

https://dspace.org/

XRF analysis of base metals prepared by fused bead method

Engelbrecht, Chantelle

2012-02-27
http://hdl.handle.net/10539/11357

Downloaded from a DSpace repository. https://dspace.org/

XRF ANALYSIS OF BASE METALS PREPARED BY FUSED BEAD METHOD

Chantelle Engelbrecht

A dissertation submitted to the Faculty of Science, University of the Witwatersrand. Johannesburg, in fulfilment of the requirements for the degree of Master of Science

Johannesburg, 2011

DECLARATION

I declare that this dissertation is my own, unaided work. It is being submitted for the Master of Science in the University of the Witwatersrand, Johannesburg. It has not been submitted before for any degree or examination in any other University.

_____

_____ day of _____ 20_____

ABSTRACT

The objective of the study was to investigate the preparation of glass beads for base metal analysis of mining samples prior to x-ray fluorescence analysis.

The research method used included the investigation of different fluxes, oxidising, non-wetting agents, fusion temperature and time. The experiments were carried out using different fusion instruments: Electrofluxer and Katanax followed by both EDXRF and WDXRF analysis. The x-ray spectrometers were calibrated with standards prepared from pure oxides and the results compared to values determined by alternative techniques. Different statistical methods were used to validate the experiments including factorial designs.

Not all the elements and oxides were recovered successfully, however, perfect glass beads were prepared. The two areas of concern were addressed successfully: firstly the loss of copper was overcome by using an alternative heating mechanism of the Katanax and sodium iodide as the non-wetting agent. Secondly, the sulphur was successfully oxidised and retained in the glass beads.

In loving memory of my Father

Johan de Lange

1952 – 2004

ACKNOWLEDGEMENTS

I would like to express my sincere gratitude to the following persons and institutions:

- First and foremost, my husband Zach Engelbrecht and my mother Wilma de Lange, without their support this would not have been possible.
- Dr. Keith McIntosh, from Anglo Research, Germiston Campus, for all the guidance, support, criticism and valued advice.
- The sponsor, Alan Buck, Anglo Platinum Group Analytical, for all the patience and financial support.
- Anglo Platinum for allowing this research project.
- Anglo Research, for the use of the equipment, resources, reagents and time.
- Prof. Ewa Cukrowska for the advice and support.
- Petra Dinham, mineralogist for Anglo American Research Centre Crown mines campus, for the mineralogical analyses.
- Rustenburg Base Metal Refineries Anglo Platinum for the time spent away to do the research.

CONTENTS

DECLARATION ii
ABSTRACT iii
ACKNOWLEDGEMENTS v
LIST OF FIGURES ix
LIST OF TABLES xi
1. INTRODUCTION 1
1.1 Background 1
1.2 Aim and objectives: 2
1.3 Outline of dissertation 3
2. THEORETICAL OVERVIEW 5
2.1 Introduction 5
2.2 Theoretical review of heterogeneity: mineralogical and particle size effects 7
2.3 Theoretical review of fusion techniques and different approaches 12
2.3.1 Fusion techniques 12
2.3.2 Inter-elemental effects and the fundamental parameter correction model 17
2.3.3 Inter-elemental effects and the Empirical influence coefficient 22
2.4 X-ray theory and principles 26
2.5 Theoretical overview of problems associated with the fusion of concentrator samples containing sulphide, copper, iron, nickel and PGM's 39
3. PRELIMINARY EXPERIMENTS 51
3.1 Introduction 51
3.2 Preliminary experiments testing flux, flux to sample ratio and the heating source 51
3.3 Preparation of secondary calibration standards 57
3.4 Preparation of secondary calibration standards with the addition of an oxidising agent and roasting the samples 62
3.4.1 Oxidising sulphur with potassium nitrate 62
3.4.2 The production of calibration standards with roasted samples 64
3.5 Calibration of the WDXRF with secondary glass bead calibration standards 65
3.6 Conclusions 68
4. NON-WETTING AGENTS 70
4.1 Introduction 70
4.2 Testing of halide salts as non-wetting agents 73
4.3 Preparation of oxide calibration standards with sodium iodide as the non-wetting agent 78
4.3.1 Preparation of calibration standards and calibration of EDXRF 78
4.3.2 Validation of calibration prepared with sodium iodide as non-wetting agent 85
4.4 Determination of mechanics of copper loss, integrating the flux and the non-wetting agent and testing other ions as non-wetting agents 87
4.4.1 Fusion of roasted samples with no non-wetting agent 88
4.4.2 Investigation into integrated flux and non-wetting agent 90
4.4.3 Investigation into alternative non-wetting agents 92
4.5 Addition of bromine gas as the non-wetting agent during the casting step and the production of oxide calibration standards 94
4.5.1 Initial investigation into bromine gas as the non-wetting agent 94
4.5.2 Bromine gas addition using a carrier gas 96
4.5.3 Preparation of oxide calibration standards with bromine gas as the non-wetting agent and validation of the calibration 100
4.6 Conclusions 107
5. PREPARATION OF FINAL CALIBRATION STANDARDS USING AN ALTERNATIVE FUSION INSTRUMENT 109
5.1 Introduction 109

5.2 Katanax operation and heating mechanism 110
5.2.1 Operation of Katanax 110
5.2.2 The heating mechanism of the Katanax and comparisons to other heating mechanisms 113
5.3 Determining whether copper is lost when fused with halide salts in the Katanax 118
5.4 Production of oxide calibration standards with potassium iodide as the non-wetting agent using the Katanax 120
5.5 Calibration of EDXRF with final set of oxide calibration standards and the empirical correction model 124
5.6 Conclusions 133
6. OXIDATION OF SAMPLES 135
6.1 Introduction 135
6.2 Oxidation step using the Electrofluxer 137
6.2.1 Oxidation with ammonium nitrate and the Electrofluxer 137
6.2.2 Oxidation with sodium nitrate and the Electrofluxer 141
6.3 Oxidation experiments using the Katanax 143
6.3.1 Oxidation factorial experiments using the Katanax 144
6.3.2 Determination of sodium nitrate, per-borate and carbonate ratio 149
6.4 Conclusions 151
7. COMPARISON OF EDXRF AND WDXRF CALIBRATIONS WITH FUNDAMENTAL PARAMETERS CORRECTION MODEL 153
7.1 Introduction 153
7.2 Determination of iodide concentration in the final oxide calibration standards 154
7.3 Calibration procedure and results for EDXRF 155
7.4 Calibration procedure and results for WDXRF 159
7.5 Comparison of calibrations achieved for EDXRF and WDXRF 165
7.6 Conclusion 166
8. VALIDATION OF FINAL WDXRF CALIBRATION 167
8.1 Introduction 167
8.2 Samples produced for validation of final calibrations 167
8.3 Comparison and discussion of copper results 171
8.4 Comparison and discussion of nickel results 175
8.5 Comparison and discussion of sulphur results 178
8.6 Comparison and discussion of iron results 181
8.7 Comparison and discussion of cobalt results 184
8.8 Comparison and discussion of aluminum oxide 186
8.9 Comparison and discussion of calcium oxide results 189
8.10 Comparison and discussion of results for magnesium oxide 191
8.11 Comparison and discussion of chromic oxide results 193
8.12 Comparison and discussion of silicon dioxide 196
8.13 Conclusion 198
9. CONCLUSIONS 203
9.1 Preliminary experiments 203
9.2 Non-wetting agents 203
9.3 Different mechanism of heating and crucibles used 205
9.4 Pure oxide calibration standards 206
9.5 Oxidation step 207
9.6 Validation of final calibrations 207
9.7 Future work and investigations 212
REFERENCES 214
APPENDIX A 219
APPENDIX B 221
APPENDIX C 226
APPENDIX D 244

APPENDIX E 250
APPENDIX F 252
APPENDIX G 260

LIST OF FIGURES

Figure 2-1: Bushveld Complex 42
Figure 3-1: Formation of buttons during secondary calibration standards production 59
Figure 4-1: Copper oxide calibration graph with sodium iodide as non-wetting agent and fundamental parameter corrections 85
Figure 4-2: Copper oxide calibration graph with bromine gas as non-wetting agent 103
Figure 4-3: Bromine calibration graph with bromine as non-wetting agent 104
Figure 5-1: K2 Katanax instrument 111
Figure 5-2: Picture illustrating heating mechanism of the Katanax 113
Figure 5-3: Picture illustrating heating mechanism of the Electrofluxer 115
Figure 5-4: Picture illustrating heating mechanism from below only 116
Figure 5-5: Calibration standards prepared with the Katanax and potassium iodide as the non-wetting agent 122
Figure 5-6: Iodide calibration graph with final calibration program and fundamental parameter correction model 127
Figure 5-7: Copper calibration graph with empirical corrections applied 129
Figure 5-8: Copper calibration graph without empirical correction 130
Figure 5-9: Sulphur calibration graph with outlier and empirical correction applied 131
Figure 5-10: Sodium oxide calibration graph with empirical corrections 132
Figure 5-11: Iodide calibration graph with empirical corrections 133
Figure 7-1: EDXRF Copper calibration graph with FP corrections 156
Figure 7-2: EDXRF Sulphur calibration graph with FP corrections 157
Figure 7-3: EDXRF Sodium calibration graph with FP corrections 158
Figure 7-4: EDXRF Iodide calibration graph with FP corrections 159
Figure 7-5: WDXRF Copper calibration graph with FP corrections 163
Figure 7-6: WDXRF Sulphur calibration graph with FP corrections 163
Figure 7-7: WDXRF Sodium calibration graph with FP corrections 164
Figure 7-8: WDXRF Iodide calibration graph with FP corrections 164
Figure 8-1: Comparison of consensus values and measured values for copper 174
Figure 8-2: Comparison of consensus values and measured values for nickel 177
Figure 8-3: Comparison of consensus values and measured values for sulphur 180
Figure 8-4: Comparison of consensus values and measured values for iron 183
Figure 8-5: Comparison of consensus values and measured values for cobalt 185
Figure 8-6: Comparison of consensus values and measured values for aluminum oxide 188
Figure 8-7: Comparison of consensus values and XRF values for calcium oxide 190
Figure 8-8: Comparison of consensus values and XRF values for magnesium oxide 192
Figure 8-9: Comparison of consensus values and XRF values for chromic oxide 195
Figure 8-10: Comparison of consensus values and XRF values for silicon dioxide 197
Figure C-0-1: Nickel oxide calibration graph with sodium iodide as non-wetting agent and FP corrections 229
Figure C-0-2: Cobalt oxide calibration graph with sodium iodide as non-wetting agent ad FP corrections 229
Figure C-0-3: Iron oxide calibration graph with sodium iodide as non-wetting agent and FP correction 230
Figure C-0-4: Chromic oxide calibration graph with sodium iodide as non-wetting agent and FP corrections 230
Figure C-0-5: Calcium oxide calibration graph with sodium iodide as non-wetting agent and FP corrections 231
Figure C-0-6: Sulphur oxide calibration graph with sodium iodide as non-wetting agent and FP correction 231

Figure C-0-7: Silicon dioxide calibration graph with sodium iodide as non-wetting agent and FP corrections 232
Figure C-0-8: Aluminum oxide calibration graph with sodium iodide as non-wetting agent and FP corrections 232
Figure C-0-9: Magnesium oxide with sodium iodide as non-wetting agent and FP corrections 233
Figure C-0-10: Sodium oxide calibration graph with sodium iodide as non-wetting agent and FP corrections 233
Figure C-0-11: Sodium oxide calibration graph with bromine gas as non-wetting agent 238
Figure C-0-12: Magnesium oxide calibration graph with bromine gas as non-wetting agent 238
Figure C-0-13: Aluminum oxide calibration graph with bromine gas as non-wetting agent 239
Figure C-0-14: Silicon dioxide calibration graph with bromine gas as non-wetting agent 239
Figure C-0-15: Sulphur oxide calibration graph with bromine gas as non-wetting agent 240
Figure C-0-16: Potassium oxide calibration graph with bromine gas as non-wetting agent 240
Figure C-0-17: Calcium oxide calibration graph with bromine gas as non-wetting agent 241
Figure C-0-18: Chromic oxide calibration graph with bromine gas as non-wetting agent 241
Figure C-0-19: Manganese oxide calibration graph with bromine gas as non-wetting agent 242
Figure C-0-20: Iron oxide calibration graph with bromine gas as non-wetting agent 242
Figure C-0-21: Cobalt oxide calibration graph with bromine gas as non-wetting agent 243
Figure C-0-22: Nickel oxide calibration graph with bromine gas as non-wetting agent 243
Figure D-0-1: Magnesium oxide calibration graph with potassium iodide as non-wetting agent and empirical corrections 246
Figure D-0-2: Aluminum oxide calibration graph with potassium iodide as non-wetting agent and empirical corrections 246
Figure D-0-3: Silicon dioxide calibration graph with potassium iodide as non-wetting agent and empirical corrections 247
Figure D-0-4: Calcium oxide calibration graph with potassium iodide as non-wetting agent and empirical corrections 247
Figure D-0-5: Chromic oxide calibration graph with potassium iodide as non-wetting agent and empirical corrections 248
Figure D-0-6: Iron calibration graph with potassium iodide as non-wetting agent and empirical corrections 248
Figure D-0-7: Cobalt calibration graph with potassium iodide as non-wetting agent and empirical corrections 249
Figure D-0-8: Nickel calibration graph with potassium iodide as non-wetting agent and empirical corrections 249
Figure F-0-1: Magnesium calibration graph on EDXRF with FP corrections 252
Figure F-0-2: Aluminum oxide calibration graph on EDXRF with FP corrections 252
Figure F-0-3: Silicon dioxide calibration graph on EDXRF with FP corrections 253
Figure F-0-4: Calcium oxide calibration graph on EDXRF with FP corrections 253
Figure F-0-5: Chromic oxide calibration graph on EDXRF with FP corrections 254
Figure F-0-6: Iron oxide calibration graph on EDXRF with FP corrections 254
Figure F-0-7: Cobalt oxide calibration graph on EDXRF with FP corrections 255
Figure F-0-8: Nickel oxide calibration graph on EDXRF with FP corrections 255
Figure F-0-9: Aluminum calibration graph on WDXRF with FP corrections 256
Figure F-0-10: Silica calibration graph on WDXRF with FP corrections 256
Figure F-0-11: Calcium calibration graph on WDXRF with FP corrections 257
Figure F-0-12: Chrome calibration graph on WDXRF with FP corrections 257
Figure F-0-13: Iron calibration graph on WDXRF with FP corrections 258
Figure F-0-14: Cobalt calibration graph on WDXRF with FP corrections 258
Figure F-0-15: Nickel calibration graph on WDXRF with FP corrections 259

LIST OF TABLES

Table 2-1: Summary of terms for equation 19
Table 2-2: Summary of terms for equation 2-3 24
Table 2-3: Summary of terms for equation 2-4 25
Table 2-4: Summary of crystals and filters in PW 2400 37
Table 2-5: Summary of collimators and detectors in PW 2400 37
Table 2-6: Measuring conditions of Quant'X EDXRF spectrometer 38
Table 2-7: Average Concentrations of base metals in concentrate type samples reported in percentage 41
Table 2-8: Melting temperatures of fluxes of interest (°C) (Lide, 1990) 46
Table 3-1: Summary of flux and samples used to produce initial glass beads 53
Table 3-2: Calibration parameters chosen for the analytes of interest 66
Table 4-1: Crucible differences before and after fusion with halides as non-wetting agents 75
Table 4-2: Recovery of copper and halides using different halides as non-wetting agents 77
Table 4-3: Concentration of oxides in calibration standards prepared with sodium iodide as non-wetting agent reported in percentage 81
Table 4-4: Measuring conditions chosen to analyse calibration standards prepared with sodium iodide as non-wetting agent 83
Table 4-5: Determination of copper recovery for unknown samples analysed with fused bead oxide calibration program 86
Table 4-6: Copper recovery of unknown samples prepared without non-wetting agent 89
Table 4-7: Crucible differences before and after fusion with integrated halide as non-wetting agent .. 90
Table 4-8: Copper recovery of unknown samples prepared with integrated flux 91
Table 4-9: Copper recovery of unknown samples prepared with alternative non-wetting agents 93
Table 4-10: Intensities measured for copper oxide and chloride with factorial design experiment 95
Table 4-11: Copper and bromide intensities measured with bromine gas addition via carrier gas 98
Table 4-12: Concentration of oxides in calibration standards prepared with bromine gas as the non-wetting agent 101
Table 4-13: Measuring conditions chosen to analyse calibration standards prepared with bromine gas as non-wetting agent 102
Table 4-14: Copper recovery of samples prepared with bromine gas as non-wetting agent 105
Table 5-1: Copper oxide recovery with halide salts by Katanax 119
Table 5-2: Fusion parameters for program used on Katanax 121
Table 5-3: Concentrations for oxide calibration standards prepared with potassium iodide as the non-wetting agent in the Katanax, reported in percentage 123
Table 5-4: Measuring conditions for the final calibration created with the standards produced with the Katanax and potassium iodide as the non-wetting agent 125
Table 5-5: Elements chosen for empirical corrections on the final calibration program 128
Table 6-1: Relative percentage difference for Sulphur with ammonium nitrate as oxidising agent 139
Table 6-2: Relative percentage difference for Sulphur after oxidation with sodium nitrate and sodium per-borate 142
Table 6-3: Oxidation factorial design using the Katanax 145
Table 6-4: Fusion parameters used in the Katanax 146
Table 6-5: Relative percentage differences for Sulphur after oxidation factorial 147
Table 6-6: Mass of sodium nitrate, per-borate and carbonate for ratio determination 150
Table 6-7: Relative percentage difference for sulphur while testing ratio of oxidizing agents 150
Table 7-1: Measuring conditions for EDXRF calibration with fundamental parameter correction model 155
Table 7-2: Summary of correlation coefficients achieved with EDXRF and fundamental parameter corrections 155

Table 7-3: Summary of calibration parameters for WDXRF calibration 160
Table 7-4: Summary of calibration graph parameters for WDXRF 162
Table 8-1: Summary of samples produced with final set of parameters 169
Table 8-2: Summary of fusion program used to produce glass beads for validation of final calibration 170
Table 8-3: Comparison of consensus and measured values for copper 171
Table 8-4: Comparison of copper results for quality control samples 173
Table 8-5: Comparison of consensus and measured values for nickel 175
Table 8-6: Comparison of nickel results for quality control samples 176
Table 8-7: Comparison of consensus and measured values for sulphur 178
Table 8-8: Comparison of sulphur results for quality control samples 179
Table 8-9: Comparison of consensus and measured values for iron 181
Table 8-10: Comparison of iron results for quality control samples 182
Table 8-11: Comparison of consensus and measured values for cobalt 184
Table 8-12: Comparison of cobalt results for quality control samples 185
Table 8-13: Comparison of consensus and measured values for aluminum oxide 186
Table 8-14: Comparison of consensus and measured values for calcium oxide 189
Table 8-15: Comparison of consensus and measured values for magnesium oxide 191
Table 8-16: Comparison of consensus and measured values for chromic oxide 193
Table 8-17: Comparison of chromic oxide results for quality control samples 194
Table 8-18: Comparison of consensus and measured values for silicon dioxide 196
Table A-1: Summary of details of reagents used 219
Table B-1: Preliminary experiment details 221
Table B-2: Comparison of results obtained by XRF and ICP for Merensky sample type reported in percentage 222
Table B-3: Comparison of results obtained by XRF and ICP for UG2 sample type reported in percentage 222
Table B-4: Details of experiments done to prepare secondary calibration standards 222
Table B-5: Details of experiments done to oxidise sulphur in Merensky and UG2 sample types with potassium nitrate 223
Table B-6: Details of experiments done to produce secondary calibration standards with roasted samples 223
Table B-7: ICP results of duplicate samples prepared with roasted and unroasted Merensky and UG2 samples types reported in percentage 224
Table B-8: ICP results of duplicate samples prepared with roasted and unroasted Merensky and UG2 sample types reported in percentage 225
Table C-1: Summary of experiments and results obtained for testing halides as non-wetting agents. 226
Table C-2: Mass of oxides, flux and non-wetting agent weighed to prepare oxides calibration standards with sodium iodide as non-wetting agent. 227
Table C-3: Calibration results for preparation of oxide calibration standards with iodide as non-wetting agent 228
Table C-4: Validation of calibration created with oxide calibration standards and sodium iodide as non-wetting agent 234
Table C-5: Summary of experimental details with no non-wetting agent 234
Table C-6: Summary of experimental details with integrated flux 235
Table C-7: Summary of experimental details with alternative non-wetting agents 235
Table C-8: Summary of experimental details with bromine gas as non-wetting agent 235
Table C-9: Mass of oxides and flux weighed to prepare calibration standards with bromine gas as non-wetting agent 236
Table C-10: Calibration results for preparation of oxide calibration standards with bromine gas as the non-wetting agent 237
Table D-1: Experimental detail of samples prepared with different halides as non-wetting agents in the Katanax 244

Table D-2: Results obtained for samples prepared with different halides as non-wetting agents in the Katanax 244
Table D-3: Mass of oxides, flux, additives ad non-wetting agent weighed to prepare oxide calibration standards with potassium iodide as the non-wetting agent in the Katanax..... 245
Table E-1: Experimental details of samples prepared during oxidation with ammonium nitrate in the Electrofluxer..... 250
Table E-2: Experimental details of samples prepared during oxidation with sodium nitrate in the Electrofluxer..... 250
Table E-3: Experimental results of samples produced during oxidation with sodium nitrate in the Katanax 251
Table G-1: Experimental detail of sample prepared for the validation of the final calibration on WDXRF 260
Table G-2: Raw results for copper oxide as analysed by WDXRF..... 261
Table G-3: Raw results for nickel oxide as analysed by WDXRF 262
Table G-4: Raw results of sulphur oxide as analysed by WDXRF 263
Table G-5: Raw results for iron oxide as analysed by WDXRF 264
Table G-6: Raw results for cobalt oxide as analysed by WDXRF 265
Table G-7: Raw results for aluminium oxide as analysed by WDXRF..... 266
Table G-8: Raw results for calcium oxide as analysed by WDXRF 267
Table G-9: Raw results for magnesium oxide as analysed by WDXRF 268
Table G-10: Raw results for chromic oxide as analysed by WDXRF..... 269
Table G-11: Raw results for silicon dioxide as analysed by WDXRF 270

1. INTRODUCTION

1.1 Background

Mining samples are analysed by x-ray fluorescence spectrometers (XRFS) for base metals using the pressed powder briquette technique. These base metals include copper, nickel, iron, cobalt, sulphur, calcium oxide, magnesium oxide, aluminum oxide, chrome oxide and silicon dioxide. XRFS are used because it is a rapid, cost effective and multi-elemental technique. The pressed powder technique used for preparation of the samples has certain advantages:

- It is a rapid preparation technique with a pulverising step of three minutes, pellet pressing step of one minute and the XRF analysis of three minutes per sample.
- The cost of this sample preparation is low due to the small amount of chemicals required.
- It is an easy, simple technique which can be performed without too many human errors and without excessive training.

The disadvantage of the pressed powder briquette preparation technique includes the heterogeneity effects which are the particle size and mineralogical effects. These effects introduce inaccuracies in the results and matrix matching is the only possible method to overcome this.

The fusion technique for preparation poses the solution to both these problems and introduces a preparation technique that will ensure more accurate XRF analysis. Fusion is the decomposition of a sample by dissolving the sample using flux at high enough fusion temperatures (Bennett and Oliver, 1992).
The advantages of the fusion technique include:

- Accurate and precise XRF analysis due to the fact that the heterogeneity effects are overcome.
- Inter-elemental effects can be reduced by diluting the sample with the flux.
- Pure oxide synthetic standards can be used for calibration and will maximise the concentration ranges of elements and oxides that can be analysed.

The fusion technique presents some disadvantages which include:

- It is more complex and time consuming to prepare a sample by fusion.
- Since more expensive and pure chemicals are used, the technique is also more expensive.

It can, however, be concluded that the advantages out-weigh the disadvantages and therefore the method was investigated.

The limitation of the fusion technique is the fusion of samples that contain sulphur. The concern with the sulphur is that unoxidised sulphides will react with the platinum ware (crucibles) and cause severe damage (Claisse, 2000). Another limitation is the fact that the glass beads can stick to the mould and easily crack or shatter as they cool. To resolve this limitation non-wetting agents are used (Claisse, 1990).

1.2 Aim and objectives:

The aim of the investigation is to produce glass beads from concentrator samples and analyse these glass beads by XRFS. An ideal fusion as defined by Blank and Eksperiandova (1998) will have the following:

- Simple and rapid fusion,
- Retention of all elements including the oxidation and retention of sulphur,
- Wide range of elemental concentration,
- Use the fundamental parameter model for the inter-element interferences,
- No damage to crucibles and moulds, no need to clean between fusions.

- Prevention of the glass bead cracking during cooling or sticking to the moulds and crucibles.

1.3 Outline of dissertation

An overview of the literature is presented (Chapter two) with regards to previous studies as well as all areas investigated previously.

Preliminary experiments were carried out with significant contributions to the considerations made for the fusion process forwards (Chapter three).

The different halides were investigated as non-wetting agents to prevent the glass beads from shattering as well as sticking to the crucibles and moulds. Alternatives to halides were also investigated as well as the mechanism of copper loss with the addition of halides as non-wetting agents (Chapter four).

A new fusion instrument was investigated and the fusion method finalised with sodium iodide as the non-wetting agent. The final set of pure oxide calibration standards were prepared (Chapter five).

The oxidation step was investigated with the aim to oxidise the sulphur in the samples and thereby retain it (Chapter six).

Both the EDXRF and the WDXRF were calibrated using the oxide calibration standards prepared and the fundamental parameters correction model applied. The calibrations were compared (Chapter seven).

The calibration for the WDXRF was validated using samples with known concentration values and the results were statistically validated (Chapter eight).

The final conclusions and recommendations as well as future work is discussed (Chapter nine).

2. THEORETICAL OVERVIEW

2.1 Introduction

In 1913 Bragg used the first type of ionization spectrometer for his research and in 1920 Hertz showed that there was regularity between atomic number and the frequency of the X-ray spectra. The X-ray fluorescence technique was used for chemical analysis in 1932 by Hevesy and Moseley who showed the regularity between the atomic number and the frequency of the spectra as a linear relationship. Instrumental analysis methods including X-ray fluorescence were introduced to mining and process industries in the 1960's as reported by Bernstein (1963).

In Anglo Platinum, X-ray fluorescent spectrometers are used for the analysis of concentrator, converter matte and slag as well as furnace matte and slag samples. The five elements analysed routinely by the X-ray fluorescence technique are copper (Cu), nickel (Ni), iron (Fe), cobalt (Co) and sulphur (S) and the five oxides are calcium oxide (CaO), magnesium oxide (MgO), aluminum oxide (Al_2O_3), chromic oxide (Cr_2O_3) and silicon dioxide (SiO_2). These results are used for both metal accounting and process control of the plants and processes.

Metal accounting is where the analytical results are used for mass balance of the metals in the plants and processes. In process control the results are used to control the process and produce products to specified requirements to attain high quality products without damage to the process. Therefore the results must be timeous in order to take action should the process go out of control.

In the Anglo Platinum laboratories the results can be produced within twenty-four hours, for metal accounting samples, if the samples are prepared manually, or within

fifteen minutes, for process control samples, if the samples are prepared by automated systems. The preparation technique used in the laboratories is pressed powder, whereby the sample is milled together with a binding agent and then pressed into a briquette, either in an aluminum cup, steel ring for the robotic laboratories or with a backing, for example boric acid. The advantages of the pressed powder technique include: speed and ease of preparation and the low cost due to the use of just the binding agent or backing chemicals.

Once the equipment for preparation has been installed, only maintenance costs need to be considered. However, pressed powders are subject to certain limitations. the X-ray fluorescence technique is based on the assumption that the sample is always homogeneous with equally sized particles. This, however, is not the case with pressed powders. Pressed powders are almost always heterogeneous and the particle size will depend on the milling efficiency of the equipment used. Claisse and Samson (1961) and Bernstein (1963) studied the effect of the particle size on the measured fluorescence and showed that for any given wavelength the fluorescence will depend not only on the particle size but also on the phases present in the sample. Norrish and Chappell (1967) reported that the effect would be insignificant only for very fine or very coarse particles. Another effect that was identified and investigated by Claisse and Samson (1967) and Bernstein (1963) is that of mineralogy. It has been found that the X-ray fluorescence will not only be affected by the particle size but also the chemical composition. The particle size effect can be reduced by milling the sample. However, this may introduce contamination from the milling vessel and the assumption is that all particles are reduced equally, which is not necessarily the case. The mineralogical effect can be reduced by matching the calibration standards to the samples. To match the mineralogy of the samples and the standards, secondary calibration standards are prepared from a range of samples obtained from the process. The secondary calibration will limit the range of concentrations that can be measured. Small changes in the process may cause a change in the mineralogy of the samples

and the samples will not match the standards, this will lead to inaccurate results (Claisse and Samson, 1961).

The solution to the above mentioned limitations are fusing the samples. The definition for fusion as discussed by Bennett and Oliver (1992) is the process whereby the sample is decomposed at a high temperature using an appropriate flux. Fusion eliminates the mineralogy effect due to the fact that the sample is dissolved and the mineralogy destroyed and will eliminate the particle size effect. Other advantages of fusion include the reduction of inter-element effects due to the dilution of the samples and also there exists the possibility of preparing pure oxide calibration standards. The technique, however, does have limitations: it is time-consuming, expensive since platinum ware and high purity chemicals and oxides are used. Norrish and Thompson (1990), Norrish and Hutton (1969) and Ingamells (1970) reported limitations regarding the analysis of samples that contain sulphur as a sulphides. Bennett and Oliver (1992) stated that the operator must be well trained to produce reproducible results. One of the advantages can also be seen as a disadvantage, Norrish and Chappell (1967), where the dilution of the sample during fusion will reduce the inter-element effects but will decrease the sensitivity of the instrument, raising the detection limits and will affect the precision achieved.

The fused bead technique addresses most of the problems associated with pressed powders and inaccurate results. This makes the technique worthwhile investigating in the field where most laboratories are ISO 17025 accredited and accurate and precise results are of the utmost importance.

2.2 Theoretical review of heterogeneity: mineralogical and particle size effects

The major concerns when analysing samples by X-ray fluorescence as pressed powders are the heterogeneity of the samples, in other words the mineralogical and

particle size effects. These effects were identified and investigated from 1957 by various scientists and will be discussed in this section.

Claisse and Samson (1961) reported that in 1957 Claisse was the first to draw experimental curves showing the effect of the size of an isolated particle on the X-ray fluorescence intensity. Claisse defined this as the heterogeneity effect and furthermore showed that the fluorescence intensity will increase as the particle size decreases. Claisse predicted that the fluorescent intensity should increase as the mean distance between the atoms in the compound are increased due to the decreased absorbance by neighbouring atoms. The greater the distance between the atoms in the compound the less absorption of the fluorescence X-rays and a greater intensity from the atom of interest will be observed. A number of other scientists reported to have seen these two effects and had done experiments to show the effect as reported by Claisse and Samson (1961). These include Smithson et al in 1960 who experimented and confirmed the particle size effect; Campbell and Thatcher in 1960 and Chados et al 1960 who experimented and observed the particle composition effect.

Claisse and Samson (1961) investigated both these effects and concluded that: the fluorescence intensity for a given wavelength will vary with particle size but in a limited region only and they described this region as the transition zone. The position of the transition zone varies with the wavelength of primary radiation as well as the composition of the fluorescence intensity. When low atomic number elements are analysed the transition zone is so low in the particle size scale that it is impossible to grind sufficiently. These conclusions yet again confirmed that grinding the samples would not necessarily compensate for these effects, particularly where low atomic number elements are analysed.

Possible solutions for these two effects are discussed in the paper by Claisse and Samson (1961). The solutions include the reduction of the particle size of the sample

and produce identically sized particles. It should be noted that vigorous grinding necessary to achieve this would introduce contamination from the grinding vessel and it is very important to note that not all particles would be reduced equally in size. Particles not reduced equally will mean that the fluorescence intensity will increase for those particles that were decreased in size and this will not be observed for all the particles present in the sample. The other solution offered by Claisse and Samson was the dissolution of the sample and therefore removing the heterogeneity effect. Grinding proved successful for Campbell and Thatcher who ground the samples extensively for ten to fifteen hours and Adler and Axelrod who added an abrasive material as a grinding aid and ground the samples for shorter times. Dissolution proved successful for Claisse and was done with sodium tetra-borate and as an alternative with aqueous dissolution by Campbell et al.

Andermann (1961) investigated the heterogeneity effects as well and classified the effects seen in powdered samples into four categories namely: variations in the sample source (mineralogical), variations from one particle to another (inter-particle effect), variations within the particle where two or more phases are present causing a concentration gradient (intra-particle size) and variation in composition (inter-element effect). Andermann defines the mineralogical differences as the effect due to changing the source of the samples. The crystalline structures of the two samples can vary and this will cause differences in the number of efficiently excited atoms per unit volume as also demonstrated by Claisse. Andermann showed improved results for SiO_2, CaO, Fe_2O_3, MgO and Al_2O_3 due to fusion when comparing the results of the same samples as pressed powder. The results of the pressed powders indicated that the accuracy approached the precision levels of the instrument for MgO and Al_2O_3 but not for SiO_2, CaO and Fe_2O_3. The experiments on the finished cements showed a striking example of how two different laboratories using two different commercially available instruments could provide the same wrong answers, data from Andermann et al and Kiley et all. The fact that both laboratories gave the same wrong answers was attributed to mineralogical effects. Andermann and Allen (1961)

used the X-ray absorption law to postulate that infinite depth is reached for an MgO particle at 20 μm. Powdered material have the usual particle size range from 40 to 150 μm and the analysis of the constituents such as MgO, Al_2O_3 and SiO_2 will present the analysis of the upper portion of each particle on the surface. If there were any in-homogeneity present this would constitute a major problem. The solution that could be considered would be extensive grinding but would present problems for the analyses of light elements. For acceptable analyses of SiO_2 the particle size of MgO would have to be less than 0.003 μm, which is not practically achievable. Andermann and Allen (1961) concluded that particle size reduction could not be expected to solve the mineralogical differences between two samples. To resolve this issue the two authors considered the fusion technique that was completed successfully in 1954 and refined in 1956 by Claisse. The fusion results compared to the powdered samples results showed an improvement in the total precision as well as an improvement in accuracy by all participating laboratories for the oxides of iron, magnesium, aluminum and calcium but not for silica. This was attributed to a decrease in instrumental precision due to loss of sensitivity because of the dilution of the samples. The final conclusion was that fusion was the solution to inhomogeneity and mineralogical effects in cement samples and the method should only be refined to improve the accuracy even further for the lighter elements.

Bernstein (1963) investigated the relationship between particle size and intensity in mining applications for minor constituents. Bernstein concluded from his results that the relationship between intensity and particle sizes for a minor constituent in a mixture became constant for relatively large and for relatively small particles. It would, therefore, appear to be feasible to work with either large or small particles. It was observed, however, that mining samples are almost never just large particles. The relative intensity of a minor constituent in a mixture is a function of both the particle size of the minor constituent as well as the particle size and absorption coefficient of the matrix material. Bernstein pointed out that after evaluating a large number of mining, cement and process samples presented as powdered samples for

X-ray analysis – normal process control was capable of producing samples with satisfactory results, in spite of the fact that the particle size did not conform to the requirements. This can be attributed to samples having a relatively constant particle size distribution achieved in the process, uniform particle sizes, reproducible sample preparation techniques and matrix matching between the samples and the calibration standards. This is not always achieved by all processes and will have to be controlled and regulated to make sure the results achieved by XRF is fit-for-purpose and that the particles are always uniform, that the sample preparation remains reproducible and that the matrices are matched. Monitoring the particle size distribution after milling will account for the particle size effect but will not overcome mineralogical effects.

To conclude:

- Heterogeneity effects were identified, classified and investigated by Claisse, Samson and Bernstein. The effect was attributed to both particle size effects and mineralogical effects.
- Solutions that were identified to compensate for these two effects were:
    - Grinding the samples extensively,
    - Fusion of the samples was the other solution identified and involved the destruction of the mineralogy of the samples due to dissolution and therefore eliminating both effects.

An important factor that should be taken into consideration at this point is that heterogeneity can also be introduced by sampling incorrectly from the bulk sample. This will introduce non-representative and biased results and cannot be compensated for by grinding or fusion and only by implementing the correct sampling methods. This study will not focus on sampling methods.

The importance of investigating the fusion of mining samples was illustrated up to now and the next section of the literature review will focus on different methods and chemicals used for these fusions for different types of samples.

2.3 Theoretical review of fusion techniques and different approaches

2.3.1 Fusion techniques

Fusion is the decomposition of the sample by dissolving the sample using a flux, at a high temperature, Bennett and Oliver (1992). It is an expensive and time-consuming technique but it is used worldwide in many application laboratories due to all the advantages of the technique. The advantages of the technique are multiple:

- Providing precise and accurate X-ray fluorescence analysis of the sample due to the fact that the glass bead presented to the spectrometer is homogeneous.
- Using flux to dissolve the sample will dilute the sample and will reduce inter-elemental effects. By choosing a constant dilution factor the magnitude of these effects can be established and corrected for by matrix correction models (fundamental parameters).
- Glass beads allow the use of pure oxides for the production of synthetic primary calibration standards. Therefore, the standards can be prepared in a manner that will enable the analyst to establish the line overlap and inter-elemental effects, providing an improved way for accounting and correcting for these effects. A calibration with pure oxides has the further advantage of calibration curves with regression coefficient closer to 1.0. The primary standards will enable the analyst to control the concentration range of all the elements measured. Therefore the X-ray fluorescence technique can be a primary technique, similar to techniques such as Inductively Coupled Plasma (ICP) spectrometry.

Another advantage was investigated and discussed by Enzweiler and Webb (1996) where it was shown that glass beads produced more accurate results than pressed

powders of the same samples. The higher accuracy of the glass beads when compared to the pressed powder results were attributed to the reduced matrix effects as well as the elimination of the mineralogical effects.

The features of an ideal fusion technique as discussed by Blank and Eksperiandova, (1998) are simplicity, rapidly, retention of the elements to be determined, high limit of sample to flux ratio, wide range of element concentration in the sample, applicability of fundamental parameters as a correction model, production of glass bead disks that are not prone to cracking, shattering or sticking in the moulds and crucibles that need no cleaning between fusions of different samples.

Borax fusion was developed in 1956 by Claisse and modified by several workers, Campbell et al in 1958, Andermann et al in 1961, Longobusso in 1962 and Rose et al in 1963. The method consisted of heating a mixture of the sample and the flux at high temperature until it is molten and cast, to cool into a solid glass bead with a flat surface that is analysed with an XRF fluorescence spectrometer. The quality of the analysis is dependant on the bead homogeneity, which in turn is dependant on the fusion process, Le Houillier and Turmel (1974).

A review of X-ray fluorescence sample preparation from 1987 to 1996 was done by Blank and Eksperiandova (1998). The review considers sample types fused, fluxes and oxidising agents used as well as crucibles and moulds. Fusions are used for the analyses of a wide range of sample types, including slimes in waste waters, geological samples, iron ores and slags, ferroalloys, raw material for blast furnaces, non-ferrous metallurgical products and metal oxides. Different fluxes investigated and used are lithium tetra-borate, lithium meta-borate and potassium pyrosulphate mixtures, lithium meta- and tetra-borate mixtures, lithium tetra-borate and carbonate mixtures, sodium tetra-borate and various combinations of the above-mentioned compounds. Seldom used are fluxes containing phosphates. Oxidising agents that were used to enhance the oxidation of the elements in the sample as well as lowering

the melting temperature of the fluxes. These included lithium nitrate, nitric acid, ammonium nitrate, sodium nitrate, sodium peroxide and sodium nitrite ($NaNO_2$). Admixtures used to lower the melt's viscosity and alternatively known as non-wetting agent or releasing agents that were reported were sodium iodide and potassium iodide but not mentioned in this review and used by other analysts are bromide and chloride compounds, for example, potassium bromide (Le Houillier and Turmel, 1977), ammonium iodide (Norrish and Thompson, 1990); (Sangenberg, Fontbote and Pernicka, 1994) and lithium iodide (Turmel and Samson, 1984).

Factors to be considered for the fusion technique were identified and discussed by Maesson and Bouman (1968), the sample type, particle size, flux, sample to flux ratio, fusion temperature as well as fusion time. Other factors of importance considered during this study were oxidising agents, oxidation steps, non-wetting agents, roasting samples, crucible and mould material as well as the furnace used.

The *selection of the flux* to be used is a very important factor and should be considered carefully taking into account the main constituents of the samples to be analysed. The oxides in the samples can be classified using two different criteria (Lee, 1996). The first manner to classify oxides depends on the structure; the second depends on the chemical properties. Oxides may be basic, amphoteric or acidic depending on the products that are formed when the oxides react with water. Metallic oxides are generally basic; sodium oxide will react with water to form sodium hydroxide. A large amount of energy is required to form an ionic oxide and therefore ionic oxides have high melting points, for example Na_2O 1275°C. Acidic oxides are usually non-metallic oxides and covalent. They will have lower melting and boiling points, for example SO_2. Some of the acidic oxides will have high melting points for example SiO_2 because it forms 'giant molecules'. They will react with water and produce an acid for example B_2O_3 will produce H_3BO_3. The oxides that do not react with water, for example, silicon dioxide, may react with sodium hydroxide showing their acidic properties. The oxides may be classified as amphoteric, in other words

they, will react with both strong acids and bases. For example Al_2O_3 will react with hydrochloric acid and then dissociate. The fluxes can be classified using the same criteria, when comparing meta- and tetra- borate fluxes (Bennett and Oliver, 1992). The meta-borate fluxes are less acidic than sodium tetra-borate fluxes when comparing the oxygen ratio. The oxygen in the meta-borate fluxes when compared to the tetra-borate fluxes contain 2 oxygen atoms to 7 oxygen atoms. Tetra-borate fluxes are therefore classified as more acidic. Reactions are more likely to occur between basic oxides and acidic fluxes and visa versa. Therefore, a sample with high silica content is considered to be highly acidic whereas the alkali's and alkaline oxides are basic.

The flux must, therefore, be considered and chosen to make sure the sample components will dissolve readily. Anhydrous borax flux (sodium tetra-borate) was used as the main flux in early fusion methods. Borax was and is still much cheaper than the other fluxes, however, borax is not ideal due to its hygroscopic nature. The beads produced with the flux have to be stored in desiccators and will have to be replaced at frequent intervals. Borax is still used by many laboratories who prepare new standards regularly rather than using the expensive lithium alternative. Tetra-borate fluxes have some disadvantages as well. They have a higher melting point compared to meta-borate fluxes and material with high silica content will not dissolve readily in tetra-borate fluxes due to its acidic nature. Therefore, meta-borate fluxes and a combination of the meta- and tetra-borate fluxes are often used. Another important consideration is the sample to flux ratio, i.e. the dilution of the sample. The degree of dilution will be a compromise between the sensitivity obtained for the analytes present in low concentrations and the ease of dissolution of all analytes present at high concentrations. To enable the use of fundamental parameters as a correction model for inter-element effects the sample to flux ratio must be constant for both the calibration standards as well as the samples. However, use of a mass balance approach will compensate for differences between the samples and standards.

The selection of the *crucibles and moulds* to be used and the material they are made of is of great importance due to both being subjected to harsh conditions. The crucibles have to withstand intense heating and rapid cooling for prolonged times together with attack from corrosive flux and additives. The mould has to withstand rapid heating and cooling of the melt at it is cast and solidifies. (Bennett and Oliver, 1992).

Crucibles and moulds used for the fusions were reviewed by Blank and Eksperiandiva (1998). Crucibles and moulds investigated and used are generally made of platinum, platinum-gold alloy, platinum-gold-ruthenium alloy, duralumin, steel, graphite and glassy carbon. The use of $CBrF_3$ was recommended by Yoshioka et al in 1988, to spray the insides of the crucible walls as well as the mould to prevent sticking of the glass bead. Another recommendation made by the authors is the use of glassy carbon crucibles. It is reported that the metal oxides will not interact with the crucible and it is cheaper than the precious metal alternatives. However, glassy carbon crucibles are subject to oxidation by oxygen at high temperatures and will limit the fusion of the samples to reducing conditions. This would not be suitable for sulphide containing material. The Pt-Au alloy is the most universally used due to it being the best non-wetting properties (Bennett and Oliver, 1992). Some modifications include the addition of rhodium, zirconia and yttria. Rhodium will increase the hardness of the crucible whereas the yttrria and zirconia will inhibit crystal formation. Norrish and Hutton (1968) reported adhesion of the melt to the crucible walls and reported the improvement with the use of Pt-Au (95% - 5%) and palau (80% Au – 20% Pt – 20% Pd) that were not wet by the melt. However, palau crucibles have a short lifetime and therefore the Pt-Au alloy is preferred. Graphite crucibles can be used, however the authors reported the presence of a graphite layer on the glass beads and this will reduce the count rates of the lighter elements, for example, silica, aluminum and magnesium. Ingamells (1970) reported that graphite crucibles should not be used due to them being reportedly porous and the flux melt will leak through the crucible into the furnace and cause great damage. Ingamells

further reported the use of platinum ware but that the flame used must be oxidising and when reducing flame conditions are applied iron, copper, lead, cobalt and manganese are extracted from the sample into the platinum, which causes loss of elements and damage to the platinum ware. Gold crucibles are reported to be less subject to contamination when compared to platinum ware. However, gold has a low fusion temperature and the crucibles will be damaged at the higher temperatures that are necessary for some samples. Gold-lined crucibles are reported to be an improvement on just pure gold crucibles.

The *type of furnaces and flames* used to fuse the samples are also of utmost importance as discussed by Bennett and Oliver (1992). A gas burner can be used for the fusion of the samples depending on the gas available as well as the local conditions. If the gas is oxygen enriched it can reach very high temperatures. Sophisticated automated devices are available where the crucibles can be swirled and the melt cast automatically, making use of Meker burners. The disadvantages of gas burners are that the temperatures and conditions cannot be kept consistent and cannot be controlled, for example; in the case of oxidation steps where the control of the temperature is of great importance. Gas burners will work effectively for certain samples where lower temperatures are sufficient for complete fusion and temperature control is of less importance. However, for samples where oxidation steps are necessary and the temperature control is of utmost importance, electrical furnaces are preferred. Electric furnaces produce more consistent conditions and temperatures, are safer and more convenient. Other factors influencing the choice of heating are the sample types in particularly those containing sulphides. This will be discussed in Section 2.5.

2.3.2 Inter-elemental effects and the fundamental parameter correction model

As reported the fusion process will overcome both the heterogeneity effects: mineralogical and particle sizes. However, another effect, the inter-element effect

will never be overcome by the preparation method. X-rays from the XRF will irradiate the sample and the X-rays are absorbed to produce primary fluorescent radiation. The primary fluorescent radiation can be absorbed by other elements present in the sample, produce secondary fluorescent radiation. The resulting intensity observed is the sum of the primary and secondary fluorescent radiation from all the components in the sample – this is the inter-element effects. The inter-elemental effects can be reduced in various ways:

- These can be corrected for by theoretical calculations using mathematical equations, for example, the Sherman equation. However, this leads to complicated mathematical calculations especially with a multi-component system (multi-elemental sample) (Hickson, 1963). To be able to calculate the line intensity is unique to XRF spectrometers. No other analytical technique allows for such a combination of theoretical physics and experimental results (Rousseau, 2004).
- By diluting of the matrix: the fluorescence intensity is dependent on the total number of atoms of any element present in the sample. The intensity for only one element is proportional to the concentration of the element and the absorption coefficient of the sample. Considering one wavelength only, an element with a high absorption coefficient at that wavelength can be selected which makes one absorption term in the denominator very large and so predominates over the absorption effects of the other elements. However, this also reduces the count rates recorded for each element (Hickson, 1963). This is also known as using a heavy absorber as mentioned by Kodoma, Brydon and Stone in 1967.

Attention is given to the development of the theoretical calculations for matrix (inter-elemental) effects as reviewed by Rousseau (2006). The methods are reviewed from a historical point of view in order to present their contribution to the modern methods currently used. These methods most suitable features are extracted to create a new modern fundamental parameters (FP) method that corresponds to the modern

analytical needs of the XRF analyst. In the XRF technique, the calculation of the sample composition is based on the relationship between the concentration (C_i) of the analyte i and the measured net intensity (I_i) which can be expressed by equation 2-1 (Rousseau, 2006). Refer to Table 2-1.

$$C_i = K_i . I_i . M_{is} \qquad \textbf{Equation 2-1}$$

Table 2-1: Summary of terms for equation

Term	Definition
C_i	Concentration of the analyte
K_i	Calibration constant factor of i
I_i	Measured net intensity
M_i	Correction factor for the matrix effect of spectrum s of i

The concentration C_i is a weight fraction of the element i in the original sample and not the specimen.

The two most efficient mathematical methods, as reported by Rousseau, are influence coefficients and fundamental parameters (FP). The synergy of influence coefficients and fundamental parameters are discussed as well as empirical influence coefficients. To simplify the calculation and discussion it must be assumed that the sample presented to the XRF spectrometer is homogeneous, flat, with a polished surface and infinitely thick.

In 1955, Jacob Sherman was the first to publish a detailed demonstration of an equation enabling the theoretical net X-ray intensity emitted by each element from a specimen of known composition to be calculated when it is irradiated by a poly-chromatic X-ray beam, equation 2-2 (Rousseau, 2006).

$$I_i = f(C_i, C_j, C_k, \ldots\ldots, C_N) \qquad \textbf{Equation 2-2}$$

In 1954 Beattie and Brissey proposed an analytical XRF method based on the Sherman equation. This method contains eight significant approximations, which delayed the development of modern methods in XRF. Only 30 years later, in 1984, these eight approximations were eliminated and a new method proposed. The eight approximations are:

1. An equation system where n solutions are possible for the composition of a sample of n elements to be determined.
2. Forced normalisation to 100% of the calculated concentration.
3. Absorption correction factors are assumed to be constant for a given concentration range.
4. Unique and effective wavelength is equivalent to the full polychromatic spectrum of the excitation source.
5. The enhancement effect is equal to the absorption effect.
6. Absorption correction factors are binary dependent only on the analyte i and a matrix element j. The rest of the matrix composition is ignored.
7. Absorption correction factors can be calculated empirically from binary samples of known compositions.
8. The total effect of the matrix on the anlalyte i is equal to the sum of the effects of each element of the matrix, each matrix effect being calculated independently.

According to Rousseau, the greatest contribution of Beattie and Brissey is their proposal of the concept of relative intensity, defined as the ratio of measured net intensity to the measured net intensity of the pure element.

In 1966, Lachance and Trail proposed a new method, but only eliminated approximation 1 and 2. Lachance and Trail contributed to a clear definition of the concept of the influence coefficient, which is defined as a coefficient that quantifies the total matrix effects of an element j on the analyte i in a given sample. In 1967 Claisse and Quintin proposed a new method where approximations 1 and 4 were

eliminated. Their contribution was to show that the influence coefficient values vary with the concentration of the analyte i and the effective wavelength is an unnecessary and undesirable approximation. They also introduced the concept of the weighting factor for each wavelength of the excitation source spectrum. The Claisse-Quintin algorithm was improved by Rousseau and Claisse in 1974, by Tertian in 1976 and Rousseau in 1984.

In 1968, Criss and Birks proposed a new method, the fundamental parameters (FP), where all the approximations are excluded. They focused on the application of the Sherman equation and disregarded the concept of influence coefficients. To overcome the difficulty of the Sherman equation that allows only the calculation of intensity and not concentration, Criss and Birks initiated the iteration process with measured relative intensity normalised to 1, for calculating a first estimate of the sample composition. The theoretical intensities are compared to the measured intensity. If the match is not within an allowed maximum error the process is repeated. The method suffers from a few weaknesses: firstly, having to normalise to 1 the measured relative intensity may introduce a bias. It is preferable to use a solution that does not require normalisation. Secondly, the Sherman equation was designed to calculate only theoretical X-ray intensities and not concentrations. Therefore the X-ray intensity can be predicted directly, if the sample composition is well known and totals 100%. Used in this manner the Sherman equation is a continuous function. The Sherman equation cannot directly predict the composition of a sample that totals 100% from a set of measured intensities. It is possible to use the Sherman equation to indirectly calculate the sample composition. This problem can be overcome by using another analytical method to calculate a first estimate as close as possible to the final composition. Thirdly, Criss and Birks used a single standard for calibration, which is not efficient.

Criss and Birks did contribute positively by proposing to use the Sherman equation for the correction of matrix effects each time that the composition of an unknown

sample has to be calculated. In 1973, Willy de Jongh proposed a method where all approximations were overcome, except for number 3. De Jongh showed that theoretical and multi-elemental influence coefficients could be calculated from the Sherman equation and the normalisation to 100% is unnecessary. Mainly, he contributed to the calibration method of plotting the measured intensity as a function of the calculated intensity. In 1974, Rasberry and Heinrich proposed an empirical method, which is in complete disagreement with the Sherman equation; however, the method is only valid for Cr-Fe-Ni alloys. Their major contribution was to show that empirically the absorption and enhancement are two different matrix effects and should be treated separately. In 1981 Lachance proposed a new method, named COLA, using the binary influence coefficients. It was the last attempt at using this approximation and was justified at the time since powerful computers were not that readily available to calculate the FP. In 1984, Rousseau proposed the fundamental algorithm (FA) where influence coefficients correcting for absorption and enhancement effects vary with the composition of every sample. The algorithm agrees with the Sherman equation and ignores completely all the approximations of Beattie and Brissey. Finally in 1985, Pella et al proposed an equation for calculating the intensity of the incident spectrum for every wavelength. It turned out to be the very last tool required allowing easy application of any FP approach. The author mentions at least two other FP methods that solved the Sherman equation correctly. They use the Sherman equation within standardless software packages, for example, the Spectra software from Bruker. Rousseau reports that these two methods are neither better not worse than the whole FA method but different and equivalent.

2.3.3 Inter-elemental effects and the Empirical influence coefficient

Empirical influence coefficients was reviewed by Rousseau (2006) and are based on the observation that the magnitude of matrix effects, both absorption and

enhancement, of any element *j* on *i* can be quantified by an overall factor noted as the empirical influence coefficient, e_{ij}.

Empirical influence coefficients are derived by calculating the best possible fit between the measured intensities and the concentrations of the reference material, with a multiple regression analysis technique that solves a series of simultaneous equations. The reference material must cover the concentration ranges of interest and must closely match the composition ranges of the unknowns. The effectiveness of the empirical influence coefficients are influenced by the latter. Furthermore, the preparation of the reference material must be identical to the preparation of the unknown samples. A minimum number of reference materials are required and expressed in the equation 2(N + 1) where N is the number of elements to be determined and therefore as the number of analytes increase so must the number of reference materials.

Some of the disadvantages of the empirical influence coefficients are summarised:

- This approach is very sensitive to any experimental error in data and can frequently and easily yield inaccurate empirical coefficients.
- The coefficient can only be applied to unknowns with similar compositions as the reference material
- The reference material and the sample preparation must be identical.
- Empirical influence coefficients are less accurate over extended composition ranges and this will depend on the compositional ranges of the reference materials therefore the application range is limited.

The only remaining advantage of the empirical influence coefficients is that they only have to be calculated once. However, it is a necessity that the sample preparation, concentration ranges of the analytes and the instrumental conditions never change.

Two algorithms can be used for the calculation of the concentration with empirical coefficients. The first equation, equation 2-3 (Rousseau, 2006) was proposed by Lucas-Tooth and Pyne in 1964.

$$C_i = C_{oi} + m_i I_i (1 + \Sigma g_{ij} I_j) \qquad \textbf{Equation 2-3}$$

Table 2-2: Summary of terms for equation 2-3

Term	Definition
C_i	Concentration of the analyte
C_{oi}	Background equivalent concentration
I_i	Net intensity of analyte i peak
I_j	Net intensity of matrix element j peak
m_i	Reciprocal of slope of the calibration line of analyte i
g_{ij}	Empirical coefficient correcting matrix effects of j on i in an intensity model

The algorithm is based on measured intensities and assumes that the matrix effect of an element j, on the analyte I, is proportional to its intensity. However, this assumption does not correspond to the reality since the measured intensities are modified by matrix effects and are not directly proportional to the concentrations. The coefficient, $g_{ij,}$ has no physical meaning.

The only advantage of this algorithm is that the concentrations can be calculated directly from the measured intensities without the iteration process.

The other algorithm, equation 2-4 (Rousseau, 2006), was proposed by Lachance - Trail in 1966 and assumes the matrix effect of element j on i is proportional to its concentration C_j.

$$C_i = C_{oi} + m_i I_i (1 + \Sigma e_{ij} C_j) \qquad \textbf{Equation 2-4}$$

Table 2-3: Summary of terms for equation 2-4

Term	Definition
C_i	Concentration of the analyte
C_{oi}	Background equivalent concentration
C_j	Concentration of matrix element j
I_i	Net intensity of analyte i peak
m_i	Reciprocal of slope of the calibration line of analyte i
e_{ij}	Empirical coefficient correcting matrix effects of j on i in a concentration model

This assumption is more in line with the reality; however, an iteration process is necessary to solve the equations.

Rousseau recommends the use of only the algorithm proposed by Lachance and Trail and not others as proposed by Rasberry and Heinrich or Lucas-Tooth and Pyne because of the extremely limited application range. He further recommends the mixing of theoretical coefficients with empirical coefficients and lists three important reasons in favour of the theoretical approach. Theoretical coefficients:

- Requires only a few reference materials for calibration
- Enable the analyst to determine wider concentration ranges
- Increase the accuracy of the results.

It is concluded by Rousseau (2004) that it is likely that fundamental parameter models based on calculated theoretical intensities will be replaced by algorithms using theoretical variable influence coefficients calculated for each sample composition. Fundamental parameters and influence coefficients are not two different solutions to the correction of matrix effects but are two parts of the same solution and the combinations of these two methods will bring the analyst an extremely effective mathematical method for matrix corrections.

Fusion is therefore the solution to mineralogical and particle size effects and mathematical models can be used to overcome the matrix effects not resolved by fusion.

2.4 X-ray theory and principles

X-rays are electromagnetic radiation with associated wavelengths and having photons with associated energies. The relationship between the energy and the wavelength is shown in equation 2-5 (Norrish and Hutton, 1967):

$$E = \frac{hc}{\lambda}$$ **Equation 2-5**

Where, E is the energy, λ is the wavelength in nm, c is the velocity of light in $m.s^{-1}$ and h is Planck's constant in $eV.s^{-1}$. The wavelengths of X-rays are in the range of 0.01 to 10 nm, which corresponds to the energy range of 0.125 to 125 keV.

The X-rays will interact with matter and can be absorbed or pass through. The interaction can be divided into:

- The X-rays can be absorbed by the sample, produce primary fluorescence radiation and characteristic lines can be measured, this is the photo electric effect or,
- Scattering: when the X-rays are scattered from the sample and not absorbed and are either Compton scattering or Rayleigh scattering. Compton scattering occurs with loss of energy and Rayleigh scattering occurs without loss of energy.

The fluorescence interaction and the scatter will depend on the thickness of the sample as well as the density of the sample. More focus will be given to the fluorescence interaction, which is the principle of X-ray fluorescence spectrometers.

To understand the origin of fluorescence the classic model of the atom must be considered. The atom has positively charged protons and non-charged neutrons in the nucleus, which is surrounded by electrons grouped in shells or orbitals. The innermost shell is the K-shell, followed by the L, M and N-shells. The energy of the electron will depend on the element to which it belongs as well as the shell it is in. When irradiating a sample, X-rays with sufficient energy can expel an electron from the atom. As soon as an electron has been removed a hole is left in the shell. This means that the atom will be unstable and at a higher energy. To restore the atom to a more stable state the hole must be filled with an electron from an outer shell. The L-shell electron has a higher energy than the K-shell electron and when the L-shell electron moves to the K-shell the surplus energy is emitted as X-rays.

Each atom has its own specific energy levels, which mean the emitted radiation is characteristic of that element. More than one hole can form at a time and therefore an atom can emit more than one energy or line. For the incoming X-rays to expel an electron, the X-rays must have a higher energy than the binding energy of the electron. If the energy is too high many X-rays will pass through the atom and few electrons will be removed. If the energy of the X-rays is just above the energy required to excite the K_{α} of a certain element, excitation will take place but not effectively. The highest yield is reached when the energy of the X-rays is three to four time that of the binding energy of the electron to be expelled. If the energy becomes lower then the binding energy, a jump or edge (absorption edge) is observed, where the energy is too low to expel electrons from that shell but too high to expel electrons effectively from the lower energy shells. When the energy is sufficient to expel an electron form the K-shell a K-line is produced and measured. Simultaneously the L-shell is expelled and the L-line is produced and measured.

Since not all the incoming photons or X-rays produce fluorescence the fluorescent yield can be calculated as the ratio of emitted fluorescent intensity and the incident intensity. The other interaction of the incoming X-rays with the sample is scatter as

mentioned before. Scatter is when some of the incoming X-rays are reflected or scattered by the sample instead of producing characteristic radiation. This will happen when the photon hits the electron but is bounced away. Compton or incoherent scatter is when the photons lose a fraction of its energy to the electron. Rayleigh scatter will take place when a photon collides with a strongly bound electron. The electron will not be expelled from the shell but will start oscillating at the frequency of the incoming photon. The electron will emit radiation at the same frequency as the oscillations and the incoming photon is reflected. Samples containing light elements will give rise to high Compton scatter and low Rayleigh scatter because they have many loosely bound electrons; therefore for the heavier elements less Compton scatter will be seen.

XRF spectrometers can be divided into two main groups: wavelength dispersive XRF spectrometer (WDXRF) and energy dispersive X-ray spectrometer (EDXRF). The elements that can be analysed as well as the detection levels of these analytes will depend on the type of spectrometer used. The WDXRF has an elemental range from beryllium to uranium while the EDXRF has a range from sodium to uranium. The basic concept of the spectrometer is a source, a sample and a detection system. The difference between the two types is found in the dispersion system. WDXRF utilises an analysing crystal to disperse the different energies form the sample. The crystal will then diffract that energy into different directions where they will be detected by detectors at certain angles. The EDXRF has a detector, which is able to differentiate the energies of the characteristic radiation directly from the sample.

The WDXRF consist of certain components, Figure 2-1

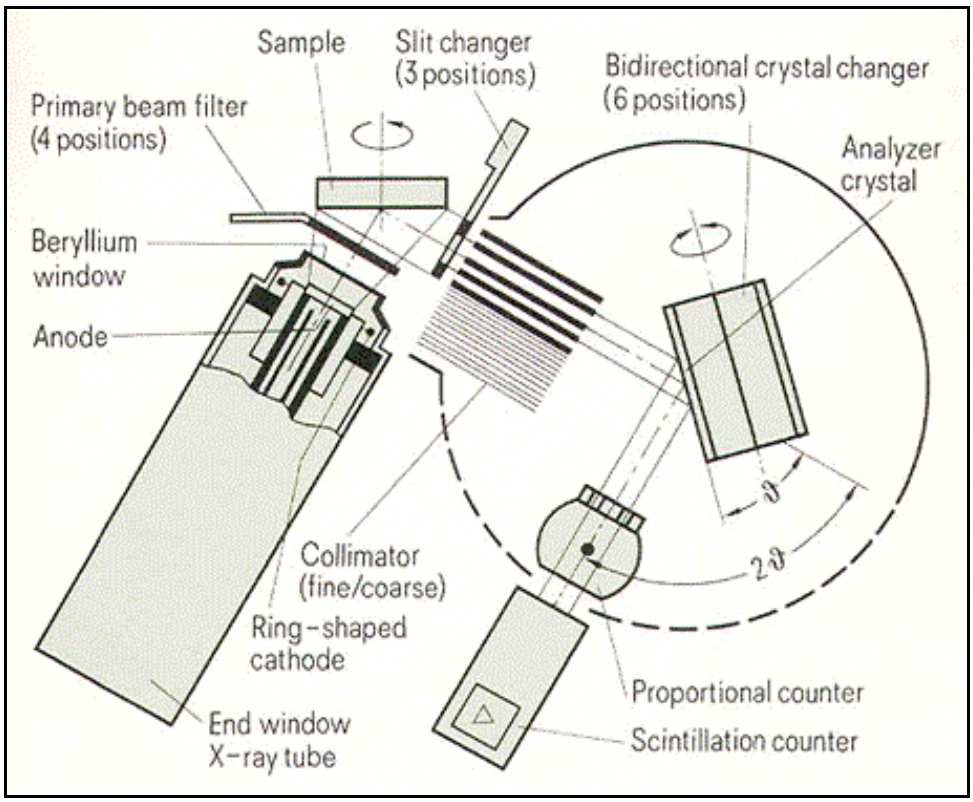


Figure 2-1: Schematic diagram of WDXRF[1]

- The X-ray source which is the tube,
- Filters between the sample and the tube,
- Collimators and analysing crystals,
- And one or more detectors

The detector is mounted on a goniometer and moves through an angular range to measure the intensities with different wavelengths. WDXRF spectrometers with moving detectors mounted on the goniometer are sequential spectrometers and they measure the intensities from the different wavelength one after the other. Simultaneous WDXRF spectrometers have fixed detection systems. In other words, each system has its own crystal and detector for a specific wavelength. The intensities at the different wavelengths are measured all at the same time.

[1] www.ksanalytical.com

One of the *source of the XRF spectrometer is* called the X-ray tube and consists of a filament or wire, made from tungsten, and an anode or target, made from copper, coated with any suitable target material, for example: chromium, molybdenum, rhodium, tungsten, scandium or gold, in a vacuum housing. An electrical current heats the filament, which produces electrons. A high voltage is applied across both the filament and the anode and the electrons will be accelerated towards the anode. When the electrons hit the anode they are decelerated and emission of X-rays occur, this is called Brems-strahlung. A spectrum of energies, each with its own intensity, is emitted and the spectrum produced is called the continuum. A fraction of the electrons accelerated towards the anode will expel electrons from the anode and cause the production of characteristic radiation dependent on the anode material. The X-rays emitted by the anode will leave the tube through a beryllium window. Not all the X-rays produced will leave the tube since X-rays with very low energies are not capable of passing through the beryllium window. The only parameters under the control of the analyst with regards to the tube are the kV and mA settings. The kV setting will influence the wavelength as well as the intensity of the continuum while the mA setting will influence the intensity only. The kV setting must be at least four times the keV of the element to be measured. A kV setting of 60 kV will be optimum for the elemental range of cesium to iron and a kV selection of 24-30 kV will be optimum for the elemental range of scandium to beryllium.

WDXRF spectrometers utilise two types of *detector*s, a gas filled detector and a scintillation detector. Two types of detector are essential to cover the full elemental range since the gas filled detector will efficiently measure the elements from beryllium to copper and the scintillation detector will efficiently measure the elements from copper to uranium. The detectors convert the X-ray photons from the sample into electrical pulses and the height of the pulse will be proportional to the energy of the incoming radiation. A multi channel analyser (MCA) will count the amplified pulses and the pulse height attenuator (PHA) will discriminate between different pulses.

There are two important properties of detectors:

- The resolution is defined as the ability of the detector to distinguish between different energy levels. A detector with high resolution can distinguish between many different energy levels.
- The sensitivity of the detector is defined as the efficiency of the detector when counting the incoming photons. The sensitivity is high when the ratio of the number of pulses against the number of incoming photons is high.

The *proportional (gas filled or gas flow) detector* consists of an aluminum cylinder at earth potential, filled with inert gas (Ar, Ne, Kr or Xe) and a tungsten wire running down the length of the detector. The anode wire is raised to a high voltage (1 300 – 2 000 V). A thin window consisting of beryllium, aluminium, mylar or polypropylene, allows the X-rays from the sample to enter the detector. The X-rays that enter the detector will ionise some of the argon in the detector making the argon conductive for a short period of time. This allows the electrons to flow through the gas to the anode wire, when it reaches the wire it creates an electric pulse. The magnitude of the pulse is proportional to the energy of the X-ray responsible for the ionisation. In some cases the detector has a flow of gas and this is to remove the ionised gas. However sealed proportional detectors are also available.

The *scintillation detector* consists of the beryllium window, a sodium iodide scintillator crystal and a photon multiplier tube with a photo cathode. When the X-rays or photons from the sample pass through the beryllium window they will hit the scintillator crystal and produce a flash of blue light. The light photons will travel into the photo multiplier tube and impact on the photo cathode from where electrons are produced. The electrons are accelerated through a series of dynodes to the anode. As soon as the electrons reach the anodes they will decrease the voltage and a negative voltage pulse is registered at the amplifier. The number of electrons is proportional to the energy of the incoming photons and the MCA counts the pulses produced. Detectors suffer from two problems namely dead time and the production of escape peaks. Dead time is the time when the detector is non-conducting and response to incoming X-rays is impossible. The conduction of the electricity through the detector

is not continuous and after a pulse is achieved the detector or tube does not conduct. Before the detector can conduct again the cations must flow back to the walls of the chamber. Dead time represents a lower limit in the response time of the detector. The dead time of a scintillation detector is significantly smaller than the dead time of a proportional detector.

Escape peaks are produced when the atoms from the gas present in the proportional detector or the phosphor in the scintillation detector are excited by the incoming X-rays and characteristic radiation is produced. A smaller peak at a lower energy than the peak of interest is observed. Escape peaks are only produced when the X-rays from the element can excite the gas or the phosphor of the detectors.

Filters are placed between the sample and the source. In EDXRF spectrometers the filter is used to modify the excitation conditions so that only the analytes of interest is excited, minimising the counting time. Filters can also be used to reduce the scatter and thereby improving the peak to background ratio as well as the limit of detection.

Diffraction crystals contain a stack of thin layers of atoms with the same spacing in a regular pattern. Diffraction crystals are used to reflect the X-rays from the sample to the detector. The condition for diffraction of X-rays is when Bragg's law is fulfilled, Figure 2-2.

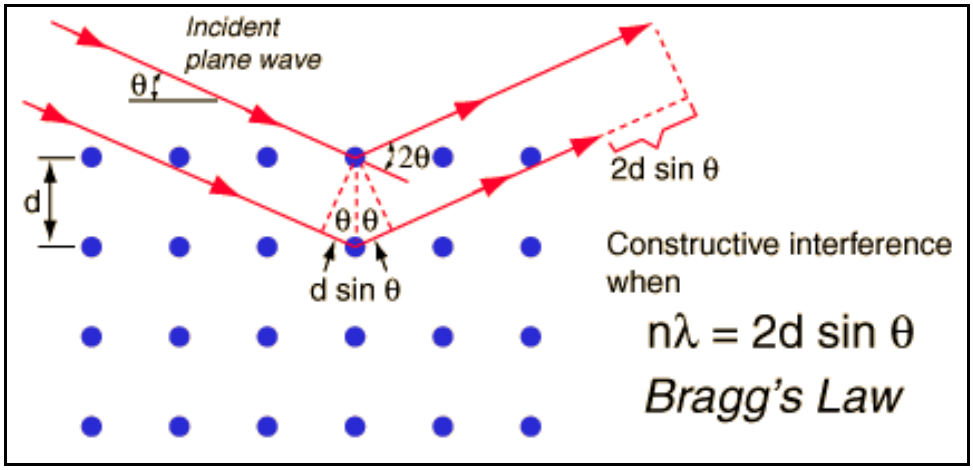


Figure 2-2: Demonstration of Bragg's law[2]

$$n\lambda = 2 d \sin\theta \qquad \textbf{Equation 2-6}$$

In equation 2-6 (Norrish and Champell, 1967), where λ is the wavelength of the incoming X-rays, n must equal an integer, d is the distance between the layers of the crystal and θ is the angle of incoming and out going X-rays. If a parallel beam of X-rays fall on the crystal, the first layer of the crystal will reflect a fraction of the X-rays, the remaining X-rays will penetrate the crystal and is reflected by subsequent layers. At a certain angle θ, all the reflected radiation with the wavelength λ and obeying Bragg's law are in phase (reinforced) and constructively interfere. All other wavelengths, at the same angle not obeying Bragg's law, will destructively interfere. Reflected wavelengths that obey Bragg's law for n = 1 are first order reflections and if n = 2 they are second order reflections. A detector placed at angle θ can measure the intensities of the corresponding wavelength.

A *collimator* is set of parallel plates used to obtain a parallel X-ray beam that falls exactly at the required angle of the crystal. The primary collimator is placed between the sample and the crystal to ensure parallel beams reach the crystal while the secondary collimators are placed between the crystal and the detector to ensure that only parallel beams from the crystal will reach the detector. The secondary collimator will increase the spectral resolution by reducing the peak width and spectral overlap.

A *mask* can be placed between the sample and the detection system to prevent characteristic X-rays from the sample cup and spectrometer reaching the detector and interfering with the radiation from the sample. A mask can be used in both the EDXRF and the WDXRF.

The *spinner* rotates the sample during analysis to even out the effects of in-homogeneity and imperfections of the samples. The spinner can be present in both XRF spectrometer types.

[2] www.xray.princeton.edu

The sample, detection systems and source of both the WDXRF and the EDXRF spectrometers are mounted in a *vacuum chamber*. Vacuum has to be reached before analysis can take place because air will absorb the X-rays between the samples and the detector. Air would have a major effect on the light elements with low energy radiation. However, for liquid and loose powder samples a vacuum system cannot be used since the liquids will evaporate and the loose powders will create an aerosol. The spectrometers can be filled with helium even though the helium will absorb the low energy radiation of all elements up to fluorine. All the other elements can be measured as liquids or loose powders.

The EDXRF spectrometers consist of the source, a multi channel analyser (MCA) and a solid state detector. EDXRF spectrometers can be divided into two groups the spectrometers with 2D optics and spectrometers with 3D optics. The difference lies in the optical path, for the 2D spectrometers the X-ray path is in one plane and for the 3D spectrometers the X-ray path is not limited to one plane only. With the EDXRF spectrometer with *2D optics,* the tube irradiates the sample directly and the fluorescence radiation from the sample is measured directly by the detector. However, scattered tube radiation will reach the detector as well and this will result in background noise. Due to the background it is difficult to detect low intensity peaks and therefore it is difficult to measure low concentration samples. In the case of the *3D optic* EDXRF spectrometer the X-ray path is not in one plane and the X-rays from the tube will irradiate a secondary target. The secondary target will emit characteristic X-rays as well as scatter some of the X-rays coming from the tube. The radiation coming from the secondary target will then excite the sample and the sample will emit characteristic radiation, which will be measured by the detector. In this case the advantage is that the scattered radiation from the tube does not reach the detector, resulting in lower background and improved the detection limits. Background will still be measured by the detector since the X-rays from the secondary target will be scattered by the samples but it will be significantly less when compared to the 2D optics, usually an order of magnitude.

The EDXRF *source* can be a tube (other sources available) with an anode made of copper and coated with a certain target material, for example, rhodium and it will function exactly the same as the WDXRF.

The *MCA* of the EDXRF spectrometer will count the pulses that enter the detector in each height interval and the number of pulses at a certain height gives the intensity of the corresponding energy. The resolution of the detector will depend on the ability of the detector and the MCA to distinguish between the different energies. The detector and the MCA are able to distinguish between 1 000 and 16 000 different energy levels.

The EDXRF spectrometer uses a *solid state detector* and not a gas filled detector or the scintillation detector. The solid state detector consists of a body of silicon, germanium or other semi-conducting material. On the front of the detector, there is a dead layer and on the back there is a collecting plate. A beryllium window will allow the X-ray photons from the sample to enter the detector and penetrate the body of the detector to produce electron-hole pairs. The number of electrons depends on the energy of the incoming photons and therefore the higher the energy the more electrons will be produced. A high voltage across the dead layer and the back means that the electrons will be attracted to the back of the detector. The potential drops as the electrons reach the back and gives a negative pulse. The depth of the pulse will be proportional to the number of electrons and proportional to the energy of the incoming radiation. The MCA will sort and count these pulses. The EDXRF spectrometer will also have a spinner, filter as well as the vacuum and helium systems.

Certain factors can be used to compare the EDXRF and the WDXRF spectrometers to show the differences. These factors are the elemental range, the detectors, the cost, the power consumption as well as moving parts.

- The elemental range for the EDXRF is from sodium to uranium while the WDXRF spectrometer can analyse from beryllium to uranium.
- The major difference between the EDXRF and the WDXRF spectrometers lies in the dispersion system and detectors. The sensitivity of the

spectrometer will depend on the type of detector as well as the energy of the incoming radiation. The WDXRF spectrometer will have good resolution for the lighter elements and less optimal resolution for the heavier elements while the opposite is true for EDXRF. The detection limits of the EDXRF spectrometers are less optimal for lighter elements and good for heavy elements while the WDXRF spectrometer has good detection limits for beryllium and all heavier elements.

- When comparing the cost of the EDXRF and the WDXRF spectrometers the EDXRF is inexpensive.

The *presentation of the sample* to the tube is of utmost important to any spectrometer whether a WDXRF or EDXRF spectrometer. For both types of spectrometers the sample in the sample container (cup) can be measured face-up or face-down. In other words, the analysing surface can face up and therefore the sample is underneath the tube or the analysing surface can be facing down and therefore the tube is underneath the sample. The advantage of the facedown option is that the positioning of the sample is by gravity important for powders and liquids, however if the sample is not prepared correctly, debris, dust or even liquid can fall on the tube and damage it.

Another important factor to consider for the presentation of the sample is the distance between the sample and the anode of the tube. The measured intensity is proportional to the inverse of the distance, between the sample and the anode, squared. Therefore, the measured intensity will change with a change in the distance and this means that the height of the sample with regards to the tube must be kept constant.

For X-ray measurements the *optimum conditions* must be chosen. Optimum measurement conditions will depend on what the analyst requires, for example the highest intensity, the lowest background or the minimum line overlap. The maximum intensity is achieved when the energy of the tube radiation is three to four times the absorption edge of the element. In terms of line overlaps the choice of crystals and collimators in a WDXRF spectrometer will have a large effect. For the EDXRF spectrometer, the setting of the MCA and the detector will determine the resolution of the peaks.

Two spectrometers were available for calibration and the measurement of unknowns. The Thermo Fisher Scientific Quant'X EDXRF spectrometer and the PANalytical PW 2400 (Axios) WDXRF spectrometer. In the case of the WDXRF spectrometer the different crystals and collimators available will be discussed while the different measurement conditions of the EDXRF spectrometer will be discussed. Both spectrometers were equipped with a rhodium tube. The WDXRF spectrometer has a 4 kW power tube. The maximum kV and mA setting for the WDXRF spectrometer tube is 60 kV and 66 mA, and it is recommended by the supplier to keep the power of the tube constant and therefore change the kV and mA so that the power setting remains is 4 kW.

The PW 2400 contains four filters and the choice of filter will depend on the elements required as well as if the analyst would want to reduce the signal to background ratio, Table 2-4. The crystals available in the PW 2400 are summarised in Table 2-4.

Table 2-4: Summary of crystals and filters in PW 2400

Crystals	Elemental range	Filters	Elemental range
LIF 200	K – U	Brass 0.3 mm	Rh – upwards
LIF 220	V – U	Brass 0.1 mm	Zr – Rh
PE 002	Al – Cl	Aluminum 0.75 mm	Br – Zr
GE 111	Al – Cl	Aluminum 0.2 mm	Ti - Se
PX 1	O - Mg		

The three collimators and two detectors available in the PW 2400 is summarised in Table 2-5.

Table 2-5: Summary of collimators and detectors in PW 2400

Collimators / µm	Advantage	Detectors	Elemental range
150	Improved resolution	Proportional	Lower energy
300		Scintillation	Higher energy
700	Improved sensitivity		

In the case of the Quant'X the EDXRF has a rhodium tube with 50 W power, but no crystals and only one detector, the SiLi detector, peltier cooled at 180 K. The

Quant'X has seven different filters that can be used together with optimum current and voltage settings to measure target elements. The Quant'X has eight different measuring conditions used for different elements from light to heavy elements, depending on the voltage setting of the tube as well as the filters used. (Table 2-6).

Table 2-6: Measuring conditions of Quant'X EDXRF spectrometer

Condition name	Filter	Voltage [kV]	Analytes
Low Za[3]	None	4	Na – S, Zn - Mo
Low Zb	Cellulose	8	Cl – Sc, Tc – Cs
Low Zc	Aluminum	12	Ti – Mn, Ba
Mid Za	Pd Thin	16	Cr – Ni
Mid Zb	Pd medium	20	Fe – Ge, Hf – Au
Mid Zc	Pd thick	28	As – Mo
High Za	Cu thin	40	Sr – Sn
High Zb	Cu thick	50	Tc - Ba

Parameters that can be changed in the condition are the voltage setting of the tube and the atmosphere (air, vacuum or helium). The voltage setting on the tube will determine which elements will be excited and which not. Care must be taken when concentrating on certain elements and their excitement of the K-shell electrons to produce the K-lines, that heavier element' L-shell electrons will be excited by the same condition and can possibly interfere if the heavier elements are present in the same sample, for example for condition Low Za. If the element of interest is between the elemental range of sodium and sulphur, the K-lines of sodium and sulphur will be produced by this condition, however, the elements zinc to molybdenum will also be excited and the L-line will be present if one of the elements are present in the sample. This overlap can be corrected for by doing a line overlap correction or measuring the K-line of the heavier element.

[3] Condition names as chosen by suppliers of XRF

2.5 Theoretical overview of problems associated with the fusion of concentrator samples containing sulphide, copper, iron, nickel and PGM's

The XRF technique is used for the analyses of base metals in various mining samples. The samples are prepared as pressed powders and analysed for ten elements of interest. Due to considerable mineralogical and particle size problems inaccurate and biased results are produced. To compensate for mineralogical effects it is the practice to match the calibration standards closely to the samples, however many challenges arose:

- Changes in the process caused a change in the matrix of the samples, which in turn made the samples significantly different from the standards which leads to inaccurate results. In this scenario, new calibration standards have to be collected and produced.
- The preparation of new calibration standards is a laborious and costly process including selecting and collecting suitable standards, with a wide concentration range, preparing the standards by mixing, splitting, analysing for the ten analytes by alternative techniques using numerous laboratories, assigning concentration values, preparing the pressed powders and calibrating the XRF spectrometer. This has to be done for all sample types and streams. The process of collecting and preparing new calibration standards can take between three and six months.
- The concentration range of these standards cannot be controlled and are usually not very wide due to the plants and processes being kept consistent.
- The in-house Quality Control samples (QC) are produced and used over several years and in most cases do not match the calibration standards prepared and fall outside the calibration concentration range, contributing to inaccurate results. Therefore the matching of the calibration standards and the samples is not successful.

The second factor contributing to inaccurate and biased results is the particle size effect. To compensate for this effect all the samples are ground with sodium stearate as a binding agent for three minutes and pressed into a briquette with an aluminium cup backing. In the automated preparation the samples are milled for 150 seconds with sucrose as the binding agent and pressed into steel rings. Factors to consider when grinding samples are:

- The efficiency of the mill and milling vessel. The pre-requisite in the group laboratories for the particle sizes are 90% less than 75 µm and this has to be tested on a regular basis to ensure the mill is consistently producing samples with this particle size.
- The milling curve and milling time has to be determined on a regular basis since it can change over time and with new milling vessels.
- Deterioration of the milling vessels causing the efficiency to decrease, the use of different vessels for different types of samples (for example high grade and low grade) to reduce possible contamination, as well as the use of the correct pairing of the puck and ring to produce the correct milling efficiency.
- The contamination of the samples from the milling vessel with for example cobalt, iron and chromium that are analytes of interest. The contamination will not always be consistent as the milling vessel will wear and deteriorate.
- The other challenge is to ensure that the standards and samples are prepared exactly the same, with the same vessels, mills, times, binding agents, press and pressure.
- The most important factor however is that not all the particles are reduced equally and therefore milling the samples to reduce the particle size proves to be problematic. Unless very stringent control measures are put in place and there is control of the particle size, reproducibility of sample preparation will become a problem.

Since the results received from the XRF spectrometer are used for metal accounting and must agree with other laboratories, the pressed powder preparation technique has

come under pressure and the progression to a more precise and accurate preparation technique has become important. This has led to the investigation of the fusion technique for mining samples. Concentrator samples are used in this study to determine whether the fusion technique will resolve these concerns and produce more accurate and unbiased results for metal accounting purposes. Only some elements and oxides are of interest and the average concentrations for these in concentrate samples are summarised in Table 2-7.

Table 2-7: Average Concentrations of base metals in concentrate type samples reported in percentage

	Lebowa (M) [4]	Lebowa (UG2)	Amandelbult (M)	Amandelbult (UG2)	Modikwa (UG2)	BRPM (M)	PPL (Platreef)
Cu	4	3	2	0.4	0.7	4	2
Ni	6	4	3	0.9	1.5	4	3
Fe	20	15	17	0.03	9.5	20	0.1
Co	0.2	0.1	0.1	8.	0.03	0.12	17
S	16	8	9	2	2.5	13	9
CaO	2	3.5	2	2	2.5	2	2
MgO	12	15.	17.8	24	23	15	15
Al_2O_3	2.5	5.5	2.7	3	3	2.5	3
Cr_2O_3	0.8	3.5	0.4	2	1.5	0.6	0.2
SiO_2	32	35	36	47	49	28	18
Total	95.5	92.6	90.0	89.3	93.2	89.2	69.3

The concentration of the elements and oxides as well as composition will differ between the concentrate samples due to the different mineralogy of the areas where these samples have been mined. The Bushveld Complex, Figure 2.4 (www.dme.gov.za), is mined for Platinum Group Metals (PGM) and base metals (BM).

[4] M for Merensky

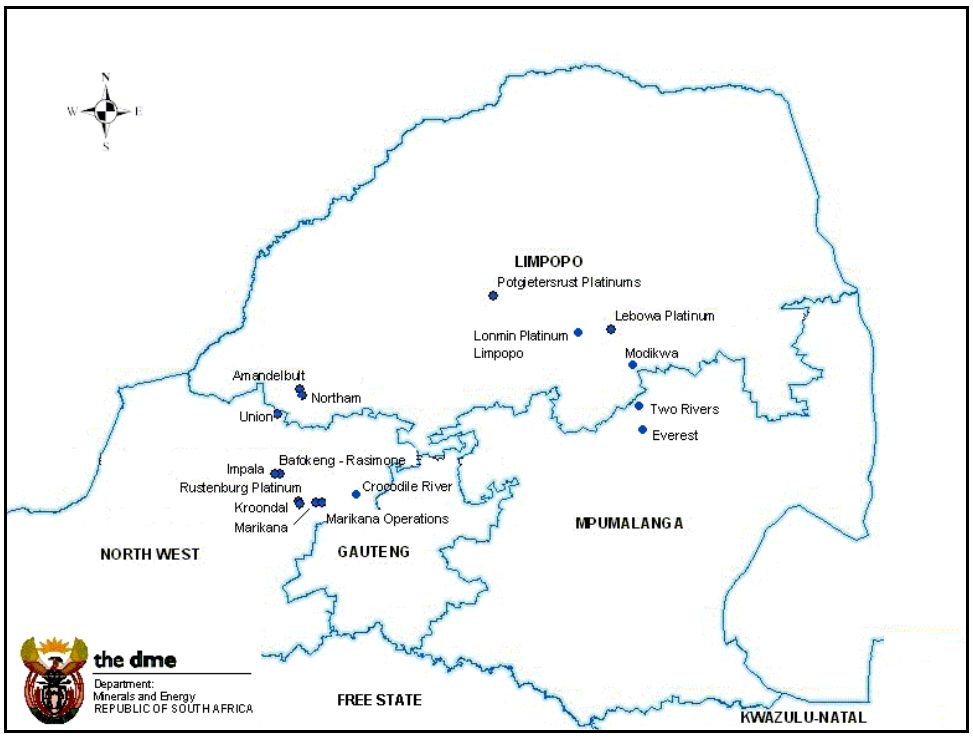


Figure 2-1: Bushveld Complex[5]

The Western limb of the bushveld complex consists of Amandelbult, Bafokeng Rasimone Paltinum Mine (BRPM), Rustenburg and Union sections. The Eastern limb of the complex consists of PPL concentrate that is Platreef and Lebowa. Both Merensky and Upper Group 2 (UG2) reef contains sulphide in the form of pentladite (Fe-Ni-S), pyrrhotite (Fe-S) and chalcopyrite (Cu-Fe-S). The UG2 reef will contain more chromitite and less sulphide than the Merensky reef. The reefs with the highest sulphur content are Lebowa Merensky and BRPM. It can be seen clearly that the Amandelbult UG2 samples have less of the base metals Cu, Ni etc and more of the oxides, especially silica, than any of the other samples.

The elements of interest for metal accounting are copper, nickel, iron, cobalt, sulphur and chromium. However, all the elements must be considered due to the effect that they will have on the choice of flux, oxidising agents, crucibles and fusion parameters. Therefore, the choice of flux and other agents must be considered

[5] www.dme.gov.za

carefully and tested vigorously. There is also inter-elemental effects that must be considered and all the elements will have an influence on one another. Matrix correction models, for example the fundamental parameters model, will correct for the inter-elemental effects but the pre-requisite is that 100% of the composition of the sample must be known.

It has been reported that samples containing sulphide and other analytes, for example copper, nickel and iron, are problematic and the fusion of these samples can cause damage to the crucibles (Baker, 1982). Sulphides such as Cu_2S and NiS will melt and the sulphide will react with Pt to produce PtS_2 causing damage to the crucible. This will happen at temperatures higher than 700ºC. The sulphide will form compounds with some of the other elements, for example copper, nickel, iron and platinum group metals and none of the analytes can be determined. However, if sulphides are oxidised to their highest oxidation state, sulphate, at a temperature lower than 700ºC, the sulphur will not react with the crucible.

S^{2-}	→	S^0	→	SO_2	→	SO_4^{2-}
Insoluble		Alloys Pt		Gas		Stable/ soluble

The chemical sequence above shows the forms that the sulphur can be present in the samples as well as the possibilities of the sulphur both being oxidised and removed from the sample or the possibility to be retained and completely oxidised. S^{2-} is reported to be insoluble in the borate fluxes and will therefore not dissolve during fusion and hence cannot be effectively determined (Claisse, 2000). When sulphide is oxidised it form S^0 when the sulphur will form compounds with the platinum of the crucible and cause damage, this stage must be avoided. Further oxidation will produce SO_2 (g), which is volatile and will be lost from the sample. If all the sulphur is converted to gas and removed from the samples the damage to the crucibles and the probability of the other metals reacting with the sulphur will be eliminated but then sulphur cannot be determined. The other concern is that not all the sulphur is converted to the gas and therefore the removal of the sulphur is not consistent. The matrices would differ and magnitude of matrix effects in each sample will also differ.

The full oxidation of the sulphur in the samples will produce SO_4^{2-} which is soluble in the flux, will not attack the crucibles or interact with other metals and can be determined by the fusion method.

The investigations proposed and executed in this study include various fluxes, oxidising agents, non wetting agents, temperature and time, heating sources, ratio of flux to sample as well as crucible and mould material taking the literature reviewed into account:

- The *fluxes* considered include sodium-hexa-metaphosphate ($(NaPO_3)_6$), pyrophosphates (Na or Li P_2O_7) and the borates. The sodium-hexa-metaphosphate was considered because of improved bead casting, without cracking. The pyrophosphates were investigated due to the reported higher reactivity of the phosphates with the samples when compared to the borates. The borates were investigated, taking into account that the concentrate samples contain silica which is an acidic oxide that will dissolve more easily in more alkaline flux, the meta-borate. The concentrate samples however also contain calcium and magnesium oxide which are alkaline oxides that will dissolve more easily in an acidic flux like tetra-borate.
- The fluxes considered for the fusion must also be able to retain the sulphur present in the samples. Sulphides can be dissolved in either a combination of acidic and basic flux or acidic flux with a basic additive.
- Baker (1982) conducted experiments to determine suitable fluxes and additives to retain sulphur. All the experiments were done under oxidising conditions using platinum ware. Baker investigated various fluxes and oxidising agents and reported combinations where the sulphur was completely oxidised. If the samples had very high sulphide concentrations, even if the conditions were oxidising some of the metal will still form compounds with the platinum in the crucibles. The sulphur results in the glass beads were compared to the gravimetric analyses of sulphur using a Leco instrument. Even though no results are published or compared and no accuracy or

precisions were discussed three combinations were reported successful in retaining sulphur. Sodium tetra-borate and sodium nitrate (80:20), lithium tetra-borate and lithium nitrate (80:20) and lithium tetra-borate and cesium nitrate (80:20). All fusions were done at 1000ºC with lithium bromide as the non wetting agent.

- In studies done by Claisse (2000) for zinc sulphide ore and concentrates he reports that factors that could lead to sulphur loss and inconsistent results are incomplete oxidation of the sulphide; the contact of the oxidising agent with the sample, whereby complete contact is necessary therefore agitation during the oxidation step and fusion is essential; the oxidation reaction is exothermic and violent and therefore matter can be ejected from the crucibles during the fusion and the loss of sulphur due to SO_3 and SO_2 gas production. This loss can be inconsistent and will cause reproducibility problems. These factors are dependent on the acidity of the flux and the temperature of the fusion. The factors can be eliminated with a 50:50 tetra-borate, meta-borate flux mixture as well as a fusion temperature of below 1050°C or the use of nitrate with tetra-borate. The method proposed by Claisse consists of both wet and dry oxidation steps followed by fusion. The sample together with the nitrate was weighed into the crucible and hydrogen peroxide solution added and left on the hotplate for five minutes so that the reaction could take place. The flux was weighed on top of the mixture in the crucible, creating a basic flux with a lower melting temperature. The results reported by Claisse for the sulphide in ZnS beads had a percentage relative standard deviation (% RSD) of 0.19% and concentration variations of ± 0.06%, for sulphur concentration of 32.78%.
- In another discussion by Claisse (1995), for a method for sulphide bearing material, the solution according to Claisse is the positioning of the samples and the flux in the crucible. The sample together with lithium nitrate and a small amount of the lithium tetra-borate flux was mixed and placed at the bottom of the crucible. The remaining flux is weighed on top with lithium bromide as the non-wetting agent added on top of the flux. The fusion then

consisted of various low temperature, slow agitation steps with a complete high temperature fusion at the end. The total fusion time was between 25 to 27 minutes. It was concluded that the method was more successful due to the full oxidation of sulphide to SO_4^{2-} before the fusion step was attempted and furthermore the sulphide was not touching the crucible material without the presence of the oxidising agent. The flux on top prevented the sulphide from making contact with the crucibles walls before complete oxidation.

- Another aspect studied was whether sodium or lithium flux must be used. The sodium borate fluxes are cheaper but hygroscopic while the lithium borates are more expensive but stable. Another important consideration is the melting point of the fluxes. Since the fusion temperature will contribute to the retention of volatiles such as sulphur, the temperature of the fusion must be as low as possible and therefore the flux with the lowest melting point will be of greater value. Table 2-8 shows the melting points of the different fluxes of interest (DR Lide, 1990).

Table 2-8: Melting temperatures of fluxes of interest (°C) (Lide, 1990)

	$(NaPO_3)_6$[6]	**$Na_2P_2O_7$[7]**	**$NaBO_2$[8]**	**$Na_2B_4O_7$[9]**	**$LiBO_2$[10]**	**$Li_2B_4O_7$[11]**
Melting point	ND*	880	966	741	845	930

- As seen, the melting temperatures for the sodium fluxes are low when compared to the same lithium flux. In the case of the sodium borates the tetra-borate has a lower melting point than the meta-borate, however the opposite is true for the lithium borates. The flux with the lowest melting temperature is sodium tetra-borate and will therefore be the flux to be tested.

[6] Sodium hexa-meta phosphate
[7] Sodium pyro-phosphate
[8] Sodium meta-borate
[9] Sodium tetra-borate
[10] Lithium meta-borate
[11] Lithium tetra-borate

It should be noted that the lithium in the lithium fluxes will absorb the X-rays from the XRF spectrometer less than the sodium salts.

- It is important to note that additives like nitrates and carbonates will lower the melting temperature of the glass beads and therefore the fusion temperature as well. Nitrates can also be used as oxidising agents to convert sulphur to its highest oxidation state. Norrish and Hutton (1968) used sodium nitrate to convert all the forms of sulphur present in the sample to sulphate. Ammonium nitrate was also used and has the advantage that it can be added in excess due to its volatility and because it decomposes and is removed. However, the authors found that sulphur was still lost and contributed this to the formation of volatile ammonium sulphate compound; furthermore, the authors reported that ores containing reducible metals like copper are problematic due to reaction with the crucible and are lost from the sample melt.
- The *dilution factor* of the sample and flux is an important consideration and is a compromise between sensitivity and dissolution. High dilutions can be made in the case where the analytes dissolves with difficulty, like chromium. However, concentrate samples contain 0.1% cobalt, that is 0.01% cobalt in a ten times diluted glass bead, already seriously compromising the sensitivity, precision and repeatability of the technique. A higher dilution factor will compromise this even more and therefore lower dilutions were given preference.
- Crucible and mould material: For the initial stages of testing the fluxes and other parameters, zirconium crucibles and fire assay pots were used. The final stages of the experiments were conducted in platinum-gold alloy crucibles and moulds. These crucibles are reported to have the best results in oxidising conditions for retaining sulphides together with other metals, for example copper, nickel and iron. The platinum-gold crucibles are however, expensive and can be damaged by the sulphides present in the samples. Graphite crucibles are considerably cheaper but are not suitable for oxidative fusions.

- *Heat sources* used are gas and electric furnaces. The electric furnace will produce higher temperatures more consistently and more conveniently. However, the important factor is the retention of sulphides and metals of interest. To retain the sulphur in the samples the conditions must be oxidising at a temperature lower than 700°C. The best retention of sulphur was reported with the use of an electric furnace. Therefore, all the test work was carried out in electric furnaces but various types are considered.
- Oxidation steps with the flux and oxidising agents before fusion, and lower temperatures are recommended and will be considered and tested. Norrish and Thompson (1990) established the importance of oxidising sulphur completely before any fusions. Various experiments were done in platinum-gold alloy (95%-5%) crucibles and moulds. The oxidation steps were carried out at different times in air, oxygen and with sodium nitrate. The oxidation of the sample was monitored in various ways. Samples tested and of importance to this study were copper concentrates ($CuFeS_2$), pyrite (FeS_2) slag and mattes. Thermal analysis indicated an immediate oxidation of pyrite after the sodium nitrate melted but the reaction takes longer for copper in converter matte. Fusion tests were performed to determine sulphur lost as well as crucible contamination with iron and copper. Different heat sources were investigated including the electric furnace and gas units. The results indicated that sulphur was lost at temperatures of 1150ºC and above. At lower temperatures the sulphur was retained the best using the furnace. Iron contamination of the crucibles was investigated and it was reported that the furnace caused no contamination. Samples containing 10% and more iron showed contamination irrespective of the heat source used. However, the addition of sodium nitrate and lithium nitrate prevented the contamination. The copper contamination was also investigated and the results indicated that all the methods of heating caused contamination. Also 0.5% was lost when using the furnace. The final fusion process, developed with these tests was, 6.8 g of 12-22 flux (12 lithium meta-borate and 22 $LiBO_2$), 1 g of sodium

nitrate and 0.66 g of sample. For oxidation everything was mixed in the crucible and heated in a furnace at 700ºC for 10 minutes. The fusion step was carried out at 1050ºC for six minutes using a gas unit. 10 mg of ammonium iodide was added after casting to the melt as releasing agent. The releasing agent is essential for samples with copper. The XRF was calibrated with pure oxide standards for each element of interest and matrix corrections applied. The final results indicated very good precision between duplicate results with a variation of less than 0.5%, and the authors felt that this was good evidence that no sulphur or metal was being lost.

- Claisse (1995) recommended mixing the samples with the oxidising agent as well as a small amount of the flux and placing this at the bottom of the crucible. This is then covered with the remaining amount of flux followed by several oxidation steps with agitation and the final fusion.
- If, however, the sulphur in the samples cannot be retained or fully oxidised, the samples will be pre-ignited to remove the sulphur before fusion. Care must be taken and loss of ignition calculations used to ensure all the sulphur is converted to SO3(g) / SO2(g) and removed. This was investigated by Spangenberg, Fontbote and Pernicka (1994) who analysed sulphide-containing sample by volatilising the sulphur before fusion. The sample was dried at 105ºC for one hour and then ignited overnight in an oxidising environment using an electric furnace at 800ºC. Samples tested in this study were pyrite (FeS_2), chalcopyrite ($CuFeS_2$) and chalcocite (Cu_2S). Loss on ignition calculations indicated 100% loss of sulphur for the pyrite and 81% for the chalcopyrite and chalcocite. Therefore, it can be concluded that the sulphur can be removed effectively where only iron is present but higher temperatures, longer time and a more oxidising environment would be necessary to remove the sulphur associated with copper. The final results with copper concentration of more than 1% indicated a standard deviation of less than 5%, representing precise and accurate copper analysis after sulphur was removed from the sample.

- Glass beads produced by fusion often tend to crack during cooling and stick to the crucibles and moulds. Compounds reported to assist in this regard are called non-wetting or releasing agents. These are mostly halides for example bromide, chloride and iodide. Non-wetting agents considered and tested are sodium and lithium halides.
- Two types of XRF fluorescence spectrometers were considered for the analyses of the samples, the WDXRF and the EDXRF spectrometers. These spectrometers and their differences are discussed in Section 2.4.

The initial experiments were carried out in zirconium crucibles and fire assay pots in hearth furnace to get familiar with the fusion technique and procedure. The final experiments were carried out in BIS Pt-Au (95%-5%) in the electrofluxer designed for single crucible fusion, automatic agitation and casting. Later fusions were carried out in the Katanax K2 furnace.

Two XRF fluorescence spectrometers were used in the investigations. Both were calibrated with glass beads produced from pure oxides to match the samples. The initial calibration work and test work was done on the Thermo Fischer Quant'X Energy-Dispersive spectrometer (EDXRF). The final calibration and test work was done on the PANalytical PW 2400 Wavelength-Dispersive spectrometer (WDXRF). The empirical and fundamental parameters of the mathematical models were used with both XRFs for the matrix effects corrections. In-house quality control samples (QC) with assigned values were used to validate the final calibration as well as the complete fusion process. The results were acquired using the software programs of the XRF spectrometers, WINTRACE for the EDXRF and SuperQ for the WDXRF. The data was evaluated statistically using Microsoft Excel.

The final fusion process is expected to produce glass beads retaining all the analytes of interest, a calibration with pure oxides and results that are unbiased and accurate thereby proving the elimination of the mineralogical and particle size effects.

3. PRELIMINARY EXPERIMENTS

3.1 Introduction

Fusion of a sample for X-ray fluorescence analysis can eliminate mineralogical and particle size effects and therefore it was decided to investigate the technique and determine a method that would prove successful for the process samples and analytes of interest. The process samples, used for the experiments, are concentrate samples as discussed in Section 2.5 Table 2-7. These samples contain many elements that are reported to be problematic, for example copper, nickel, iron, sulphur and chromic oxide. Preliminary fusion experiments were carried out testing; flux to be used, sample to flux ratio and heating sources.

The preliminary experiments were carried out testing different fluxes, ratios as well as heating sources, Section 3.2.
Secondary calibration standards were prepared to improve on the standardless analyses of elements present in the samples, Section 3.3.
The secondary standard preparation was changed by investigating the addition of an oxidising agent and roasting samples to be used for standard production, Section 3.4.
The WDXRF was calibrated using the secondary calibration standards, Section 3.5.

3.2 Preliminary experiments testing flux, flux to sample ratio and the heating source

The initial experiments were done with Lebowa concentrate samples. The Lebowa concentrate samples have the highest concentration of copper, nickel, iron and sulphur present when compared to other concentrate samples and are therefore ideal for test work.

Two fluxes were chosen to be tested, sodium hexa-meta-phosphate and sodium tetra-borate. Only sodium salts were chosen for the initial experiments due to the lower melting point and cost when compared to the lithium salts. The sodium tetra-borate was preferred to the sodium meta-borate due to the findings reported that supports the use of the tetra-borate flux for samples containing sulphur (Baker, 1982) as well as the fact that high purity sodium tetra-borate is more easily obtainable.

The phosphate was tested due to the reported improved solubility of samples when compared to borate fluxes as well as higher reactivity (Blank and Eksperiondova, 1998). Sodium carbonate was added to some of the samples to make the flux more basic in order to improve the dissolution of the acidic oxides present in the sample. It would also produce $CO_2(g)$ that will be released during the fusion and will assist in mixing the sample and the flux.

A higher sample to flux ratio was considered which would mean an easy dissolution of the sample due to the high amount of flux present however the sensitivity of the XRF when analysing low concentration elements will decrease, which in turn means a decreased repeatability due to decreased instrument precision.
The first ratio considered was 5:1, however the samples did not dissolve completely and the mould was not filled with glass during casting. It was therefore decided to rather consider a 10: 1 ratio.

Equipment and reagents used:

- Refer to Appendix A, Table A-1 for the summary of the reagents used.
- Zirconium crucibles
- Hearth furnace
- Bi-directional Sieb mill supplied by Dickie and Stockler with six ferro-chrome pots
- Press supplied by Dickie and Stockler: maximum power 40 kN.

- Aluminium cups: 40 mm diameter
- Panalytical WDXRF spectrometer PW 2400.
- Merck convection oven
- Furnace pots, size four
- Conical cast-iron moulds also used for furnace samples
- Hearth furnace supplied by Ultrafurn. E-con 14/16 model, front loading with spiral silicon carbide elements. Rated to 1400°C and 6.6 kW.

The samples were produced in duplicate: eighteen glass beads were produced in total with six blanks, Table 3-1. All the details are given in Table B-1 in Appendix B.

Table 3-1: Summary of flux and samples used to produce initial glass beads

Number of glass beads	Flux used	Sample Type
Two	Sodium hexa-meta-phosphate	Merensky
Two	Sodium hexa-meta-phosphate	UG2
Two	Sodium hexa-meta-phosphate	Blank
Two	Sodium tetra-borate	Merensky
Two	Sodium tetra-borate	UG2
Two	Sodium tetra-borate	Blank
Two	Sodium tetra-borate and sodium carbonate	Merensky
Two	Sodium tetra-borate and sodium carbonate	UG2
Two	Sodium tetra-borate and sodium carbonate	Blank

One sample with sodium hexa-meta-phosphate and one sample with sodium tetra-borate as the flux were fused using a Bunsen burner, however the flame did not reach a high enough temperature to dissolve the sample and flux, therefore it was decided to use the hearth furnace instead. The samples were fused at 1000°C for ten minutes in the hearth furnace. Zirconium crucibles, with a melting point of 1857°C (Greenwood and Earnshaw, 1997), were used for the initial experiments, and not platinum, to save

costs. After the fusions the molten glass was cast into graphite moulds left at room temperature.

Since all the glass beads cracked due to thermal shock, the samples could not be measured on the X-ray fluorescence spectrometer as glass beads. It was decided to produce briquettes and to investigate a solution for the cracking of the glass beads at a later stage.

The pressed briquettes were analysed using the standardless semi-quantitative program (IQ+) of the PANalytical WDXRF spectrometer. The IQ+ software works in various steps (PANalytical user guide). Firstly, an intensity measurement, was made for all elements present in the sample (in order to correct for matrix effects). An automatic qualitative analysis was done in order to find a suitable line for each element present. The net intensity of the line which was most sensitive with no line overlaps was used for the calculation of the concentration. The calculations were done using theoretical formulae and fundamental parameters. The calculation is "standardless" meaning no standards similar to the unknown samples are necessary. The 'intrinsic' spectrometer sensitivity has to be determined in order to scale the obtained theoretical intensity with the measured intensity. For unknown samples, the composition of the sample was varied in an iterative process until the measured intensity matches the calculated intensity. The measurement conditions used for the calibration of the WDXRF should be identical to the conditions used for the measurement of the unknown samples. For quantification to be accurate the sample preparation must be specified correctly. The elements or oxides that cannot be measured by an X-ray spectrometer must be calculated and specified. The Na_2O, B_2O_3 and P_2O_5 content was calculated for each glass bead and entered into the program. Since the Loss of ignition (LOI) was not determined experimentally it was assumed that only $CO_2(g)$ was lost during the fusion.

After analysing the glass beads, the concentrations of the elements of interest were quantified. The X-ray spectrometer did not indicate any cobalt present in the samples even though it is known that these samples contained cobalt. The results obtained from the X-ray spectrometer for the blanks were used for blank correction. The results obtained by X-ray spectrometer for each flux type for the elements of interest were compared to the assigned values for these samples. The assigned values were determined by sodium peroxide fusions and the analyses of the samples in solution with an ICP spectrometer. The samples were fused and analysed at least four times to obtain these values. Refer to Appendix B, Table B-2 and B-3 for the comparison of the results obtained by XRF and ICP for both the Merensky and UG2 type samples.

The results for the Merensky concentrate indicated poor comparisons for almost all the elements of interest between the different fluxes as well as the assigned values, especially for the sodium tetra-borate, sodium carbonate combination. In the case of the sodium hexa-meta phosphate and sodium tetra-borate fluxes the copper oxide, nickel oxide and iron oxide is the same magnitude as the assigned values, both these fluxes are acidic and could account for similar recoveries. The sulphur in the samples was not retained by any of the fluxes. The result of the duplicates indicated that the fusions were not reproducible.

The results of the UG2 sample type also indicate poor comparisons for almost all the elements of interest between the different fluxes as well as the assigned values. The sulphur was not retained by any of the fluxes of the UG2 sample; the fusions were also not reproducible.

The *conclusions* that can be made from the experiments, observations and results are discussed:

- The lower fusion temperature of the sodium salts should improve the retention of volatiles for example sulphur. However, the results for the Merensky as well as the UG2 sample types for all fluxes indicate a loss in sulphur. It is

reported that sulphur can only be retained with extra care and controlled oxidation, which was not investigated at this stage.

- It is reported that the phosphate flux is more reactive when compared to the borate fluxes and therefore the sample should dissolve easier. This was seen for both the Merensky and UG2 sample types, however it was seen that the sodium tetra-borate was effective for both sample types as well. The phosphate flux has a lower melting point when compared to the borate fluxes and therefore decreased viscosity and improved flow of the glass from the crucible to the mould.
- Both the sodium tetra-borate flux and the sodium hexa-meta-phosphate flux are acidic and showed improved results when compared to the more basic sodium meta-borate and the combination of sodium tetra-borate and sodium carbonate.
- The results of the UG2 samples also indicate that the more basic flux was not as effective as the acidic flux. UG2 samples contain more chromic oxide than the Merensky samples and would need a more acidic flux.
- It should be taken into account that the samples do not only contain basic oxides but also acidic oxides. For example, silicon dioxide in concentration ranges of 30 to 50% and therefore basic fluxes or basic additives must also be taken into consideration.
- The Bunsen burner could not be considered for fusion of the samples due to the temperature of the flame being insufficient without using enriched air.
- The hearth furnace can be operated at temperatures of 1400°C which are suitable for the fusions. The hearth furnace was considered for future experiments.
- The fusion temperature of 1000°C, and the fusion time of ten minutes were sufficient for fusion to take place and for the samples to dissolve.
- Due to the moulds being at room temperature and could not be placed into the hearth furnace or on the Bunsen flame, all the glass beads cracked during the

casting and cooling period due to thermal stress, this can be resolved by heating the moulds.

- High viscosity was observed for all the glass beads and the possibility of adding a non-wetting agent to resolve this would be investigated.
- The cobalt was not detected by the X-ray spectrometer indicating poor sensitivity. This could be improved by changing the ratio of sample to flux or optimising the X-ray spectrometer. The X-ray spectrometer parameters cannot be changed due to for the standardless software and for the use of the fundamental parameters to be effective the parameters for "calibration" must be identical to the parameters used to analyse the unknowns.

Since this was the initial experiments it was decided to rather prepare calibration standards specific to the sample types and to repeat the process.

3.3 Preparation of secondary calibration standards

The initial experimental results indicated the necessity of having a well-known calibration with parameters that could be changed to improve sensitivity for certain elements. To create a calibration, calibration standards have to be available and should be prepared in the same manner and with the same fusion parameters as the samples.

The two samples used in the initial experiments, Lebowa Merensky and UG2 concentrates were used to create secondary calibration standards. Preparing secondary standards for calibration has been the only method available to the Anglo Platinum laboratories. Not many samples with different concentrations are available and therefore it was decided to combine different masses of the two Lebowa concentrate samples to produce calibration standards with different concentrations for all the elements. The copper concentration of both samples was used to calculate

masses of the samples to be combined to obtain a range of copper from 0.05% to 0.6%. Summary of experiments are reported in Appendix B, Table B-4.

The flux of choice was sodium tetra-borate and in some cases sodium carbonate was added. One standard was prepared with phosphate together with sodium tetra-borate. The flux, as well as the additives, was dried for one hour in a convection oven at 105°C. Eight calibration standards were prepared in the hearth furnace at 1100°C for one hour in size four furnace pots; the standards were not agitated during this hour. These experiments were carried out in large scale since the furnace pots allowed large volumes. A total of 100 g of sample, flux and additives were weighed and glass beads of between 87 and 96 g were produced. This allowed for improved observation during the experiments. After the hour the pots were removed and the molten glass cast into the conical cast-iron moulds and left to cool to room temperature.

The pots were weighed before and after the fusion. It was observed that all the pots showed evidence of being corroded on the inside by the flux. The reaction of the flux on the pots means that the samples were contaminated with alumina and silica. The amount of contamination could not be quantified, since not all the pots reacted in the same manner, therefore the contamination cannot be corrected for. Both aluminium oxide and silicon oxide are of interest and contamination would mean increased concentration in the results. The pots used for the production of standards six and seven showed greater attack of the flux when compared to the other pots since it contained a combination of sodium carbonate and sodium tetra-borate. The more vigorous reaction of the flux with the pots was attributed to the higher sodium content. Glass was left behind in all the pots after casting.

As the glass was poured, from the pots into the moulds, a corrosive pattern in the bottom of all eight pots was evident, indicating the formation of a button. It was suspected that these buttons could contain sulphides as the reaction of sulphides with copper, nickel and iron has been observed (Claisse, 2000).

The glass beads shattered due to thermal stress and were removed from the moulds. This was not a concern since the glass beads were going to be crushed and pulverised to produce briquettes. The buttons were separated from the glass; however no button was found for standard seven, Figure 3-1.

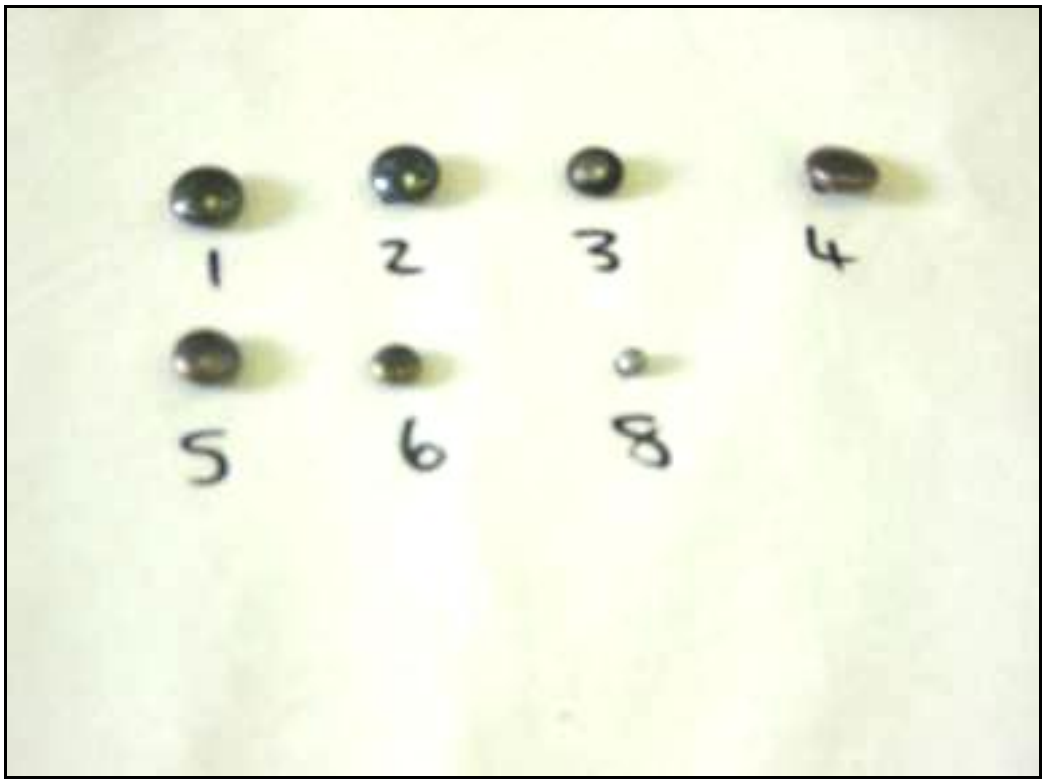


Figure 3-1: Formation of buttons during secondary calibration standards production

The sum of the glass bead and button were compared to the initial mass of sample and flux. There was a weight loss for all eight standards. The weight loss was contributed to the glass left behind in the pots as well as the loss of CO_2(g) from standards six and seven. The buttons that formed were submitted to the mineralogical department for investigation.

The glass beads were investigated and standards one to five and eight were homogeneous with no bubbles. Standards six and seven showed signs of crystallisation due to the presence of too much sodium oxide which resulted in a separation of phases. The glass beads were crushed in a pestle and mortar and pulverised in a bi-directional Sieb mill for one minute with no binding agent. The objective was to obtain the glass beads in a fine powdered form to improve dissolution for ICP analysis.

The mineralogical department reported the methodology and procedures followed as well as results obtained (Dinham, 2005). The buttons were smashed into smaller pieces since they were too small to be sectioned with a diamond saw. The fragments were mounted as polished sections and examined using reflected light optical microscopy and scanning electron microscope (SEM) techniques. The major component of the button was sulphide-bearing minerals and the different sulphides that developed were analysed using the Energy Dispersive Spectrometer (EDS) option of the SEM. All seven buttons contained nickel-rich sulphides with smaller amounts of copper-rich sulphides and traces of Platinum Group Element (PGE) alloys. The nickel-rich sulphides form the matrix of the buttons with the copper-rich sulphides forming along specific crystallographic directions. Fine-grained PGE bearing alloy particles were present in the nickel-rich sulphide matrix.

Three distinct nickel-rich sulphides were identified in the buttons and closely resemble three types of minerals: pentladite, heazlewoodite and millerite. All buttons contained copper-rich sulphides with either iron-enriched or iron-depleted varieties.
The conclusion was made that there does not appear to be any correlation between the microstructure developed in the buttons and the amount of concentrate or flux added.

Certain conclusions that can be made from these experiments:

- The major contribution of these experiments was not the secondary calibration standards but the formation of the sulphide buttons.
- The experiment was conducted in large scale and proved to be insightful since the formation of the buttons could be observed.
- The sulphide buttons formed due to the sulphides being melted during fusion and settled at the bottom of the pots due to their higher density. The sulphides did amalgamate to form mixed masses. The sulphides were separated from the flux and not part of the dissolution of the rest of the sample and therefore did not react with the flux and additives. The flux and additives did not effectively react, oxidise or dissolve the sulphide button.
- The potassium nitrate was also consumed in a side reaction with the sodium tetra-borate and therefore did not oxidise the sulphur.
- The mineralogical results indicated buttons with copper- and nickel- rich sulphides. The presence of the PGE (Platinum Group Elements) bearing alloys in the sulphide buttons indicated that the sulphide will alloy with the platinum and accounts for the samples containing sulphur attacking the platinum crucibles.
- Due to the fact that the buttons contained copper, nickel, iron and sulphide, the elements were removed from the calibration standards and therefore the calibration standards would not be useful as the concentration of these elements present in the standards would not cover the analytical range.

Since the X-ray spectrometer could not be calibrated it was decided to repeat the preparation of secondary standards using oxidising agents to oxidise the sulphide to prevent the formation of buttons.

3.4 Preparation of secondary calibration standards with the addition of an oxidising agent and roasting the samples

In the process of producing secondary calibration standards, using Merensky and UG2 samples with sodium tetra-borate flux, glass beads were produced. However, for each glass bead produced a sulphide button formed. The formation of the button removed the copper, nickel, iron and sulphur from the glass bead calibration standards. These glass bead standards were not used for the calibration of the X-ray spectrometer.

3.4.1 Oxidising sulphur with potassium nitrate

The objective for this section was to oxidise the sulphur completely to its highest oxidation state and therefore prevent the formation of the buttons. The first step was to oxidise the sulphur by adding an oxidising agent, namely potassium nitrate. Potassium nitrate was selected instead of sodium nitrate since potassium nitrate was available at higher purity and lower cost. Nitrate was used due to it being the most commonly used oxidant, as reported in the literature (Baker, 1982; Claisse, 1995). The nitrate was added to the flux in different masses, and the highest being 50.5 g. However, even the glass bead produced with the 50.5 g of potassium nitrate produced a sulphide button.

As in the case of section 3.3, eight calibration standards were prepared with the Lebowa Merensky and UG 2 sample types. The sodium tetra-borate mass was kept constant and the sodium carbonate and potassium nitrate masses were increased for standards one to five. From standard six the potassium nitrate mass was increased significantly, the sodium tetra-borate mass was increased slightly and the sodium carbonate was kept constant. The increase in oxidising agent mass was to ensure that

the sulphide buttons which was observed during the casting of standards one to five would not form for standards six to eight. Details of the experiments are summarised in Appendix B, Table B-5.

All eight pots were fused in the hearth furnace at 1100°C for one hour; the samples were not agitated manually during this hour but some agitation took place due to the production of CO_2(g). After the hour, the pots were removed and the molten glass cast into cast-iron moulds and left to cool to room temperature. The pots were weighed before and after fusion to determine the difference in mass.

Observations made during casting showed that all the pots had signs of corrosion due to the flux reacting with the pots. Glass was left behind in all the pots and all the pots had corrosion patterns at the bottom indicating the formation of buttons, even for standards six to eight for which the nitrate added was increased significantly. All the glass beads cracked upon cooling and the buttons and the glass beads were separated.

It was concluded that:

- The buttons were still being produced even when more than enough potassium nitrate was added to the mixture to completely oxidise the sulphides. This was attributed to the sulphides still melting, settling at the bottom of the crucibles and amalgamating. Therefore, it was not in the sample, flux, oxidising agent mixture and only the top of the button was in contact with the oxidising agent. The sulphides were not oxidised effectively due to separation.
- At the higher temperature, the potassium nitrate was consumed in a side reaction with sodium tetra-borate.
- Introducing an oxidising step at a lower temperature some time before commencing with the full fusion process could ensure the reaction of the sulphide with the oxidising agent before it melts. If the sulphide is oxidised first, separation will not take place.

3.4.2 The production of calibration standards with roasted samples

The objective was reviewed and it was decided to produce calibration standards from roasted samples. Therefore, the sulphur would be removed from the samples during roasting to prevent sulphide button formation. Both the Merensky and UG2 samples types were roasted overnight in an oven at 800°C.

The only analyte for which the X-ray spectrometer would not be calibrated for would be sulphur. This was not a great concern, since sulphur could be determined by alternative techniques and methods. Details of the experiments are summarised in Appendix B, Table B-6.

Observations made of the pots during casting showed no signs of button formation. The pots were corroded by the flux and glass was left behind after casting. Pots used to produce standards nine and ten were damaged during the fusion and showed signs of sample loss. Since no sulphide buttons formed during the fusion it showed that the roasting of the sample to remove the sulphur was successful. The glass bead standards produced with the potassium nitrate, as well as the roasted samples, were evaluated for calibration of the WDXRF.

The conclusion that could be made from these experiments:

- Roasting the samples to remove the sulphide proved successful since no sulphide buttons formed during fusion.

3.5 Calibration of the WDXRF with secondary glass bead calibration standards

It was decided to calibrate the WDXRF using the glass bead calibration standards produced. The objective of the calibration was to obtain as wide a concentration range as possible for all elements present in the samples. To calibrate the X-ray spectrometer the true concentration of the elements present in the glass bead standards had to be determined. The glass beads were analysed using ICP-OES.

The glass bead standards were prepared for ICP by crushing and pulverising them to produce a fine powder. A small portion of the fine powder was fused with sodium peroxide in zirconium crucibles in a muffle furnace at 800°C for three minutes. Once the crucibles were removed and cooled, hydrochloric acid was used to leach the sample and a solution with a final matrix of 20% HCl and 50 $mg.L^{-1}$ yttrium, as the internal standard, was produced. The solutions were analysed with the ICP spectrometer using a standard set of calibration standards.

The results obtained from the ICP spectrometer (Appendix B, Table B-7 and Table B-8) showed poor precision between replicates. The chrome in the sample was below the detection limit of the ICP and therefore could not be determined for any of the glass bead standards. It was decided to use these results to select glass bead standards with good replicate agreement.

The glass bead standards chosen as calibration standards were dissolved in duplicate and analysed by ICP again, matching the sodium content of the ICP calibration standards to that of the glass beads. The results obtained were more precise due to improved agreement between the replicates. It was decided that the average of the two replicates could be used to calibrate the WDXRF.

Since the glass bead standards cracked during cooling they were pulverised and pressed powder briquettes were prepared for the calibration of the WDXRF. The glass bead standards were weighed together with sodium stearate as binding agent. The glass bead and binding agent were pulverised for three minutes in a bi-directional mill and pressed into 40 mm diameter aluminium cups.

The X-ray spectrometer calibration program was created to calibrate and analyse for copper, nickel, iron, cobalt, magnesium oxide (MgO), aluminum oxide (Al_2O_3), calcium oxide (CaO), chromic oxide (Cr_2O_3) and silicon dioxide (SiO_2). The WDXRF was not calibrated for sulphur since it was assumed that the sulphur had been removed.

The spectrometer parameters available and selected to be used for calibration were discussed in full detail in Chapter two, section 2.4 and will be referred to regularly in this section to justify the use of certain parameters. The parameters were chosen for the calibration, as well as the subsequent analyses of samples, for optimum intensity, sensitivity and resolution, depending on the analyte. The choice of parameters that were used to optimise the WDXRF was the crystals, collimators and detectors. Refer to Table 3-2 for the parameters chosen.

Table 3-2: Calibration parameters chosen for the analytes of interest

Channel	Crystal	Collimator [µm]	Detector
Mg	PX 1	300	Flow
Al	PE 002	700	Flow
Si	PE 002	300	Flow
Ca	LiF 200	700	Flow
Cr	LiF 200	700	Scintillation
Fe	LiF 220	300	Scintillation
Co	LiF 220	300	Scintillation
Ni	LiF 220	300	Scintillation
Cu	LiF 220	300	Scintillation

The kV and mA were kept at 60 kV and 50 mA to keep the power of the tube constant at 3 kW as recommended by the supplier. The LiF 200 crystal was used for calcium and chromic oxide and the LiF 220 crystal for iron, cobalt, nickel and copper. The PE 002 crystal can be utilised for the elemental range of aluminum to chloride and in this calibration it was used for aluminum and silica. The PX 1 crystal is a synthetic crystal and was used for magnesium.

Resolution is more important for elements where the peaks are closer to one another, for example iron Kβ and the cobalt Kα. In the case of elements with high concentrations, the intensities were high and were reduced by using the 300 µm collimator. The scintillation detector is more sensitive for nickel, copper, cobalt, chromium and iron, while the flow detector is more sensitive for calcium, magnesium, aluminum and silica.

The standards were measured for three minutes using these conditions. After measurement, the calibration unknowns were calculated. This included the intercept, slope as well as the inter-elemental corrections. The fundamental parameters model was used to correct for inter-element effects. The calibration graphs were evaluated and showed that the calibration was unsuccessful. The calibration lines were non-linear with only some of the calibration standards on the calibration line even with inter-element corrections. For some analytes, for example, aluminum, iron and cobalt the intercept was negative and had to be forced through zero.

The following conclusions were made:

- The results obtained from the ICP indicated poor replicate results for the samples. This was attributed to the samples and the ICP standards not being matrix matched with regards to the sodium content and some of the samples had a silica precipitate.
- The reason for the non-linear calibration lines on the XRF was attributed to certain factors:

    - The calibration range was not wide enough
    - The calibrations standards were very dilute due to the high dilution when preparing glass beads and then preparing powdered briquettes from the glass beads.
    - The possibility that not all the sulphur was removed and had enhancing and absorbing effects on some of the elements that were measured.
- The XRF could not be calibrated for chrome since the concentration of the chromium could not be determined by the ICP.
- Since a secondary calibration is dependant on the results obtained by ICP the uncertainty in the XRF calibration is increased. Due to the many factors that could have attributed to poor ICP replicate results, the XRF calibration could not be considered to be accurate, or precise, and therefore it was concluded that the secondary calibration of the XRF and the secondary standards produced were unsuccessful.

3.6 Conclusions

- The initial experiment indicated that acidic flux should be considered. More resistant crucibles, other than zirconium, should be considered. The hearth furnace could be used for future fusions, the time and temperature used for the experiments were sufficient. The moulds must be heated to prevent thermal stress.
- The production of secondary calibration standards contributed to the investigation due to the formation of sulphide buttons. The sulphides melted at a lower temperature than the fusion temperature and settled at the bottom of the crucibles. The sulphide in the samples had to be oxidised before continuing with the fusions.

- The next set of secondary calibration standards was prepared by adding potassium nitrate to oxidise the sulphur present in the sample. The buttons formed again indicating that even though more than enough potassium nitrate was added to oxidise the sulphur this was insufficient. The sulphides were still melting and settling at the bottom of the crucible where the flux and oxidising agents only reacted with the top of the buttons. A possible solution would be the oxidation of the sulphur with an oxidising agent at a lower temperature for a preset time.
- For now, the samples were roasted to remove the sulphides and the secondary standards prepared with the roasted samples. No buttons formed, indicating that the sulphur was removed from the samples. These secondary standards were used to calibrate the WDXRF.
- The concentration of the elements present in the glass beads were determined by ICP. ICP results were not accurate or precise and the replicates were poor. This was attributed to the samples and the ICP calibration standards not being matched, the samples had silica precipitate and most probably the secondary XRF calibration standards were analysed at the lower end of the ICP calibration range.
- The WDXRF calibration was not successful. This was attributed mostly to the secondary calibrations only being as good as the analyses of the concentration of the elements present in these standards.

Since the secondary calibration standards were not successful, primary calibration standards would be considered for future work.

The next investigation was into the use of non-wetting agents which prevents the cracking of the glass bead during cooling and casting. If non-wetting agents are used, the glass beads can be analysed on the XRF without further preparation and without pulverising and preparing briquettes. This will also allow for the preparation of primary calibration standards.

4. NON-WETTING AGENTS

4.1 Introduction

The objective of the fusion technique is to produce homogenous samples to eliminate the particle size and mineralogical effects. In many of the early experiments the glass beads cracked or shattered. Non-wetting agents were investigated to prevent the cracking and shattering of samples.

Non-wetting agents are reported to reduce the cracking of the glass beads during cooling as well as reduce the molten glass viscosity so that more glass can be removed from the crucible during pouring. The borates from the flux will produce long chain structures during the formation of the glass bead. During the cooling of the glass bead the chains will contract putting the glass bead under stress and causing it to crack. Non-wetting agents introduce counter ions that produce shorter chains and therefore reduce the stress in the glass bead, preventing it from cracking.

The most commonly used non-wetting agents reported in the literature are the ionic halides and they are used as salts or solutions, and can be introduced during the casting step or from the beginning of the fusion procedure. Different salts of halides are used, including potassium-, sodium- and lithium-, of fluorides, bromides, chlorides and iodides. Examples are:

- Potassium bromide as a salt, added together with the sample and the flux, for the complete fusion process (LeHouillier, Turmel and Claisse, 1977),
- Lithium fluoride and lithium iodide salts added together with the flux and sample from the beginning of the fusion procedure (Turmel and Samson, 1984),

- Ammonium iodide salt (Norrish and Thompson, 1990); (Spangenberg, Fontbote and Pernicka, 1994),
- An aqueous solution of lithium bromide added on top of the sample and flux mixture for the complete fusion procedure (Claisse, 1990),
- Potassium iodide tablets introduced to the melt after the fusion steps and just before the casting step (Claisse, 1990).
- Sodium iodide and potassium iodide as mentioned in the review by Blank and Eksperiandova in 1998.

Counter ions will reduce the formation of long chains, by associating with the sodium and the borate. These counter ions include the halides (X^-) as well as the sodium (Na^+), potassium (K^+) and lithium (Li^+) ions. The sizes of the halides can be expressed as F < Cl < Br < I so that the smallest halide is fluoride and the largest is iodide (Lee, 1996). The largest halide would be expected to have the best non-wetting agent capabilities, the larger the counter ion the better the dissociation of the long chains of the flux. Hence, the most used salt is iodide. Even though the non-wetting agents and the halides offer a solution to the cracking of the glass bead in the moulds and the reduction of the melt viscosity there are limitations and disadvantages to using halides as non-wetting agents:

- When selecting the halide the possibility of line overlaps with the elements of interest must be considered. For example, the overlap of the L-lines of bromine with the K-lines of aluminum, the possible overlap of the L-lines of iodide with the K-lines of potassium and calcium.
- It is reported by manufacturers of WDXRF spectrometers that fluoride can be analysed. However, the fluorescence yield is low due to the electrons being bound so strongly that fluorescence is less likely to occur. The assumption is made that fluoride cannot be measured accurately by XRF and can therefore not be corrected for.

Even though disadvantages have been reported, halide can be chosen that will not interfere with elements of interest. The possibility of copper being lost in association with the halide can be investigated with all the available halides. The advantage of not having to pulverise the glass bead and producing a perfect bead directly after casting is worth investigating.

The objective of the experiments done and discussed in this chapter was to test the non-wetting agents with regard to the possibility of the glass beads not cracking as well as the retention of copper. Since copper is a very important element in the mining industry it has to be retained during the fusion process. Chlorides, bromides as well as iodides were tested in different experiments and primary oxide calibration standards prepared with the non-wetting agents.

The non-wetting agent properties of the halides were tested in Section 4.2. The halides tested were sodium – chloride, chlorate, bromide, iodide and iodate. Primary oxide calibration standards were prepared with sodium iodide as the non-wetting agent, Section 4.3.1. Samples were used for the validation of the calibration as well as to determine whether the copper was retained or lost, Section 4.3.2. The theory of integrating the non-wetting agent and the flux was investigated in Section 4.4. Alternative non-wetting agents were tested, focussing on alternative small counter ions to react with the flux, for example, SO_4^{2-}, Na+ and K^+, Section 4.4. The next set of experiments was carried out by adding the non-wetting agent only during casting and not for the complete fusion process. Bromine gas was tested and another set of calibration standards were prepared with bromine as the non-wetting agent, Section 4.5.

Equipment and reagents used:

- All the experiments were carried out with platinum-gold (95% - 5%) alloy crucibles and moulds. Specific BIS crucibles were used with a lip that could fit the clip of the Electrofluxer for automatic loading and unloading. 40 mm

diameter glass beads were produced and the final mass of the glass bead was 10 g.

- The crucibles were cleaned in 20% hydrochloric acid solution on a hotplate in between all the samples.
- Refer to Appendix A, Table A-1 for the list of reagents used.
- A 7170 Electrofluxer, Figure 4-1, supplied by Spex SamplePrep, was used for the production of the glass beads. It can produce one sample at a time and consists of a controller unit and a heater module. The Electrofluxer has a small furnace that uses a spiral Superthal™ molybdenum di-silicide heating element. This type of furnace can produce exceptionally fast heating rates compared to other resistively heated furnaces. The Electrofluxer has a clip arm assembly for loading and unloading the crucible into the furnace as well as automatically casting the melt. The clip also holds the mould directly above the crucible where it is preheated during the fusion process. The Electrofluxer is equipped with a fan underneath the mould in the casting position for efficient cooling of the glass bead after casting. It also has a motor that moves the furnace unit in a circular fashion for agitation of the sample. It can be programmed to run through a fusion process with controlled parameters. The parameters that can be changed are the temperature, time, agitation and fan cooling. The temperature of fusion can be set together with the time that the specified temperature must be held. The agitation rate and delay time can be chosen as well as the fan delay time.

4.2 Testing of halide salts as non-wetting agents

The objective was to test the different halides and determine the most suitable halide to be used as non-wetting agent.

The halides that were tested were 0.5 to 4% sodium iodide salt, 1% sodium chloride, 1% sodium bromide and 1 to 4% potassium iodate. The potassium salt was used to

determine whether the potassium ion could act as a counter ion for the long chains of the flux.

Four glass beads were produced with sodium iodide as the non-wetting agent, one glass bead with no non-wetting agent, one glass bead with sodium chloride, one glass bead with sodium bromide and three glass beads with potassium iodate. Sodium tetra-borate was used as the flux and all the glass beads were produced at 1100°C with a fusion time of twelve minutes in the Electrofluxer with the platinum-gold alloy crucibles. The copper oxide mass was kept constant at 0.1 g. The crucibles and moulds were weighed before and after fusion. See Appendix C, Table C-1 for the details of the experiments.

To determine the best halide to act as the non-wetting agent, the glass bead appearance, the glass lost to the crucible, loss on ignition (LOI), halide recovery and copper recovery was all taken into consideration.

During cooling the following glass beads cracked: the glass bead with no non-wetting agent, 0.5% NaI, 1% NaCl, 1% NaBr, 1% $NaIO_3$ and 2% $NaIO_3$. Since the glass bead produced with 0.5% of NaI cracked, it can be concluded 0.5% of sodium iodide was insufficient. The same can be concluded for the glass beads which contained 1% sodium chloride and sodium bromide. The glass bead with no non-wetting agent cracked as expected. The glass beads with 1% and 2% of potassium iodate cracked however, the glass bead with 4% potassium iodate did not crack. Indicating that the iodate can be considered, but a high amount would be required. The glass bead appearances, therefore indicate the best non-wetting agent was 2, 3, 4% sodium iodide and 4% potassium iodate.

The loss of glass in a crucible will indicate the efficiency of the non-wetting agent to release the glass from the crucible during the casting stage, Table 4-1.

Table 4-1: Crucible differences before and after fusion with halides as non-wetting agents

Non-wetting agent	Loss of glass in crucible [g]	Glass bead mass [g]	LOI [%]
0.5% NaI	0.9	9.7	2.6
1% NaI	0.4	9.7	2.4
2% NaI	0.3	9.6	2.5
4% NaI	0.1	9.5	4.6
None	1.2	9.8	2.1
1% NaCl	1.2	9.8	1.9
1% NaBr	0.2	9.8	1.6
1% $NaIO_3$	1.2	9.7	2.4
2% $NaIO_3$	0.5	9.7	3.2
4% $NaIO_3$	0.3	9.5	4.1

The highest mass was for the glass bead that contained 1% of sodium chloride and cracked. This indicated the worst releasing properties even when compared to the glass bead with no non-wetting agent. It was attributed to only 1% of sodium chloride being used and the greater loss of glass indicated that if sodium chloride is to be used it must be more than 1% of the total glass bead mass. In the factorial design, the amount of sodium chloride added was never less than 0.2 g, which is 2%, and in the factorial design results, Section 4.2, the loss of glass was not as great. The smallest loss of glass, indicating the best releasing property, was for the glass bead that contained 4% of sodium iodide and did not crack. This would indicate the best releasing agent. When comparing the crucible differences for all the 1% added of the halides it can be seen that the loss for 1% sodium chloride 1.2 g, for 1% sodium bromide 0.2 g, for 1% sodium iodide 0.4 g and for 1% potassium iodate 1.2 g. It can be concluded that the best releasing properties for the same amount of halide would be for the 1% of sodium iodide.

The loss of ignition will indicate the volatile portion of the flux, as well as the possible loss of halides recurred during fusion. The loss of oxygen from the iodates was taken into account. The greatest loss on ignition was for the glass beads produced with 4% sodium iodide and 4% sodium iodate, indicating a loss of iodide. The lowest loss on ignition for these glass beads was the sodium bromide, indicating the lowest possibility of halide loss, as well as copper loss, however. the glass bead cracked. The most important factor is to consider whether the copper was recovered or lost.

The glass beads were measured using the standardless program of the EDXRF with the following parameters:

- 24 kV and 40 keV,
- No filter,
- An auto current, and
- Using vacuum.

The standardless program was used as an indication of the copper and halide recovery since it is unknown whether correct values were found.

From the measured copper oxide and halide concentrations, the copper and halide recovery was calculated, as discussed in Section 4.2 and shown in Table 4-2. The measured concentrations are reported in Appendix C, Table C-1.

Table 4-2: Recovery of copper and halides using different halides as non-wetting agents

Non-wetting agent	Copper recovery [%]	Halide recovery [%]
0.5% NaI	54.84	0.57
1% NaI	55.96	2.75
2% NaI	57.24	2.33
4% NaI	59.47	3.01
None	54.92	-
1% NaCl	53.62	108.9
1% NaBr	55.08	47.43
1% $NaIO_3$	53.63	0.33
2% $NaIO_3$	53.46	0.33
4% $NaIO_3$	53.10	0.36

The copper recovery for all the glass beads, with all three halides used, as well as no non-wetting agent, showed a recovery of 55%. The four glass beads produced with sodium iodide recovered between 54 and 59% and this did not decrease as the iodide was increased, therefore indicating that the loss of copper was not linear with respect to the amount of iodide. The halide recovery for the sodium iodide was very low, indicating that iodide was lost during fusion. The recovery of the copper in the glass bead produced with no non-wetting agent was only 54.9%, indicating that the copper was "lost" regardless of the presence of the non-wetting agent or the type of halide used. The copper recovery in the glass bead produced with potassium iodate was 53% and the copper recovered was not influenced by the increase in iodate. The halide recovery for the iodate was as low as in the case of the sodium iodide, again indicating the loss of iodide during fusion. The copper recovery with sodium chloride was 53% and with sodium bromide 55% indicating that not one of the two was better than the other. The halide recovery for the chloride was 108%, indicating that all the chloride was recovered and did not volatilise with the copper. The bromide recovery was 47%, indicating that some of the bromide was lost during fusion.

The conclusion made was:

- The results indicate copper loss. The mechanism of the copper loss is not known and can be attributed to incorrect measurements, the copper plating out in the crucibles or the copper being lost is association with the halides.

To improve on the copper measurement it was decided to produce calibration standards with a non-wetting agent. It was decided to use sodium iodide since the glass loss in crucible was the lowest for the 4% sodium iodide. However, the loss on ignition for the 4% sodium iodide was high and therefore it was decided to use the 1% sodium iodide. Since the halide recovery was very low for iodide, it can be used without fear of significant interferences with other elemental lines.

4.3 Preparation of oxide calibration standards with sodium iodide as the non-wetting agent

Calibration standards were prepared to calibrate the EDXRF and determine the copper and hence the true copper recovery. The calibration standards were prepared from pure oxides and sodium iodide was used as the non-wetting agent. The salt was added, together with oxides, sodium tetra-borate and sodium carbonate, as the flux. The sodium carbonate was used to improve mixing as well as the alkalinity of the flux to further dissolution.

4.3.1 Preparation of calibration standards and calibration of EDXRF

The concentration range of each oxide was calculated to have standards lower and higher than the concentrate samples. The oxides were combined in different standards to be able to correct for inter-elemental interferences as well as possible

line overlaps. The concentration of the oxides to be weighed was calculated for the final glass bead mass of 10 g.

Two blanks were prepared, one with sodium tetra-borate and carbonate and one with sodium tetra-borate, carbonate and the non-wetting agent. The sodium tetra-borate was weighed as the difference between the oxides and carbonate taking the loss of the CO_2(g) and iodide into account. 0.5 g of the sodium carbonate was weighed into each sample. All the standards were prepared in platinum-gold alloy crucibles and moulds in the Electrofluxer. The fusion temperature was set at 1100°C for ten minutes to ensure that all the oxides dissolved. The crucibles and moulds were weighed before and after fusion. The crucibles were also weighed after everything was weighed into the crucibles to check the masses. The experimental details are summarised in Appendix C, Table C-2.

The oxide standards two, four and six, cracked during cooling and after investigation it was seen that undissolved solids were present that caused the glass beads to crack. The undissolved solids were attributed to the presence of refractory oxides, for example, chromic and titanium oxide. The glass beads were returned to the crucible and re-fused and re-cast into the moulds and the glass beads did not crack the second time.

The loss on ignition calculated was higher than the expected and this was attributed to the sodium tetra-borate, Appendix C, Table C-3. The component of flux that was lost during fusion was identified by using the software HSC version 4.0 from Outotech (www.outotech.com, Outotech Research Information Centre, PO Box 69, FIN 28101, PORI, Finland) and calculating the thermodynamically favoured reaction. The most likely portion that was identified as the volatile component of the flux was $NaBO_2$(g).

The concentration of each oxide was calculated after the fusion to calibrate the EDXRF. The mass of oxide weighed was divided by the glass bead mass and

multiplied by a hundred to get the percentage of the oxide present. A factor was used to account for the presence of the oxide in a compound, for example the CaO in calcium carbonate and the SO_3 in sodium sulphate. The sodium oxide (Na_2O) concentration was calculated as the sum of all the oxides that will contribute that oxide (sodium sulphate, sodium carbonate, sodium tetra-borate and sodium iodide) minus the sodium oxide loss from the volatile component of the flux ($NaBO_2$). The boron oxide (B_2O_3) concentration was calculated as 100% minus the sum of all the oxides. These concentration values were used to calibrate the EDXRF, Table 4-3.

Table 4-3: Concentration of oxides in calibration standards prepared with sodium iodide as non-wetting agent reported in percentage

Oxide	Oxide Std 1	Oxide Std 2	Oxide Std 3	Oxide Std 4	Oxide Std 5	Oxide Std 6	Oxide Std 7	Oxide Std 8	Oxide Std 9	Oxide Std 10
SiO_2	4.1	-	3.1	-	2.1	-	1.0	-	0.5	-
Fe_2O_3	-	0.5	1.0	-	-	1.5	-	2.0	2.5	-
MgO	-	1.5	-	1.2	-	-	0.9	-	0.6	0.3
SO_3	0.3	-	-	0.6	-	-	0.9	1.2	-	1.5
CaO	-	0.5	-	0.4	0.3	0.2	-	-	-	0.1
Al_2O_3	-	-	0.5	-	0.4	0.3	0.2	0.1	-	-
CuO	-	0.1	-	0.2	0.3	0.5	-	-	-	0.5
NiO	-	0.5	-	-	0.4	-	0.3	0.2	0.1	-
Cr_2O_3	-	0.5	-	0.4	-	0.3	0.1	-	-	0.2
Co_2O_3	0.1	0.2	-	0.3	-	0.4	-	-	-	0.6
TiO_2	-	0.5	-	0.4	-	0.3	-	-	0.2	0.1
ZnO	-	-	-	0.1	0.2	-	0.3	0.4	-	0.5
ZrO_2	0.5	-	0.4	0.3	-	0.2	-	-	0.1	-
TeO_2	-	0.2	0.1	-	0.3	-	0.5	-	0.5	-
V_2O_5	0.1	-	-	0.2	-	0.3	-	0.4	-	0.5
As_3O_4	-	0.1	-	0.2	0.3	0.4	-	-	0.6	-
SeO_2	-	0.4	-	0.5	0.3	-	0.2	0.1	-	-
SnO_2	-	-	-	0.2	0.1	-	0.3	0.4	-	0.5
Sb_2O_4	-	-	-	-	0.4	0.5	0.1	0.2	-	0.3
MnO_2	-	-	-	-	-	0.2	0.3	-	-	-
B_2O_3	63.3	61.5	63.3	63.8	63.9	63.2	63.3	63.2	64.2	63.1
Na_2O	31.6	33.5	31.6	31.1	30.9	31.6	31.6	31.7	30.7	31.8

These concentration values were used to calibrate the EDXRF and the Fused Bead oxide standard calibration program was created. The calibration was created in the method explorer section of the software, the calibration standards and the concentration values of all the oxides are entered into a file in the standards library section of the software and finally the standards as well as the samples were analysed using the acquisition manager. The following steps were used for the creation of the calibration:

- Elemental peak profiles are imported from a library where they are stored. These peak profiles are collected from pure elements as liquids, powders, glass beads or pressed powder briquettes.
- The next step is to select the elements that will be analysed as well as the conditions to be used to obtain the best possible intensity.
- The spectra are processed, which means the region of interest (ROI) is selected to make sure that only the peaks of interest are measured and not background or any other interfering lines. The deconvolution method used is a linear least-square fitting method with digital filtering (randy.cone@thermofisher.com)
- The unknown components are identified. As the elements are selected for analysis from the periodic table, it is updated in this section. Since oxygen cannot be measured, it must be included in the unknowns for the software to calculate the correct concentration of all oxides present. The boron oxide (B_2O_3) is added as an unmeasured component.
- The glass bead standards were imported from the file in the standards library section. In the standards library section the standards must be created and the concentration values of all the oxides entered as percentages. The values are then certified and can be stored as the standards file for later use.

- The next step is to analyse the glass bead standards, the standards are placed in the sample holders of the EDXRF.
- After analysis, the spectra were viewed and the calibration results calculated. The correction model can be chosen and is usually the fundamental parameters theoretical method. This correction model is based on the approximations made by Criss and Birks in 1968. However, the analysis of the elements is normalised (randy.cone@thermofisher.com). The calibration graphs are created by the software and the alpha corrections are displayed. At this point the correction model, intercept and calibration graphs, can be modified if necessary.
- The EDXRF is calibrated and unknowns can be analysed using the calibration obtained.

For the Fused Bead oxide standards calibration program five conditions were chosen, twenty one elements were analysed and twelve standards were used (ten oxide standards plus the two blanks). The conditions were chosen as to be able to analyse all the elements of interest, (Table 4-4).

Table 4-4: Measuring conditions chosen to analyse calibration standards prepared with sodium iodide as non-wetting agent

Condition name	Filter	Voltage [kV]	Medium	Live time [s]	Analytes
High Zb	Cu thick	50	Vacuum	30	Sn, Sb, Te
Mid Zb	Pd medium	20	Vacuum	60	Fe, Co, Ni, Cu, Zn
Mid Zc	Pd thick	28	Vacuum	30	As, Se, Zr
Low Za	None	4	Vacuum	100	Na, Mg, Al, Si, S
Low Zc	Al	12	Vacuum	60	Ca, Ti, V, Cr, Mn

The condition name is a default chosen by the supplier and gives the selection of possible filters, voltage, chamber medium (vacuum, air or He), live times and recommends the analytes that will be measured effectively with those condition. The

filter will enable the operator to reduce the background intensity as well as the intensities of elements that will be excited by that condition, but are not of interest. The voltage setting will excite only certain elements. The filter is situated between the source and the sample and will reduce unwanted fluorescence by absorbing X-rays of energies below the absorption edge, reducing the excitation of elements that could absorb those X-rays. The medium is a selection between air, vacuum and helium gas. The helium gas is used for liquids and loose powders while the vacuum is used for pressed powders and solid samples. The heavier elements can be analysed using air since the absorption of the X-rays by air will have a less significant effect on the results, while the lighter elements will be influenced significantly. The live time is the time chosen for the analyses of those elements under the selected condition. The elements of great interest, as well as the light elements, will be measured for 60 to 100 seconds to improve the counting statistics whereas the elements of less importance will be measured for 30 seconds. The twelve oxide calibration standards were analysed using these conditions, fundamental parameters was chosen as the correction model and the calibration graphs were obtained.

The iodide in the oxide calibration graphs were not measured and calibrated for because it was assumed that most of the iodide was lost during the fusion. The calibration graphs were constructed using Excel and comparing the calculated concentration with the given concentration. The calibration graph of most importance is copper oxide, Figure 4-1. Refer to Appendix C Figures C-1 to C-10 for the other oxides calibration graphs.

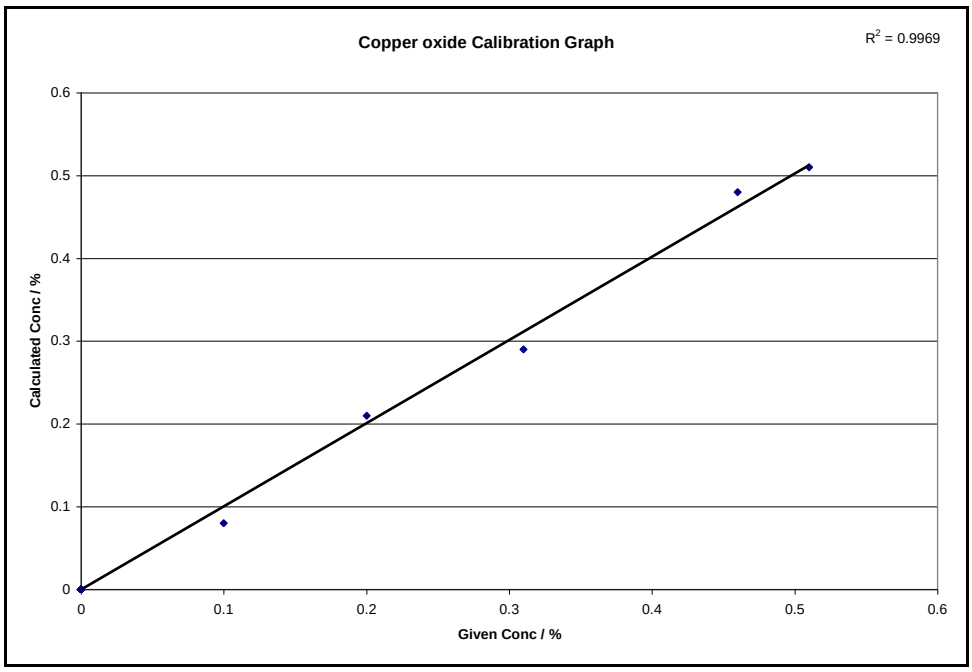


Figure 4-1: Copper oxide calibration graph with sodium iodide as non-wetting agent and fundamental parameter corrections

The correlation coefficient of the line is 0.997, indicating good correlation between the calculated concentration and the given concentration. The calibration is not a perfect line through all the data points. The fundamental parameters are correcting for all enhancement and absorption effects, however the outliers in the graph may be due to inter-element effects unaccounted for. Unknown samples were prepared and analysed using this calibration to determine whether the calibration was a success.

4.3.2 Validation of calibration prepared with sodium iodide as non-wetting agent

Since the calibration graphs for copper oxide indicated no concerns, it was decided to use unknown samples to validate the calibration. The samples would indicate whether the copper was retained during fusion.

Two samples were available for the validation: the Lebowa concentrates as mentioned in Chapter three. The sample was roasted over night to remove the sulphur.

Two glass beads were prepared with the sample and 1% sodium iodide and sodium tetra-borate. The samples were prepared at 1100°C for ten minutes and the crucibles and moulds weighed before and after fusion. The first glass bead that was prepared was inhomogeneous and the crucible had black smears at the top. The sodium tetra-borate and the sample was not mixed manually before the fusion and the inhomogeneous glass bead indicated that not all the sample particles were in direct contact with the flux for oxidation and dissolution. The sample also crept up the sides of the crucible producing the black smears. While preparing the second glass bead, the sample, sodium tetra-borate and sodium iodide were manually mixed by way of paper rolling and the glass bead produced was homogenous. Both samples were analysed with the fused bead oxide calibration program and the copper and halide recovery determined (Table 4-5). The experiment details are summarised in Appendix C, Table C-4.

Table 4-5: Determination of copper recovery for unknown samples analysed with fused bead oxide calibration program

Glass bead number	Copper concentration in glass bead [%]	Copper assigned concentration [%]	Copper recovery [%]
Bead 1	2.90	3.37	86.05
Bead 2	3.09	3.37	91.69

The copper recovery for Glass bead 1 was only 86% which was higher than the 54% achieved previously. The copper recovery for Glass bead 2 was 91.7%, a definite improvement when compared to the copper measured with the standardless program. However, the recovery was still not 100% and indicated a possible copper loss. The way in which the copper was lost was still uncertain and had to be determined.

It was concluded that:

- The fused bead oxide calibration indicated that the measurement of the copper recovery amounting to 54% was not accurate and with the calibration more accurate results were achieved.
- Calibration graphs were obtained and indicated a calibration graph with 0.997 correlation coefficient, for copper, even though the line is not perfect with data points off the line.
- The copper recovery was 86% and 91.7%, an improvement on the previously achieved recoveries, showing the potential of using sodium iodide as a non-wetting agent and using the calibration program for analysing unknown samples.

It was determined that the standardless program was not producing correct results for copper and the halides measured. A calibration was created with calibration standards and the results of the samples indicated copper lost. Since the measurement was improved, the mechanism of the copper loss was either copper plating out or reacting with the halide. This was investigated.

4.4 Determination of mechanics of copper loss, integrating the flux and the non-wetting agent and testing other ions as non-wetting agents

The calibration created with the calibration standards and sodium iodide as the non-wetting agent showed improved accuracy for the measurement of the copper in unknown samples. However, the recovery was not hundred percent indicating that the copper was definitely lost, even if in small quantities. The objective of these experiments were to determine whether the copper was lost or plated out in the crucible during fusion, reacting with the platinum in the crucible rather than the flux.

In these experiments the roasted samples were fused with flux only and no non-wetting agent was added.

4.4.1 Fusion of roasted samples with no non-wetting agent

Three glass beads were prepared (FB 45, 47 and 49) in the Electrofluxer for five, seven and a half and ten minutes respectively. The crucibles and moulds were weighed before and after fusion and the differences calculated. Three glass beads were produced with sodium tetra-borate flux only, in the crucibles used to produce glass beads FB 45, 47 and 49. These samples (FB 46, 48, 50) were produced to determine if a significant amount of copper was left in the crucibles after the production of the glass beads.

The crucible losses for samples FB 45, 47 and 49, were between 0.9 and 1.3 g indicating the high mass of glass left behind during casting if no non-wetting agent was used, Appendix C, Table C-5. All three samples (FB 45, 47 and 49) produced glass beads with a mass of 9.8 g, indicating that the fusion time did not have a significant effect on the mass of the glass bead. All six glass beads cracked during cooling. The pieces of the glass beads were stuck together with tape on the opposite side of the measuring surface and measured using the Fused Bead oxide calibration program to determine the copper recovery. The copper concentration measured was used to calculate the copper recovery for beads FB 45, 47 and 49 and are found in Table 4-6.

Table 4-6: Copper recovery of unknown samples prepared without non-wetting agent

Glass bead number	Copper concentration in glass bead [%]	Copper assigned concentration [%]	Copper recovery [%]
FB 45	3.32	3.32	98.5
FB 47	3.32	3.32	98.5
FB 49	3.37	3.37	100.0

The recoveries of glass beads FB 45 and 47 were 98.5% and FB 49 was 100% indicating that the copper was recovered completely in the absence of the non-wetting agent, confirming that the copper was not plating out or reacting with the crucibles. Conclusions made included:

- All six glass beads cracked during cooling indicating the necessity of the non-wetting agent.
- The copper recovery indicated that the fusion time did not have a significant influence but ten minutes is recommended.
- The fact that close to 100% of the copper was recovered for all three glass beads also indicated that the copper was not plating out in the crucibles during fusion.

It could be concluded that the copper was lost in association with the halide. The type of halide or non-wetting agent as well as the method of addition had to be investigated. An alternative method of addition was investigated in the next set of experiments.

4.4.2 Investigation into integrated flux and non-wetting agent

A suggestion from S. Rivard from Claisse (www.clasisse.com, srivard@claisse.com) was to integrate the flux and the non-wetting agent prior to the fusion procedure and thereby preventing the loss of copper in association with the halide. The integrated flux and non-wetting agent is a standard product in the Claisse range and can be purchased. To integrate the flux and the non-wetting agent, the glass bead was created in a normal fusion procedure. The glass beads were pulverised to a fine powder and the integrated powder was then used during subsequent fusions as a flux.

Six glass beads were produced to make the integrated flux and the glass beads were crushed using a mortar and pestle and pulverised in a mill. Three samples were fused using the integrated flux (FB 40, 41 and 42), one blank and two with the roasted Lebowa concentrate sample. The blank was produced to determine the possible contaminants in the integrated flux introduced by the milling vessel. The glass beads were produced using the platinum-gold alloy crucibles and moulds and the Electrofluxer. The fusions were performed at 1100°C with a fusion time of ten minutes. The crucibles and moulds were weighed before and after the fusions and the differences calculated. The experimental details are summarised in Appendix C, Table C-6.

Table 4-7: Crucible differences before and after fusion with integrated halide as non-wetting agent

Glass bead number	Loss of glass in crucible [g]	Glass bead mass [g]
FB 40	0.197	9.94
FB 41	0.066	9.95
FB 42	0.183	9.93

The loss of glass was between 0.1 g and 0.20 g and higher than achieved with the non-wetting agent and the flux not integrated. This could be an indication that some of the non-wetting properties of the sodium iodide were lost during the integration fusion. Glass beads FB 40 and 41 were inhomogeneous, indicating that the sample was not in full contact with the integrated flux. FB 42 cracked, indicating that the integrated flux was not effective as a non-wetting agent. The glass beads were stuck together and measured using the Fused Bead oxide calibration program. The concentration of copper measured was converted to the copper mass in the glass bead and the recovery calculated, Table 4-8.

Table 4-8: Copper recovery of unknown samples prepared with integrated flux

Glass bead number	Copper concentration in glass bead [%]	Copper assigned concentration [%]	Copper recovery [%]
FB 41	1.97	3.37	58.5
FB 42	2.30	3.37	68.2

The copper recovery for the two glass beads prepared with the integrated flux was 58.5% and 68.9%. The copper recovery was lower than expected.

It was concluded that:

- The glass beads cracked indicating that some of the sodium iodide was already lost during the integration fusions.
- The integration of the flux and the sodium iodide was expected to prevent the reaction of the copper with the halide, however this did not occur and the copper in the sample was not recovered.

The integrated flux and non-wetting agent method of iodide introduction was unsuccessful and the copper was not recovered. It was decided to investigate alternative non-wetting agents to the halides to determine whether the copper could be recovered.

4.4.3 Investigation into alternative non-wetting agents

During the previous experiments it became clear that the copper was being lost in association with the halides. When glass beads were prepared without any halides present the copper was recovered. Different approaches were tried and not even integrating the halides and the flux improved the copper recovery. It was decided to investigate alternative non-wetting agents with the focus on breaking the sodium bonds of the flux and reducing the thermal stress that these longs chains were subjected to. Therefore, small negative and positive ions were investigated as alternatives.

The alternative non-wetting agents that were investigated included:

- Sodium sulphate (SO_4^{2-} and Na^+)
- Potassium hydrogen phosphate (PO_4^- and K^+)
- Sodium hydroxide (Na+ and O^{2-} ions)
- Potassium carbonate (K_2O – K^+ and O^{2-})
- And combinations of the above mentioned compounds.

Nine samples were prepared with sodium tetra-borate as the flux and the Lebowa concentrate sample as used in the above sections, Appendix C, Table C-7.

- Five glass beads were prepared with 10% of sodium carbonate (FB 52), sodium sulphate (FB 53), potassium hydrogen phosphate (FB54) and sodium hydroxide (FB 55),
- One glass bead was prepared with 5% potassium hydrogen phosphate (FB 60) and one glass bead with the combination of 5% potassium hydrogen phosphate and 5% potassium carbonate (FB 61).

The objectives were to find the best suited alternative non-wetting agent, where the glass beads did not crack during cooling and the copper was recovered. The glass

beads were prepared in the Electrofluxer with the platinum-gold alloy crucibles and moulds.

During the cooling period, all the glass beads cracked or shattered, however it was decided to determine the copper recovery before any final conclusions were made. The beads were analysed using the Fused Bead oxide calibration program, Table 4-9.

Table 4-9: Copper recovery of unknown samples prepared with alternative non-wetting agents

Glass bead number	Alternative non-wetting agent used	Copper recovery [%]
FB 52	Na_2CO_3	92.5
FB 53	Na_2SO_4	94.0
FB 54	KH_2PO_4	94.1
FB 55	NaOH	94.1
FB 60	KH_2PO_4	96.4
FB 61	Combination	93.9

The copper recovery varied between 92.5% and 96.4% depending on the compound used. The best recovery was for the glass bead produced with 5% potassium hydrogen phosphate. Copper was lost because previous recoveries of between 98% and 100% was achieved when no non-wetting agent was used, Section 4.5.1. All the glass beads cracked, showing that these compounds did not have enough non-wetting properties.

The conclusions that were made from this section included:

- The glass beads produced with possible alternatives to the halides as non-wetting agents all cracked.
- The copper recovery was high, but not between 98% and 100% as previously achieved without any non-wetting agents.
- This indicated that the alternative non-wetting agents were not effective as alternatives for the halides.

Alternative non-wetting agents to halides could not be found. Therefore, the addition of the halides after fusion and during casting was considered.

4.5 Addition of bromine gas as the non-wetting agent during the casting step and the production of oxide calibration standards

The experiments up to now indicated the necessity of adding a non-wetting agent to prevent the glass beads from cracking. An alternative method for introduction of the halides had to be investigated. The possibilities, as mentioned in the literature, were to add the halide salt as a powder or liquid during the fusion period or to add the powder or solution during the casting step. Adding the halide during the casting procedure would mean that the copper was already oxidised by the flux and would not be able to react with the halide. However, the halide addition must be fast enough to have an influence on the cracking of the glass bead. The Electrofluxer casting step was automatic and the mechanism did not allow for the addition of the halide during casting and an alternative way of addition had to be considered. The option considered was to add the non-wetting agent during the casting step as a gas. None of the halides exist as a gas at room temperature. However, bromine at room temperature is a liquid and if poured into a larger container would immediately fill the volume with gas.

4.5.1 Initial investigation into bromine gas as the non-wetting agent

The first set of experiments that were carried out was to test whether using the bromine gas would prevent the glass beads from cracking. The bromine was poured into a plastic wash bottle and the addition was done manually. The glass bead

appearances and copper recovery was used to determine the success of the addition of the bromine gas.

The first five glass beads were produced with the addition of the bromine gas done manually from a plastic wash bottle. The glass beads were prepared with 10.0 g of flux with no sample. The bromine was squirted from the plastic bottle and aimed into the crucible in the casting position. The bromine gas came into contact with the crucible as well as the glass. Two glass beads were produced by continuously squirting the bromine gas into the crucibles, while the other samples were produced with intermittent squirts of two, four and eight at a time. Only one of the five glass beads did not crack during cooling, the glass bead produced with continuous squirting of the bromine gas. The glass beads were analysed using the EDXRF, but since the EDXRF was not calibrated for bromine, the bromine intensities were determined with the standardless function of the software. The intensities were compared and used to determine whether the bromine was absorbed by the glass beads, (Table 4-10).

Table 4-10: Intensities measured for copper oxide and chloride with factorial design experiment

Glass bead number	Bromine gas addition	Bromine intensity measured [cps]
FB 70	Continuous squirts	255
FB 71	Two squirts	359
FB 72	Four squirts	480
FB 73	Eight squirts	652
FB 75	Continuous squirts	432

The intensity measured for the bromide indicated that the bromine gas was absorbed by the glass beads. The intensities for the glass beads were not comparable and were significantly different.

It was concluded that:

- The addition of the bromine gas using the plastic wash bottle was inconsistent and not reproducible.
- Due to the manual nature of addition it would be operator dependant and not reproducible.
- The fact that the bromine attacked the plastic and destroyed the bottle within two days indicated the impractical use of the plastic wash bottle.

Another way of introducing the bromine gas more consistently had to be investigated.

4.5.2 Bromine gas addition using a carrier gas

The carrier gas chosen was nitrogen, which is inert and should not influence the glass bead produced or the elements of interest. The bromine liquid was poured into a 250 ml Dresce bottle and coupled to the carrier gas. The tube used to introduce the bromine gas to the crucibles and mould during casting was coupled to the other side of the Dresce bottle. The tube was fixed to the Electrofluxer and aimed at the crucible and mould casting position. As soon as the Electrofluxer came to a stop, after mixing for the casting step, the carrier gas was opened and the bromine gas introduced. The nitrogen gas flow was regulated and could change the flow of bromine gas addition.

Eight glass beads were produced, seven (FB 80 – FB 85 and FB 87) using nitrogen as the carrier gas for the bromine gas addition and one bead (FB 86) without the bromine gas introduction. Copper oxide was used as the sample to determine whether the copper was recovered with bromine gas addition. Three of these glass beads (FB 80, 81 and 87) were produced without copper oxide and five glass beads were produced with 0.5% copper oxide (FB 82, 83, 84, 85, 86), Appendix C, Table C-8. The glass bead produced with copper oxide and without bromine gas as the non-wetting agent (FB 86) was used to compare the copper recovery when using the

bromine gas. Two other glass beads were produced, one glass bead without copper oxide and bromine gas as the blank and one glass bead with 1% of sodium bromide salt and no copper oxide. This sample would be used to determine the intensity of 0.77% bromine and to compare with the samples produced with the bromine gas addition via the carrier gas. The carrier gas flow was set at 5 $L.min^{-1}$ for the addition of the bromine gas.

During the cooling period glass beads FB 80, 81, 83 and 84, cracked and this was not expected and upon investigation it was determined that the Electrofluxer did not stop in the same position after mixing and before casting and therefore the bromine gas addition was not consistent. Due to the bromine gas tubing being placed at a fixed position, the position that the Electrofluxer came to stop during the casting step was of great importance. Glass beads 82 and 85 did not crack during cooling, indicating that the bromine gas addition could be effective if the position the fluxer stopped, were consistent.

The samples were measured using the fundamental parameter standardless function of the EDXRF and the intensities of the copper and the bromine determined, (Table 4-11).

Table 4-11: Copper and bromide intensities measured with bromine gas addition via carrier gas

Glass bead number	Loss of glass in crucible [g]	Copper oxide weighed [g]	Normalised Copper oxide intensity measured [cps]	Bromine gas addition	Bromine intensity measured [cps]
FB 76	1.2	0	0	None	51
FB 77 (NaBr)[12]	0.4	0	0	0.77 % Br	29812
FB 86	1.4	0.052	1	None	45
FB 80	0.1	0	0	5 $L.min^{-1}$	669
FB 81	0.4	0	0	5 $L.min^{-1}$	4417
FB 82	0.3	0.051	0.98	5 $L.min^{-1}$	270
FB 83	0.9	0.066	1.27	5 $L.min^{-1}$	360
FB 84	0.1	0.049	0.99	5 $L.min^{-1}$	148
FB 85	0.2	0.052	0.99	5 $L.min^{-1}$	545
FB 87	0.2	0	0	5 $L.min^{-1}$	600

The loss of glass in the crucible was high for the two samples where no bromine was added, FB 76 and FB 86. The loss for FB 77 where the sodium bromide salt was used was 0.4 g and of the same magnitude as the losses for the samples prepared with the bromine gas. The loss of glass in the crucible does not compare to the bromine intensity, where the bromine intensity was very high, FB 81. It is expected that the loss would be low but this is not the case.

The bromine intensity does not show a correlation to the glass beads that cracked during cooling. FB 80 and FB 81 cracked, the samples were both exposed to bromine gas at a flow rate of 5 $L.min^{-1}$, and both contained no copper. However, the bromine intensity varies from 669 cps to 4417 cps. For FB 83 and FB 84, both glass beads cracked, both samples were exposed to 5 $L.min^{-1}$ bromine gas flow and contained copper, however the intensities, for bromine, varied between 360 cps to 148 cps.

[12] Salt was added and not gas, for comparison reasons

The bromine intensities also show that the bromine measurement was inconsistent and that the intensity of the bromine varied 187% between the glass beads. The bromine gas intensity for the glass bead produced with 1% NaBr was also significantly higher than the samples produced with the gas.

The copper intensities were normalised to the intensity achieved with FB 86 where no bromine was added to the sample. The same mass of copper was added to samples FB 86, FB 82 and FB 85 and the normalised intensities showed that the copper intensity was very close to 1. The intensities of the samples where the bromine was added indicate that the copper was either not lost or an insignificant amount was lost. The copper intensity for FB 83 was higher than the other glass beads because more copper was weighed into the sample.

The conclusions made were:

- The addition of the bromine gas had to be controlled more efficiently.
- The bromine gas addition was not consistent but the bromine gas was absorbed by the glass beads and in some cases prevented the cracking of the glass beads.
- The glass loss to crucibles indicates that less glass was lost than in the case where no non-wetting agent was used. Therefore, the bromine gas was acting as a releasing agent even though it was not added consistently.
- The copper recovery was not influenced by the addition of the bromine gas, indicating that the bromine gas was not interacting with the copper. This was due to the bromine gas being added after the fusion and during the casting process.

Since these results showed no significant effect on the copper recovery it was decided to prepare another set of oxide calibration standards with bromine gas as non-wetting

agent introduced via the carrier gas. The calibration standards previously prepared were prepared with iodide as the halide and it was proven that iodide influenced the copper recovery.

4.5.3 Preparation of oxide calibration standards with bromine gas as the non-wetting agent and validation of the calibration

The preparation of the oxide calibration standards was repeated but instead of using the sodium iodide, bromine gas delivered by a carrier gas was used.

Ten oxide calibration standards were prepared combining different oxides in different concentration ratios. Each oxide was present in five standards and the concentration ranges were (Appendix C, Table C-9):

- Between 0.1 and 0.5% of the elements of interest in a sample with the total mass of 10 g for calcium, aluminium, copper, nickel, chromic oxide, cobalt and manganese.
- Between 0.5 and 4.0% for silicon dioxide,
- Between 0.5 and 2.5% for iron,
- Between 0.3 and 1.5% for magnesium and sulphur.

Sodium carbonate and sodium nitrate was weighed with the oxide. The nitrate was added as an extra oxidising agent. The amount of sodium tetra-borate to be weighed was calculated as the difference between the total glass bead mass of 10 g and the sum of all the components weighed. The loss of the CO_2 (g), N_2(g) and O_2(g) was taken into account for the calculation. The calibration standards were fused in the Electrofluxer at 1100°C for twelve minutes. The bromine gas was added during the casting period and the carrier gas flow was set at 5 $L.min^{-1}$. The crucibles and moulds were weighed before and after fusion for the calculation of the glass bead mass and loss on ignition. The loss on ignition was consistent between 0.09 g and 0.21 g (Appendix C, Table C-10).

The calculated concentration values were used to calibrate the EDXRF, refer to Table 4-12 for the concentrations of all the oxides. One glass bead was prepared with a known concentration of bromide and this was used to calculate the bromide concentration in the calibration standards and to calibrate for the bromide.

Table 4-12: Concentration of oxides in calibration standards prepared with bromine gas as the non-wetting agent

Oxide	Oxide Std 1	Oxide Std 2	Oxide Std 3	Oxide Std 4	Oxide Std 5	Oxide Std 6	Oxide Std 7	Oxide Std 8	Oxide Std 9	Oxide Std 10
SiO_2	4.07	-	3.07	-	2.08	-	1.01	-	0.52	-
Fe_2O_3	-	0.52	1.02	-	-	1.50	-	2.02	2.67	-
MgO	-	1.52	-	1.18	-	-	0.91	-	0.61	0.30
SO_3	0.32	-	-	0.64	-	-	1.00	1.23	-	1.55
CaO	-	0.07	-	0.40	0.31	0.20	-	-	-	0.11
Al_2O_3	-	-	0.52	-	0.41	0.34	0.22	0.10	-	-
CuO	0.10	-	-	0.22	0.31	0.40	-	-	-	0.54
NiO	-	0.50	-	0.00	0.43	-	0.33	0.20	0.11	-
CrO_3	-	0.72	-	0.53	-	0.40	0.14	-	-	0.27
Co_2O_3	0.11	0.20	-	0.31	-	0.40	-	-	-	0.51
MnO_2	-	0.12	0.20	0.49	-	-	0.30	0.48	-	-
K_2O	-	0.34	-	0.25	-	0.19	0.06	-	-	0.13
B_2O_3	64.59	65.15	64.62	64.92	65.46	65.49	64.63	64.43	65.18	64.61
Na_2O	30.79	30.85	30.57	31.08	31.00	31.08	31.40	31.55	30.90	31.98

For the Oxide calibration standards with bromine gas calibration program four conditions were chosen, Table 4-13.

Table 4-13: Measuring conditions chosen to analyse calibration standards prepared with bromine gas as non-wetting agent

Condition name[13]	Filter	Voltage [kV]	Medium	Live time [seconds]	Analytes
Mid Zb	Pd medium	20	Vacuum	40	Cr, Mn,Fe, Co, Ni, Cu
Mid Zc	Pd thick	28	Vacuum	20	Br, Rh
Low Za	None	4	Vacuum	100	Na, Mg, Al, Si, S, Rh, Br
Low Zb	Cellulose	8	Vacuum	60	Ca, K

Two conditions were available for the measurement of the bromide, Mid Zc and Low Za. The Mid Zc condition will excite the K-lines of the bromide while the Low Za will excite the L-lines of bromine which will possibly overlap with aluminium. The bromide L-line has to be measured to be able to correct for the line overlap.

The ten oxide calibration standards and the blank were analysed using these conditions, theoretical fundamental parameters were chosen as the correction model and the calibration graphs were obtained. The calibration graphs of importance were the copper and bromide graphs, Figures 4-2 and 4-3 (Appendix C, Figures C-11 to C-22).

[13] Name of condition as chosen by supplier of instrument (Za, Zb, Zc)

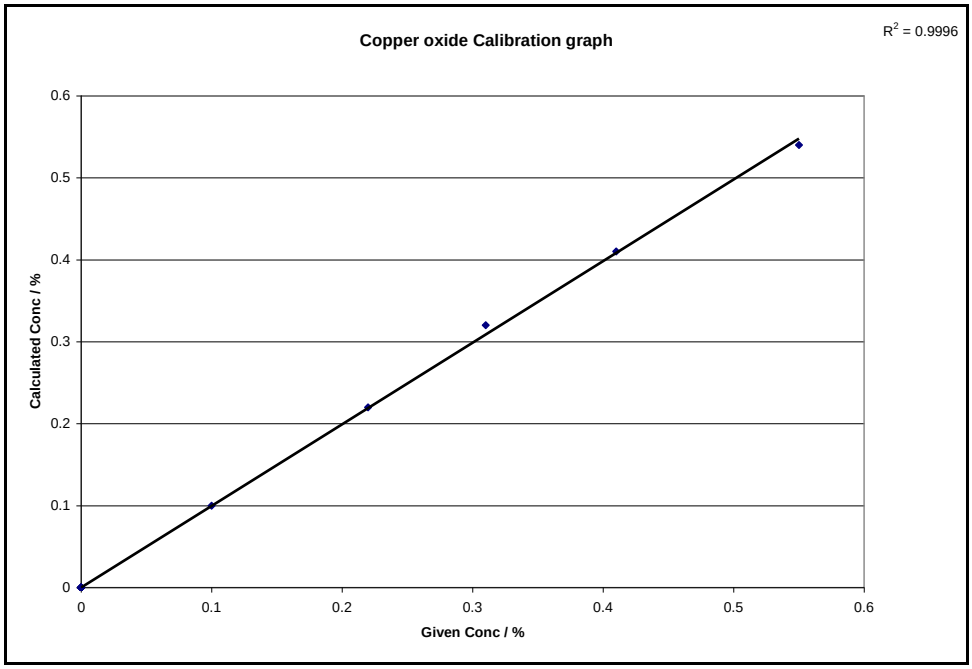


Figure 4-2: Copper oxide calibration graph with bromine gas as non-wetting agent

The graphs are constructed by the software and are a representation of the calculated concentration % (as done by the software) and the given concentration (%). The copper line has a correlation coefficient of 0.9996 which is close to one indicating an almost perfect straight line with no outliers. The graph indicates a successful calibration for copper.

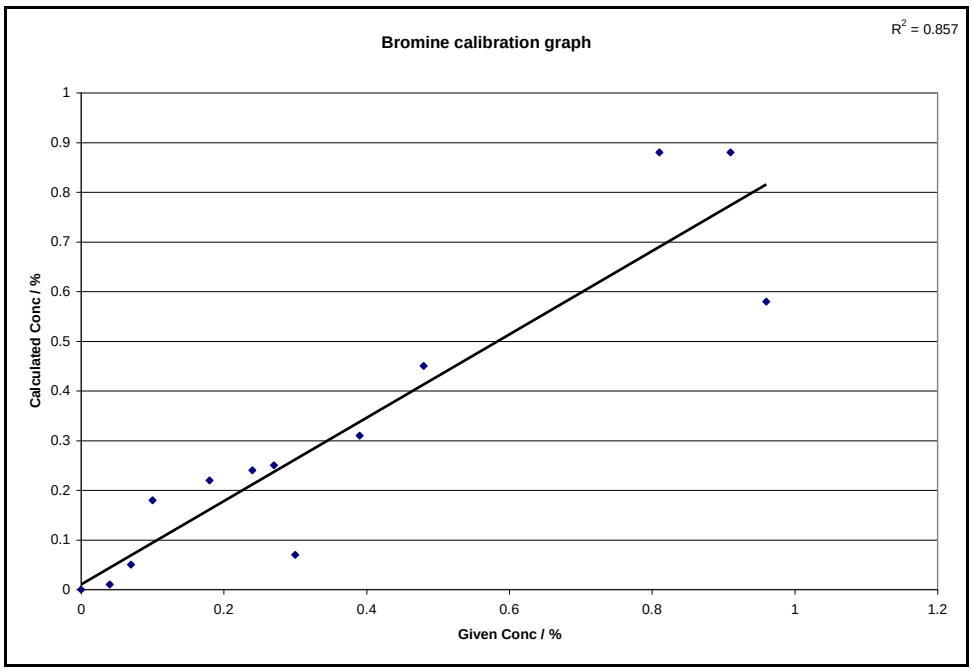


Figure 4-3: Bromine calibration graph with bromine as non-wetting agent

The bromide graph however has many outliers and a correlation coefficient of 0.857. The first conclusion that can be made is that the determination of the bromide concentration, with one standard, was inaccurate. The graph indicates that the bromine is not added and absorbed consistently and will pose a problem for calibration. Since the concentration of the bromine is inconsistent it does pose a problem when it comes to matrix effects since the bromine concentration cannot be calculated accurately. Despite these concerns it was decide to first validate the calibration with samples and determine the copper recovery before any changes or improvements were made.

Eight samples were chosen to be used for validation. These samples are used as quality control samples in the mine laboratories and the concentration; for copper, nickel, iron, cobalt, chromic oxide and sulphur were determined by alternative techniques by various laboratories in the group. The known concentrations are

reported with lower and upper limits indicating the uncertainty in the concentration, as well as the limits within which the laboratories must operate.

A portion of the samples were weighed and roasted in an oven before fusion. The samples were fused at 1100°C for twelve minutes in the Electrofluxer. The crucibles and moulds were weighed before and after fusion to calculate the glass bead mass. The crucibles were investigated after the fusion and it was found that the crucible used to produce the sample Amandelbult Merensky Concentrate (AMC) had black spots at the bottom, indicating that the sample was not completely roasted to remove the sulphur and that some of the sulphur reacted to produce sulphides. It was not seen in any of the other samples. Only one glass bead cracked, LUC QC 02, indicating that possibly undissolved particles were present after fusion.

The glass beads were analysed using the oxide calibration standards with bromine gas calibration program. The copper recovery was calculated and used to evaluate the calibration produced with the bromine gas as the non-wetting agent.

Table 4-14: Copper recovery of samples prepared with bromine gas as non-wetting agent

Sample material used	Copper concentration in bead [%]	Copper assigned concentration [%]	Relative percentage difference [%]	Uncertainty in assigned concentration [%]
AMC	2.22	2.02	9.90	Not known
LMC QC 03	4.37	4.28	2.10	± 2.34
LUC QC 02	2.58	2.55	1.18	± 6.27
BMC QC 02	3.66	3.44	6.40	± 5.23
MUC QC 03	0.51	0.56	- 8.93	± 3.57
PPC QC 02	1.90	1.92	- 1.04	± 2.60

The relative percentage difference was calculated between the concentrations of copper in the sample minus the assigned concentration of the copper, as a percentage of the assigned copper value. These percentages range from -8.9% to 9.9% indicating

that the copper in the sample does not give a systematic error, being either consistently lower or higher than the assigned value. For two samples (MUC QC 03 and PPC QC 02), the copper concentration was lower in the glass beads than the assigned value and for four glass beads (AMC, LMC QC 03, LUC QC 02 and BMC QC 02) the copper concentration was higher in the beads. The uncertainty of the assigned values is calculated statistically using the different concentrations as reported by the different participating laboratories and is used by the mining laboratories to assign limits to the concentration value of the sample. These limits are then used by the laboratories to establish whether the technique and results they report are accurate. In the case of the AMC sample, it was not distributed to different laboratories and the uncertainty of the value is not known. In the case of the other samples, three of the glass beads (LMC QC 03, LUC QC 02 and PPC QC 02) passed the uncertainty limits since there percentage difference is less than the uncertainty. For two of the glass beads, the percentage difference is more than the uncertainty and these samples failed. In other words, the copper is not within the range and for BMC QC 02 the copper is over-recovered. In the case of MUC QC 03 the copper is under-recovered. The results indicate the copper was recovered and in some samples the copper was not within limits. This could be due to sample mass uncertainty or preparation irregularities.

Conclusions that were made:

- The recovery of the copper of the unknown samples indicated that the calibration with the bromine gas could be used for further investigations.
- Bromine gas could be used as the non-wetting agent since the calibration results showed that the copper in the glass beads were recovered.
- The addition of the bromine gas was not consistent and therefore the bromine calibration was not perfect. The matrix effect that the bromine will have on the other elements would differ. This would be investigated at a later stage.

4.6 Conclusions

The following conclusions were made in this chapter regarding the investigations into the non-wetting agents and the copper recovery:

- Non-wetting agents are necessary to prevent the glass bead produced from cracking and to release the glass from the crucibles during the casting step.
- The most commonly used non-wetting agents are halides, however the use of halides influences the recovery of copper in the samples. Since it is of economical importance the analysis of copper cannot be compromised.
- Halides were investigated and all the halides: chloride, iodide as well as bromide salts, showed a poor recovery of copper. The copper loss was attributed to possible measurement errors.
- Calibration standards were produced with sodium iodide as the non-wetting agent. The calibration results showed no concern regarding copper. To validate the calibration, samples were prepared with sodium iodide and copper recoveries of more than 80% were achieved. This was the best recovery at the time. Samples prepared with no non-wetting agent showed a copper recovery of 100%, indicating that the copper measurement was correct and the copper was not plating out as previously suspected but was definitely reacting with the halides and being lost. This result also indicated that the copper recovery determined with the intensities only was not as accurate as with the calibration procedure.
- The addition of bromide as gas during the casting step and not for the complete fusion was investigated. Calibration standards were produced and the calibration was successful. Validation of the calibration showed that the addition of the non-wetting agent after the fusion and during the casting step prevented the reaction of the copper and the halide. The copper in the glass beads was recovered.
- The bromide calibration was not perfect and this was due to the inconsistent absorption of the gas by the glass beads produced. The varying intensities of

the bromine gas would have an effect on the other elements present in the glass bead as well as aluminum due to line overlap. It would be difficult to correct for matrix effects due to the varying intensities of the bromide as well as the inability to calculate bromide concentrations.

The next step was to continue with the oxide calibration standards with bromine gas calibration program and produce more unknown samples. Roasting of the samples is not part of the ideal fusion, therefore the oxidation of the samples was investigated.

5. PREPARATION OF FINAL CALIBRATION STANDARDS USING AN ALTERNATIVE FUSION INSTRUMENT

5.1 Introduction

In the previous chapter it was shown that non-wetting agents are a necessity to prevent glass beads from cracking and the loss of glass in crucibles. The method of addition as well as the halide used is of great importance. In Chapter four a successful calibration was produced with oxide calibration standards and bromine gas as the non-wetting agent and in some samples the copper was recovered successfully. The objective was to test the oxidation of the samples in various ways with a factorial design experiment, however during these experiments the Electrofluxer broke and was decommissioned.

A Katanax K2, an automatic fluxer, was used for subsequent fusions and experiments. The Katanax heating mechanism and operation is different to that of the Electrofluxer and introduced the possibility of non-wetting agent addition as a salt, for the complete fusion process, without copper loss. Due to this possibility the halide salts were re-investigated. Even though the use of the bromine gas was successful, the bromine gas was damaging the equipment and it was unsafe to work with. The heating mechanism and operation of the Katanax will be discussed in Section 5.2.2.

The halides were investigated with the objective of determining whether the copper will be lost during fusion while using one of the halide salts. Three halide salts were investigated, namely sodium chloride, sodium bromide and potassium iodide, Section 5.3. To determine the recovery of the copper in the glass beads prepared, the EDXRF

was calibrated using the different concentrations of the halides and copper oxide. Oxide calibration standards were prepared with potassium iodide as the non-wetting agent, Section 5.4, and used to calibrate the EDXRF, Section 5.5.

5.2 Katanax operation and heating mechanism

5.2.1 Operation of Katanax

The Katanax K2; refer to Figure 5-1, is an automatic electrical fluxer equipped to handle five samples at a time. The Katanax consists of a furnace, furnace door, crucible holder unit, crucible agitator, cooling fans and control unit with display. The crucible holder can accommodate five crucibles with their moulds. Stepper motors and position detectors automatically open the furnace door and move the crucible holder into the furnace. When the fusion cycle is completed, the crucibles and moulds will automatically be removed from the Katanax and the melt poured into the moulds. The fans at the bottom of the moulds are used to cool the glass beads.

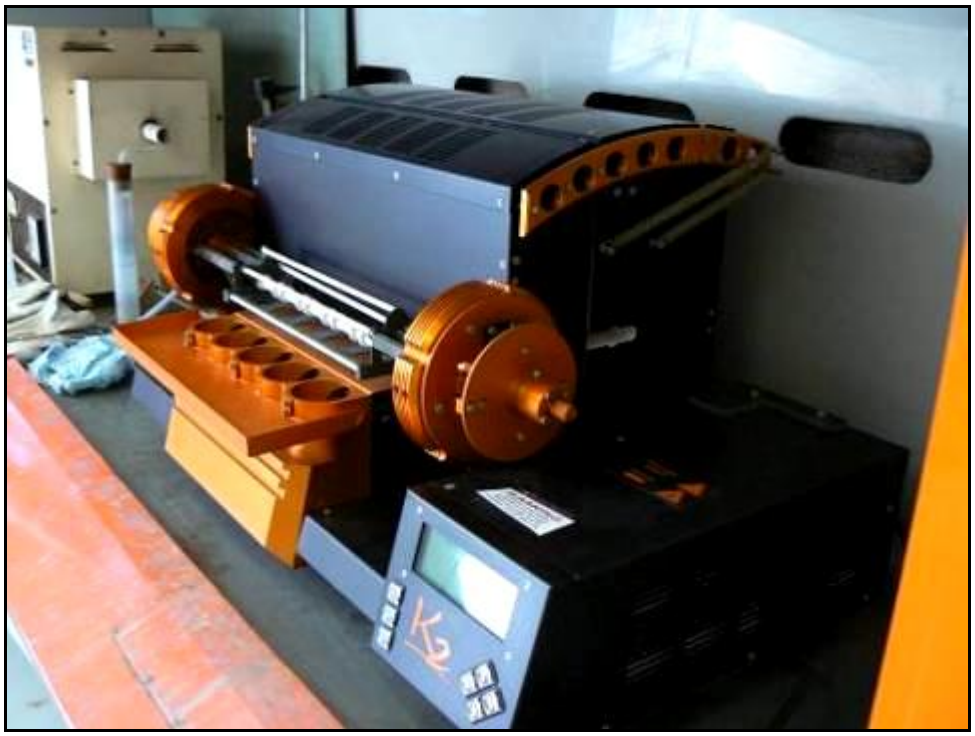


Figure 5-1: K2 Katanax instrument

The Katanax is equipped with a holding temperature function. The holding temperature is selected by the user and once the temperature is reached, by the furnace, it will be maintained at that temperature for one to five hours. The samples will also only be loaded into the furnace, for fusion, once the holding temperature has been reached.

The Katanax has predefined programs but custom programs can also be created by the user. Each program contains seven steps, including four heating steps, a pouring step, a cooling step and the forced cooling of the mould. For each step certain parameters can be changed. For example, the duration of the step, the temperature of the step, the rocking speed of the crucible holder and the tilting angle of the crucible holder.

The user guide also contains a formula for the calculation of the total glass bead mass depending on the inner diameter of the mould. The total mass is equal to the square of the diameter of the mould divided by 150. Therefore, if the mould has a diameter of 32 mm the square is calculated and divided by 150 to reach a total of 7.0 g. This theory was used for the production of glass beads in the 32 mm diameter moulds. The moulds previously used were 40 mm in diameter and the glass beads were produced with a final mass of 10.0 g. This was changed to incorporate the smaller moulds.

The main features and advantages of the Katanx are discussed:

- Increased precision due to the entire fusion process being automated. The fusion method is reproducible due to the parameters being kept identical by the instrument. The production of the glass beads is reproducible due to the closed electric furnace and the effective temperature control. All the crucibles will be at the same temperature for the same time and the real-time temperature display makes temperature monitoring easy.
- Increased safety due to no gasses being used for the fusions.
- Since five samples can be fused at the same time, productivity is increased when compared to fluxers that can only produce one or two samples simultaneously. The throughput of the instrument will depend on the fusion time of the method used.
- The holding temperature, as set by the user, has the added benefit of the furnace temperature being maintained at a temperature ready for the next fusion; a decreased temperature ramping time thereby, increasing productivity due to decreased total fusion time.

5.2.2 The heating mechanism of the Katanax and comparisons to other heating mechanisms

The Katanax uses heating elements above and below the crucibles and moulds. The temperature is closely monitored and controlled with the platinum thermocouple and the furnace is a closed electric furnace. The crucibles and moulds both enter the furnace and therefore the moulds are at the same temperature as the crucibles during the pouring step, decreasing thermal stress on the glass beads. The cooling step is also controlled by the fans at the bottom of the moulds.

The prime benefit of the heating of the Katanax is that the samples are heated from above and below, Figure 5-2.

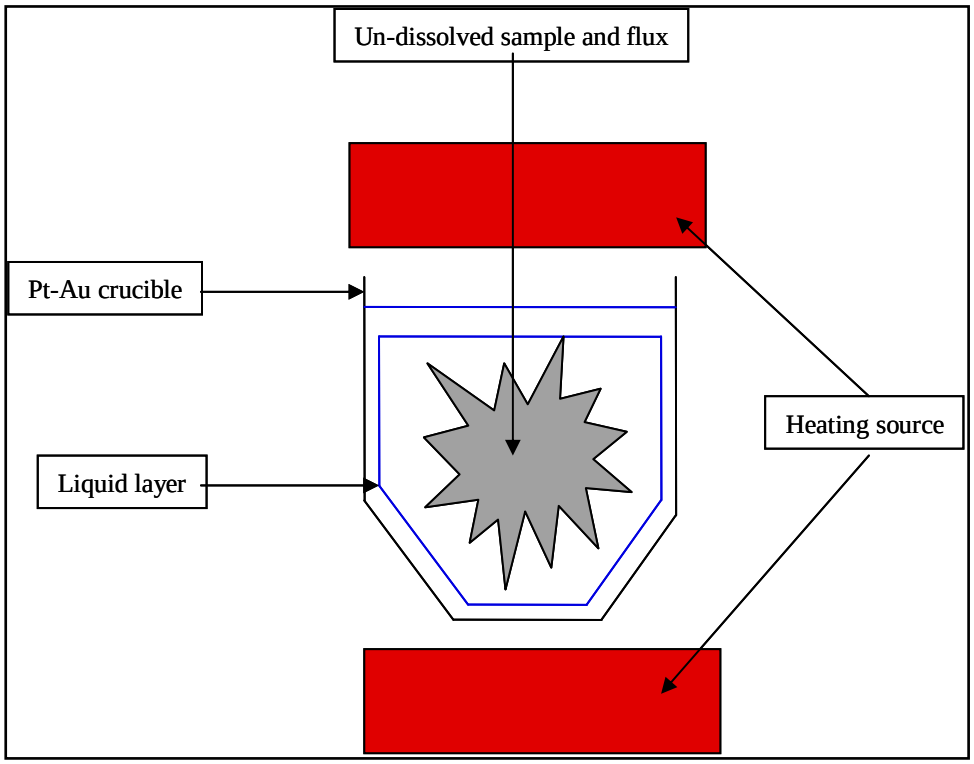


Figure 5-2: Picture illustrating heating mechanism of the Katanax

Since the samples are heated from the top and the bottom of the crucible, the oxidising agents and flux will melt at the bottom of the crucible as well as the top and this form a liquid layer. The liquid layer will enclose the sample completely and the sample will be surrounded by the reagents. This will improve reactivity and oxidation of the sample and reduce the loss of sample due to creeping up the sides of the crucible. The reaction will occur from the top and bottom until it reaches the middle and by then the entire sample would have reacted with the molten flux. Another advantage is that gas produced during fusions will have to pass through the liquid layer on top of the sample and therefore no sample particles or volatiles will be lost and the entire sample will react with the oxidising agent and flux.

The crucibles are also rocked forwards and backwards, increasing mixing as well as improving reactions. Due to agitation, the sides of the platinum crucibles will be covered with the molten flux and oxidising agent, preventing the reaction of the sample with the crucible. Due to the sample being covered by a liquid layer, prediction was made that the copper would not be lost.

The heating mechanism of the Electrofluxer consists of a heating element coiled in a spiral around the crucible, Figure 5-3. In other words, the crucible is lowered into the furnace and is heated from right around due to the element coiled around the furnace wall. The sample is heated from the sides and the liquid layer will therefore form on the inside of the crucible but not on top of the sample as in the case of the Katanax. The same can be said for samples that are only heated from the bottom, for example the Bunsen flame, or an instrument with only one element at the bottom, Figure 5-4.

Any gas produced during the fusion can therefore escape through the top of the sample which is granular/ powdery and with it particles of the sample and flux and additives can be lost. The reaction of the sample with the flux and agents present will be from the bottom and sides of the crucible and since there is no liquid layer at the top the volatiles can escape. It is hypothesised to be the reason why the copper was

lost when using the Electrofluxer. Since the sides of the crucibles will not be covered with molten flux and oxidising agents, as in the case of the Katanax, the samples can react with the crucibles and also cause loss of sample as well as crucible damage.

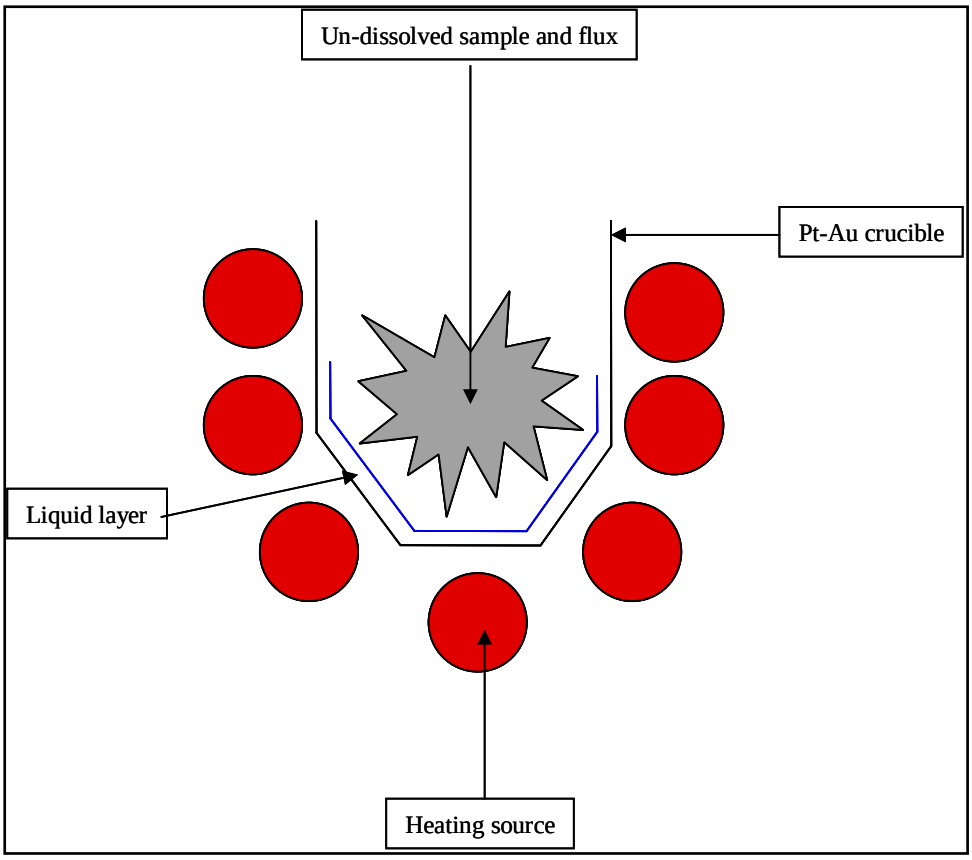


Figure 5-3: Picture illustrating heating mechanism of the Electrofluxer

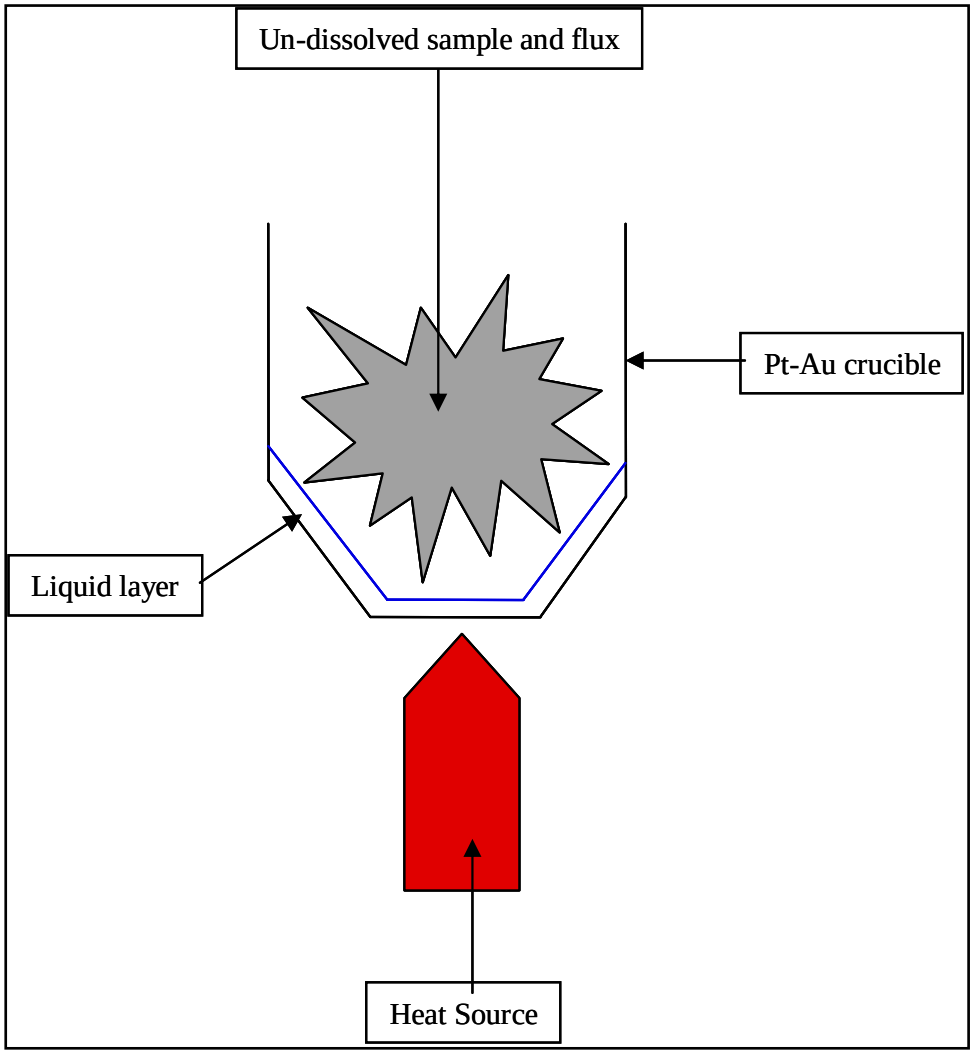


Figure 5-4: Picture illustrating heating mechanism from below only

The comparison of the Katanax and Electrofluxer does not just include the heating mechanism but many other factors:

- Another important difference is the fact that the Katanax has a closed temperature controlled environment where the crucibles are at exactly the same temperature for the same time. Whereas the Electrofluxer is not an entirely closed environment and the temperature control is not as effective. This influences the precision of the fusions as well as the reproducibility.

- The heating rates on the Electrofluxer are exceptionally fast and therefore there is very little difference in overall heating time when compared to the Katanax.
- In the case of the Katanax, the crucibles and moulds are loaded together into the furnace. The Electrofluxer loads the crucible into the furnace while the mould is covering the opening of the crucible but not entering the furnace. Therefore, during casting, the mould is considerably cooler than the crucible, increasing the thermal stress on the glass bead during casting. It should also be taken into account that if the moulds are kept at high temperatures for long times, as in the case of the Katanax, the moulds can deteriorate.
- The Electrofluxer can load one sample at a time whereas the Katanax can handle up to five samples at a time, increasing productivity and throughput. Even though the Katanax can load five samples, it was used to produce only three at a time since only four moulds were available. Therefore, the number of samples produced at a time can also depend on the number of available crucibles and moulds.
- The physical positioning of the crucibles and moulds into the loading positions are considerably easier with the Katanax compared to the Electrofluxer.
- Both the fluxers can fit onto a bench and under a fume hood.

The Katanax was used to investigate the halide salts as non-wetting agents, added for the full fusion process.

5.3 Determining whether copper is lost when fused with halide salts in the Katanax

If the experiments showed that halide salts could be used instead of bromine gas a great concern would be overcome in that the bromine gas was attacking the Electrofluxer and causing damage to the instrument and also posed considerable health risks to the operator. Therefore, using the salts instead of the bromine gas would be considered an advance.

Glass beads were prepared with sodium chloride, sodium bromide and potassium iodide and the copper recovery was determined by EDXRF. The glass beads were prepared with sodium tetra-borate as flux and known, and varied, concentrations of copper oxide (Appendix D, Table D-1). The iodide and bromide concentrations were varied between 0.5% and 2.0%. The concentrations of the copper oxide, bromide and iodide were varied, to be able to calibrate the EDXRF, and consequently measure the copper recovery more accurately. The concentrations were also varied to determine whether an increase in the halides would affect the copper recovery.

The samples were prepared in the Katanax at 900°C. Some of the glass beads produced with the sodium bromide shattered while cooling, indicating that not enough sodium bromide was used as non-wetting agent. None of the glass beads produced with the potassium iodide shattered.

The EDXRF was calibrated for copper and bromide using glass beads. The glass beads were produced with 0%; 0.5% and 1% copper oxide and 0% and 2% sodium bromide. Two glass beads were used to calibrate the EDXRF for iodide, one bead with 2%. The other bead with 0.5% potassium iodide. The rest of the glass beads, not used for the calibration, were analysed using this calibration, and the copper recovery determined, Table 5-1. (Appendix D, Table D-2)

Table 5-1: Copper oxide recovery with halide salts by Katanax

Halide used	Copper oxide recovery [%]
1% Sodium chloride	95.7
1% Sodium bromide	96.2
1.5% Sodium bromide	103.4
0.5% Sodium bromide	100.0
1% Sodium bromide	101.2
2% Sodium bromide	109.2
0.5% Potassium iodide	98.7
1% Potassium iodide	116.3
2% Potassium iodide	106.4

The recovery of the copper oxide was above 95% for all the glass beads and all three halide salts used. For sodium bromide, the recovery varied between 96.2% (1% sodium bromide) and 109.2% (2% sodium bromide). The copper recovery when using the potassium iodide was between 98.7% (0.5% potassium iodide) and 116.3% (1% potassium iodide). The recovery of the copper oxide was promising and no correlation was found between the increased addition of halides and the copper recovery. The apparent over recovery of the copper can be attributed to the calibration and regression, only three glass beads were used to calibrate for copper and this contributes to a greater uncertainty in the calibration. There is also uncertainty in the copper concentration. If the oxide was not 100% copper oxide that could also explain the possible under-recovery. Another uncertainty was the mass of the copper oxide used.

It was concluded that:

- The copper oxide was recovered with the use of the halide salts added during the complete fusion process.
- There is evidence indicating that the heating mechanism of the Katanax prevented the loss of copper.

- Using a halide salt as a non-wetting agent was a great improvement when compared to the use of the bromine gas.

All three halide salts indicated good copper recovery however it was decided to use the iodide rather than the bromide since the bromide L-lines would interfere with the aluminium, K-lines. Since the non-wetting agent addition, the fusion instrument and fusion parameters had changed, new oxide calibration standards were prepared.

5.4 Production of oxide calibration standards with potassium iodide as the non-wetting agent using the Katanax

The importance of an accurate calibration with primary standards from pure oxides has been discussed in previous chapters. Up to now standards were produced with sodium iodide and sodium bromide as well as bromine gas. Since the preparation of samples as well as heating mechanism changed, new calibration standards had to be prepared with potassium iodide.

Certain changes were made to the preparation of the calibration standards when compared to the preparation as discussed in Chapter four, Section 4.5.3, including the fusion parameters as well as some of the compounds used to produce the oxides of interest. Since some of the oxides used for the production of the standards were refractory and proved difficult to dissolve at the fusion temperature of 1100°C, alternatives were considered for magnesium, aluminum, chrome and manganese. The alternatives chosen were hydrated magnesium sulphate, hydrated aluminum nitrate, potassium dichromate and potassium permanganate, the lower melting points ensuring dissolution during fusion.

Fourteen glass bead standards and two blanks were produced combining different oxides in different concentration ratios (Appendix D, Table D-3). Different masses

of potassium iodide were used to be able to calibrate the EDXRF for iodide. Sodium nitrate (0.25 g), sodium carbonate (0.25 g) and sodium tetra-borate were used for the fusion to produce a glass bead with the total mass of 7 g. The amount of sodium tetra-borate to be weighed was calculated as the difference between the total glass bead mass and the sum of all the other components; taking into account the loss of gasses due to carbonates, nitrates and hydrates. The concentration ranges are summarised:

- Between 0.5% and 6.0% for silicon dioxide; 0.5 to 2.5% for iron oxide; 0.3 to 1.5% for magnesium oxide; 0.3 to 3.4% for sulphur oxide and 0.1 to 0.5% for calcium-, copper- and cobalt oxide.
- Between 0.1% and 0.8% for aluminum oxide; 0.1 to 0.7% for chromic oxide; 0.1 to 0.6% for manganese oxide and nickel oxide; and 0.5 to 1.5% of potassium iodide.

The sodium carbonate and sodium nitrate were weighed into the bottom of the crucible followed by the sample covered by the sodium tetra-borate and the potassium iodide.

The fusion programme was created and included the following options and parameters Table 5-2.

Table 5-2: Fusion parameters for program used on Katanax

Step	Temperature [°C]	Time [minutes]	Rocking
First heating	600	5	No
Second heating	1000	2	Yes
Third heating	800	0.5	Yes
Fourth heating	900	0.5	Yes
Casting	900	To cast	No

All the oxides dissolved and none of the glass bead standards shattered or contained any gas bubbles. The loss on ignition was between 0 g and 0.4 g. Refer to Figure 5-5

for a picture of the calibration standards and Table 5-3 for the concentrations of the calibration standards (OCS).



Figure 5-5: Calibration standards prepared with the Katanax and potassium iodide as the non-wetting agent

Table 5-3: Concentrations for oxide calibration standards prepared with potassium iodide as the non-wetting agent in the Katanax, reported in percentage

	OCS 1	OCS 2	OCS 3	OCS 4	OCS 5	OCS 6	OCS 7	OCS 8	OCS 9	OCS 10	OCS 11	OCS 12	OCS 13	OCS 14
SiO_2	6.06	-	5.05	-	4.04	1.86	3.17	0.81	2.01	-	1.35	-	0.53	-
Fe_2O_3	-	1.24	-	0.57	-	-	1.15	0.70	1.44	-	-	2.03	-	2.51
MgO	-	1.52	-	1.19	-	1.20	0.91	-	-	0.57	-	0.30	0.78	-
SO_3	0.31	3.02	-	2.36	0.94	3.40	1.80	1.20	-	2.65	-	0.60	1.56	-
CaO	-	0.51	-	0.41	-	-	-	-	-	0.11	-	0.30	0.29	-
Al_2O_3	-	-	0.11	-	-	0.79	-	0.41	-	-	0.19	0.78	-	-
CuO	0.10	-	-	0.26	0.32	0.27	-	-	0.14	0.52	-	0.20	-	-
NiO	-	0.51	-	-	0.47	-	0.33	0.24	-	-	0.57	-	0.23	0.15
CrO_3	-	-	-	0.57	-	0.46	0.14	0.69	-	0.27	-	-	-	-
Co_3O_4	0.10	0.20	-	0.30	-	-	-	-	0.41	-	-	-	0.48	-
MnO_2	-	-	0.60	-	0.14	-	0.15	-	0.19	-	0.22	-	-	0.30
KI	1.39	1.35	1.21	1.14	0.97	1.60	0.80	0.71	0.61	0.50	0.57	0.70	0.83	0.89
K_2O	-	-	0.26	0.22	0.06	0.18	0.12	0.26	0.08	0.10	0.10	-	-	0.13
Na_2O	30.70	31.17	30.58	31.43	31.41	30.44	30.94	32.31	31.54	32.73	33.20	31.67	31.99	31.80
B_2O_3	61.35	62.01	61.96	62.69	61.59	61.22	61.32	62.60	63.51	63.09	63.70	63.72	64.09	64.11

Conclusions made during the production of the calibration standards:

- None of the glass beads cracked proving potassium iodide as a good choice.
- The use of alternative compounds for the production of the oxides of magnesium, aluminum, chrome and manganese proved successful due to all the compounds being dissolved and the production of perfect glass bead standards with no un-dissolved solids.
- The heating program used for the production of the calibration standards proved successful since the oxides reacted with the oxidising agents as well as the flux in the time and temperature used.

The calibration standards were produced successfully and were used for the calibration of the EDXRF.

5.5 Calibration of EDXRF with final set of oxide calibration standards and the empirical correction model

The oxide calibration standards produced with potassium iodide in the Katanax was used to calibrate the EDXRF. Due to the inconsistency in the difference between the calculated concentration and the measured concentration of iodide in the glass beads it was decided fundamental parameters could not be used. The concentration of the iodide present in the glass beads was calculated. However, due to the loss of iodide during fusion, the concentration of the iodide was inaccurate. For fundamental parameter corrections to be applied successfully, one of the pre-requisites is that all the elements concentrations should be known > 99%. Since the iodide content in the beads was not known, the fundamental parameter model could not be used, and therefore the empirical correction model was investigated. The fundamental parameters and empirical corrections models were discussed in Chapter two, Section 2.3.2 and 2.3.3.

Empirical corrections are used to calculate the best possible fit between the measured intensities of the calibration standards and the calculated concentration of the calibration standards. The mathematical model used by the Quant'X is least square fitting of a large number of calibration standards to establish alpha coefficients which describe the effect of one element on another. The intensity correction model is attributed to the Lucas, Tooth and Pyne (randy.cone@thermofisher.com).

The calibration program Final Calibration was created and the following analytical measuring conditions chosen for the calibration of the EDXRF, Table 5-4.

Table 5-4: Measuring conditions for the final calibration created with the standards produced with the Katanax and potassium iodide as the non-wetting agent

Condition name	Filter	Voltage [kV]	Medium	Live time [sec]	Analytes
High Zb	Cu thick	50	Vacuum	20	I
Mid Zb	Pd medium	20	Vacuum	60	Cr, Mn, Fe, Co, Ni, Cu
Mid Zc	Pd thick	32	Vacuum	30	Rh
Low Za	None	4	Vacuum	100	Na, Mg, Al, Si, S
Low Zb	Cellulose	8	Vacuum	40	K, Ca, I

The iodide was measured using two measuring conditions, High Zb for the K-lines of the iodide as well as Low Zb for the L-lines of the iodide. All the conditions were measured in vacuum and for a certain live time. The Mid Zc condition was used for the measurement of the rhodium lines of the tube. The element rhodium was not included in the calibration, however it was used for Compton scattering correction.

Compton scattering was discussed in Chapter two, Section 2.4, and entails the scattering of photons or X-rays with loss of energy. The most observed example of Compton scattering is when the tube spectrum is scattered by the sample and the

entire tube spectrum shifts. The advantage of the Rh K-line Compton scatter is that the ratio of the $RhK\alpha_{Compton}$ peak is always constant to the background wavelength in that region. The Compton ratio can be used to correct for changes in the mass absorption coefficient and will only correct for absorption effects. Compton scatter corrections were done on the final calibration programme since the samples contain many lights elements and should have a high occurrence of Compton scatter.

For reporting reasons, some of the elements are kept as oxides and some are reported as the elements, for example, copper, nickel, iron, sulphur and cobalt. The calculated concentrations and given concentrations were used to construct the calibration graphs in Excel.

The calibration was first evaluated using the fundamental parameter correction model and the greatest concern identified was the iodide calibration graph. The correlation between the concentration given by the user for calibration and the concentration as calculated by the EDXRF software was 0.594 with the Low Zb measurement condition and 0.529 with the High Zb measuring condition. The calibration line is therefore far from straight due to the inconsistent concentration of the iodide in the glass beads, Figure 5-6.

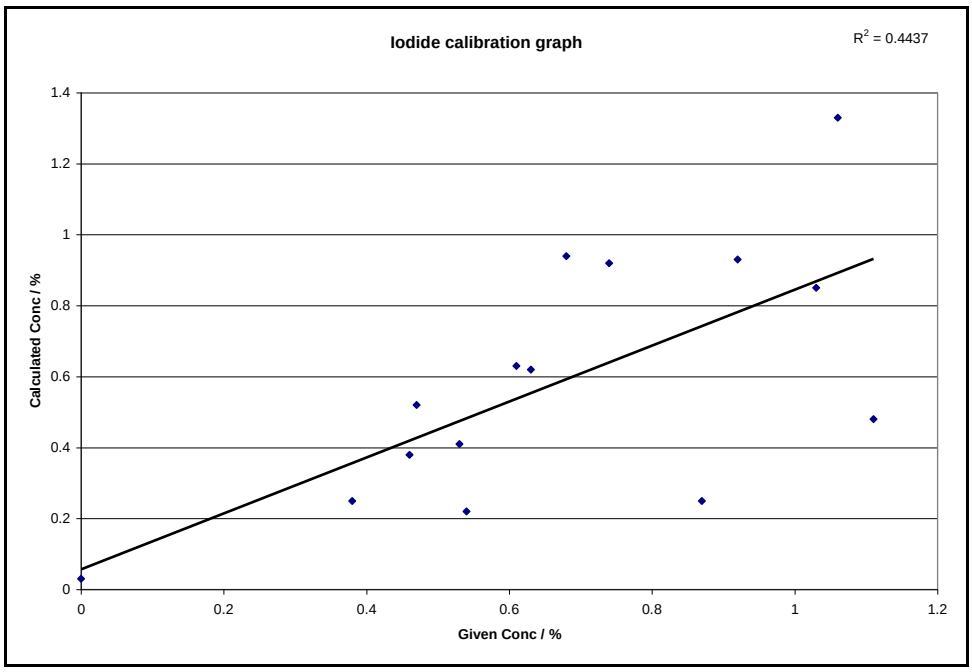


Figure 5-6: Iodide calibration graph with final calibration program and fundamental parameter correction model

To apply empirical correction certain considerations were made to identify the elements that could attribute most to enhancement and absorption effects:

- The compounds with the highest concentrations (matrix elements) were identified as sodium oxide (32%), iron oxide (2%), magnesium oxide (1%), sulphate (3%), potassium iodide (calculated as 1.6%) and silicon dioxide (6%).
- The compounds with the greatest difference in concentration between the highest and lowest concentration was identified as silicon dioxide, sulphate, potassium oxide and iron.
- Elements closest on the periodic table to the element of interest for example in the case of nickel both copper and cobalt were considered.

For every correction addition to an element, the calibration line was evaluated and the correction only considered if the correlation coefficient improved. In some cases, the software prompted with a warning of negative sensitivity for the calibration line

indicating that too many corrections were applied to a single element and the correction was removed. Refer to Table 5-5 for the corrections applied to all the elements as well as the final correlation coefficient. The correlation coefficient is calculated between the given concentration and the calculated concentration and is an indication of the linearity of the line.

Table 5-5: Elements chosen for empirical corrections on the final calibration program

Element of interest	Elements used for inter-elemental corrections	Correlation coefficient of calibration line
Na_2O	Si, S, Fe	0.464
MgO	Na, Al, K, Fe	0.997[14]
Al_2O_3	Na, Fe	0.997
SiO_2	Na, S	1.000
S	Na, K, Fe	0.999[15]
K_2O	Na, Mg, S, Ca	1.000
CaO	S, Fe, Cu	1.000
Cr_2O_3	Mg, Cu	1.000
Mn_2O_7	Na, Mg, Si, Fe	1.000
Fe	Na, Cr, Ni	1.000
Co	Na, Mn, Cu	1.000
Ni	Na, Co, Cu	1.000
Cu	Na, Si, S, Fe	1.000
I	Na	0.592

Oxide calibration standard six was excluded, as an outlier, from all the calibration graphs**.** The calibration graphs of interest will be discussed and shown in the chapter, refer to the Appendix D (Figures D-1 to D-8) for the rest of the calibration graphs. The elements and calibration graphs of interest are copper, sodium, sulphur and iodide. A correlation coefficient of 0.999 is used to show good correlation and, in this case, is true for most of the elements and oxides except sodium, magnesium oxide and iodide.

[14] Outlier was removed and correlation coefficient re-calculated
[15] Outlier was removed and correlation coefficient re-calculated

Copper is the element of greatest concern with regards to recovery. The correlation coefficient for copper is 1.000 (Table 5-5) and shows a straight line without any of the calibration standards deviating. The copper calibration graph with empirical corrections, Figure 5-7, and the calibration graph without any corrections, Figure 5-8, is used to illustrate the improvement when corrections are applied.

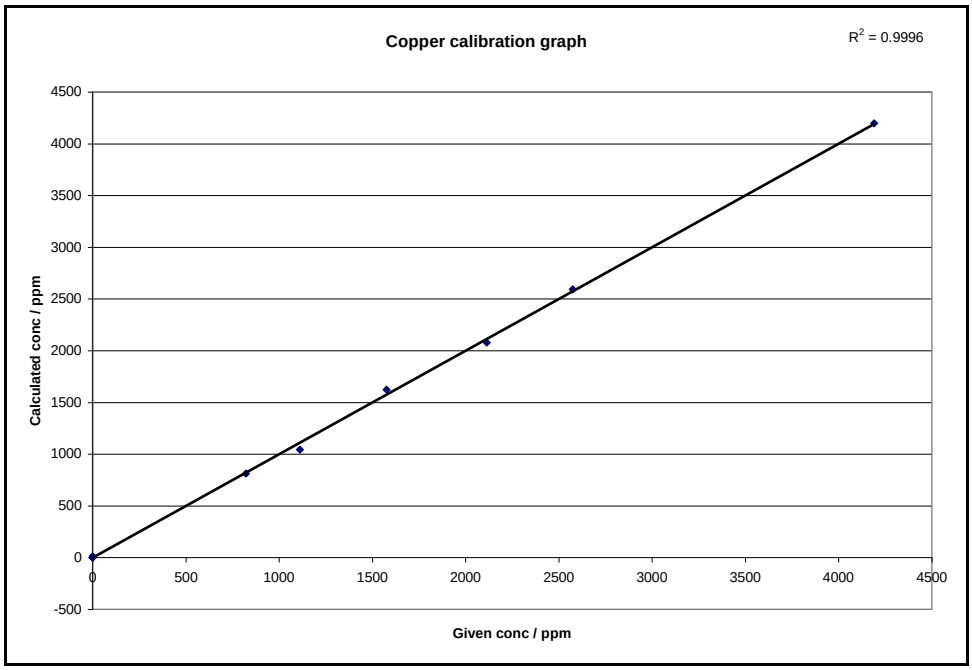


Figure 5-7: Copper calibration graph with empirical corrections applied

The graph with empirical corrections clearly shows a perfect straight line. The line fits all the calibration standards and therefore shows no deviation due to enhancement or absorption. At this stage it can be assumed that the correct inter-element corrections were chosen for the element.

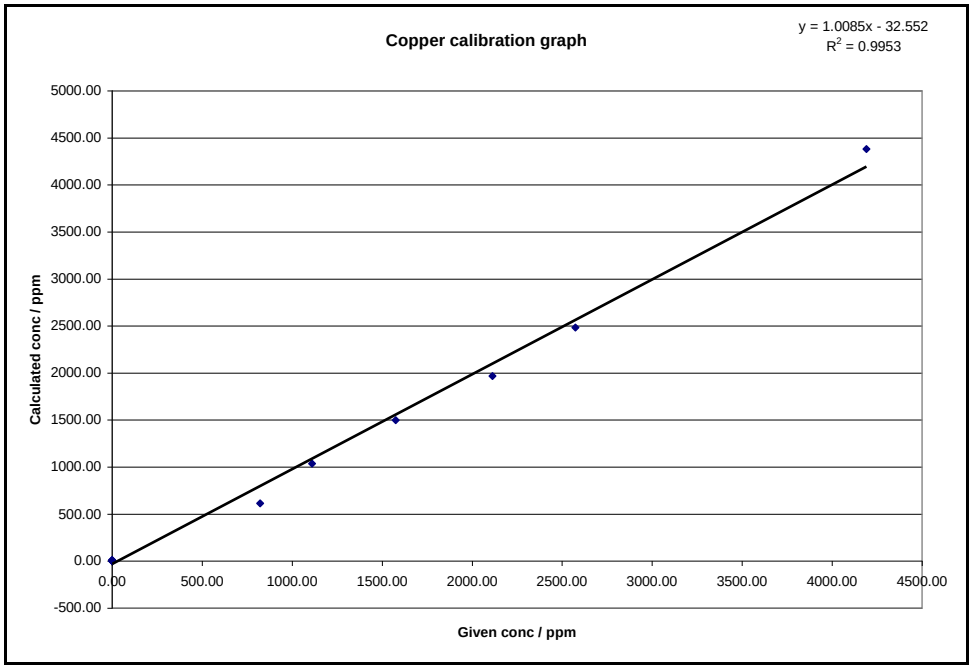


Figure 5-8: Copper calibration graph without empirical correction

As can be seen from Figure 5-8, the line is not a perfect fit to the calibration standards and shows definite inter-element effects. By comparing the two calibration lines of copper, before and after applying corrections, it clearly shows the improvement of applying inter-element corrections.

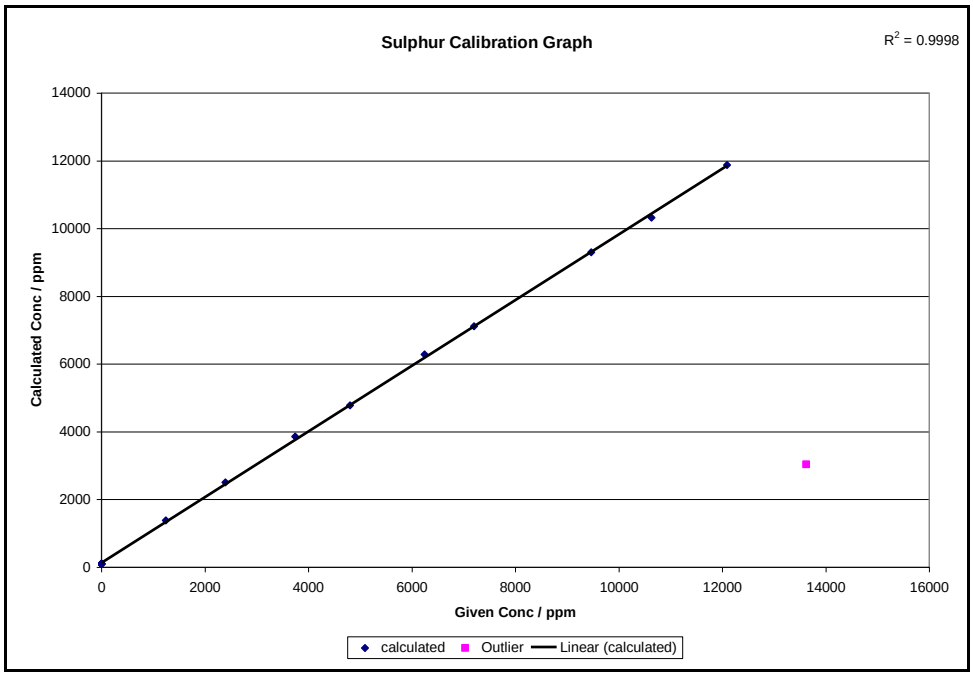


Figure 5-9: Sulphur calibration graph with outlier and empirical correction applied

As can be seen, oxide calibration standard six is a definite outlier. Once the outlier is removed, the sulphur calibration line improves, and gives a straight line through all the standards. It can be assumed at this stage that the correct empirical corrections were used for the sulphur.

Another calibration of interest was the sodium oxide calibration. The correlation coefficient was 0.46 and an indication of a poor regression. However, it should be noted that the sodium is contributed from the flux and the additives and therefore the concentration of the sodium oxide is consistently between 30 and 33%. This is not a substantial range and therefore the oxide calibration standards are all grouped in a bundle and will not give a perfect calibration line, Figure 5-10. The regression line can be restricted through zero or be allowed to cut the axis.

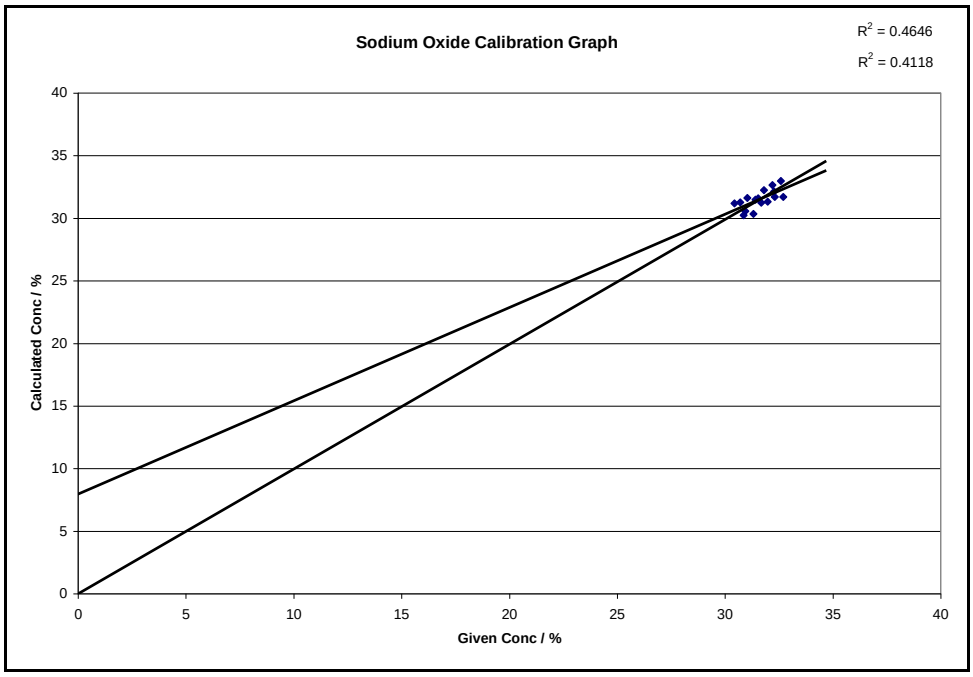


Figure 5-10: Sodium oxide calibration graph with empirical corrections

Another element of interest was the iodide. As discussed previously, the calculated concentration is not a true representation of the concentration of iodide in the glass beads. This calibration line with empirical corrections could not be improved and shows poor regression, Figure 5-11.

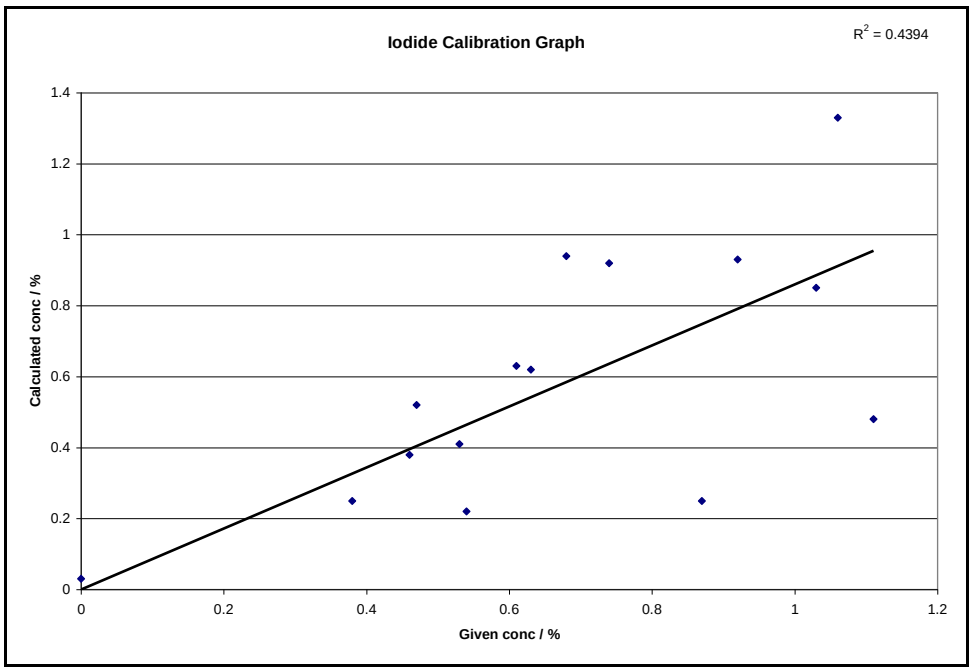


Figure 5-11: Iodide calibration graph with empirical corrections

The correlation coefficients were used to determine whether the calibration graphs were straight and if the regression between the calculated and given concentration were good. The correlation coefficients, as well as the appearance of the calibration graphs, were used to indicate the relevance of the empirical corrections used. A true indication of the accuracy of a calibration as well as the corrections applied would be the recovery of all the elements in QC samples. Samples were prepared to validate the final calibration and this will be discussed in Chapter Six.

5.6 Conclusions

The following conclusions were made in this chapter regarding the use of the Katanax, non-wetting agents and the final calibration:

- Since the Electrofluxer was decommissioned, the Katanax was obtained, and introduced the possibility of adding halide salts during the fusion rather than using bromine gas.

- Experiments with the halide salts, sodium chloride, sodium bromide and potassium iodide, showed copper recoveries of above 95% for all the salts tested. This showed that the heating mechanism of the Katanax was preventing the loss of copper as hypothesised.
- Calibration standards were prepared with the potassium iodide as the non-wetting agent and compounds for the refractory oxides. The calibration standards were prepared successfully and none of the glass beads cracked or shattered and none of the glass bead standards had undissolved solids or gas bubbles.
- The initial calibration was done with fundamental parameters, however the calibration graph of iodide showed that the regression between the calculated and given concentrations was poor. This indicated that the concentration of the iodide in the calibration standards was not consistent and that iodide was lost during the fusion procedure. Since the concentration of the iodide varied to such an extent, and was not known, it was decided to move away from the fundamental parameter correction model to the empirical correction model.
- The correlation coefficients for all the other elements were 0.999 and above, illustrating straight lines with good correlations and no signs of inter-element effects. The preparation of the calibration standards with potassium iodide and the calibration of the EDXRF was successful.

The final set of calibration standards was prepared successfully. Roasted samples were used to prepare samples in all the previous experiments; however, the sulphur was never retained. The next step was to oxidise the samples, retain the sulphur and to validate the calibration achieved.

6. OXIDATION OF SAMPLES

6.1 Introduction

One of the features of an ideal fusion, as defined by Blank and Eksperiandova (1998), is the retention of all elements. Up to now most of the experiments completed were to investigate the retention of copper, together with the use of a non-wetting agent. In most cases this was done with roasted samples, where the sulphur in the samples was removed or oxidised. The objective was to create a glass bead with all the elements of interest present.

The concern with sulphur is that the unoxidised sulphides will react with the platinum ware and could cause severe damage. However, if the sulphides are oxidised to the highest oxidation state of SO_4^{2-} it will not react with the platinum or the other elements but will be stable and soluble in the borate flux (Claisse, 2000).

Oxidising agents investigated and reported include, sodium nitrate or ammonium nitrate as used by Norrish and Hutton (1969), combinations of sodium tetra-borate and sodium nitrate (80:20) or lithium tetra-borate and lithium nitrate (80:20) or lithium tetra-borate and cesium nitrate (80:20), as reported by Baker (1982). Claisse (2000) recommended the use of a 50:50 tetra-borate, meta-borate flux or tetra-borate together with the nitrate. In most cases the more acidic tetra-borate (when compared to meta-borate) was used with addition of nitrates.

Claisse (1995) claimed that the positioning of the sample and flux are important factors: the flux must always be weighed on top of the sample and oxidising agent mixture. This allows for the oxidising agent and the sample to react and for the sulphides to be completely oxidised before commencing with a full fusion procedure.

It will also prevent the physical loss of sulphur due to manual agitation or a vigorous reaction.

Temperature control for sulphur retention is very important and must be controlled as closely as possible and at a low as possible temperature. This is done by the addition of nitrates to the borate fluxes. The nitrate will lower the temperature at which the reaction takes place (Baker, 1982).

In the preliminary experiments, Chapter three, sodium tetra-borate flux together with potassium nitrate was used to oxidise the sulphide in the samples. The copper-, nickel-, iron-, cobalt-, PGE- sulphide buttons formed due to the sulphides melting at 700°C, settled at the bottom of the crucibles and amalgamated. The sulphide buttons were present even though enough potassium nitrate was added to oxidise the sulphur. These buttons formed because the fusion reaction occurred above the sulphides that had settled, and therefore oxidation only occurred at the top of the button which was in contact with the flux and oxidising agent. In addition, at the temperature of the fusion, 1100°C, the potassium nitrate had a side reaction with the sodium tetra-borate and was consumed, so the oxidising effect of the nitrate was lost. The conclusion made was that the sulphides must be fully oxidised below 700°C. This formed the basis of the investigation of an oxidation step whereby the sample, oxidising agent and flux are fused at a temperature lower than 700°C for a chosen time and then the full fusion process commence at a higher temperature.

Different oxidation steps were investigated with different heating sources, temperatures, times and oxidising agents. The first oxidising agent that was investigated was ammonium nitrate. The oxidation was carried out in the Electrofluxer and a hotplate, Section 6.2. Oxidation steps were investigated with the Electrofluxer, sodium nitrate and hydrated sodium per-borate, Section 6.3. The Electrofluxer was decommissioned after these experiments; therefore another set of oxidation factorial experiments was carried out using the Katanax and investigating

sodium carbonate, sodium nitrate and hydrated sodium per-borate as the oxidising agents, Section 6.3.

6.2 Oxidation step using the Electrofluxer

Experiments done so far indicated the necessity of an oxidation step at temperatures below 700°C. The first oxidation experiments were carried out using the Electrofluxer, with Lebowa Merensky concentrate sample (16% sulphur), ammonium nitrate as the oxidising agent and sodium iodide as the non-wetting agent, Section 6.2.1. The second set of oxidation experiments carried out in the Electrofluxer was done with sodium nitrate and hydrated sodium per-borate, Section 6.2.2.

6.2.1 Oxidation with ammonium nitrate and the Electrofluxer

The ammonium nitrate was chosen since it would decompose at higher temperature to produce N_2(g) and H_2(g) and NO_2(g) and NO(g). No metal oxide, for example Na_2O or K_2O, will be produced when using ammonium nitrate and therefore the basic and acidic properties of the flux would not be influenced.

The objectives of the experiments were to determine:

- Whether ammonium nitrate would oxidise the sulphides completely.
- Whether this oxidation could be completed before the Electrofluxer reached 700°C.

The crucibles were investigated to determine whether the sulphide interacted with the platinum ware as an indication that the sulphides were not oxidised. Another consideration was the appearance of the glass bead and whether the glass bead had any undissolved particles.

For the first experiment, sample (0.25 g) was weighed together with 1.0 g ammonium nitrate, 0.1 g sodium iodide and sodium tetra-borate flux (Appendix E, Table E-1). The crucible was loaded into the Electrofluxer when the Electrofluxer reached 600°C and was unloaded just before the Electrofluxer reached 700°C. The sample was loaded and unloaded manually. The sample did not spend a full ten minutes in the Electrofluxer and the oxidation step was dependant on how fast 700°C was reached. The full fusion process was then commenced at 1100°C for ten minutes.

The crucible was investigated after the fusion and it had black smears on the inside as well as black spots at the bottom. This indicated that the oxidation step was not efficient. The glass bead cracked during cooling, indicating the possible loss of non-wetting agent or the presence of undissolved particles.

The second glass bead was produced with 0.25 g sample, 1.0 g ammonium nitrate and sodium tetra-borate as the flux but this time the crucible was loaded into the Electrofluxer at 540°C and left for an oxidation step of ten minutes. It was decided to concentrate on the time rather than temperature and in the ten minutes the temperature of the Electrofluxer increased to 740°C. The sample was left to cool and the non-wetting agent added after the crucible was cool. The sample was loaded for a complete fusion process of ten minutes at 1100°C. After the fusion process the crucible was investigated and black smears were seen inside the crucible. The glass bead did not crack upon cooling indicating that the non-wetting agent was not lost and no undissolved particles were observed.

With the third glass bead produced a completely different methodology was followed. The oxidation step was carried out on a hotplate. The crucible was left on the hotplate at 400°C and weighed every two minutes. Once the mass was constant it would be seen as the end point of the reaction of the ammonium nitrate and the sample. The hotplate was used since the temperature could be controlled at 400°C and closely monitored. After forty minutes the mass of the sample was constant and

the potassium nitrate and potassium iodide was added and the sample fused at 1050°C for ten minutes. The potassium nitrate was added to make sure all of the sulphides were oxidised after the oxidation step.

Again the crucible was inspected and black smears were seen inside the crucible, indicating another incomplete oxidation of sulphides. The black smears indicated the possibility of the sample creeping up the sides of the crucible and reacting with the crucible before complete oxidation could take place. The glass bead did not crack and did not have un-dissolved particles.

All three the glass beads were analysed on the EDXRF with the calibration as created and discussed in Chapter four, Section 4.4.1. The sulphur recovery was calculated, Table 6-1.

Table 6-1: Relative percentage difference for Sulphur with ammonium nitrate as oxidising agent

Glass bead number	Sulphur concentration measured [%]	Known Sulphur concentration [%]	Relative percentage difference [%]
Glass bead 1	0.038	0.051	-34.2
Glass bead 2	0.040	0.051	-27.5
Glass bead 3	0.050	0.051	-2.0

The percentage differences indicate that the best result was achieved for glass bead 3 which was oxidised with ammonium nitrate on the hotplate at 400°C for forty minutes and then a full fusion commenced with the added potassium nitrate. The sulphur percentage difference is much higher for the two oxidations carried out in the Electrofluxer. The percentage difference for glass bead three is significantly improved when compared to the other two samples.

Conclusion that can be made from these experiments:

- The black smears in the crucibles indicate incomplete oxidations however, it is assumed that the samples crept up the sides of the crucibles during the fusion and the sulphides had the chance to react with the crucible walls before a complete oxidation was done. To prevent this, the oxidising agent and flux must be weighed on top of the sample.
- The ammonium nitrate does not appear to be an efficient oxidising agent and the sulphur recovery increased significantly with the addition of potassium nitrate. This could be due to the potassium nitrate contributing a basic oxide (K_2O) to the process while the ammonium nitrate only contributes the oxidant. The counter ion of the potassium nitrate will balance the acidic oxide of the sulphide, essentially forming K_2SO_4.
- Another factor that could contribute have to the poor recovery of sulphur while using ammonium nitrate as the oxidising agent, is the possibility of physical loss of the sample due to loss of nitrogen and oxygen.
- The Electrofluxer's temperature control is not efficient at lower temperatures and oxidations are done for ten minutes with the sample being unloaded at a temperature above the desired 700°C or unloaded at a lower temperature with a considerably shorter oxidation time. The glass beads produced indicated that not enough time at a lower temperature was achieved for the oxidation to be completed.
- The solution to the time and temperature control of the Electrofluxer was to complete the oxidation step on a hotplate and weigh the crucible to ensure the oxidation was completed. However this took forty minutes and is not a time that can be considered for producing results in a process control laboratory.

Since the ammonium nitrate did not prove successful the possibilities of other oxidising agents were investigated.

6.2.2 Oxidation with sodium nitrate and the Electrofluxer

The next set of oxidation experiments were carried out after the non-wetting agent was changed from sodium iodide to bromine gas, Chapter four, Section 4.6.3.

Since the previous oxidation experiments with ammonium nitrate were not successful in completely oxidising the sulphur present in the samples, it was decided to use sodium nitrate as well as hydrated sodium per-borate ($NaBO_3.4H_2O$). These will dissociate during the oxidation phase to produce basic oxides, sodium nitrate will produce Na_2O and per-borate will produce $NaBO_2$ (sodium meta-borate) which will both contribute to the basicity of the fusion. The objectives of these oxidation experiments were:

- To prevent the creeping of the samples up the sides of the crucibles by weighing the oxidising agents as well as the flux on top of the sample.
- Using a hydrated oxidising agent with a very low melting point to wet the sample.
- Fully oxidising the sulphides at the correct temperature and time.
- To improve sulphur recovery.

Four glass beads were produced using in-house Quality Control samples:

- PPL concentrate with 6.7% sulphur,
- Amandelbult Merensky (AMB MER) concentrate with 8.7% sulphur,
- Amandelbult UG2 (AMB UG2) concentrate with 3.3% sulphur, and
- Lebowa Merensky (LMER) concentrate with 18.1% sulphur.

All the glass beads were produced by weighing 0.25 g of the sample with 0.5 g sodium nitrate and 1.0 g sodium per-borate, then the flux and lastly 0.5 g sodium per-borate (Appendix E, Table E-2). The Electrofluxer was programmed for an oxidation step at 600°C for ten minutes followed by a full fusion of twelve minutes at 1100°C.

The oxidation step was not being controlled by the user, no manual loading and unloading at certain temperatures.

Even though the Electrofluxer was programmed at 600°C for ten minutes this temperature was not maintained very closely. The crucibles and glass beads were observed after cooling and for the PPL sample black smears could be seen inside the crucible. All three of the other glass beads had black residue left in the crucibles. None of the glass beads cracked during cooling and were analysed on the EDXRF. The sulphur recovery was calculated, Table 6-2.

Table 6-2: Relative percentage difference for Sulphur after oxidation with sodium nitrate and sodium per-borate

Sample	Sulphur concentration measured [%]	Known Sulphur concentration [%]	Relative percentage difference [%]
PPL	0.016	0.017	-6.3
AMB MER	0.020	0.022	-10.0
AMB UG2	0.008	0.008	0.0
LMER	0.044	0.047	-6.8

The percentage differences were between 0% and – 10% indicating a definite improvement from the previous set of oxidation experiments.

The conclusions that were made:

- The percentage differences indicate successful oxidation of the sulphur even though the crucible had residue.
- It was decided that the sample and oxidising agents must be mixed before adding the flux on top to ensure the entire sample is surrounded by the oxidising agents and will be wetted by the hydrated per-borate.

- Even though the temperature control of the Electrofluxer was not that efficient it allowed enough time, at the lower temperature, for the oxidation to take place.
- The improved oxidation can be attributed to the sodium nitrate being used instead of ammonium nitrate. Both the sodium nitrate as well as the sodium per-borate contributed basic oxides.
- The fact that less creep could be seen was an indication that the hydrated sodium per-borate was wetting the sample and preventing the creeping of the samples and assisting in the oxidation of the sample at a lower temperature.

These oxidation experiments were successful and optimising the oxidation step was the next consideration.

6.3 Oxidation experiments using the Katanax

The oxidation with the hydrated sodium per-borate improved the recovery of the sulphur in the samples as well as reduced the creeping of the sample up the sides of the crucibles. An oxidation factorial design experiment was designed to optimise the oxidation step. These experiments were carried out in the Katanax since the Electrofluxer had been decommissioned.

A factorial experiment is defined as an experimental design that consists of two or more factors with discrete possible values and the experimental units can take all possible combinations of these values across all factors. The factor is defined as a major independent variable with subdivisions or levels. Interaction effects can occur when a difference in one factor depends on the level of another factor (www.socialresearchmethods.net). Experimental designs address two different issues; one: how to design the optimal experiment and two: how to analyse the results. The objective of the experimental design is to allow the experimenter to

evaluate data in an unbiased fashion (www.statsoft.nl). Experimental design can be divided into various types depending on the outcome. For example, if the objective is to discover important factors: Plackett-Burman or fractional experimental designs can be used. If the objective is to determine effects and interactions of several factors: factorial and fractional experimental designs can be used. If the experimental design is done for optimisation: central composite, Box-Behnken, simplex or D-optimal experimental designs can be used (www.twi.co.uk). The factorial design results can be analysed using an ANOVA, regression analysis, interaction plots and probability plots (www.statsoft.nl). Diagnostic plots can be used to make observations of the effects of different factors on the response of the experiments. For example, a one factor or interaction graph and probability plot (www.statease.com, Industa Pro, 1 Peeka street, Die Boord, Stellenbosch, RSA, 7600).

6.3.1 Oxidation factorial experiments using the Katanax

The factorial design experiments were designed with the following objectives:

- Complete oxidation of the sample with the oxidising agents at the correct conditions.
- To prevent the creeping of the sample up the sides of the crucibles by the addition of the correct amount hydrated per-borate.
- Improved oxidation by improving the temperature control of the Katanax.
- Optimisation of the oxidation step with regard to the mass of the oxidising agents, oxidation temperature and time.
- Improved recovery of the sulphur in the samples, glass beads that do not crack and no undissolved particles in the glass beads.

The sample chosen for the oxidation factorial experiments was Amandelbult Merensky concentrate with a sulphur concentration of 8.65%. The sample mass,

sodium carbonate and flux mass were kept constant. Sodium iodide was used as the non-wetting agent. The parameters to be changed and tested were:

- The oxidation temperature between 400 and 600°C.
- The oxidation time between four and ten minutes.
- The sodium nitrate mass between 0 and 0.35 g.
- The hydrated sodium per-borate mass between 0.2 and 0.6 g.

The parameters to be measured were the glass bead appearance, the crucible appearance and the percentage difference between the measured sulphur concentration and the known sulphur concentration. The statistical program Design-Expert from Stat-Ease was used to determine the experimental design with these factors to consider and each parameter done in duplicate, Refer to Table 6-3 for the factorial design used to produce the glass beads, duplicate parameters are not shown.

Table 6-3: Oxidation factorial design using the Katanax

Glass bead number	Sodium nitrate [g]	Sodium per-borate [g]	Oxidation temperature [°C]	Oxidation Time [min]
POF 1	-	0.2	400	4
POF 3	0.350	0.2	400	4
POF 5	-	0.6	400	4
POF 7	0.350	0.6	400	4
POF 9	-	0.2	600	4
POF 11	0.350	0.2	600	4
POF 13	-	0.6	600	4
POF 15	0.350	0.6	600	4
POF 17	-	0.2	400	10
POF 19	0.350	0.2	400	10
POF 21	-	0.6	400	10
POF 23	0.350	0.6	400	10
POF 25	-	0.2	600	10
POF 27	0.350	0.2	600	10
POF 29	-	0.6	600	10
POF 31	0.350	0.6	600	10
POF 33	0.175	0.4	500	7
POF 35	0.175	0.4	500	7

The program used on the Katanax was set-up with a holding temperature of 395°C; refer to fusion parameters in Table 6-4

Table 6-4: Fusion parameters used in the Katanax

Step	Time [minutes]	Temperature [°C]	Rocking [%]	Tilting [°]
1	Factorial	Factorial	0	0
2	10	1000	90	24
3	0.5	800	90	24
4	0.5	900	90	24

The fusion parameters used during the factorial experiments show an initial temperature of 1000°C for ten minutes, which resulted in the fusion, thereafter the temperature was brought down to force any bubbles or air trapped in the glass bead to come out. The temperature was increased again to 900°C before casting to make sure the glass bead viscosity is correct and the casting easy.

Thirty six glass beads were produced and the crucible and glass bead appearances classified. Only two of the thirty six glass beads appeared to have black un-dissolved particles in the glass beads: POF 21 and 22 produced with no sodium nitrate and the maximum amount of sodium per-borate at the longest oxidation time of ten minutes showed that this condition was not optimal. Some of the crucibles had major residue after the fusion, indicating an incomplete oxidation step: POF 16, 18, 21, 26 and 36. However, this was only one of each duplicate glass bead. Refer to Appendix E, Table E-3 for the experimental results.

The glass beads were analysed using the final calibration program on the EDXRF created in Chapter Five Section 5.5. Values are compared to the known concentration in the sample used, Refer to Table 6-5. Refer to Appendix E, Table E-3 for the EDXRF results.

Table 6-5: Relative percentage differences for Sulphur after oxidation factorial

Glass bead number	Sulphur concentration measured [%]	Known Sulphur concentration [%]	Relative percentage difference [%]
POF 1	7.69	8.65	-12.5
POF 2	7.55	8.65	-14.5
POF 3	8.63	8.65	-0.2
POF 4	8.67	8.65	0.2
POF 5	8.08	8.65	-7.0
POF 6	7.71	8.65	-12.2
POF 7	8.61	8.65	-0.5
POF 8	8.87	8.65	2.5
POF 9	8.16	8.65	-6.0
POF 10	8.21	8.65	-5.3
POF 11	8.65	8.65	-0.1
POF 12	8.55	8.65	-1.1
POF 13	8.25	8.65	-4.8
POF 14	8.25	8.65	-4.9
POF 15	7.47	8.65	-15.7
POF 16	9.84	8.65	12.1
POF 17	8.05	8.65	-7.5
POF 18	7.86	8.65	-10.1
POF 19	8.82	8.65	1.9
POF 20	7.90	8.65	-9.4
POF 21	8.08	8.65	-7.0
POF 22	8.52	8.65	-1.6
POF 23	8.58	8.65	-0.8
POF 24	8.60	8.65	-0.6
POF 25	8.27	8.65	-4.6
POF 26	8.34	8.65	-3.7
POF 27	8.62	8.65	-0.4
POF 28	8.75	8.65	1.2
POF 29	8.39	8.65	-3.0
POF 30	8.67	8.65	0.2
POF 31	8.74	8.65	1.0
POF 32	8.74	8.65	1.0
POF 33	8.43	8.65	-2.6
POF 34	8.59	8.65	-0.7
POF 35	8.35	8.65	-3.6
POF 36	8.54	8.65	-1.3

The measured sulphur concentrations are blank corrected. The percentage difference between the measured concentration and the known concentration varies between –12.1 and 15.7%. There is no indication of a bias, where the sulphur measured is consistently lower or higher than the known sulphur concentration. Of all the glass beads prepared, twelve had percentage differences of more than five percent and the other twenty four glass beads had acceptable percentage differences.

The appearance of the glass bead and crucible together with the percentage difference were used in the statistical program to produce results and make conclusions regarding which parameters would be considered the best oxidation step. The results of the statistical program showed:

- The samples POF 15, 16 and 20 were identified as outliers with regards to all the other samples and their data was not further considered.
- An improved crucible appearance was observed with increased sodium nitrate.
- It also showed that the amount of sodium nitrate added had a more significant effect on the recovery of sulphur than the amount of sodium per-borate added.
- Sodium carbonate showed no effect on the parameters monitored since the mass was kept constant.
- The experiments also showed that the recoveries increased with increasing oxidation time and the optimal time was identified as ten minutes.

The conclusions made with the results of the oxidation factorial included:

- The best oxidation parameter was chosen as 600°C for ten minutes in the Katanax. The temperature close to the fusion temperature and will reduce the time spent in ramping up from 600°C instead of 400°C. The ten minutes will allow for complete oxidation of the sample before commencing with the fusions.

- The experiments showed that mixing the sample with the oxidising agents and covering the flux prevented the creeping of the samples up the sides of the crucibles and also contributed to a more complete oxidation of the sample.
- The sodium per-borate prevented the creeping of the sample up the sides of the crucible due to the loss of the water at 70°C and the wetting of the samples. However, it did not have a significant effect on the recovery of sulphur.
- The sodium nitrate played an important role in the oxidation of the sample by contributing sodium oxide which is a basic oxide.
- Sodium carbonate will contribute to the fusions by making the sodium tetra-borate flux more basic as well as contributing to the mixing of the sample due to the loss of CO_2(g).

Since no conclusion could be made regarding the mass of nitrate and per-borate to be added, this was investigated.

6.3.2 Determination of sodium nitrate, per-borate and carbonate ratio

The oxidation factorial indicated that sodium nitrate, sodium per-borate and sodium carbonate were of importance but the mass to be added could not be deduced with certainty. It was decided to test the contribution of the sodium carbonate, nitrate and per-borate with three experiments. In these experiments three glass beads were prepared and the mass of the sodium carbonate and nitrate was changed for each sample to establish the ideal mass of nitrate and carbonate to be used.

Three glass beads were produced with Amandelbult Merensky concentrate sample together with potassium iodide as the non-wetting agent and sodium tetra-borate as the flux. The mass of the nitrate and carbonate was changed as shown in Table 6-6 while the mass of the sodium per-borate was kept constant.

Table 6-6: Mass of sodium nitrate, per-borate and carbonate for ratio determination

Glass bead number	Sodium nitrate [g]	Sodium per-borate [g]	Sodium carbonate [g]
POF 37	0.50	0.50	0.50
POF 38	0.75	0.50	0.25
POF 39	0.25	0.50	-

The glass beads were produced with the optimal oxidation conditions, 600°C for ten minutes. The appearance of the glass bead and crucible as well as the relative percentage differences of sulphur were used to make a final decision regarding the ratio of the sodium oxidising agents to add.

The glass beads POF 37 and 38 did not crack, however POF 39 did crack, indicating that the masses used for the production of POF 39 were not ideal. The glass beads were analysed on the EDXRF using the final calibration program and the sulphur relative percentage differences determined, Table 6-7.

Table 6-7: Relative percentage difference for sulphur while testing ratio of oxidizing agents

Glass bead number	Sulphur concentration measured [%]	Known Sulphur concentration [%]	Relative percentage difference [%]
POF 37	8.69	8.65	0.4
POF 38	8.52	8.65	-1.5
POF 39	8.70	8.65	0.6

The relative percentage differences indicate that the best sulphur recovery was made with glass bead POF 37, indicating that the optimal conditions were 0.5 g of all three the oxidising agents.

The conclusions reached:

- Sodium carbonate is necessary to produce samples with perfect appearances.
- The amount of sodium nitrate added will influence the sulphur recovery.
- The best amount of oxidising agents is 0.5 g, of sodium nitrate, per-borate and carbonate.

Since the optimal oxidation conditions and the ideal masses for oxidising agents were determined the final set of samples were chosen and produced to validate the final calibration.

6.4 Conclusions

The final conclusions that were made regarding the use of the oxidising agents, temperature control, time for oxidation and weighing methodology followed is discussed:

- It was confirmed that at temperatures higher than 700°C the sulphur will melt and react and will not be recovered even if enough oxidising agent was used.
- Using a hotplate to control the temperature, and weighing the crucible until a constant mass was achieved increased the oxidation time to almost forty minutes which is not acceptable for process control or metal accounting laboratories in the mining environment. This will not be considered.
- The ammonium nitrate did not prove a good option as an oxidising agent since the sulphur was not recovered. This was attributed to sample loss due to the loss of gas as well as the ammonium nitrate not contributing a basic oxide.
- The sodium and potassium nitrates were a better choice of oxidising agents, however they did not prevent the creeping of the samples up the sides of the crucibles. Both wetting the sample as well as weighing the oxidising agents and flux on top of the samples were investigated and proved successful.

- Most of the crucibles showed evidence of the sample creeping up the sides of the crucible and reacting with the crucible instead of the oxidising agent and the flux. This was limited by the use of hydrated sodium per-borate. The hydrated sodium per-borate has a lower melting point and once this temperature is reached the hydrated per-borate will wet the sample and prevent the creeping of the sample up the sides of the crucible. It will also increase the contact of the oxidising agent and flux with the sample.
- The ideal combination of time, temperature and oxidising agents were achieved with the Katanax.
- The optimal oxidation step was at 600°C for ten minutes. The ideal oxidising flux was 0.5 g of sodium nitrate, 0.5 g of hydrated sodium per-borate and 0.5 g sodium carbonate.

Both XRFs would be calibrated with the calibration standards and it was decided to move away from empirical corrections to fundamental parameter corrections. Once both XRFs were calibrated with fundamental parameters the calibrations were compared.

7. COMPARISON OF EDXRF AND WDXRF CALIBRATIONS WITH FUNDAMENTAL PARAMETERS CORRECTION MODEL

7.1 Introduction

A set of calibration standards were prepared from pure oxides using the Katanax. Potassium iodide was the final choice as non-wetting agent and the empirical correction model was chosen instead of the fundamental parameter correction model for the calibration of the EDXRF (Chapter 5, Section 5.5). This was done since the concentration of the iodine was not known and could not be corrected for. Hence the fundamental parameter model did not work.

It was decided to determine the concentration of the iodide in the calibration standards and use that concentration to calibrate the XRFs to enable the use of the fundamental parameters correction model. The fundamental parameter corrections are preferred to the empirical corrections due to some of the disadvantages of the empirical corrections. The empirical correction model requires similar compositions for the samples and the calibration standards. The samples and the calibration standard preparation must be identical and the parameters used for calibration must stay the same for the analyses of the unknowns. Empirical corrections are very sensitive to any experimental error in data and can yield inaccurate results. The empirical corrections are also subjective to the operator that is calibrating the XRF and selecting the elements to be used for corrections. The fundamental correction model is a mathematical model that will take all effects for all elements in the matrix into account.

The iodide concentration in the calibration standards were determined, Section 7.2 and used to calibrate the EDXRF, Section 7.3 as well as the WDXRF, Section 7.4. The calibrations as well as calibration results of both XRFs are compared in Section 7.5.

Equipment and reagents used:

- Refer to Table A-1 for the list of reagents used.
- The powdered briquettes were prepared with a methacylate plastic vial with three plastic balls using the Spectromill from Chemplex.
- A hydraulic press was used to press the pulverised samples into briquettes with an aluminium backing cup.
- The briquettes were analysed on the Quant'X EDXRF.

7.2 Determination of iodide concentration in the final oxide calibration standards

The EDXRF was calibrated with powdered briquettes with known amounts of sodium iodide. Sodium iodide and sodium tetra-borate and wax binder was weighed together and mixed for three minutes. The mixture was then pressed into powdered briquettes using a hydraulic press with pressure at 20 tones. The calibration from the powdered briquettes was used to measure the final set of oxide calibration standards (prepared in Section 5.4) to determine the iodide concentration.

Once the iodide concentration was known the oxide calibration standards were used to calibrate both the EDXRF and the WDXRF, using the fundamental parameter correction model instead of the empirical correction model.

7.3 Calibration procedure and results for EDXRF

The EDXRF was calibrated with the oxide calibration standards and the determined iodide concentration using the parameters as summarised in Table 7-1.

Table 7-1: Measuring conditions for EDXRF calibration with fundamental parameter correction model

Condition name	Filter	Voltage [kV]	Live time [s]	Analytes
High Zb	Cu Thick	50	40	I
Mid Zb	Pd medium	20	60	Cr, Mn, Fe, Co, Ni, Cu, Zn
Low Za	None	4	60	Na, Mg, Al, Si, S
Low Zb	Cellulose	8	60	S, K, Ca, Ti, I

The calibration graphs were achieved; refer to Figures 7-1 to 7-4 and Appendix F, Figures F-1 to F-8 for the other calibration graphs and Table 7-2 for the summary of the correlation coefficient as determined by the XRF software for all elements.

Table 7-2: Summary of correlation coefficients achieved with EDXRF and fundamental parameter corrections

Element	Correlation coefficient
Na	0.7535
Mg	0.9999
Al	0.9993
Si	0.9996
S	0.9998
Ca	0.9992
Cr	0.9996
Fe	0.9999
Co	0.9998
Ni	0.9996
Cu	0.9991
I	1.0000

Most of the correlation coefficients are above 0.999 indicating very good correlations between the calculated and the known concentrations. The sodium correlation

coefficient is not close to 0.999 due to the sodium not representing a range of concentrations. The iodide coefficient is 1.000 and has improved considerably when compared to the calibration graph achieved when the iodide concentration was not determined, Chapter five, Section 5.5, Figure 5-12.

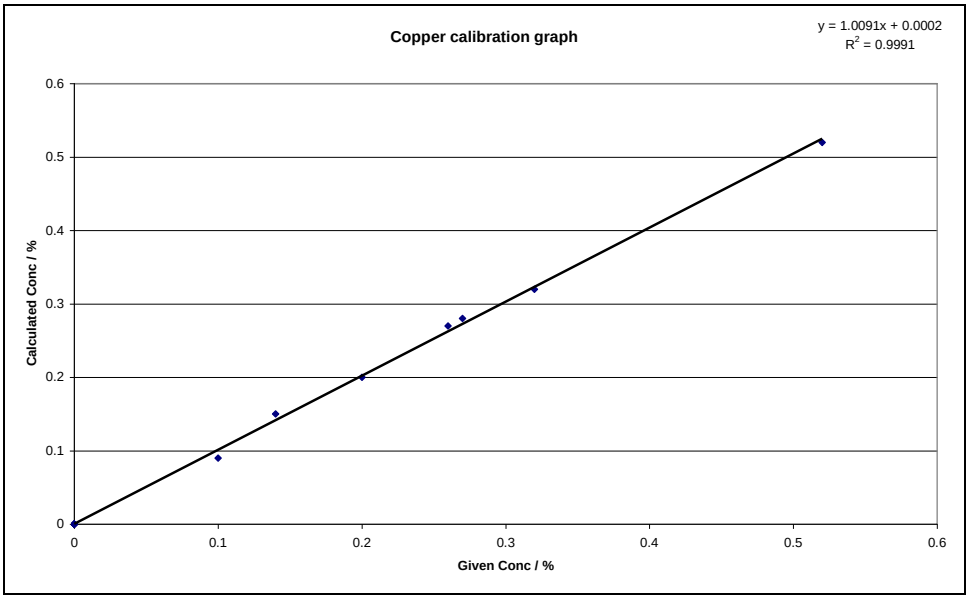


Figure 7-1: EDXRF Copper calibration graph with FP corrections [16]

The correlation coefficient for the copper calibration graph with fundamental parameter corrections is 0.999 and shows good correlation between the calculated and given concentration. No calibration standards were eliminated as outliers.

When comparing the regression achieved with the empirical corrections (Chapter five, Figure 5-7) the correlation coefficient for both are above 0.999 and the fundamental parameter calibration does not show a significant improvement. However, the fundamental parameter is the preferred correction model because it does not have the same limitations as the empirical correction model.

[16] Fundamental parameter correction model

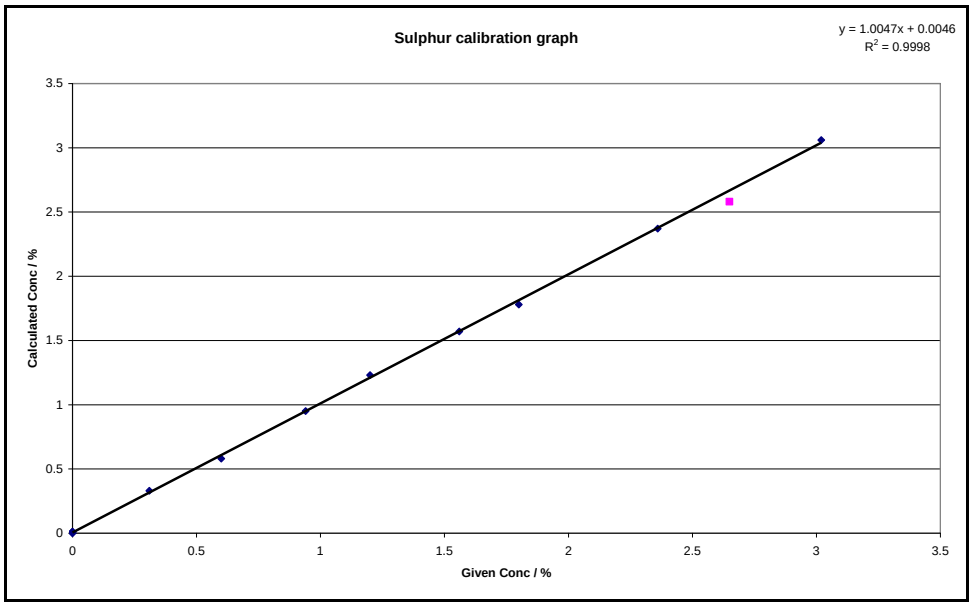


Figure 7-2: EDXRF Sulphur calibration graph with FP corrections

As in the case of the empirical corrections calibration, standard six is a clear outlier and was removed from the calibration graph. Calibration standard ten was also removed to improve the correlation of the graph. The correlation coefficient is 0.9998 and indicates a good correlation between the given and calculated concentrations. When comparing the empirical correction calibration (Chapter five, Figure 5-9) with the fundamental parameter calibration it does not indicate a significant improvement, however the fundamental parameters correction model is preferred.

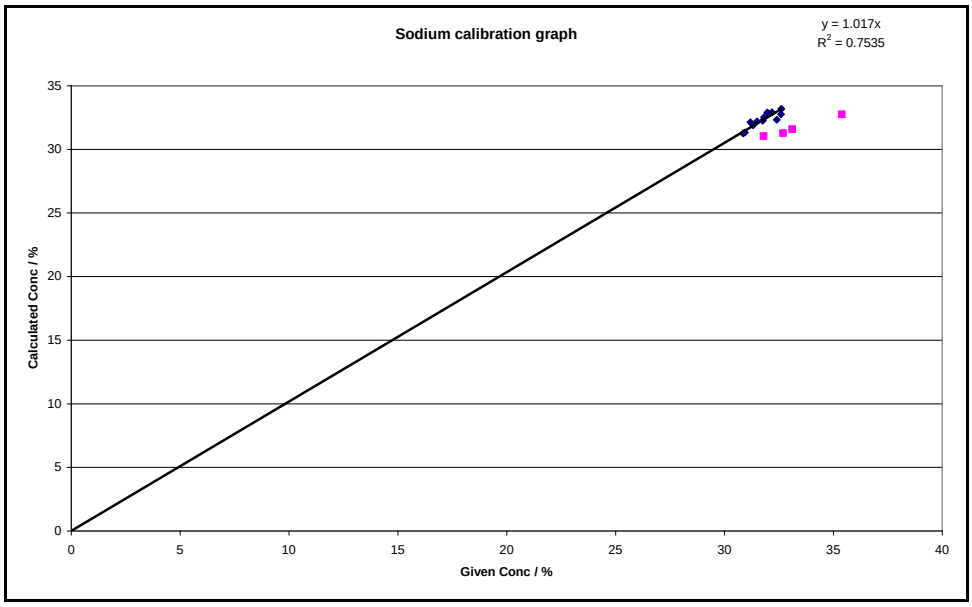


Figure 7-3: EDXRF Sodium calibration graph with FP corrections

Since almost all the calibration standards have the same sodium oxide content the points are grouped together. The correlation coefficient achieved with the empirical corrections (Chapter five, Figure 5-10) differs significantly from the fundamental parameters model. It shows that the fundamental parameter correction model has a greater influence on the lighter elements and could possibly also indicate that the iodide had an influence on the sodium which is now corrected for. Calibration standards ten, twelve as well as blank one and two were eliminated from the graph as outliers.

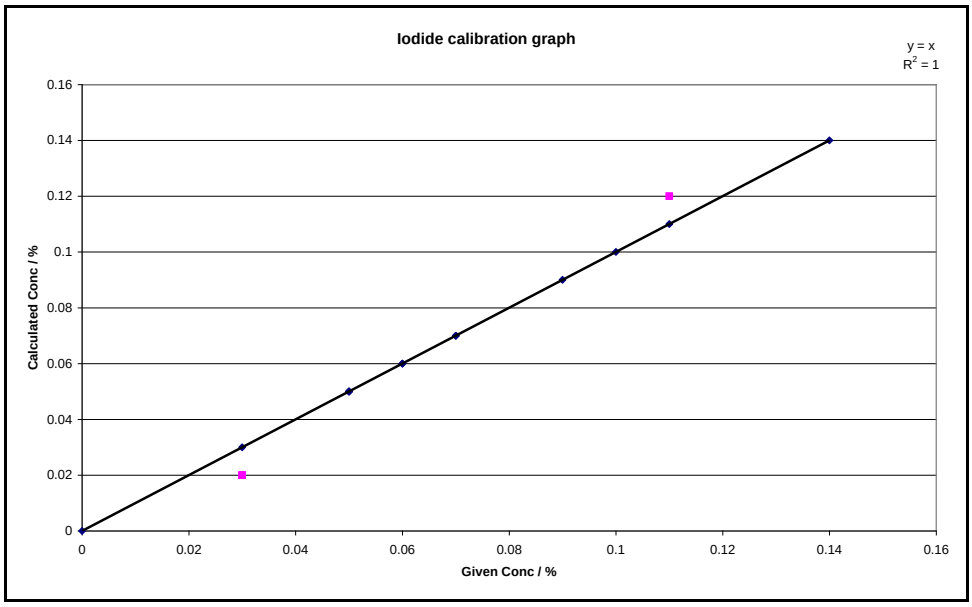


Figure 7-4: EDXRF Iodide calibration graph with FP corrections

The correlation coefficient of the iodide calibration line is 1.0000 and indicates a very good correlation between the given and calculated concentrations. This indicates that the determination of the iodide concentration was successful. Three calibration standards were eliminated as outliers, eight, ten and fourteen. When compared to the correlation coefficient of the empirical corrections with the concentration of iodide unknown (Chapter five, Figure 5-11) the improvement is significant.

The determination of the iodide concentration was clearly a success and enables the use of the fundamental parameter corrections, improving some of the calibration graphs, in particular with regards to the lighter elements.

7.4 Calibration procedure and results for WDXRF

In the case of the WDXRF, many more options are available as parameters when compared to the EDXRF. The calibration AP Float Conc was created on the PANalytical PW 2400 WDXRF. The application was created with a 27 mm mask,

which was used to limit the X-rays that reach the detector from the sample cup holder. The spinner was selected to remain on and this kept the glass bead spinning during analysis ensuring an overall exposure of the entire glass bead to the X-rays. The sample type was selected as solid and no loss of ignition corrections were made. The channels were selected and were element specific with reference to the crystals, angles, detectors and collimators to be used, refer to Table 7-3 for a summary of parameters selected.

Table 7-3: Summary of calibration parameters for WDXRF calibration

Element	Crystal	Collimator µm	Detector	kV	mA	Time [sec]
Al	PE 002	550	Flow	25	160	8
Ca	LiF 200	300	Flow	30	133	6
Co	LiF 220	150	Duplex	60	66	8
Cr	LiF 220	150	Duplex	50	80	4
Cu	LiF 220	150	Duplex	60	66	4
Fe	LiF 220	150	Duplex	60	66	4
I	LiF 220	150	Scint	60	66	8
K	LiF 220	300	Flow	25	160	6
Mg	PX1	550	Flow	25	160	12
Mn	LiF 220	150	Duplex	60	66	4
Na	PX1	550	Flow	25	160	6
Ni	LiF 220	150	Duplex	60	66	4
O	PX1	550	Flow	25	160	4
S	Ge 111	550	Flow	25	160	4
Si	PE 002	550	Flow	25	160	4
Zn	LiF 220	150	Scint	60	66	4

The selection and reasons for the selections was discussed in Chapter two Section 2.4. The time of analyses is much shorter as in the case of the EDXRF because more power can be produced. A 4 kW tube was used and the system was more sensitive to the lighter elements. The time reported in Table 7-3 includes, the time taken to analyse the element as well as the set-up of the background positions. Background corrections were determined by measuring standards with different concentrations of the elements of interest and checking whether there was any peak in the background

that could influence the peak of interest. For some elements line overlap corrections were applied, namely iron, cobalt, nickel, copper, chrome and manganese. In some cases the peaks of the elements were close to one another and the line overlap corrections corrected for this overlap. For example, the Fe Kβ was close to the Co Kα line. Before analysing the calibration standards the detector and angles for each element must be checked – this is called the PHD and angle checks. During the check angle, background positions and line overlap corrections were determined. The PHD is the pulse height selection and it is an electronic way of removing unwanted pulses which are present in the measured signal but which do not originate from the element of interest. Circuitry of the PHD selector acts like an electronic filter removing unwanted pulses and passing the pulses of interest. The unwanted pulses can be created by low voltage electronic noise, reflections from the crystals and crystal fluorescence. The fluorescence can only be removed provided that the energy is sufficiently different from the element that is being measured.

After analysing the calibration standards the fundamental parameter correction was applied and the calibration graphs evaluated. The regression analysis in the software of the WDXRF includes an error weighting function which enables the operator to force the regression analysis to concentrate on certain areas of the concentration range. In this calibration the square root error weighting function was chosen. The goodness of fit or correlation coefficient is the K-factor and it should have a value of between 0.01 and 0.10.

Refer to Table 7-4 for the summary of the calibration parameters for the calibration graphs as achieved with the WDXRF. The factors to consider with the WDXRF software is D, E and K where the D is the negative value of the background equivalent concentration (usually in %) and E is the inverse of sensitivity (usually kcps / %).

Table 7-4: Summary of calibration graph parameters for WDXRF

Element	D	E	K
Al	-0.002	0.016	0.0
Ca	-0.001	0.021	0.0
Co	-0.0	0.050	0.0
Cr	-0.0	0.070	0.0
Cu	-0.001	0.032	0.01
Fe	-0.002	0.056	0.0
I	0.001	0.163	0.01
K	-0.0	0.020	0.01
Mg	0.005	0.008	0.0
Mn	-0.0	0.066	0.0
Na	Locked	0.014	0.08
Ni	-0.001	0.037	0.0
O	Locked	0.827	0.08
S	-0.002	0.013	0.0
Si	-0.006	0.02	0.01

In the case of sodium and oxygen, the D value is locked which indicates that the calibration line was forced through zero. This is done since the original calibration line would cut the Y or X-axis. Since there were no blank calibration standards for sodium or oxygen, the calibration standards were grouped together and therefore the line is constrained through zero. As previously discussed, a very good fit will be indicated with a K-factor of between 0.01 and 0.1, as can be seen for copper, iodide, potassium, sodium, oxygen and sulphur. The calibration graphs as configured by the WDXRF software are displayed in Figures 7-5 to 7-8.

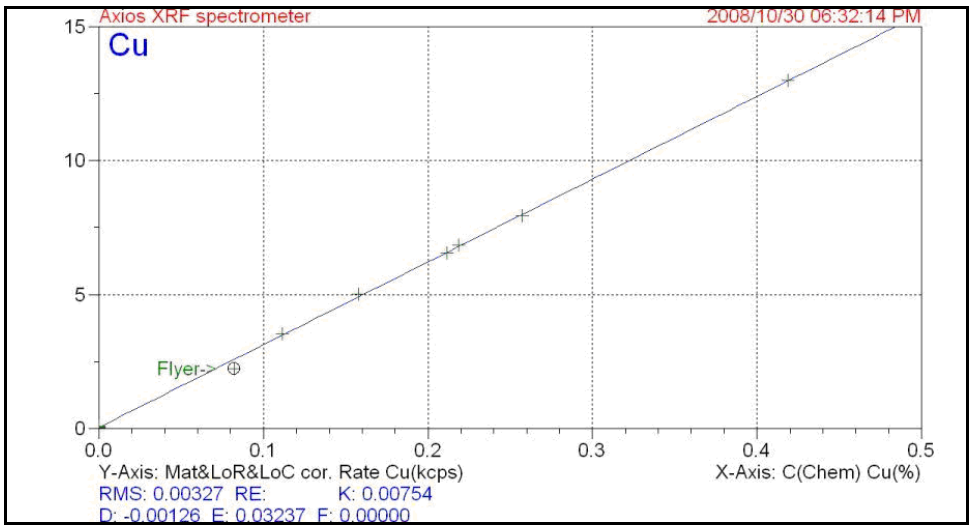


Figure 7-5: WDXRF Copper calibration graph with FP corrections

The calibration graph indicates a good correlation between the intensities measured for copper and the chemical value as specified by the operator when calibrating. No significant outlier could be identified and no calibration standard was eliminated.

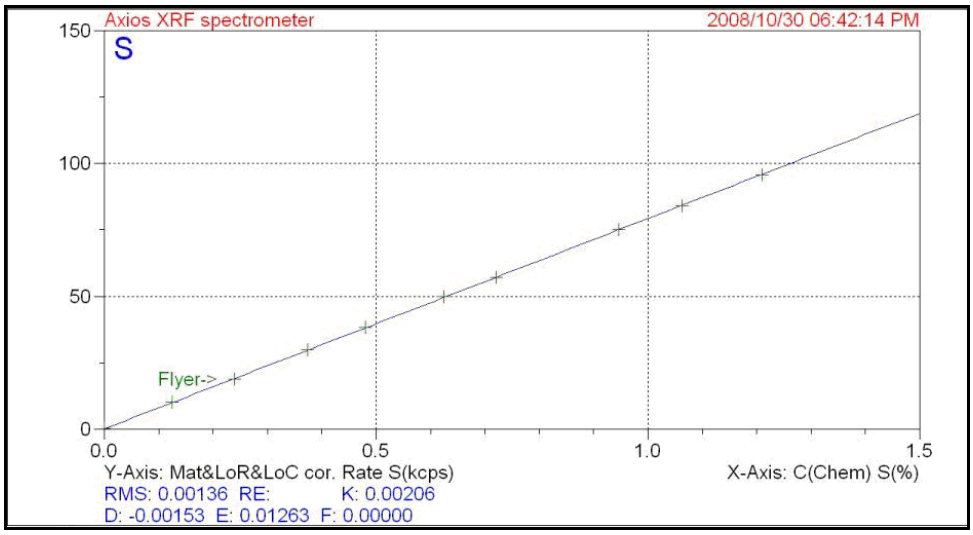


Figure 7-6: WDXRF Sulphur calibration graph with FP corrections

As can be seen from the graph, a very good correlation was achieved between the measured intensities and the concentration of the standards. Calibration standard six

was removed from the calibration as an outlier; this was done for the EDXRF calibration as well.

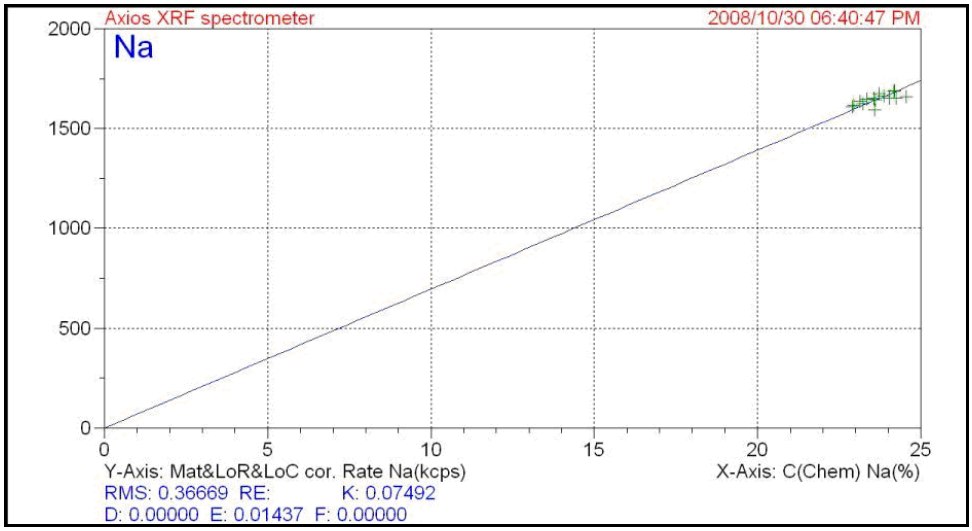


Figure 7-7: WDXRF Sodium calibration graph with FP corrections

As can be seen from the graph and as discussed earlier the calibration standards for sodium are grouped together. The intercept must be constrained through zero since there is not a wide enough range to obtain a good line.

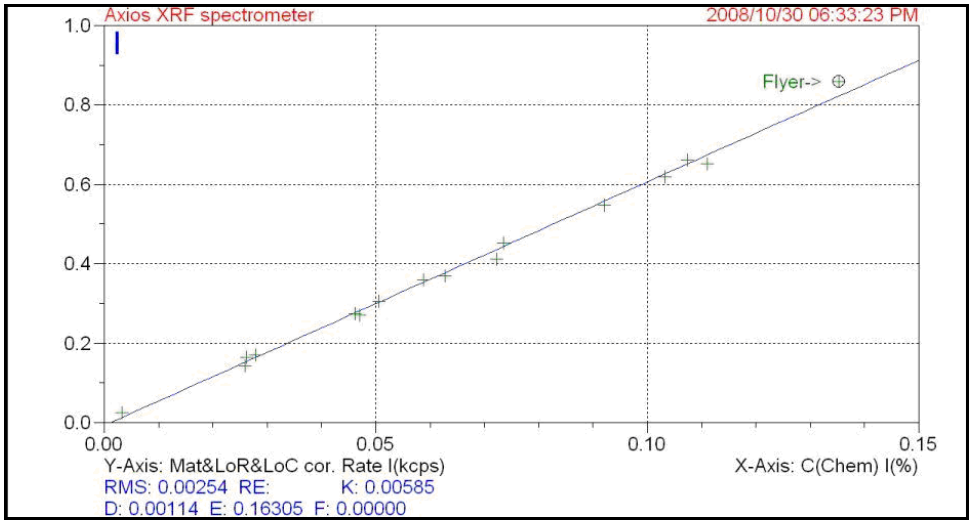


Figure 7-8: WDXRF Iodide calibration graph with FP corrections

As can be seen from the graph, good correlation was achieved between the intensities measured for iodide as well as the calculated concentration of iodide. No outliers were identified or eliminated.

The calibration graphs of the other elements are shown in the Appendix F, Figures F-F-9 to F-15.

7.5 Comparison of calibrations achieved for EDXRF and WDXRF

Since the software of the EDXRF and the WDXRF summarises the calibration parameters differently the correlation coefficients cannot be compared. The calibration graphs will be compared in overall.

For lighter elements a great improvement can be seen when comparing the results from the WDXRF and EDXRF. More of the calibration standards are on the straight line when compared to the EDXRF. An overall improvement can also be seen for the heavier elements when comparing the results of WDXRF to those of the EDXRF. The calibration for iodide is significantly improved when compared.

The improvements are contributed to the more powerful WDXRF, when compared to the EDXRF, which improves the sensitivity for the lighter elements. The WDXRF has three detectors to cover a variety of elements and improves the sensitivity by choosing the more sensitive detector. The EDXRF only uses one detector and this detector is not as sensitive to the lighter elements as the heavier elements.

7.6 Conclusion

- It can be seen from the calibration graphs achieved for iodide by both the EDXRF and the WDXRF that the determination of the iodide concentration by using the powdered briquettes was successful. The determination of the iodide concentration allowed the use of fundamental parameter corrections for both XRFs.
- The fundamental parameter corrections are more accurate when compared to the empirical corrections due to the empirical corrections being subject to the operator's choice. The fundamental parameters correction model corrects for all matrix effects of all elements on one another, mathematically. With empirical corrections the coefficient can only be applied to unknowns with similar compositions as the samples. The calibration standards and the sample preparation must be identical. This will limit the sample type that can be fused and analysed.
- The comparison of the calibration graphs for the EDXRF empirical versus fundamental parameter corrections does not indicate significant improvements. However, the known iodide concentration definitely improved the calibration achieved for iodide.
- The comparison of the EDXRF and WDXRF calibration lines with fundamental parameters indicate significant improvements for almost all the elements but especially the lighter elements. The improvements are attributed to the higher power available to the WDXRF. The resolution of the WDXRF detectors is good, whereas the deconvolution of the EDXRF detector is limited.

The next step was to produce samples with known concentrations using the final program as created with the Katanax in Chapter Six. These samples will be used to validate the calibration as achieved with the WDXRF; since it was proven that the WDXRF calibration is better than the EDXRF.

8. VALIDATION OF FINAL WDXRF CALIBRATION

8.1 Introduction

Both XRFs were calibrated with the final set of calibration standards and the calibrations compared in Chapter seven. Since the conclusion was made that the WDXRF calibration was better it was decide to validate this calibration. The only way to validate the accuracy and determine the success of the calibration, as well as the use of the fundamental parameters, is to prepare and analyse samples with known concentrations and compare the results achieved by fusion.

One of the features of an ideal fusion as discussed by Blank and Eksperiandova (1998) is the retention of all elements present. In Chapter five, the copper retention, with potassium iodide as the non-wetting agent and the alternative heating mechanism of the Katanax, was resolved and in Chapter Six the retention of sulphur, with an oxidation step was achieved. In this Chapter the unknown samples were used to determine whether an ideal fusion was achieved.

8.2 Samples produced for validation of final calibrations

The validation will include the final set of calibration standards produced, the success of the non-wetting agent used, the success of the copper recovery, the oxidation step as well as the sulphur recovery.

The objectives of the production of the glass beads were:

- Complete oxidation of the sulphur in the sample together with complete recovery of sulphur,

- The use of non-wetting agent that prevents the cracking of the glass bead together with complete copper recovery,
- Perfect glass beads with no bubbles, no undissolved particles or cracks, and
- The recovery of all elements of interest.

The glass beads were divided into two groups, samples with known concentrations, determined by different laboratories and statistically evaluated to determine the uncertainty in the measurements. These samples have assigned concentrations with determined higher and lower concentration limits and are used in the mining laboratories as Quality control samples (POF 46 – 55). For the other group of glass beads; the concentrations were determined by one laboratory and these samples are not used as QC samples but just as samples with known concentrations for comparative reasons.

All the glass beads were prepared in duplicate and only the average results will be discussed in this Chapter. For the full detail of preparation and raw data refer to Appendix G, Table G-1.

Table 8-1: Summary of samples produced with final set of parameters

Glass bead number	Sample used	Sample Type	Sample mass [g]
POF 46, 47	LMC QC[17] 03	Lebowa Merensky	0.3
POF 48, 49	LUC QC 02	Lebowa UG2	0.7
POF 50, 51	BMC QC 02	BRPM Merensky	0.5
POF 52, 53	MUC QC 03	Modikwa UG2	0.7
POF 54, 55	PPC QC 02	PPL concentrate	0.7
POF 40, 41	KM AMC	Amandelbult Merensky	0.7
POF 42, 43	KM AUC	Amandelbult UG2	0.7
POF 44, 45	KM PPC	PPL concentrate	0.7
VOC 1, 2	AMCPS	Amandelbult Merensky	1.0
VOC 3, 4	AMMCW	Amandelbult Merensky	1.0
VOC 5, 6	ANUCPS	Amandelbult UG2	1.0
VOC 7, 8	AUGPS	Amandelbult UG2	1.0
VOC 9, 10	BRFDC 258	BRPM Merensky	1.0
VOC 11, 12	BRFDC 284	BRPM Merensky	1.0
VOC 13, 14	LMRPS	Lebowa Merensky	1.0
VOC 15, 16	LUGPS	Lebowa UG2	1.0
VOC 17, 18	MDCPS	Modikwa Concentrate	1.0
VOC 19, 20	MTCPS	Modikwa concentrate	1.0
VOC 21, 22	PPLPS	PPL concentrate	1.0
VOC 23, 24	UWCPS	Union feed	1.0
VOC 25, 26	WNXPS	Waterval feed	1.0
VOC 31, 32	AMCPS	Amandelbult Merensky	0.5
VOC 33, 34	AMMCW	Amandelbult Merensky	0.5
VOC 35, 36	BRFDC 258	BRPM Merensky	0.5
VOC 37, 38	BRFDC 284	BRPM Merensky	0.5
VOC 39, 40	LMRPS	Lebowa Merensky	0.5
VOC 41, 41	LUGPS	Lebowa UG2	0.5

In the case of the POF samples, the mass was calculated dependent on the sulphur concentration and therefore varied between 0.3 g and 0.7 g. In the case of the VOC samples, 1.0 g of the sample was used and 0.5 g for VOC 31 to 41. The oxidising agents chosen were sodium nitrate, sodium carbonate and hydrated sodium per-borate, 0.5 g of each was mixed with the sample and weighed at the bottom of the crucible. This was covered by the sodium tetra-borate and potassium iodide as the

[17] QC Quality control sample used by group laboratories

non-wetting agent. The oxidation step was carried out,m followed by the full fusion program as summarised in Table 8-2.

Table 8-2: Summary of fusion program used to produce glass beads for validation of final calibration

Step	Time [minutes]	Temperature [°C]	Rocking [%]	Tilting [°]
1	10	600	0	0
2	10	1000	90	24
3	0.5	800	90	24
4	0.5	900	90	24

All the glass beads prepared were perfect with no bubbles or cracks and no un-dissolved particles. The results of the duplicate samples were averaged and the average concentrations will be compared to the consensus values (known concentrations). All the samples compared by determining the relative percentage difference between the measured concentration in the glass bead and the known concentration in the sample as well as doing a student t-test to determine whether the concentrations are significantly different. For the QC samples, the uncertainty in the known value will be used to determine whether the concentrations in the glass beads are similar. This will also be used to determine whether the glass beads fail or pass the limits as used in the laboratories for quality control. The results are represented in a graph comparing the measured concentrations to the known concentrations and the correlation coefficient determined. Outliers were removed based on statistical analyses, relative percentage differences and t-calc values, as well as visual inspection.

8.3 Comparison and discussion of copper results

Table 8-3: Comparison of consensus and measured values for copper

Sample Type	Average measured copper concentration [%]	Standard deviation	Consensus value [%]	Relative percentage difference [%]	t-calc[18]
KM AMC	2.01	0.00	2.04	-1.72	7.15
KM AUC	0.82	0.03	0.78	4.30	0.84
KM PPC	1.48	0.01	1.46	1.41	1.09
LMC QC 03	4.19	ND[19]	4.28	-2.15	ND
LUC QC 02	2.49	0.01	2.55	-2.50	6.81
BMC QC 02	3.35	0.02	3.44	-2.78	3.07
MUC QC 03	0.62	0.00	0.56	9.37	68.61
PPC QC 02	1.92	0.02	1.92	0.15	0.12
AMCPS	1.61	0.02	1.88	-16.92	11.85
AMMCW	1.83	0.06	2.19	-19.88	4.49
ANUCPS	0.35	0.06	0.30	13.56	0.56
AUGPS	0.47	0.06	0.41	12.38	0.63
BRFDC 258	2.56	0.05	3.00	-16.96	6.64
BRFDC 284	2.15	0.02	2.57	-19.54	14.49
LMRPS	1.27	0.06	1.41	-10.95	1.74
LUGPS	0.84	ND	0.91	-8.48	ND
MDCPS	0.79	0.07	0.72	8.43	0.67
MTCPS	0.34	0.02	0.30	10.88	1.65
PPLPS	1.66	0.01	1.65	0.55	0.48
UWCPS	0.57	0.02	0.52	8.01	1.41
WNXPS	1.66	0.03	1.78	-7.12	3.13
AMCPS	1.93	0.10	1.88	2.44	0.34
AMMCW	2.16	0.02	2.19	-1.51	0.96
BRFDC 258	2.99	0.04	3.00	-0.42	0.22
BRFDC 284	2.50	0.07	2.57	-2.80	0.69
LMRPS	1.28	0.04	1.41	-10.48	2.61
LUGPS	0.87	0.04	0.91	-4.14	0.64

The standard deviations calculated for the replicate samples indicate good replicates and good precision for the method. In the case of LUGPS and LMC QC 03, the one replicate sample was significantly different and the results represented are not the average.

[18] Absolute values are reported
[19] Not determined – only one of the duplicate samples were used for the comparison

The relative percentage differences vary between -19.8% for AMMCW and 13.56% for ANUCPS. The relative percentage differences for all the glass beads were both negative and positive indicating that the measured concentrations were above and below the consensus values and do not represent a bias or systematic error. The student t-test for a comparison to a known value was used and the t-calc determined for each sample. The t-crit value is 12.71 and represents the degrees of freedom of one at a confidence interval of 95% (Skoog, West and Holler, 1996).

Only two samples had a t-calc larger than t-crit indicating a significant difference between the measured and the consensus value. These samples are MUC QC 03 and BRFDC 284. The two samples do not have the lowest or highest copper content and fall well within the copper calibration range. The percentage differences for the two samples indicate that the measured concentrations were above and below the assigned values. The difference in copper concentration can be attributed to errors while preparing the glass beads or the possibility that the consensus values were determined incorrectly.

The QC samples are also compared to the uncertainty in the consensus value, Table 8-4. These uncertainties are used to determine limits wherein the QC must fall during analyses for quality control. If the percentage difference between the measured concentration and the consensuses value is less than the uncertainty in the consensus value then the results will pass the limits and will be accepted as accurate.

Table 8-4: Comparison of copper results for quality control samples

Sample type	Average measured Copper concentration [%]	Consensus value [%]	Uncertainty in consensus value [%]	Relative percentage difference [%]	Pass or fail
LMC QC 03	4.19	4.28	± 2.34	-2.22	Pass
LUC QC 02	2.49	2.55	± 6.27	-2.50	Pass
BMC QC 02	3.35	3.44	± 5.23	-2.78	Pass
MUC QC 03	0.62	0.56	± 3.57	9.37	Fail
PPC QC 02	1.92	1.92	± 2.60	0.15	Pass

The comparison indicates that only one of the glass beads failed the limits and was not accepted as accurate. The MUC QC 03 results were also indicated as significantly different as seen in Table 8-3 and therefore the result of this sample was inaccurate. This QC sample has the lowest copper concentration compared to other QC samples and could indicate an error on the lower range of the copper calibration. From Figure 7-5, it can be seen that one of the lower calibration standards was slightly off the calibration line. This could influence the analyses of all the lower concentration copper samples. In the comparison of the results it can be seen that samples with a similar concentration to the QC sample, yielded measured values that were higher than the consensus values. It could, however, also be a sample preparation error for this sample. Another consideration is an error in the determination of the consensus value; the possibility exists that this QC could have been contaminated. A graphic comparison was made between the measured and the consensus values as seen in Figure 8-1.

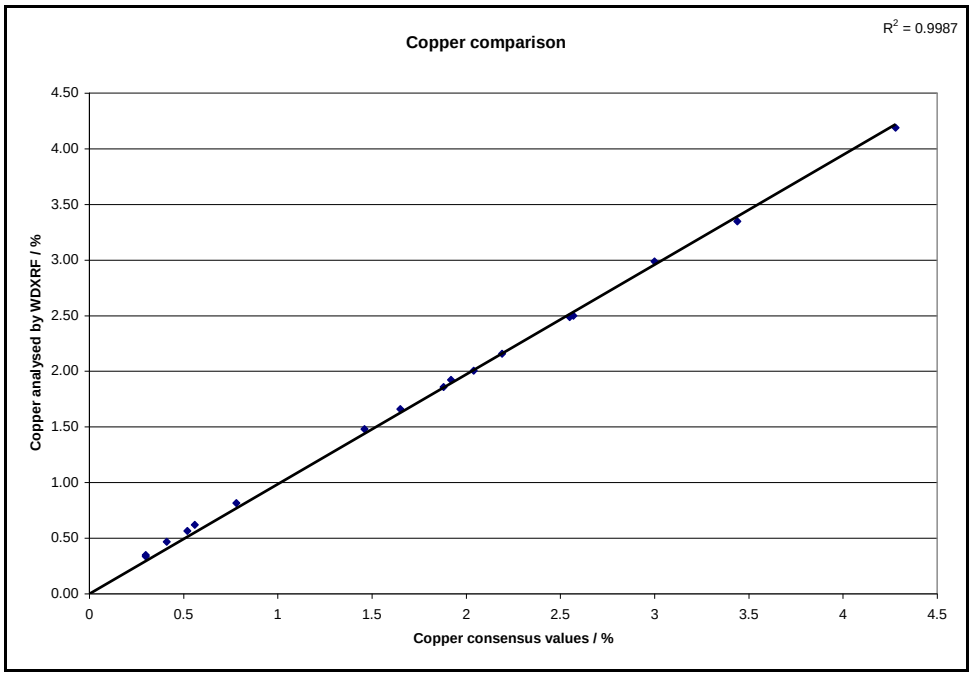


Figure 8-1: Comparison of consensus values and measured values for copper

Of the twenty seven samples prepared, eight were removed from the graph as outliers. The eight included the samples with the high percentage differences as well as the significantly different MUC QC03 sample. The comparison shows a correlation coefficient of 0.999, indicating a very good comparison between the measured results and the consensus values.

8.4 Comparison and discussion of nickel results

Table 8-5: Comparison of consensus and measured values for nickel

Sample Type	Average measured nickel concentration [%]	Standard deviation	Consensus value [%]	Relative percentage difference [%]	t-calc
KM AMC	3.49	0.0	3.69	-5.64	210.97
KM AUC	1.44	0.0	1.42	1.07	2.82
KM PPC	2.71	0.01	2.72	-0.54	0.93
LMC QC 03	7.44	ND	7.59	-2.06	ND
LUC QC 02	3.80	0.0	3.90	-2.61	28.78
BMC QC 02	4.91	0.01	5.10	-3.93	27.25
MUC QC 03	0.93	0.0	0.88	5.48	19.05
PPC QC 02	3.39	0.03	3.40	-0.37	0.30
AMCPS	3.20	0.04	3.43	-7.30	4.06
AMMCW	3.62	0.06	3.98	-10.03	4.02
ANUCPS	0.61	0.03	0.56	8.08	1.06
AUGPS	0.97	0.05	0.94	3.21	0.47
BRFDC 258	4.24	0.02	4.49	-5.79	11.32
BRFDC 284	3.56	0.12	3.28	7.98	1.63
LMRPS	1.47	0.02	1.85	-25.95	11.45
LUGPS	1.26	ND	1.54	-22.22	ND
MDCPS	1.16	0.06	1.09	6.23	0.90
MTCPS	0.79	0.02	0.79	0.15	0.05
PPLPS	2.65	0.01	2.59	2.33	4.12
UWCPS	1.13	0.01	1.04	8.00	8.41
WNXPS	2.81	0.02	3.10	-10.21	9.31
AMCPS	3.37	0.07	3.43	-1.89	0.66
AMMCW	3.91	0.02	3.98	-1.87	2.98
BRFDC 258	4.51	0.02	4.49	0.39	0.51
BRFDC 284	3.82	0.04	3.28	14.19	8.53
LMRPS	1.47	0.01	1.85	-25.86	19.86
LUGPS	1.26	0.0	1.54	-22.17	103.26

The standard deviations between the replicate glass beads are small and indicate good precision for the method. The relative percentage differences varied between 14.19% for BRFDC 284 and – 25.95% for LMRPS. The nickel concentrations in these two samples were not the lowest or highest in the range. There were both positive and negative percentage differences indicating no bias or systematic error. For the

student t-test, six samples have a higher t-calc than t-crit indicating that the measured concentration are significantly different. These samples are KM AMC, LUC QC 02, BMC QC 02, MUC QC 03, LMRPS (0.5 g) and LUGPS (0.5 g). These samples have high and low nickel concentrations and the difference cannot be attributed to the range of nickel or an error in the calibration at a certain concentration. It can be assumed that the samples had preparation errors, for example, weighing errors or fusion errors. It can also indicate that the consensus values were assigned incorrectly and the alternative methods were not accurate. Three of the significantly different samples are QC samples and the same could be seen for MUC QC 03 for copper. The QC values and the uncertainties are compared in Table 8-6.

Table 8-6: Comparison of nickel results for quality control samples

Sample type	Average measured nickel concentration [%]	Consensus value [%]	Uncertainty in consensus value [%]	Relative percentage difference [%]	Pass or fail
LMC QC 03	7.44	7.59	3.69	-2.06	Pass
LUC QC 02	3.80	3.9	6.15	-2.61	Pass
BMC QC 02	4.91	5.1	3.92	-3.93	Pass
MUC QC 03	0.93	0.88	3.41	5.48	Fail
PPC QC 02	3.39	3.4	3.24	-0.37	Pass

If the uncertainties in the consensus values are taken into account only one of the QC samples failed the limits and that was MUC QC 03. This QC sample also failed the limits for copper. The measured value was more than the consensus value and as in the case of copper this sample has a low nickel concentration when compared to the other QC samples. All the samples with low nickel concentrations measured higher than the consensus values. Since the nickel calibration graph does not show any error, Figure F-14, it cannot be attributed to the lower concentration calibration range. However, the error could lie with the calibration standards and the possibility that the values used to calibrate the WDXRF at lower ranges were incorrect. This could indicate that the purity of the nickel oxide used for standard preparation was

questionable and would have a greater effect at lower concentration ranges. The significant difference for MUC QC 03 could also indicate sample preparation errors since the same can be seen for copper and the possibility also exists that the QC was contaminated or the consensus values are incorrect.

The QCs that were significantly different do not fail the limits, indicating that the uncertainty in the determination of the consensus value was higher than the percentage difference between the measured and consensus value. The concentrations obtained was acceptable and the results accurate according to the quality requirements of the mining laboratories.

The graphic presentation of the results can be seen in Figure 8-2.

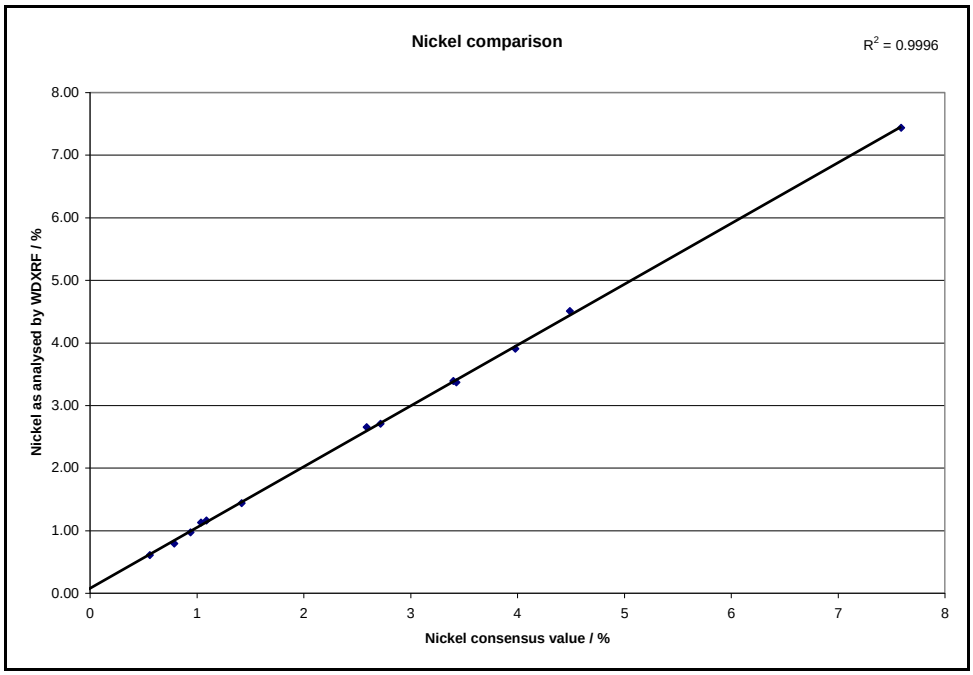


Figure 8-2: Comparison of consensus values and measured values for nickel

Of the twenty seven glass beads prepared, fourteen were removed from the graph as outliers. The samples removed as outliers included the samples with high percentage differences as well as the QCs that were significantly different. The correlation

coefficient between the measured and consensus values was 0.9996 and indicated a good comparison and good nickel recovery.

8.5 Comparison and discussion of sulphur results

Table 8-7: Comparison of consensus and measured values for sulphur

Sample Type	Average measured sulphur concentration [%]	Standard deviation	Consensus value [%]	Relative percentage difference [%]	t-calc
KM AMC	8.74	0.10	8.65	0.99	0.59
KM AUC	3.23	0.02	3.23	-0.01	0.01
KM PPC	7.10	0.04	6.95	2.13	2.73
LMC QC 03	17.98	ND	18.1	-0.67	ND
LUC QC 02	8.00	0.03	8.02	-0.20	0.40
BMC QC 02	12.22	0.08	12.2	0.13	0.15
MUC QC 03	1.98	0.0	1.83	7.44	675.96
PPC QC 02	9.20	0.06	9.06	1.55	1.80
AMCPS	8.85	0.06	8.27	6.55	6.60
AMMCW	9.95	0.07	10.19	-2.40	2.34
ANUCPS	1.36	0.01	1.34	1.39	2.36
AUGPS	1.81	0.01	1.49	17.56	18.37
BRFDC 258	12.08	0.05	12.34	-2.18	3.97
BRFDC 284	9.69	0.58	10.42	-7.58	0.90
LMRPS	3.64	0.0	4.01	-10.21	73.57
LUGPS	2.63	ND	3.04	-15.48	ND
MDCPS	2.18	0.0	2.25	-3.17	120.47
MTCPS	1.48	0.01	1.39	6.03	5.82
PPLPS	7.32	0.06	6.7	8.53	7.38
UWCPS	2.12	0.01	2.12	0.18	0.19
WNXPS	7.51	0.06	7.69	-2.33	2.25
AMCPS	8.82	0.02	8.27	6.23	19.35
AMMCW	10.02	0.05	10.19	-1.66	2.30
BRFDC 258	12.23	0.01	12.34	-0.93	6.02
BRFDC 284	10.04	0.0	10.42	-3.83	69.68
LMRPS	3.66	0.02	4.01	-9.57	15.51
LUGPS	2.61	0.03	3.04	-16.26	10.84

The standard deviations of the duplicates are low indicating good replicates and good precision for the fusion method.

The relative percentage differences vary between -16.26% for LUGPS (0.5 g) and 17.56% for AUGPS. The percentage differences were both positive and negative indicating no bias. Seven of the samples have a t-calc larger than the t-crit, indicating a significant difference between the measured and consensus concentrations. These samples were MUC QC 03, AUGPS, LMRPS (1.0 g and 0.5 g), MDCPS, AMCPS and BRFDC 284 (0.5 g). This included MUC QC 03 which was significantly different for copper and nickel, as well as two samples with the highest percentage differences. These samples have varying concentrations of sulphur and the error does not occur for low or high concentration samples only. The comparison with the QC control samples are shown in Table 8-8.

Table 8-8: Comparison of sulphur results for quality control samples

Sample type	Average measured nickel concentration [%]	Consensus value [%]	Uncertainty in consensus value [%]	Relative percentage difference [%]	Pass or fail
LMC QC 03	17.98	18.10	2.54	-0.67	Pass
LUC QC 02	8.00	8.02	2.00	-0.20	Pass
BMC QC 02	12.22	12.20	5.74	0.13	Pass
MUC QC 03	1.98	1.83	6.01	7.44	Fail
PPC QC 02	9.20	9.06	2.65	1.55	Pass

The samples all pass the quality control limits except for MUC QC 03; this was seen for copper and nickel. Again this sample has the lowest sulphur concentration. The samples with similar sulphur concentrations have higher measured values than consensus values and could indicate a concern with the lower range of the sulphur calibration. In Figure 7-6, all the lower calibration standards are on the calibration line and there are enough standards at the lower level so this is not considered. Since this was seen for copper, nickel and sulphur it can be assumed that it was either due to sample preparation, contamination of the QC or incorrect consensus values. The results are presented graphically in Figure 8-3.

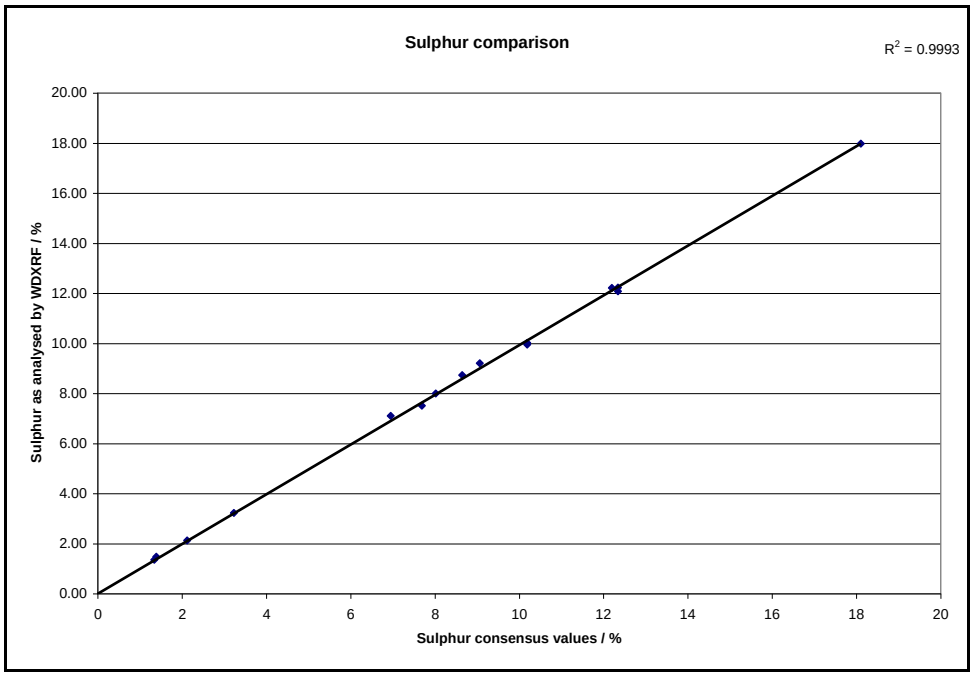


Figure 8-3: Comparison of consensus values and measured values for sulphur

Of the twenty seven samples prepared, twelve were removed from the graphic presentation as outliers. These twelve samples include the samples with high relative percentage differences as well as the samples that were significantly different. The correlation coefficient of 0.9993 indicated a good comparison between the measured and the consensus values.

8.6 Comparison and discussion of iron results

Table 8-9: Comparison of consensus and measured values for iron

Sample Type	Average measured iron concentration [%]	Standard deviation	Consensus value [%]	Relative percentage difference [%]	t-calc
KM AMC	16.29	0.10	16.86	-3.47	4.18
KM AUC	10.60	0.09	10.88	-2.66	2.11
KM PPC	14.56	0.02	14.83	-1.85	10.50
LMC QC 03	21.61	ND	21.92	-1.43	ND
LUC QC 02	13.51	0.09	13.80	-2.16	2.20
BMC QC 02	22.72	0.13	23.70	-4.29	5.44
MUC QC 03	9.52	0.09	9.41	1.19	0.91
PPC QC 02	16.75	0.09	16.70	0.30	0.40
AMCPS	16.91	0.09	17.26	-2.05	2.60
AMMCW	18.03	0.07	17.34	3.82	6.60
ANUCPS	9.50	0.02	9.47	0.28	1.05
AUGPS	8.37	0.02	8.50	-1.54	3.93
BRFDC 258	18.57	0.03	18.97	-2.17	8.95
BRFDC 284	16.04	0.75	17.18	-7.13	1.08
LMRPS	10.64	0.04	10.52	1.14	2.13
LUGPS	11.54	ND	11.41	1.14	ND
MDCPS	9.34	0.09	9.33	0.13	0.10
MTCPS	9.01	0.03	9.16	-1.64	3.27
PPLPS	14.15	0.08	13.89	1.86	2.39
UWCPS	8.87	0.12	8.53	3.82	1.96
WNXPS	14.84	0.14	15.92	-7.29	5.53
AMCPS	16.89	0.03	17.26	-2.21	8.74
AMMCW	18.11	0.08	17.34	4.24	6.50
BRFDC 258	18.62	0.04	18.97	-1.86	5.78
BRFDC 284	16.49	0.03	17.18	-4.19	18.32
LMRPS	10.69	0.03	10.52	1.55	4.20
LUGPS	11.41	0.06	11.41	0.03	0.04

The standard deviations for the duplicate samples were low and indicated good precision for the method. The relative percentage differences for iron were much lower than that of copper, nickel and sulphur. The percentage differences varied between -7.29% for WNXPS and 4.24% for AMMCW. The relative percentage differences were both positive and negative, indicating no bias or systematic error.

Only one sample has a t-calc bigger than the t-crit, BRFDC 284 (0.5 g), and this indicates that the measured value was significantly different from the consensus value. The iron concentration of this sample was not high or low, indicating possible sample preparation errors or errors in the consensus value. This was the only element so far where the MUC QC 03 was not significantly different.

Table 8-10: Comparison of iron results for quality control samples

Sample type	Average measured iron concentration [%]	Consensus value [%]	Uncertainty in consensus value [%]	Relative percentage difference [%]	Pass or fail
LMC QC 03	21.61	21.92	3.19	-1.43	Pass
LUC QC 02	13.51	13.80	5.36	-2.16	Pass
BMC QC 02	22.72	23.70	2.11	-4.29	Fail
MUC QC 03	9.52	9.41	1.38	1.19	Pass
PPC QC 02	16.75	16.70	2.99	0.30	Pass

Only one of the samples failed the quality control limits and that was BMC QC 02. BMC QC 02 contains the highest iron concentration and the measured value was lower than the consensus value. Samples with similar iron concentrations were also measuring lower than the consensus value. This could indicate a possible error in the high concentration ranges of the calibration. Figure F-12 indicated that the standards are all on the calibration line and there was no reason for concern. There was only one calibration standard at the higher range of the calibration curve and the iron concentration at higher levels might improve if more calibration standards were used. The significant difference of BMC QC 02 could be attributed to sample preparation errors, however it was not seen for any of the other elements so far.

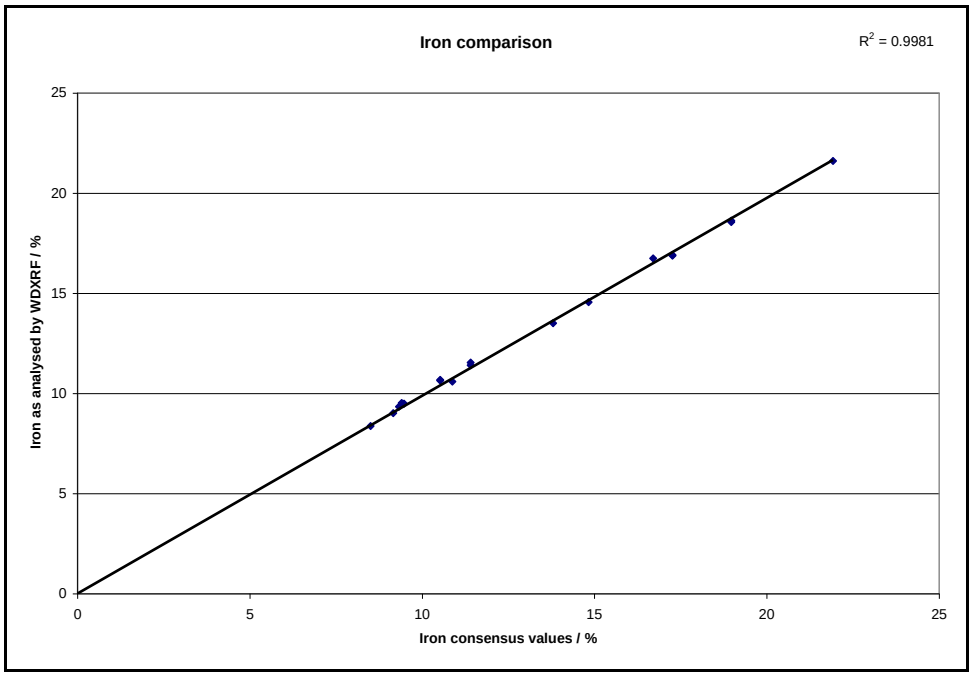


Figure 8-4: Comparison of consensus values and measured values for iron

Of the twenty seven samples prepared, nine were identified as outliers and removed from the graph. The correlation coefficient of 0.9981 indicates a good comparison between measured and consensus values, but could be improved.

8.7 Comparison and discussion of cobalt results

Table 8-11: Comparison of consensus and measured values for cobalt

Sample Type	Average measured cobalt concentration [%]	Standard deviation	Consensus value [%]	Relative percentage difference [%]	t-calc
LMC QC 03	0.11	0.0	0.12	-6.66	ND
LUC QC 02	0.07	0.0	0.08	-8.70	2.16
BMC QC 02	0.15	0.0	0.15	-0.67	0.25
MUC QC 03	0.03	0.0	0.03	-4.79	0.34
PPC QC 02	0.10	0.0	0.11	-8.55	7.28
AMCPS	0.09	0.0	0.10	-7.44	2.15
AMMCW	0.11	0.0	0.11	-2.72	8.08
ANUCPS	0.03	0.0	0.03	-0.29	0.21
AUGPS	0.03	0.0	0.03	9.45	4.66
BRFDC 258	0.10	0.0	0.10	3.37	0.63
BRFDC 284	0.09	0.01	0.09	-2.70	0.26
LMRPS	0.03	0.0	0.04	-22.61	3.84
LUGPS	0.03	0.0	0.04	-32.02	ND
MDCPS	0.03	0.0	0.04	-31.69	3.09
MTCPS	0.03	0.0	0.03	-2.86	0.86
PPLPS	0.09	0.0	0.09	0.95	1.97
UWCPS	0.04	0.0	0.04	-4.79	0.77
WNXPS	0.07	0.0	0.07	1.47	6.24
AMCPS	0.09	0.01	0.10	-8.41	0.58
AMMCW	0.11	0.0	0.11	3.71	2.77
BRFDC 258	0.11	0.0	0.10	8.58	2.31
BRFDC 284	0.09	0.0	0.09	-5.79	1.56
LMRPS	0.03	0.0	0.04	-33.44	2.94
LUGPS	0.03	0.0	0.04	-22.20	6.08

For cobalt not all the samples had consensus values and are therefore not compared. The standard deviations were very low indicating good replicates and a very good precision for the method.

The percentage differences varied between 9.45% for AUGPS and -33.44% for LMRPS (0.5 g). Most of the percentage differences were negative indicating that the measured value was less than the consensus value. None of the samples had a t-calc larger than the t-crit, indicating no significant difference.

The QC samples are compared in Table 8-12.

Table 8-12: Comparison of cobalt results for quality control samples

Sample type	Average measured cobalt concentration [%]	Consensus value [%]	Uncertainty in consensus value [%]	Relative percentage difference [%]	Pass or fail
LMC QC 03	0.11	0.12	8.33	-6.66	Pass
LUC QC 02	0.07	0.08	12.50	-8.70	Pass
BMC QC 02	0.15	0.15	6.67	-0.67	Pass
MUC QC 03	0.03	0.03	6.67	-4.79	Pass
PPC QC 02	0.10	0.11	9.09	-8.55	Pass

The comparison with the QC samples and the uncertainties in these values indicated that all the QCs passed the limits. This means that the uncertainties in the assigning of these values were larger than the uncertainty in the preparation method and calibration. According to the quality system in the laboratory these results are accepted as accurate. The graphic comparison can be seen in Figure 8-5.

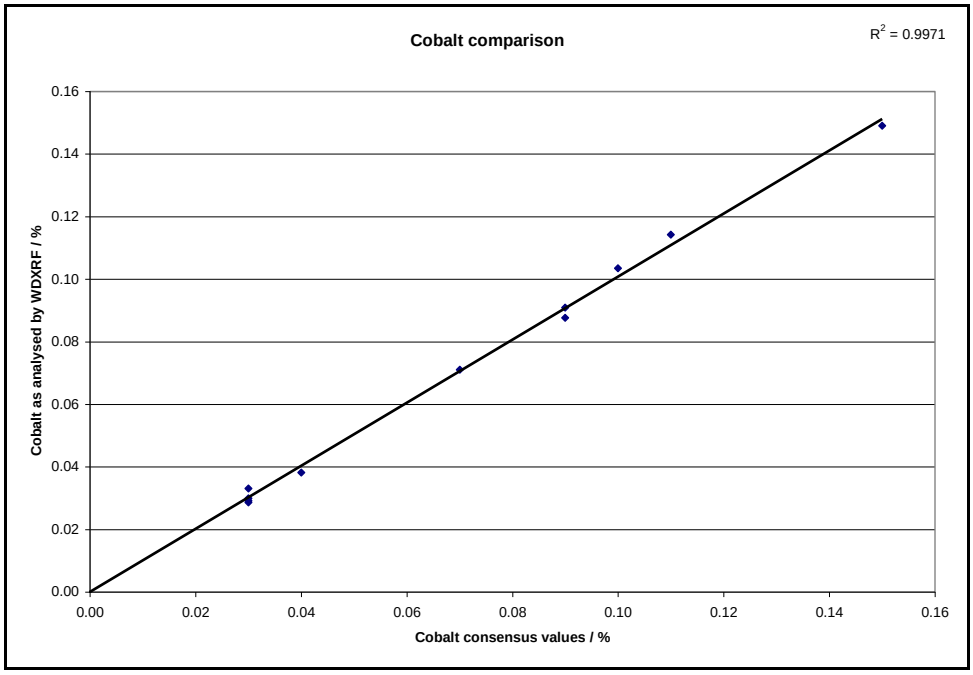


Figure 8-5: Comparison of consensus values and measured values for cobalt

The correlation coefficient for the comparison between the two concentrations was 0.997 indicating a good comparison. Of the twenty four samples prepared, thirteen were removed as outliers from the graph and these were the samples with high percentage differences. It should be noted, however, that most of the measured concentrations differ by 0.01% from the consensus values and even though the difference in concentration is small, they appear as outliers.

8.8 Comparison and discussion of aluminum oxide

Table 8-13: Comparison of consensus and measured values for aluminum oxide

Sample Type	Average measured aluminum oxide concentration [%]	Standard deviation	Consensus value [%]	Relative percentage difference [%]	t-calc
KM AMC	3.75	0.11	3.53	5.89	1.39
KM AUC	4.39	0.11	4.12	6.24	1.80
KM PPC	3.54	0.07	3.29	7.05	2.36
AMCPS	2.44	0.01	2.07	15.25	39.92
AMMCW	2.60	0.02	2.28	12.25	13.65
ANUCPS	4.62	0.09	4.24	8.24	3.14
AUGPS	2.84	0.05	2.62	7.70	3.06
BRFDC 258	4.12	0.0	3.80	7.71	46.45
BRFDC 284	4.17	0.13	3.99	4.20	0.93
LMRPS	5.85	0.0	4.46	23.78	2813.95
LUGPS	10.39	ND	7.99	23.11	ND
MDCPS	3.75	0.04	3.04	18.94	12.17
MTCPS	3.79	0.02	3.25	14.16	19.65
PPLPS	4.07	0.02	3.24	20.32	33.83
UWCPS	2.78	0.03	2.41	13.33	9.96
WNXPS	5.23	0.02	4.82	7.79	15.21
AMCPS	2.63	0.09	2.07	21.20	4.36
AMMCW	2.83	0.01	2.28	19.41	33.64
BRFDC 258	4.34	0.06	3.80	12.42	5.91
BRFDC 284	4.37	0.01	3.99	8.60	20.55
LMRPS	6.05	0.08	4.46	26.22	14.46
LUGPS	10.40	0.08	7.99	23.19	21.81

For aluminum oxide not all the samples had consensus values and therefore not all the samples were compared. The standard deviations were low, indicating good replicates and good precision for the method.

The percentage differences varied between 4.20% for BRFDC 284 and 26.22% for LMRPS (0.5 g). All the percentage differences were positive, indicating that the measured concentrations were all higher than the consensus values. This might indicate a bias and systematic error.

Ten samples have a t-calc larger than the t-crit, indicating a significant difference between measured and consensus values for samples AMCPS, AMMCW (1.0 g and 0.5 g), MTCPS, BRFDC 258, LMRPS (1.0 g and 0.5 g), PPLPS, WNXPS and BRFDC 284 (0.5 g). Some of these samples were previously significantly different or had high percentage differences for the other elements and could indicate sample preparation errors. This was not true for all the samples and another possibility should also be considered. The fact that there was a bias and systematic error indicated a possibility of a calibration error. For example, the purity of the oxide used to prepare the calibration standards. The standards were consistently higher or lower in aluminum oxide and the concentrations used to calibrate the WDXRF might have been questionable. Since the aluminum oxide in these samples varied between high and low concentrations it cannot be attributed to the range of the calibration. Figure F-8 indicates that all the calibration standards are on the line.

The possibility also exist that the consensus values were not determined correctly. None of the QC samples have consensus values or uncertainties for aluminum oxide and no comparison could be made.

The graphic presentation can be seen in Figure 8-6.

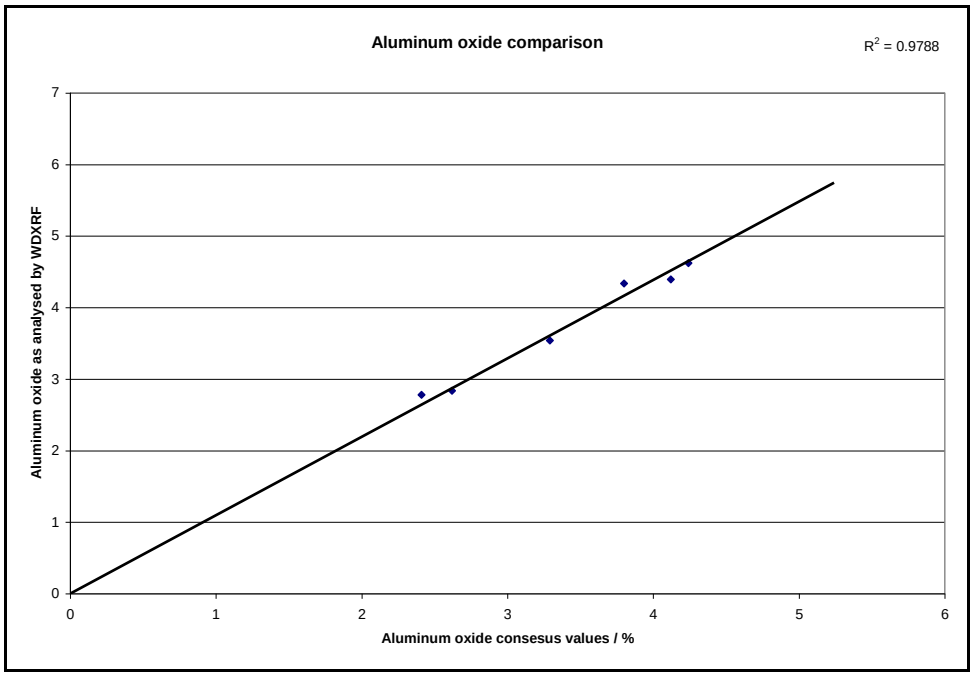


Figure 8-6: Comparison of consensus values and measured values for aluminum oxide

Of the twenty two samples prepared, sixteen were removed as outliers from the graph to get a straight line constrained through zero. The correlation coefficient of 0.979 indicated a poor comparison, taking into account that all the measured concentrations were higher than the consensus values. The systematic error was attributed to the calibration standards and the purity of the oxide used to prepare the standards. Hydrated aluminum nitrate was used for the preparation of the calibration standards and it is possible that the chemical absorbed or lost water and the hydrate factor used to calculate the aluminum oxide was incorrect. This would contribute to a systematic error. It was also possible that all the consensus values were incorrect; however the use of the ICP technique for aluminum oxide determination was not reported to be problem some.

8.9 Comparison and discussion of calcium oxide results

Table 8-14: Comparison of consensus and measured values for calcium oxide

Sample Type	Average measured calcium oxide concentration [%]	Standard deviation	Consensus value [%]	Relative percentage difference [%]	t-calc
KM AMC	2.68	0.0	3.11	-16.21	135.45
KM AUC	2.84	0.02	3.24	-14.28	17.00
KM PPC	5.36	0.05	5.92	-10.48	8.26
AMCPS	2.10	0.01	2.55	-21.71	50.02
AMMCW	2.18	0.0	2.75	-26.00	166.91
ANUCPS	3.19	0.02	3.49	-9.49	10.25
AUGPS	2.08	0.0	2.57	-23.73	902.61
BRFDC 258	2.97	0.03	3.41	-14.65	10.37
BRFDC 284	2.97	0.15	3.61	-21.50	3.00
LMRPS	3.98	0.04	3.97	0.26	0.19
LUGPS	3.81	ND	4.12	-8.15	ND
MDCPS	2.53	0.03	2.86	-13.03	8.24
MTCPS	2.51	0.01	2.82	-12.45	16.71
PPLPS	5.15	0.01	5.24	-1.67	6.68
UWCPS	2.01	0.01	2.23	-10.91	14.69
WNXPS	3.47	0.03	3.93	-13.18	12.38
AMCPS	2.10	0.02	2.55	-21.18	16.63
AMMCW	2.21	0.0	2.75	-24.39	188.08
BRFDC 258	2.98	0.01	2.75	7.86	29.32
BRFDC 284	3.05	0.03	3.61	-18.27	13.73
LMRPS	4.02	0.0	3.97	1.21	28.52
LUGPS	3.83	0.01	4.12	-7.45	19.67

The standard deviations were low indicating good replicates and good precision for the method. The percentage differences varied between – 26.0% for AMMCW and 7.86% for BRFDC 258 (0.5 g). Most of the percentage differences were negative indicating that the measured concentrations were lower then the consensus values. This constitutes a consistent negative bias and confirms another systematic error. Again the possibility exists of a calibration error and the most likely error would be the calibration standards concentrations. Thirteen of the samples had t-calc larger than t-crit and differs significantly from the consensus values. These samples have high and low calcium oxide concentrations and the error cannot be attributed to the

calcium oxide calibration range. Figure F-10 indicates a good calibration with one of the standards slightly off the calibration line. None of the QC samples had consensus values and uncertainties for calcium oxide. The results are presented in Figure 8-7.

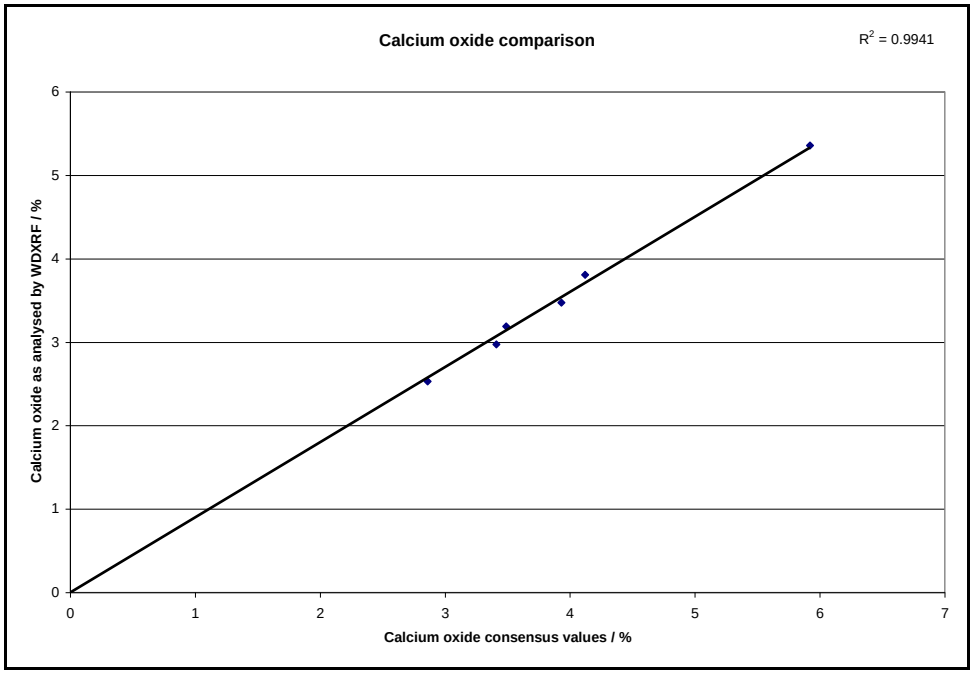


Figure 8-7: Comparison of consensus values and XRF values for calcium oxide

Of the twenty two samples prepared, sixteen were removed from the graph as outliers. These sixteen samples were identified as the samples with high percentage differences as well as being significantly different. The line was constrained through zero and the correlation coefficient of 0.994 represents a good comparison, taking into account that more than half of the samples were removed as outliers. This is attributed to the systematic error.

8.10 Comparison and discussion of results for magnesium oxide

Table 8-15: Comparison of consensus and measured values for magnesium oxide

Sample Type	Average measured magnesium oxide concentration [%]	Standard deviation	Consensus value [%]	Relative percentage difference [%]	t-calc
KM AMC	16.84	0.48	18.01	-6.97	1.73
KM AUC	21.30	0.61	22.45	-5.39	1.32
KM PPC	17.88	0.42	18.77	-4.97	1.51
AMCPS	19.02	0.20	19.90	-4.65	3.14
AMMCW	17.94	0.03	18.91	-5.43	24.49
ANUCPS	23.04	0.09	23.30	-1.13	2.02
AUGPS	24.59	0.15	23.41	4.81	5.62
BRFDC 258	14.47	0.09	14.42	0.34	0.39
BRFDC 284	15.30	1.26	16.58	-8.36	0.72
LMRPS	19.10	0.04	19.40	-1.58	4.84
LUGPS	16.14	ND	14.75	8.64	ND
MDCPS	22.19	0.52	23.01	-3.70	1.11
MTCPS	23.61	0.10	22.56	4.43	7.14
PPLPS	17.71	0.01	16.75	5.40	51.59
UWCPS	23.83	0.36	23.61	0.94	0.44
WNXPS	15.47	0.23	17.46	-12.86	6.16
AMCPS	18.33	0.0	19.90	-8.59	1028.50
AMMCW	17.50	0.31	18.91	-8.04	3.25
BRFDC 258	14.23	0.01	14.42	-1.32	19.67
BRFDC 284	15.36	0.01	16.58	-7.95	99.61
LMRPS	18.92	0.04	19.40	-2.55	9.11
LUGPS	15.75	0.15	14.75	6.36	4.73

The standard deviations for magnesium oxide were higher than the other elements and oxides so far compared; the results still indicated good replicates as well as good precision. The percentage differences varied between -12.86% for WNXPS and 8.64% for LUGPS. The percentage differences were both negative and positive indicating no consistent bias or systematic error.

Five of the samples had a t-calc larger than the t-crit and were significantly different; these samples were AMMCW, PPLPS, AMCPS, BRFDC 258 (0.5 g) and BRFDC 284 (0.5 g). These samples all had lower magnesium oxide concentrations and lie in

the lower range of the magnesium oxide calibration. This could indicate some uncertainties in the lower range of the calibration and possibly the lower range calibration standards. Sample preparation errors should also be considered since some of the samples had high percentage differences and were significantly different for the other elements and oxides.

The graphic presentation for the results can be seen in Figure 8-8.

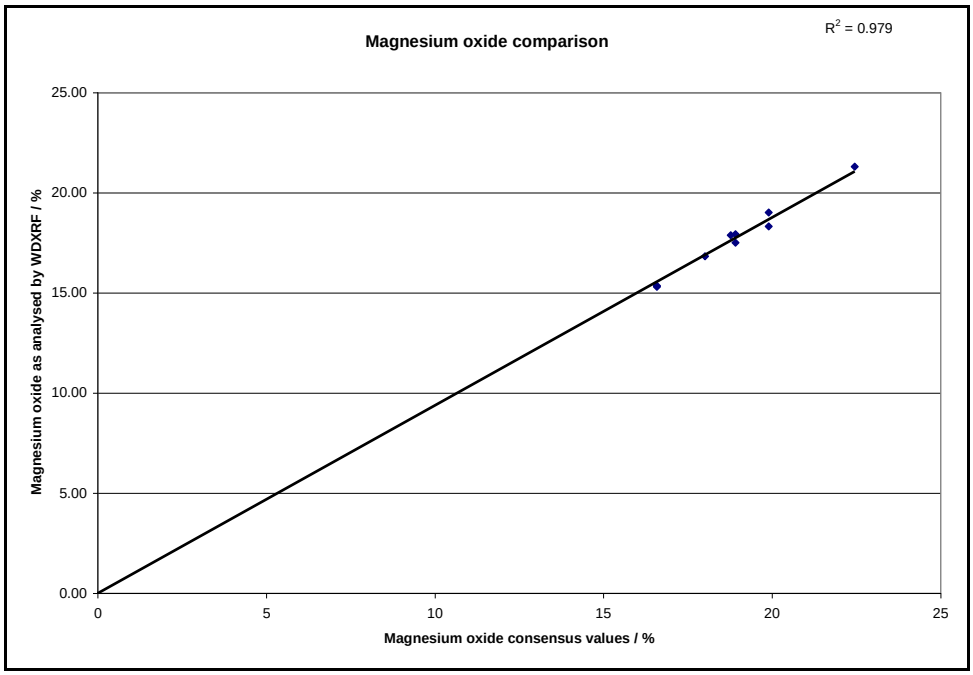


Figure 8-8: Comparison of consensus values and XRF values for magnesium oxide

Of the twenty two samples prepared, twelve was removed from the graph as outliers. These were the significantly different samples as well as the samples with high percentage differences. Samples were removed by visual inspection as outliers once the line was constrained through zero. The correlation coefficient of 0.979 was not close to a straight line.

8.11 Comparison and discussion of chromic oxide results

Table 8-16: Comparison of consensus and measured values for chromic oxide

Sample Type	Average measured chromic oxide concentration [%]	Standard deviation	Consensus value [%]	Relative percentage difference [%]	t-calc
KM AMC	1.09	0.01	1.14	-4.67	2.57
KM AUC	2.61	0.02	2.67	-2.48	2.36
KM PPC	0.17	0.01	0.23	-33.50	6.88
LMC QC 03	0.31	ND	0.39	-26.00	ND
LUC QC 02	4.30	0.03	4.32	-0.46	0.55
BMC QC 02	0.80	0.0	0.91	-14.13	30.70
MUC QC 03	1.27	0.02	1.29	-1.34	0.62
PPC QC 02	0.19	0.01	0.22	-15.70	3.80
AMCPS	0.39	0.01	0.41	-5.30	1.81
AMMCW	0.36	0.0	0.43	-20.96	23.54
ANUCPS	1.25	0.02	1.29	-3.56	1.72
AUGPS	1.59	0.0	1.70	-6.90	394.14
BRFDC 258	0.32	0.01	0.36	-12.22	2.52
BRFDC 284	0.33	0.02	0.40	-22.00	3.29
LMRPS	1.61	0.0	1.46	9.21	327.98
LUGPS	9.92	ND	9.72	2.01	ND
MDCPS	1.78	0.01	1.78	0.26	0.24
MTCPS	2.10	0.0	2.09	0.69	2.15
PPLPS	0.22	0.0	0.23	-2.78	1.30
UWCPS	1.64	0.02	1.62	1.07	0.56
WNXPS	0.83	0.0	0.89	-7.45	29.81
AMCPS	0.38	0.01	0.41	-8.83	2.34
AMMCW	0.36	0.01	0.43	-19.92	6.53
BRFDC 258	0.30	0.01	0.36	-20.66	4.21
BRFDC 284	0.33	0.01	0.40	-21.75	5.56
LMRPS	1.60	0.01	1.46	9.03	8.17
LUGPS	9.90	0.03	9.72	1.81	4.32

The standard deviations were low, indicating good replicates and good precision for the method. The percentage differences varied between -33.5% for KMPPC and 9.21% for LMRPS. The percentage differences were both positive and negative and did not indicate bias or systematic errors.

Five samples had a t-calc larger than the t-crit, indicating significant differences between the measured and the consensus values. These samples were BMC QC 02, AMMCW, AUGPS, LMRPS and WNCPS. The chromic oxide content of these samples was low; however, there were samples with the same chromic oxide content that were not significantly different. The QC samples had consensus values for chromic oxide and the comparison is given in Table 8-17.

Table 8-17: Comparison of chromic oxide results for quality control samples

Sample type	Average measured chromic oxide concentration [%]	Consensus value [%]	Uncertainty in consensus value [%]	Relative percentage difference [%]	Pass or fail
LMC QC 03	0.31	0.39	12.82	-26.00	Fail
LUC QC 02	4.30	4.32	6.94	-0.46	Pass
BMC QC 02	0.80	0.91	6.59	-14.13	Fail
MUC QC 03	1.27	1.29	3.10	-1.34	Pass
PPC QC 02	0.19	0.22	9.09	-15.70	Fail

Three of the QCs failed the quality control limits, indicating a larger uncertainty in the measured results than the uncertainty in the consensus values. The QC samples that failed all had low chromic oxide concentrations and this could indicate a problem with the lower range of the calibration. All the QCs with lower chromic oxide concentrations as well as samples with similar chromic oxide concentrations had lower measured results than the consensus values. It should also be taken into account that the dilution factor was large and could influence the sensitivity of the WDXRF for the lower concentrations and would increase the measurement uncertainty. Values in Figure F-11 do not indicate that any of the calibration standards are off the calibration line. More standards might be required at the lower concentration levels to increase the accuracy. BMC QC 02 had failed before for iron, however this does not indicate sample preparation error because it passed the limits for all the other elements. The results are presented graphically in Figure 8-9.

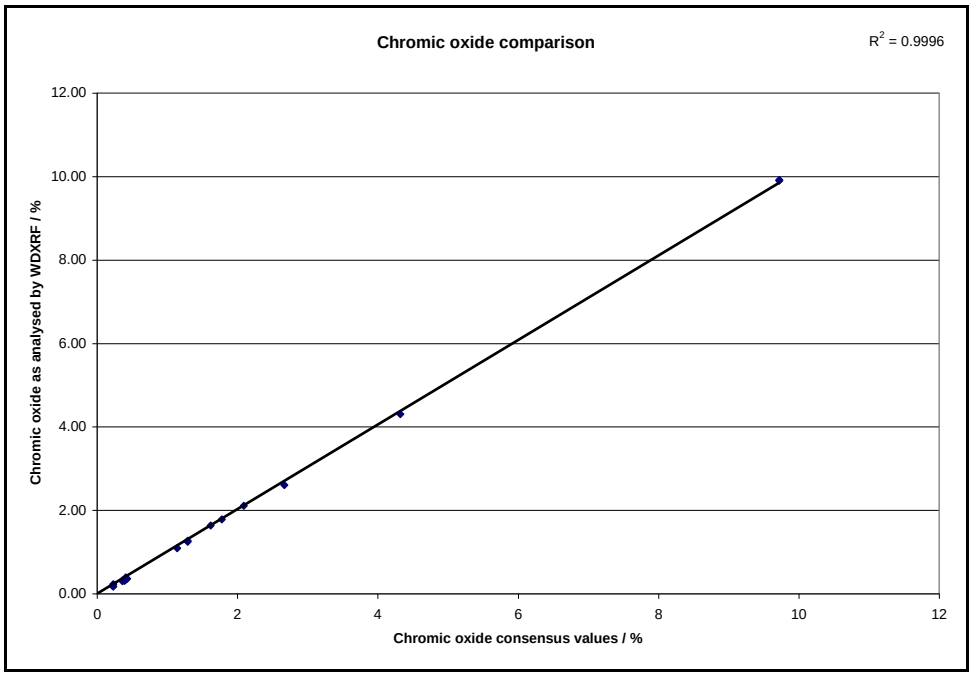


Figure 8-9: Comparison of consensus values and XRF values for chromic oxide

Of the twenty seven samples, six were removed as outliers. The correlation coefficient of 0.9996 indicated a very good comparison between the measured and consensus values.

8.12 Comparison and discussion of silicon dioxide

Table 8-18: Comparison of consensus and measured values for silicon dioxide

Sample Type	Average measured silicon dioxide concentration [%]	Standard deviation	Consensus value [%]	Relative percentage difference [%]	t-calc
AMCPS	39.18	0.10	37.58	4.10	10.97
AMMCW	37.30	0.06	34.76	6.80	31.58
ANUCPS	50.25	0.16	48.76	2.96	6.61
AUGPS	50.59	0.25	44.43	12.18	17.23
BRFDC 258	35.37	0.03	33.57	5.09	49.43
BRFDC 284	37.50	1.74	38.18	-1.81	0.28
LMRPS	47.16	0.32	52.65	-11.65	12.02
LUGPS	36.83	ND	32.73	11.13	ND
MDCPS	48.35	0.48	47.47	1.81	1.28
MTCPS	50.16	0.33	46.77	6.76	7.26
PPLPS	40.01	0.05	36.68	8.33	50.72
UWCPS	49.50	0.25	45.66	7.76	10.80
WNXPS	39.56	0.15	38.30	3.18	5.90
AMCPS	38.90	0.13	37.58	3.40	7.09
AMMCW	37.22	0.40	34.76	6.61	4.39
BRFDC 258	35.13	0.0	33.57	4.43	362.33
BRFDC 284	38.05	0.16	38.18	-0.33	0.58
LMRPS	47.42	0.04	52.65	-11.03	82.63
LUGPS	36.69	0.28	32.73	10.78	10.08

The standard deviations were low, indicating good replicates and good precision for the method. The relative percentage differences varied between -11.65% for LMRPS and 12.18% for AUGPS. There were more positive percentage differences than negative and this indicates that the measured silicon dioxide was higher than the consensus values. In the case of silicon dioxide, the possibility of errors with the determination of the consensus values must be considered. There are many concerns with the preparation technique as well as the analysis of silicon dioxide as determined by ICP. Therefore, the possibility exists that the consensus values reported are too low. None of the QC samples had consensus values for silicon dioxide. Six of the samples had t-clac larger than t-crit, indicating significant differences. These samples were AUGPS, AMMCW, PPLPS, BRFDC 285 (0.5 g and 1.0 g) and LMRPS (0.5 g).

The silicon dioxide concentrations of these samples were both high and low and can therefore not be attributed to a calibration error. In some cases, these samples had high percentage differences and were significantly different for other elements as well and could indicate sample preparation errors. However, not one of the samples were significantly different for all elements and oxides and the sample preparation error can be eliminated. It is again attributed to the consensus values and the errors made in determining them. The results are presented in Figure 8-10.

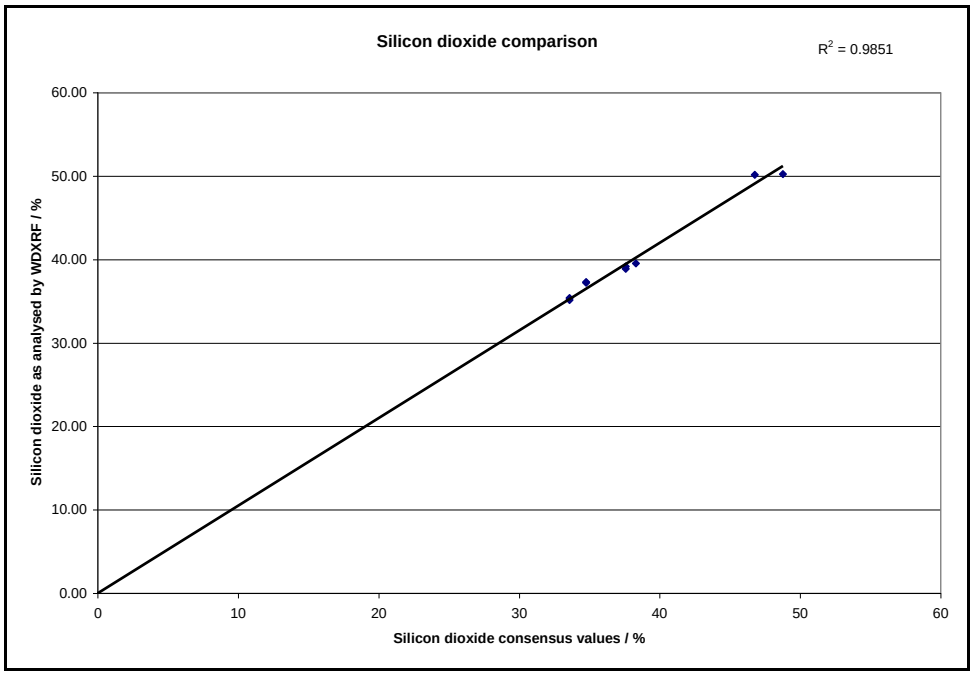


Figure 8-10: Comparison of consensus values and XRF values for silicon dioxide

Of the eighteen samples prepared, seven were removed as outliers. These samples had high percentage differences and were significantly different. The correlation coefficient of 0.985 did not indicate a very good comparison.

The concern is with the accuracy of the consensus values since the results were determined by sodium peroxide fusion and ICP analyses. With ICP analyses, hydrofluoric acid (HF) is usually added to the samples to keep the silicon dioxide in

solution. The question here is whether the HF was added to the samples and standards during the determination of the silicon dioxide consensus values. If it was not, the silicon dioxide might have precipitated out of solution and the true values would not have been determined.

8.13 Conclusion

- All the glass beads prepared were perfect with no bubbles or cracks and no undissolved particles. The crucibles had no black smears or indication of an interaction between the samples and the crucibles. This indicates that the flux, oxidation agents and non-wetting agent were correct. The fusion and oxidation step, temperature and time were sufficient.
- The replicate sample for LUGPS and LMC QC 03 was significantly different for all elements and oxides and therefore only one result was used in the comparisons. The difference between the replicates was attributed to sample preparation error. All the other samples have low standard deviations indicating good replicates and good precision for the fusion method as well as the analyses.
- The results for copper indicate no bias or systematic error. Two samples were significantly different. One of these samples was MUC QC 03. This QC sample also failed the limits of quality control, indicating inaccurate results. Since the same can be seen for nickel and sulphur but not iron and chromic oxide it was concluded that this significant difference was not due to sample preparation error, QC contamination or an error in the consensus value. MUC QC 03 contains a low concentration of copper and the significant difference was attributed to the lower end of the calibration, where one of the calibration standards was not on the calibration line. The accuracy can be improved by preparing more standards at the lower concentration range and making sure they fit the calibration line perfectly. The other QC samples all passed the

limits and indicate accurate results for the fusion method. The comparison between the results was very good and indicated a successful preparation method and analyses for copper. This indicated that the use of potassium iodide as well as the heating mechanism of the Katanax was successful.

- The nickel results indicated a good comparison with no bias or systematic error. The t-test indicated six samples that were significantly different. Only one of the three significantly different QCs failed the quality control limits. Possible sample preparation errors could be expected as well as errors while determining the consensus values. MUC QC 03 also failed the limits for nickel. As in the case of copper, the sample has a low concentration of nickel. In the case of nickel, the calibration line is perfect at the lower concentration range. It is suspected that the purity of the nickel oxide used to prepare standards could be incorrect and this would attribute to incorrect values used when calibrating the WDXRF. The error will also be more significant at lower concentration levels. The correlation of the measured and consensus values was very good, indicating a successful preparation and analyses method for nickel. Further investigation must be done to determine the purity of the nickel oxide used to prepare the calibration standards and to prepare more calibration standards at the lower concentration range.
- The results for sulphur indicated good comparisons with no bias or systematic error, seven significantly different samples and only one QC failing the t-test and the quality control limits. MUC QC 03 failed the limits and was significantly different for copper, nickel and sulphur. The concentration of the elements in this sample are lower than the concentrations of the other QC samples. No errors could be seen in the sulphur calibration and the error was not attributed to the calibration. The possibility does exist that the consensus value is incorrect. The determination of sulphur by ICP is not as accurate as, for example, the gravimetric method. It is not known which technique the other laboratories used to determine the consensus value. The correlation of

the results was good indicating a successful sample preparation method as well as analyses. The oxidation step as well as the fusion were successful.

- The results of the iron indicated good comparisons, with only one sample that was significantly different. The sample, BRFD 284, had been identified with high percentage differences for other elements and therefore the significant difference could be attributed to sample preparation error. Only one of the QC samples failed the limits. This was attributed to the higher range of the calibration; the highest calibration standard was on the calibration line; however, more standards are required at the higher concentration range to improve accuracy. The correlation between the compared results was not very good however, on overall the results were best for iron with the lowest percentage differences. This indicated a successful preparation method and analyses for iron.
- The results overall indicated very good cobalt comparisons with no significant differences and no QCs failing the limits. The fact that most of the measured values were lower then the consensus values could indicate a systematic error, however, this was not seen for all the samples and in this case could be attributed to the low cobalt concentration and the high dilution of the samples. This makes the WDXRF sensitivity lower and increases measurement error. Many of the samples were removed as outliers from the graph, and it should be noted that the concentration differences of these outliers were 0.01%. The results indicated a successful method for cobalt. Further investigation can be considered into the dilution.
- In the case of aluminum oxide, the percentage differences were all positive and ten samples were significantly different from the consensus values. The graph indicated poor correlation. This was all expected since the measured results indicated a consistent high bias. The systematic error was attributed to errors in calibration and the errors include the preparation of the standards and the purity of the oxide used. The fusion method was successful for

aluminium, however, the calibration should be investigated further with the possibility of using another oxide for the preparation of standards.

- The results for calcium oxide indicate a consistent bias and systematic error. The samples have high and low calcium oxide concentrations and the error cannot be attributed to the calibration range. Thirteen of the samples were significantly different. However not all the samples were significantly different or had high percentage differences for the other elements, therefore sample preparation cannot be the only contributor to the error. The contribution of the calibration standards and a possible error with the concentration of the calibration standards was suspected. Calcium carbonate was used for the preparation of the standards. The calibration standards must be re-prepared with another oxide to eliminate the systematic error.
- The results for magnesium oxide show no bias or systematic error. Five samples that differed significantly all had low magnesium oxide concentrations. This indicated some error in the lower range of the magnesium oxide calibration. This can be resolved by adding more calibration standards at the lower range. It is also possible that the consensus values are incorrect.
- The chromic oxide results indicated five samples significantly different and three failing QC samples. The three QCs that failed the limits were low in chromic oxide and indicated a concern with the lower range of the chromic oxide calibration. The calibration graph did not give any reason for concern. Since the dilution used in the method was substantial it could also indicate that the sensitivity of the WDXRF for the low concentrations was compromised and this will increase the measurement error. To reduce the error in the lower range, more calibration standards must be prepared and included. The dilution factor should also be investigated to reduce the uncertainty in the measurement and to improve the sensitivity of the WDXRF. The preparation method was successful.

- The results of the silicon dioxide indicated good comparisons; however, most of the percentage differences indicated that the measured results were higher than the consensus values. The differences were attributed to the consensus values and errors while determining the values. Since the WDXRF results were higher than the consensus values it is assumed that HF, used during sodium peroxide fusion and ICP analyses, was not added to the samples, and the silicon dioxide precipitated out of solution contributing to incorrect consensus values.

The results of the samples indicated good comparisons with some of the problems lying with the calibration ranges, the purity of the oxide used for calibration standard preparation as well as errors while determining the consensus values. The results indicated a successful fusion method including the flux, the oxidising agents, the non-wetting agent, Katanax, oxidising step as well as the fusion temperature and time. The analyses were successful and the calibration and use of the WDXRF was successful. The ideal fusion of Blank and Eksperiandova (1998) was achieved with perfect glass beads and the recovery of all elements and oxides of interest.

9. CONCLUSIONS

9.1 Preliminary experiments

Preliminary experiments were carried out using Lebowa concentrate samples and testing different fluxes, crucibles, heating mechanisms as well as trying to create secondary calibration standards by fusion. The fluxes investigated included sodium salts due the lower melting temperatures and cost when compared to lithium salts. Sodium tetra-borate was chosen as the ideal flux due to it improving the dissolution of basic oxides and was reported to improve the oxidation of sulphides in the sample. Dissolution of the samples proved more successful with sodium tetra-borate flux when compared to the more basic meta-borate flux and the improved reactivity of phosphate fluxes was not found.

The attempted production of secondary calibration standards using samples in different ratios contributed to the overall fusions when sulphide buttons formed during these experiments. The sulphide buttons showed that the sulphide will settle at the bottom of the crucibles and will not react with the flux or oxidising agent and would therefore have to be oxidised at lower temperatures before it melted and settled. Roasting the samples to remove the sulphides proved successful.

9.2 Non-wetting agents

All the glass beads in the preliminary experiments cracked or shattered indicating the necessity for non-wetting agents. Non-wetting agents will reduce the cracking or shattering of the glass bead by interacting with the long chains formed by the borate, by preventing the formation of the long chains. Non-wetting agents also reduce the molten glass viscosity making it easier to remove all the glass from the crucibles.

The major concern with using halides as the non-wetting agents is the loss of copper in association with the halide.

The copper recovery was tested using different halides, including iodide, bromide and chloride. The copper recovery was around 50% for all the halides as well as the glass bead with no non-wetting agent, confirming that the copper measurement was incorrect.

After calibrating the XRF, glass beads were prepared using sodium iodide as the non-wetting agent. The recovery of the copper improved to 92%, indicating that the calibration resulted in an improvement of determination of copper and that copper was lost in association with the halides. It was tested whether the flux and the non-wetting agent could be integrated to prevent the loss of copper in the sample. This was investigated by producing glass beads with roasted concentrate samples and the integrated flux. The copper recovery was around 69%. This confirmed that integrating the flux and the non-wetting agent did not resolve the problem.

Alternatives to halides were investigated and included sulphate, phosphate, hydroxide, potassium oxide and sodium oxide. The copper recovery was close to 100%. However, all the glass beads cracked or shattered, indicating that even though the copper was not lost the alternative ions were not acting effectively as non-wetting agents.

An alternative method of introduction was investigated and included adding the halide as a gas. Bromine gas was introduced onto the glass bead during the casting step. The copper recovery was close to 100%, indicating that the bromine gas was acting as a non-wetting agent and the copper did not have time to react with the bromine, so the copper was not lost. The bromine gas was not being added consistently and would have been a problem when using fundamental parameter corrections. The bromine gas was attacking the Electrofluxer and had health

concerns associated with working with it. The experiments with bromine gas were discontinued. Halide salts were investigated again using the Katanax with its alternative heating mechanism.

9.3 Different mechanism of heating and crucibles used

Different methods of heating the samples were investigated which included the Bunsen burner. It was found that the temperature of the flame was insufficient to dissolve the sample. Hearth furnaces were investigated and fusions can be carried out at temperatures of up to 1400°C. However, loading and unloading the pots from the furnaces requires a skilled operator. Another consideration was to use the furnace pots as crucibles, however, this was not practical since the flux attacked the pots and this contaminated the samples. Zirconium crucibles were considered as well, since fusions could be done at 1000°C, however, exposing the crucibles to the flux at these temperatures for longer then ten minutes would damage the crucibles and increase crucible consumption.

The 7170 Electrofluxer was used for fusions in platinum gold alloy crucibles after the samples were roasted to remove the sulphur. This furnace has exceptionally high heating rates, however only one sample can be fused at a time. This can be overcome by using more than one Electrofluxer if it is deemed cost effective. The fusions were done successfully, however, copper was lost in association with the halide and another heating mechanism was investigated. The Electrofluxer was decommissioned and the Katanax K_2 used for subsequent fusions.

Due to the de-commissioning of the Electrofluxer and the commissioning of the Katanax, a different heating mechanism was introduced. The Katanax heats the samples from the top as well as the bottom of the crucible causing the flux and additives to melt and enclose the samples. The liquid layer on top of the sample

should prevent the loss of copper. The copper will also have enough exposure to the flux and additives to be oxidised and therefore preventing the reaction with the halides. Pure copper oxide glass beads were prepared with chloride, bromide and iodide as the non-wetting agents. The copper recovery was above 95% for all the glass beads prepared. This proved the assumption with regards to the heating mechanism of the Katanax preventing the loss of copper in association with the halide.

9.4 Pure oxide calibration standards

In the initial stages it was attempted to calibrate the XRF with secondary calibration standards rather than using programs with standardless functions. Samples were used in different ratios to produce these calibration standards. This was not successful due to many factors. Firstly, the XRF calibration will be dependant on the analyses of the glass beads by an alternative technique. Poor replicates were obtained for the glass beads produced and the results did not give good calibrations. Secondly, some of the elements could not even be calibrated because they were below the limit of quantification of the alternative technique. The production of secondary calibration standards were unsuccessful and showed the necessity for primary calibration standards.

Subsequently, primary calibration standards were prepared using pure oxides in various concentrations and producing glass beads with various oxides present. Many attempts were made with different non-wetting agents, sodium iodide, bromine gas and finally with potassium iodide. The final set of calibration standards consisted of fourteen glass beads. Alternative oxides were used for the more refractory oxides and all the oxides dissolved and perfect glass beads were produced. The final calibration achieved on both the EDXRF and the WDXRF was successful with good regressions and wide concentration ranges for all the oxides. This showed the advantages of

using pure oxides to produce calibration standards and the final attempt was successful.

9.5 Oxidation step

The oxidation step is to oxidise the sulphur present in the sample at temperatures lower than the fusion temperature and therein preventing the reaction of the sulphide with the platinum gold alloy crucible and retention of the sulphur. The first experiments were done in the Electrofluxer with ammonium nitrate as oxidising agent. The oxidation was not successful and this was attributed to the ammonium not contributing a counter ion with basic oxide properties.

The next set of the experiments was carried out with sodium nitrate as oxidising agent together with hydrated sodium per-borate. This combination showed better recoveries for the sulphur in the sample. The hydrated sodium per-borate was wetting the samples and preventing the sample from creeping up the sides of the crucible and therefore preventing the sulphur from interacting with the crucible walls.

A factorial design experiment was used to optimise the oxidation step in the Katanax using a combination of sodium nitrate and hydrated sodium per-borate. The temperature of 600°C was chosen and showed to be the ideal temperature before the sulphides could react and amalgamate at the bottom of the crucible. The glass beads produced did not have black particles and the crucibles were not damaged during the validation of the fusion. The sulphur recovery for most of the samples was close to 100% indicating a successful oxidation.

9.6 Validation of final calibrations

The first calibration achieved was on the EDXRF with the pure oxide calibration standards and empirical corrections. The empirical corrections were used because the

iodide concentration in the calibration standards was not known and not consistent. One of the requirements for the fundamental parameter correction model is that the sample composition must be known > 99%. Due to the inconsistency of the iodide in the calibration standards and samples, the empirical correction model was used. The calibration was evaluated using regression parameters and the correlation coefficients for all the calibration lines of all the elements were above 0.999, indicating good calibrations.

Since the empirical corrections are not ideal, the iodide concentration in the calibration standards was determined and the fundamental parameter model was used. The empirical correction model requires similar compositions for samples and calibration standards, the corrections are sensitive to any experimental error in data and can yield inaccurate results. The empirical corrections are also subject to the operator that is calibrating the XRF and selecting the elements to be used for corrections. The fundamental correction model is a mathematical model that will take all effects of all the elements in the matrix into account.

The calibrations created on the WDXRF and the EDXRF with fundamental parameters were compared and the following conclusions highlighted. The calibration lines achieved on the WDXRF for the lighter and heavier elements were improved when compared to the EDXRF. This was attributed to the WDXRF being more powerful, with improved sensitivity as well as improved resolution due to the three different detectors. It was decided to validate the final calibration with fundamental parameters on the WDXRF.

The calibration was validated with samples with known concentrations. The samples were grouped into two: the one group that is used in the laboratories for quality control. These samples have limits and the consensus values were determined by various laboratories with various techniques and the values assigned statistically. The

other group was samples with consensus values that were determined with one technique and in one laboratory on different days.

The samples were prepared with the final fusion program, including the oxidation step and the glass beads obtained were perfect with no bubbles, cracks or undissolved particles. The crucibles had no black smears and indicated no reaction between the samples and the crucibles.

The glass beads were analysed on the WDXRF calibration with fundamental parameters. The consensus values and the measured values were compared and the relative percentage differences calculated. The t-values were calculated and the data were presented graphically. For some elements the measured value was compared to the quality control limits of the QC samples. The following conclusions were made: Overall the results indicated a successful fusion for all elements, successful oxidation, since the sulphur results compared very well, successful use of sodium iodide since none of the glass beads shattered and the copper compared well. This was taking into account that there are uncertainties in the results obtained which included, uncertainties in the preparation of both the glass beads and the calibration standards as well as uncertainties in the analyses. There are also uncertainties in the consensus values.

For copper and nickel the comparison of results was very good with few samples that were significantly different. The error in the results was attributed to the lower range of the calibration curve and can be resolved with more, lower range calibration standards. In the case of nickel, the significant difference was also attributed to the purity of the oxide used to prepare the calibration standards. The copper results indicated the successful recovery of copper with the use of potassium iodide as non-wetting agent and the heating mechanism of the Katanax.

The sulphur results compare very well, but with MUC QC 03 failing at the lower range of the calibration. Since the calibration and the calibration standards are considered to be correct, the error was attributed to the consensus values. The determination of sulphur was done by different laboratories by different techniques and it is assumed that in some cases an ICP was used. The ICP is not as accurate for sulphur determination as gravimetry and the results were biased, therefore not comparing well with the WDXRF.

The iron results indicated very good comparisons, with only one significantly different sample. Since the sample was low in iron the difference is attributed to the lower range of the iron calibration and can be corrected with more calibration standards in that region.

The cobalt results compare very well, especially since the samples contained very low concentrations of cobalt. The difference in comparison is attributed to the high dilution of the sample, increasing the uncertainty in the measurement due to the decreased sensitivity of the WDXRF.

The aluminum and calcium oxide results showed a systematic error and a constant bias. The measured results were consistently higher than the consensus value for aluminum oxide and consistently lower for calcium oxide. This was attributed to the calibration and specifically to the oxide used to calibrate for both aluminum and calcium oxide. It is assumed that the aluminum oxide and calcium oxide contribution was not identical to the calculated values used to calibrate the WDXRF and lead to the consistent bias.

The magnesium oxide results compared very well and the significant different samples were in the lower range of the magnesium oxide calibration. The difference is attributed to the lower range of the calibration and can be improved by adding more calibration standards at the lower range.

The chromic oxide results compare very well and the chromic oxide concentration is also low in the samples. Again, the differences are attributed to the high dilution in the sample, increasing the measuring error due to the decreased sensitivity of the WDXRF.

In the case of silicon dioxide the results compare well, however, most of the measured results are higher than the consensus values. Since there was no problem with the calibration or the calibration standards this was attributed to the consensus values. It is known that the method of preparation and determination on the ICP is not very accurate and requires the addition of hydrofluoric acid to keep the silicon dioxide in dilution. Since the measured results were higher than the consensus values it is concluded that the silicon dioxide precipitated during ICP analyses and the consensus values are incorrect. The silicon dioxide did dissolve in the glass beads and would not precipitate as is the case of the ICP solutions.

The results indicate a successful fusion with the correct flux, oxidising agent, non-wetting agent as well as fusion time and temperature. The oxidation as well as the use of the Katanax was successful. The calibration and the use of the fundamental parameters were successful, however in some cases the calibrations can be extended in the lower and higher concentration ranges. In the case of nickel, the purity of the oxides used must be investigated. For aluminum oxide and calcium oxide possible alternatives oxides for the standards should be investigated. In the case of cobalt and chromic oxide dilution of the sample attributed to higher uncertainty in the measurement. This can be corrected with a different dilution.

In terms of the ideal fusion as defined by F Claisse and discussed in Blank and Eksperiandova (1998) the following can be concluded:

- The oxidation and fusion method is simple and rapid with the sample, additives and flux all weighed together at the beginning followed by an

oxidation step of ten minutes and a fusion of ten minutes therefore the production of up to five glass beads in a total of twenty two minutes.

- All the elements and oxides were recovered and showed very good comparisons to consensus values. Where the QCs fail, or the results are significantly different, work can be done to improve these results.
- A wide concentration range was achieved for all elements and oxides with the pure oxide calibration standards. For some elements and oxides the calibration range can be extended to the higher and lower range by preparing more calibration standards.
- In the final fusions, glass beads were produced without sticking and cracking due to the use of the potassium iodide as non-wetting agent. The copper indicated good comparisons and the conclusion can be made that none of the copper was lost.
- Glass beads were produced without any damage to the crucibles and the moulds. The crucibles could be used directly after fusion, however they were all rinsed with hot 20% hydrochloric acid and dried before fusing the next sample to prevent contamination between samples.
- The fundamental parameter correction model was used as the final option for the inter-elemental effects and was successful.

9.7 Future work and investigations

- The ideal sample mass can be investigated with a factorial design experiment to determine the optimum dilution for cobalt and chromic oxide.
- Further investigation can be done into the calibration standards. This should include the investigating the purity of the oxide used for nickel. Possible alternatives for aluminum oxide and calcium oxide should be sought. The range of the calibration can be extended both in the lower and higher ranges.

- These experiments were used as the ground work for further method development. The final method implemented by the laboratory, for samples containing base metals, are using similar fusion techniques with lithium tetra-borate as the flux of choice.

REFERENCES

Andermann, G. (1961), Improvements in the X-ray Emission Analysis of Cement Raw Mix, *Analytical Chemistry*, vol. 33, pp. 1689-1695.

Andermann, G. and Allen, J.D. (1961), The Evaluation and Improvement of X-ray Emission Analysis of Raw-Mix and Finished Cements, *Advances in X-ray Analysis*, vol. 4, pp. 414-432.

Baker, J.W. (1982), Volatilization of Sulphur in Fusion Techniques for Preparation of Discs for X-ray Fluorescence Analysis, *Advances in X-ray Analysis*, vol. 25, pp. 91-94.

Bennett, H. and Oliver, G. (1992), *XRF Analysis of Ceramics, Minerals and Allied Materials*, 1st ed. England: Wiley, 1992.

Bernstein, F. (1963), Particle Size and Mineralogical Effects in Mining Applications, *Advanced X-ray Analytical*, vol. 6, pp. 436-445.

Blank, A.B. and Eksperiandova, L.P. (1998), Specimen Preparation in X-ray Fluorescence Analysis of Materials and Natural Objects, *X-ray Spectrometry*, vol. 27, pp. 147-160.

Brouwer, P. (2003), *Theory of XRF, Getting Acquainted with the Principles*, 1st ed. Netherlands: PANalytical B.V., 2003.

Claisse, F. (1990), *Fusion Procedure for Copper Sulfides*, JCI Laboratory, 1990, pp. 1-6.

Claisse, F. (1995), Cu, Ni, Zn, Pb, Fe Refineries Cement Plants and Geological Services, *Message to Labs involved with Sulphides.*

Claisse, F. (2000), *Borate Fusion of Sulphides: Application to Zinc Sulphide Ores and Concentrates*, Corporate Scientifique Claisse, 2000, pp. 1-8.

Claisse, F. and Samson, C. (1961), Heterogeneity Effects in X-ray Analysis, *Advances in X-ray Analysis*, vol. 5, pp. 335-354.

Dinham, P. (2005), *Memorandum: Composition of matte buttons from XRF glass beads preparation*, Anglo Platinum Research Centre, 2005.

Enzweiler, J. and Webb, P.C. (1996), Determination of Trace Elements in Silicate Rocks by X-ray Fluorescence Spectrometry on 1:5 Glass beads Discs: Comparison of Accuracy and Precision with Pressed Powder Pellet Analysis, *Chemical Geology*, vol. 130, pp. 195-202.

Greenwood, N.N. and Earnshaw, A., (1997), *Chemistry of the Elements*, 2nd ed. Oxford: Butterworth-Heinemann, 1997, pp. 957.

Hickson, K. (1963), The Place of Emission Spectrography and X-ray Fluorescence in Chemical Analysis, *First Ceramic Chemistry Conference Special Publication*, no. 43, pp. 37-55.

Ingamells, C.O. (1970), Lithium Metaborate Flux in Silicate Analysis, *Analytica Chimica Acta*, vol. 52, pp. 323-334.

Kodama, H., Brydon, J.E. and Stone, B.C. (1967), X-ray Spectrochemical Analysis of Silicates Using Synthetic Standards with a Correction for Interelemental Effects by a Computer Method, *Geochimica et Cosmochimica Acta*, vol. 81, pp. 649-659.

Lee, J.D. (1996), *Concise Inorganic Chemistry*, 5th ed. London: Blackwell Science Ltd, 1996.

LeHouilier, R. and Turmel, S. (1974), Bead Homogeneity in the Fusion Technique for X-ray Spectrochemical Analysis, *Analytical Chemistry*, vol. 46, no. 6, pp. 734-736.

LeHouillier, R., Turmel, S. and Claisse, F. (1977), Loss on Ignition in Fused Glass beads Buttons, *Advanced X-ray Analysis*, vol. 20, pp. 459-469.

Lide, D.R. (1990-1991), *Handbook of Chemistry and Physics*, 71st ed. Boston: CRC Press Inc, 1990-1991

Maessen, F.J.M.J. and Boumans, P.W.J.M. (1968), Critical Examination of the Borate Technique for Spectrochemical Trace Analysis of Geological Materials using the D.C. Arc, *Spectrochimica Acta*, vol. 23B, pp. 739-749.

Norrish, K. and Chappell, B.W. (1967), *Physical Methods in Determinative Mineralogy*, (editor Zussman, J.), Academic Press, 1967, vol. 1, pp. 161-209.

Norrish, K. and Hutton, J.T. (1969), An Accurate X-ray Spectrographic Method for the Analysis of a Wide Range of Geological Samples, *Geochimica et Cosmochimica Acta*, vol. 33, pp. 431-453.

Norrish, K. and Thompson, G.M. (1990), XRF Analysis of Sulphides by Fusion Methods, *X-ray Spectrometry*, vol. 19, pp. 67-71.

PANalytical user guide, (2004), *SuperQ software*, Chapter 13, 2004, pp. 1-51.

Rousseau, R.M. (2004), Some Considerations on How to Solve the Sherman Equation in Practice, *Spectrochimica Acta,* Part B, vol. 59, pp. 1491-1502.

Rousseau, R.M. (2006), Corrections for Matrix Effects in X-ray Fluorescence Analaysis – A tutorial, *Spectrochimica Acta,* Part B, vol. 61, pp. 759-777.

Skoog, DA., West, DM. and Holler, FJ. (1996), *Fundamentals of Analytical Chemistry,* 7th ed. London: Saunders College Publishing, 50.

Spangenberg, J., Fontbote, L. and Pernicka, E. (1994), X-ray Fluorescence Analysis of Base Metal Sulphide and Iron-Manganese Oxide Ore Samples in Fused Glass beads Disc, *X-ray Spectrometry*, vol. 23, pp. 83-90.

Turmel, S. and Samson, C. (1984), X-ray Fluorescence Analysis of Iron Ore Concentrates, *X-ray Spectrometry,* vol. 13, no. 2, pp. 87-90.

www.archaeometry.missouri.edu

www.claisse.com

www.des.umd.edu

www.dme.gov.za

www.ksanalytical.com

www.outotech.com

www.socialresearchmethods.net

www.statease.com

www.statsoft.nl

www.thermofisher.com (randy.cone@thermofisher.com)

www.twi.co.uk

www.xray.princeton.edu

APPENDIX A

Table A-1: Summary of details of reagents used

Name	Chemical formula	Supplier	Purity
Sodium hexa-meta-phosphate	$(NaPO_3)_6$	Merck	Analytical
Sodium tetra-borate	$Na_2B_4O_7$	Merck	Analytical
Sodium carbonate	Na_2CO_3	Merck	99.9%
Potassium nitrate	KNO_3	Merck	Analytical
Potassium hydrogen phosphate	KH_2PO_4	Merck	Analytical
Sodium stearate		Merck	Analytical
32% Hydrochloric acid	HCl	Merck	Analytical
Sodium peroxide	Na_2O_2	Merck	$\geq$ 95%
Yttrium 1g/L	Y	Merck	Analytical
Sodium chloride	NaCl	Merck	99.5%
Sodium chlorate	$NaClO_3$	Merck	Analytical
Sodium iodide	NaI	Merck	Analytical
Sodium bromide	NaBr	Merck	CP Grade
Potassium iodate	$NaIO_3$	Merck	99.5%
Sodium nitrate	$NaNO_3$	Merck	99.5%
Copper oxide	CuO	Johnson and Matthey	99.0%
Nickel oxide	NiO	Johnson and Matthey	99.9%
Iron oxide	Fe_2O_3	Johnson and Matthey	99.0%
Cobalt oxide	Co_2O_3	Johnson and Matthey	71.0%
Calcium carbonate	$CaCO_3$	Merck	Analytical
Magnesium oxide	MgO	Johnson and Matthey	99.0%
Aluminum oxide	Al_2O_3	Johnson and Matthey	99.0%

Chromic oxide	Cr_2O_3	Johnson and Matthey	99.0%
Silicon dioxide	SiO_2	Johnson and Matthey	99.995%
Titanium oxide	TiO_2	Merck	Analytical
Zinc oxide	ZnO	Merck	Analytical
Zirconium oxide	ZrO_2	Merck	Analytical
Tellurium oxide	TeO_2	Merck	Analytical
Vanadium oxide	V_2O_5	Merck	Analytical
Arsenic oxide	As_3O_4	Merck	Analytical
Selenium oxide	SeO_2	Merck	Analytical
Tin oxide	SnO_2	Merck	Analytical
Antimony oxide	Sb_2O_4	Merck	Analytical
Manganese oxide	MnO_2	Merck	Analytical
Sodium sulphate	Na_2SO_4	Merck	Analytical
Sodium hydroxide	NaOH	Merck	Analytical
Potassium carbonate	K_2CO_3	Merck	Analytical
Bromine gas	Br(g)	SAARCHEM	Analytical
Nitrogen gas	N_2(g)	Afrox	Analytical
Hydrated magnesium sulphate	$MgSO_4.6H_2O$	Merck	Analytical
Hydrated Aluminum nitrate	$Al(NO_3)_3.9H_2O$	Merck	Analytical
Potassium dichromate	$K_2Cr_2O_7$	Merck	Analytical
Potassium permanganate	$KMnO_4$	Merck	Analytical
Ammonium nitrate	NH_4NO_3	Merck	Analytical
Hydrated sodium per-borate	$NaBO_3.4H_2O$	Merck	Analytical

APPENDIX B

Table B-1: Preliminary experiment details

Glass bead number	Sample type	Sample mass [g]	Flux used	Flux mass [g]	Na_2CO_3 [g]	Glass bead mass [g]
1	Mer[20]	1.0	SHP[21]	10.0	-	8.5
2	Mer	1.0	SHP	10.0	-	8.3
3	UG2[22]	1.0	SHP	10.0	-	8.3
4	UG2	1.0	SHP	10.0	-	7.9
5	Blank	-	SHP	10.0	-	8.1
6	Blank	-	SHP	10.0	-	8.2
7	Mer	1.0	STB[23]	10.0	-	8.6
8	Mer	1.0	STB	10.0	-	8.3
9	UG2	1.0	STB	10.0	-	7.8
10	UG2	1.0	STB	10.0	-	7.9
11	Blank	-	STB	10.0	-	7.0
12	Blank	-	STB	10.0	-	7.5
13	Mer	1.0	STB + SC[24]	6.6	3.4	8.2
14	Mer	1.0	STB + SC	6.6	3.4	7.9
15	UG2	1.0	STB + SC	6.6	3.4	7.5
16	UG2	1.0	STB + SC	6.6	3.4	7.1
17	Blank	-	STB + SC	6.6	3.4	5.3
18	Blank	-	STB + SC	6.6	3.4	4.2

[20] Lebowa Merensky sample type
[21] SHP: Sodium hexa-meta-phosphate
[22] Lebowa UG2 sample type
[23] STB: Sodium tetra-borate
[24] STB + SC: Sodium tetra-borate and sodium carbonate

Table B-2: Comparison of results obtained by XRF and ICP for Merensky sample type reported in percentage

Oxides	SHP	STB	STB + SC	ICP[25]
CuO	4.7	2.9	1.7	4.1
NiO	10.2	4.7	3.5	7.7
Fe_2O_3	35.4	23.6	6.3	26.3
SO_3	2.7	21.0	10.4	36.9
CaO	3.6	2.7	0.9	3.0
MgO	3.4	7.7	9.2	14.1
Al_2O_3	7.0	6.5	2.3	2.9
Cr_2O_3	2.0	0.1	0.6	0.9
SiO_2	5.2	25.8	26.4	36.5

Table B-3: Comparison of results obtained by XRF and ICP for UG2 sample type reported in percentage

Oxides	SHP	STB	STB + SC	ICP
CuO	2.6	2.0	0.7	3.2
NiO	5.1	1.7	0.1	5.0
Fe_2O_3	20.8	15.0	6.6	19.2
SO_3	1.6	9.6	4.0	19.0
CaO	4.3	3.7	1.3	3.6
MgO	7.6	11.5	10.2	16.1
Al_2O_3	13.0	12.1	4.4	6.1
Cr_2O_3	8.3	4.2	2.3	4.4
SiO_2	10.6	33.3	29.0	34.9

Table B-4: Details of experiments done to prepare secondary calibration standards

Stand number	Mer [g]	UG2 [g]	STB [g]	Na_2CO_3 [g]	KH_2PO_4 [g]	Pots Before [g]	Pots after [g]	Diff [g]	Glass bead mass [g]
1	7.0	6.5	90.0	-	-	555.8	Lost	-	92.0
2	10.0	-	90.0	-	-	559.5	560.8	-1.3	95.5
3	-	10.0	90.0	-	-	555.7	558.3	-2.6	87.9
4	5.0	5.0	90.0	-	-	551.9	553.8	-1.9	87.4
5	3.8	3.0	90.0	-	-	559.4	562.9	-3.5	84.1
6	2.5	2.5	70.0	35.0	-	561.3	555.4	5.9	94.3
7	1.0	1.5	55.0	55.0	-	559.4	545.9	13.5	96.3
8	0.5	0.8	85.0	-	11.5	556.5	559.8	-3.3	85.3

[25] ICP: Inductively Coupled Plasma Spectrometer

Table B-5: Details of experiments done to oxidise sulphur in Merensky and UG2 sample types with potassium nitrate

Standard number	$Na_2B_4O_7$ [g]	Na_2CO_3 [g]	Pot before [g]	Pot After [g]	Difference [g]	Glass bead mass [g]
1	80.0	-	555.9	563.0	-7.1	93.8
2	80.0	2.1	546.6	561.9	-15.3	78.0
3	80.0	5.3	539.1	543.9	-4.8	95.2
4	80.0	7.3	537.4	540.7	-3.3	94.6
5	80.0	10.8	535.7	534.0	1.7	97.2
6	80.3	5.4	577.5	581.8	-4.3	103.0
7	80.5	5.5	543.6	552.8	-9.2	98.7
8	80.0	5.3	528.3	541.1	-12.8	102.8

Table B-6: Details of experiments done to produce secondary calibration standards with roasted samples

Standard number	Sample type	Sample [g]	$Na_2B_4O_7$ [g]	Na_2CO_3 [g]	Pot Before [g]	Pot After [g]	Diff [g]	Glass bead mass [g]
9	Mer	10.0	90.5	-	566.8	569.3	-2.5	95.7
10	Mer	10.0	60.0	32.1	544.3	539.5	4.8	85.2
11	UG2	10.2	90.2	-	533.0	535.2	-2.2	96.0
12	UG2	10.2	60.3	32.2	549.9	541.3	8.6	96.1

Table B-7: ICP results of duplicate samples prepared with roasted and unroasted Merensky and UG2 samples types reported in percentage

Standard number	Cu A	Cu B	Ni[26] A	Ni B	Fe A	Fe B	Co A	Co B
1.2[27]	0.4	0.5	1.0	1.0	49.5	50.5	0.1	0.1
3.2	0.7	0.5	1.0	1.0	32.5	32.9	0.1	0.1
4.2	0.5	0.3	1.0	1.0	30.6	32.0	0.1	0.1
5.2	2.1	0.3	1.0	1.0	23.3	22.5	0.1	0.1
6.2	2.3	1.5	2.3	1.0	19.6	20.6	0.1	0.1
7.2	3.2	0.9	2.1	1.0	12.7	6.3	0.1	0.1
8.2	1.0	0.3	1.0	1.0	3.7	4.8	0.1	0.1
1.3[28]	5.5	3.9	13.1	11.7	43.1	43.5	0.2	0.2
2.3	11.0	3.4	14.6	10.3	41.8	41.5	0.3	0.2
3.3	6.7	3.9	11.6	10.9	43.6	41.9	0.2	0.2
4.3	3.1	3.1	9.5	9.2	42.8	43.5	0.2	0.2
5.3	2.5	2.0	6.7	6.7	43.6	44.4	0.2	0.2
6.3	5.4	5.4	12.3	12.6	39.8	40.9	0.2	0.2
7.3	5.4	5.5	12.7	12.5	39.5	40.2	0.2	0.2
8.3	5.6	5.7	12.7	12.4	39.8	39.9	0.2	0.2
9.3	6.3	6.4	11.3	10.8	38.5	38.3	0.2	0.2
10.3	6.1	6.2	11.0	11.0	40.2	40.8	0.2	0.2
11.3	18.0	4.9	20.5	6.8	27.4	27.6	0.2	0.1
12.3	5.4	4.9	7.1	6.9	29.4	30.4	0.2	0.2

[26] The limit of detection of the ICP Ni is 1.0%
[27] The standard numbers indicated as #.2 was prepared in section 3.3
[28] The standard numbers indicated as #.3 was prepared in section 3.4.2

Table B-8: ICP results of duplicate samples prepared with roasted and unroasted Merensky and UG2 sample types reported in percentage

Standard number	Ca A	Ca B	Al A	Al B	Cr[29] A	Cr B	Mg A	Mg B	Si A	Si B
1.2	4.7	9.6	32.5	33.0	3.0	3.0	18.8	18.6	55.4	71.6
3.2	4.0	8.6	31.6	31.5	3.0	3.3	16.0	16.1	60.3	63.1
4.2	3.7	8.6	21.3	21.5	3.0	3.0	14.6	14.0	48.8	49.1
5.2	2.5	7.3	18.5	18.4	3.0	3.0	9.6	9.7	38.6	38.8
6.2	2.1	6.5	53.5	52.6	3.0	3.0	7.0	6.8	83.7	83.2
7.2	1.6	5.6	78.1	39.0	3.0	3.0	3.6	1.8	86.3	57.6
8.2	1.8	5.5	15.7	15.7	3.0	3.0	2.1	1.9	22.5	22.2
1.3	3.3	7.4	40.9	40.5	3.0	3.0	11.8	11.6	60.4	62.2
2.3	3.1	7.5	67.2	65.9	3.0	3.0	11.2	11.0	32.3	88.7
3.3	3.2	7.7	45.9	46.3	3.0	3.0	11.9	11.1	68.2	68.1
4.3	3.1	7.9	46.9	46.6	3.0	3.0	11.8	11.6	69.7	69.5
5.3	3.3	7.7	60.9	59.7	3.0	3.0	12.1	11.8	85.0	84.4
6.3	2.8	7.7	54.1	53.6	3.0	3.0	10.7	10.9	76.5	76.7
7.3	2.8	7.3	51.9	51.6	3.0	3.0	10.5	10.9	75.0	74.3
8.3	2.9	7.4	58.2	58.1	3.0	3.0	10.5	10.4	82.0	81.5
9.3	4.9	8.9	56.4	55.6	3.0	3.0	16.4	15.6	87.2	84.6
10.3	4.8	8.9	111.0	107.0	3.0	3.0	16.2	15.9	148.0	143.0
11.3	5.7	10.0	56.0	54.2	4.2	4.2	19.4	18.8	28.6	84.2
12.3	5.4	9.4	95.4	95.1	5.2	5.5	19.3	18.9	112.0	131.0

[29] The limit of detection of the ICP for chrome is 3.0%

APPENDIX C

Table C-1: Summary of experiments and results obtained for testing halides as non-wetting agents

Non-wetting agent	Non-wetting agent [g]	Flux [g]	Mould Before [g]	Mould after [g]	Mould diff [g]	CuO measured [%]	Halide measured [%]
0.5% NaI	0.05	9.85	34.14	42.92	8.78	0.57	0.00
1% NaI	0.10	9.80	34.14	43.46	9.32	0.58	0.02
2% NaI	0.20	9.70	34.14	43.45	9.31	0.60	0.04
4% NaI	0.40	9.50	34.14	43.61	9.47	0.63	0.11
None	0.00	9.90	34.14	42.70	8.56	0.58	-
1% NaCl	0.10	9.80	34.14	42.76	8.49	0.62	0.68
1% NaBr	0.10	9.80	34.14	43.81	8.62	0.57	0.38
1% $NaIO_3$	0.10	9.80	34.13	42.69	8.56	0.55	0.00
2% $NaIO_3$	0.20	9.71	34.14	43.28	9.14	0.55	0.01
4% $NaIO_3$	0.40	9.50	34.14	43.32	9.19	0.56	0.02

Table C-2: Mass of oxides, flux and non-wetting agent weighed to prepare oxides calibration standards with sodium iodide as non-wetting agent.

	Blank 1	**Blank 2**	**Oxide Std 1**	**Oxide Std 2**	**Oxide Std 3**	**Oxide Std 4**	**Oxide Std 5**	**Oxide Std 6**	**Oxide Std 7**	**Oxide Std 8**	**Oxide Std 9**	**Oxide Std 10**
SiO_2	-	-	0.40	-	0.30	-	0.20	-	0.10	-	0.05	-
Fe_2O_3	-	-	-	0.05	0.10	-	-	0.15	-	0.20	0.25	-
MgO	-	-	-	0.15	-	0.12	-	-	0.09	-	0.06	0.03
Na_2SO_4	-	-	0.05	-	-	0.11	-	-	0.16	0.21	-	0.27
$CaCO_3$	-	-	-	0.09	-	0.07	0.05	0.04	-	-	-	0.02
Al_2O_3	-	-	-	-	0.05	-	0.04	0.03	0.02	0.01	-	-
CuO	-	-	-	0.01	-	0.02	0.03	0.05	-	-	-	0.05
NiO	-	-	-	0.05	-	-	0.04	-	0.03	0.02	0.01	-
Cr_2O_3	-	-	-	0.05	-	0.04	-	0.03	0.01	-	-	0.02
Co_3O_4	-	-	0.01	0.02	-	0.03	-	0.04	-	-	-	0.05
TiO_2	-	-	-	0.05	-	0.04	-	0.03	-	-	0.02	0.01
ZnO	-	-	-	-	-	0.01	0.02	-	0.03	0.04	-	0.05
ZrO_2	-	-	0.05	-	0.04	0.03	-	0.02	-	-	0.01	-
TeO_2	-	-	-	0.02	0.01	-	0.03	-	0.04	-	0.05	-
V_2O_5	-	-	0.01	-	-	0.02	-	0.03	-	0.04	-	0.05
As_2O_3	-	-	-	0.01	-	0.02	0.03	0.04	-	-	0.06	-
SeO_2	-	-	-	0.04	-	0.05	0.03	-	0.02	0.01	-	-
SnO_2	-	-	-	-	-	0.02	0.01	-	0.03	0.04	-	0.05
Sb_2O_4	-	-	-	-	-	-	0.04	0.05	0.01	0.02	-	0.03
MnO_2	-	-	-	-	-	-	-	0.02	0.03	-	-	-
NaI	-	0.10	0.10	0.10	0.10	0.10	0.10	0.10	0.10	0.10	0.10	0.10
Na_2CO_3	0.50	0.50	0.50	0.50	0.50	0.50	0.50	0.50	0.50	0.50	0.50	0.50
Flux	9.71	9.61	9.11	9.11	9.11	9.17	9.18	9.11	9.12	9.11	9.26	9.10

Table C-3: Calibration results for preparation of oxide calibration standards with iodide as non-wetting agent

	Blank 1	**Blank 2**	**Oxide Std 1**	**Oxide Std 2**	**Oxide Std 3**	**Oxide Std 4**	**Oxide Std 5**	**Oxide Std 6**	**Oxide Std 7**	**Oxide Std 8**	**Oxide Std 9**	**Oxide Std 10**
Crucible Before [g]	26.7	30.9	26.7	30.9	26.7	30.9	26.7	30.9	26.7	30.9	26.7	30.9
Crucible After [g]	27.6	30.9	26.7	31.0	26.7	30.9	26.7	31.0	26.7	30.9	26.7	31.0
Crucible Diff [g]	0.9	0.0	0.0	0.1	0.0	0.0	0.0	0.1	0.1	0.0	0.0	0.1
Mould before [g]	34.1	34.1	34.1	34.1	34.1	34.1	34.1	34.1	34.1	34.1	34.1	34.1
Mould after [g]	43.1	44.0	43.9	44.0	43.9	43.8	43.7	43.3	43.9	44.0	44.0	43.9
Mould diff [g]	9.0	9.8	9.8	9.9	9.7	9.7	9.6	9.2	9.8	9.9	9.9	9.8
Bead Mass [g]	9.9	9.9	9.7	10.0	9.7	9.7	9.6	9.8	9.8	9.9	9.9	9.9
LOI [%]	1.1	1.4	2.7	3.2	2.6	2.7	3.7	2.1	1.7	1.4	1.0	1.1

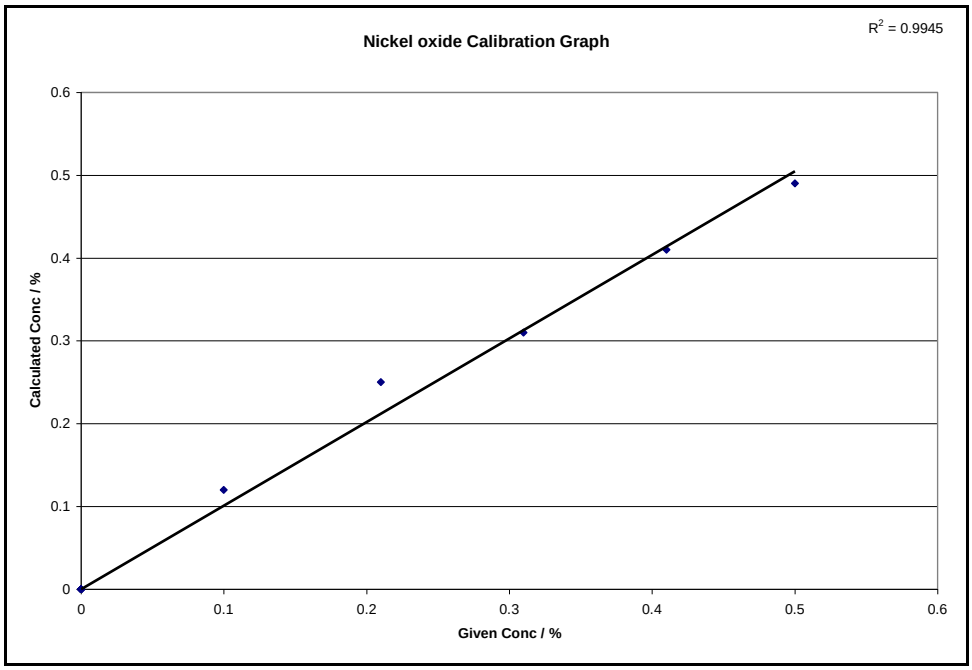


Figure C-0-1: Nickel oxide calibration graph with sodium iodide as non-wetting agent and FP corrections

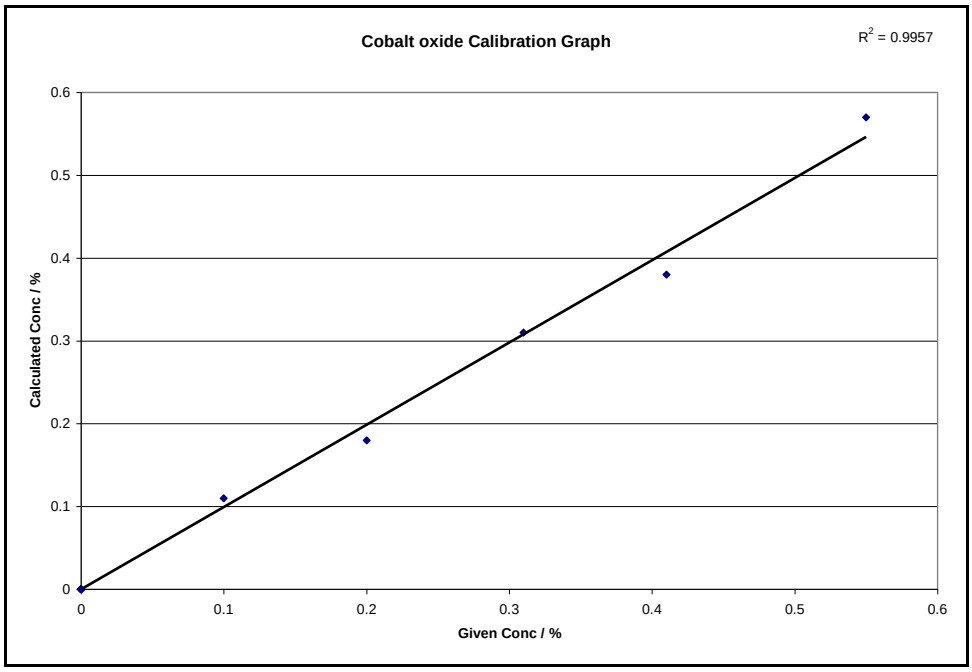


Figure C-0-2: Cobalt oxide calibration graph with sodium iodide as non-wetting agent ad FP corrections

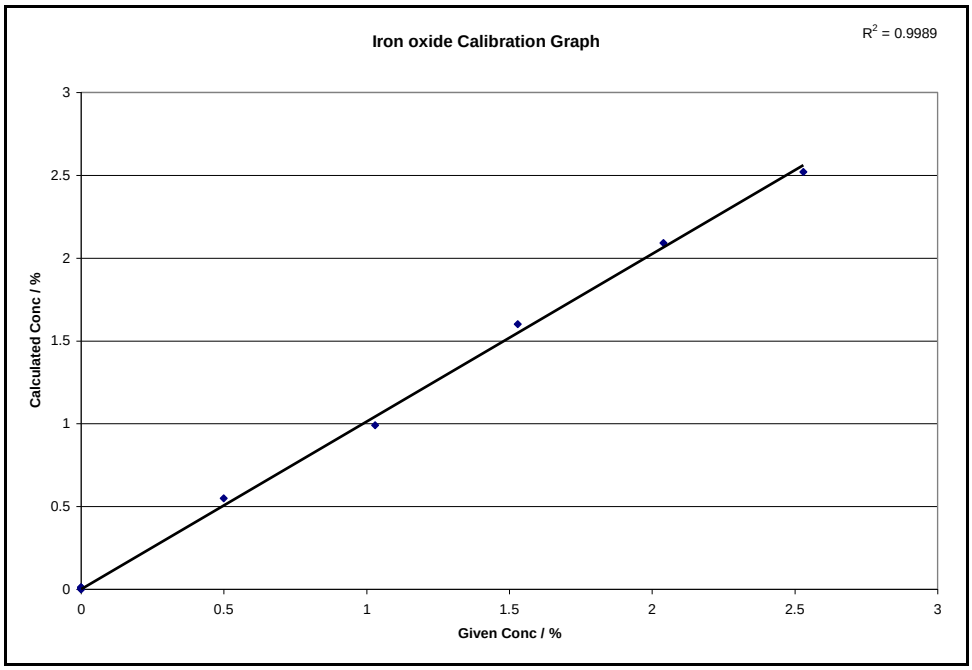


Figure C-0-3: Iron oxide calibration graph with sodium iodide as non-wetting agent and FP correction

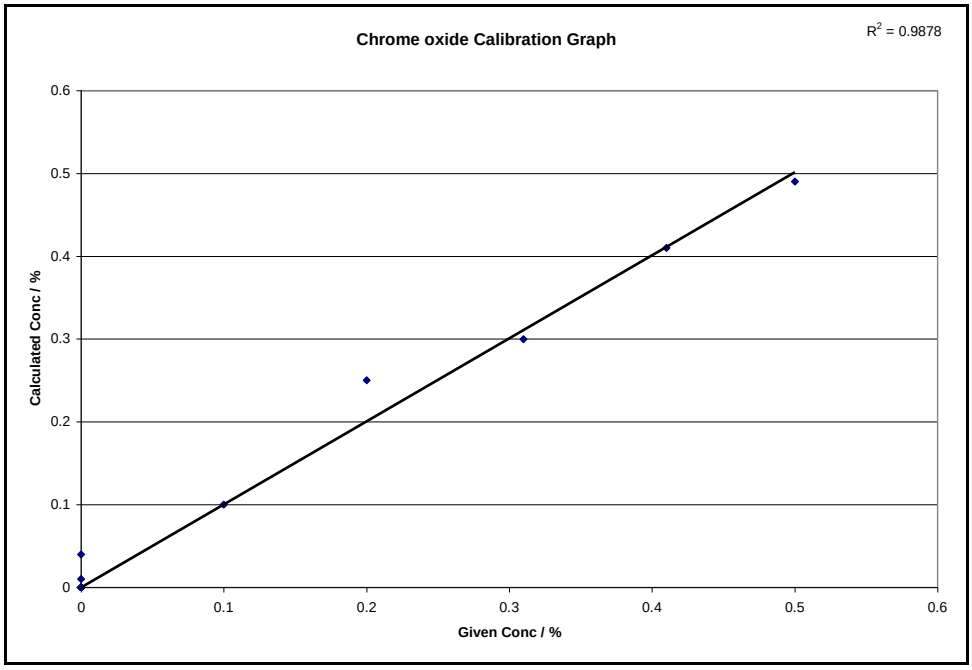


Figure C-0-4: Chromic oxide calibration graph with sodium iodide as non-wetting agent and FP corrections

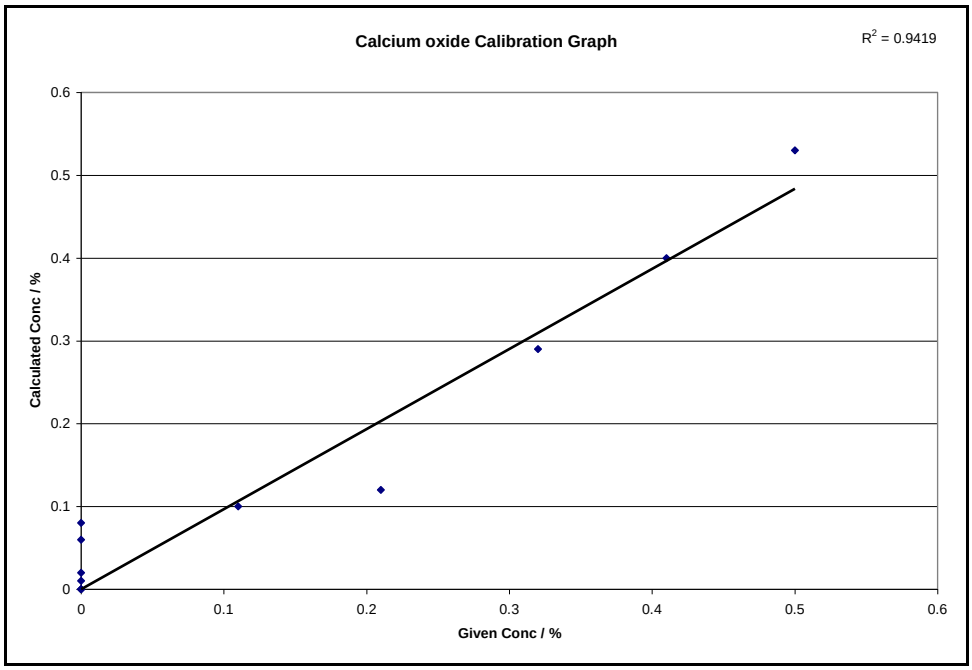


Figure C-0-5: Calcium oxide calibration graph with sodium iodide as non-wetting agent and FP corrections

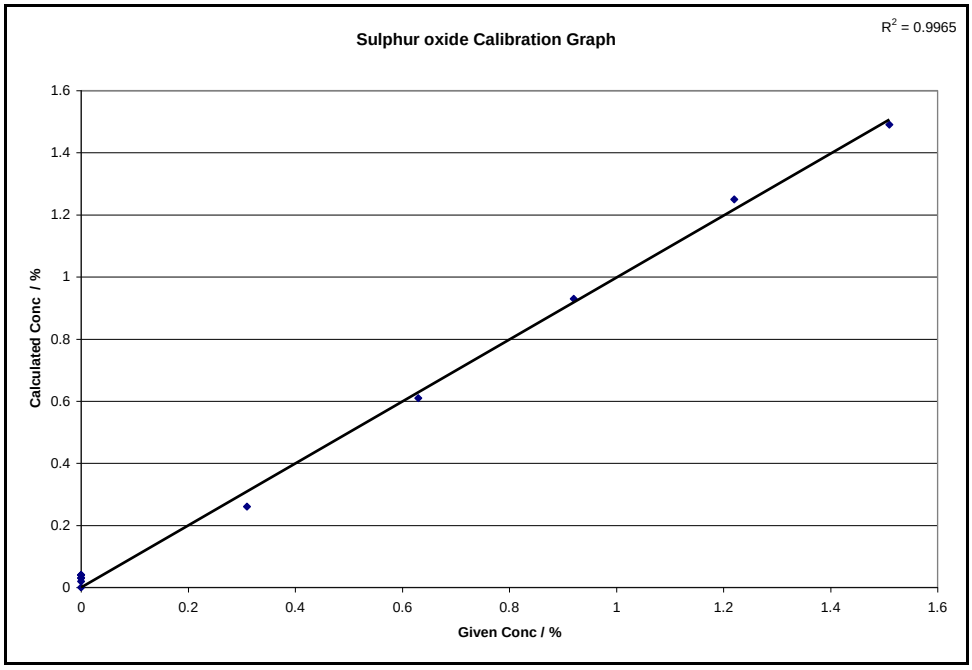


Figure C-0-6: Sulphur oxide calibration graph with sodium iodide as non-wetting agent and FP correction

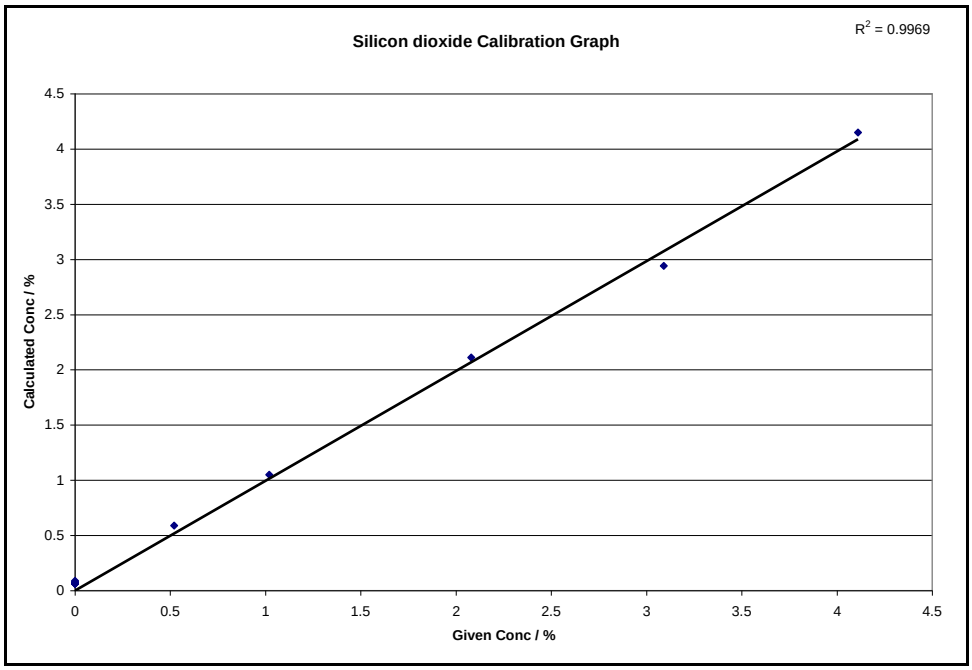


Figure C-0-7: Silicon dioxide calibration graph with sodium iodide as non-wetting agent and FP corrections

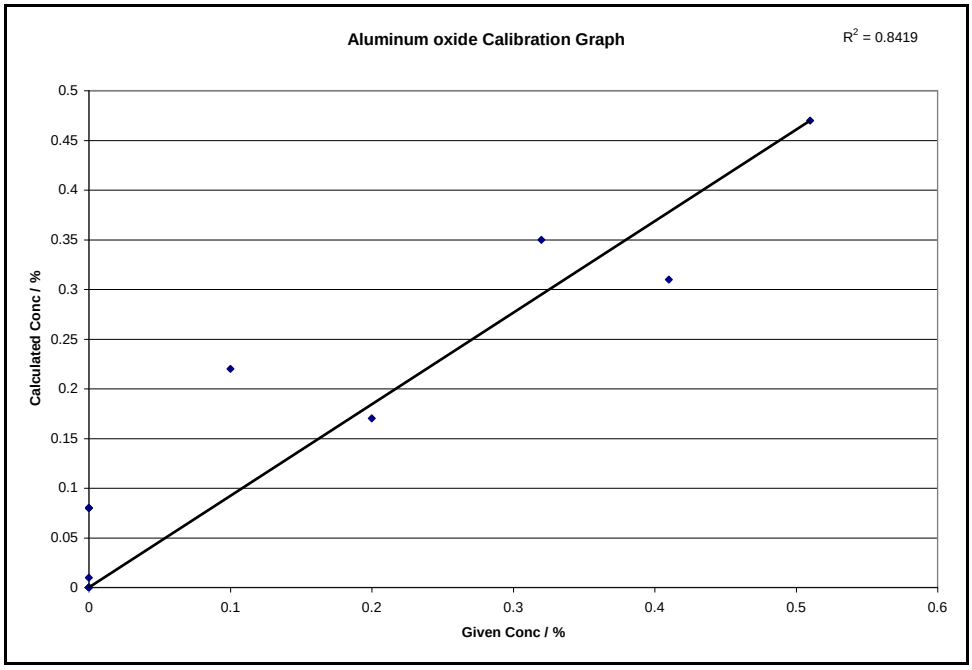


Figure C-0-8: Aluminum oxide calibration graph with sodium iodide as non-wetting agent and FP corrections

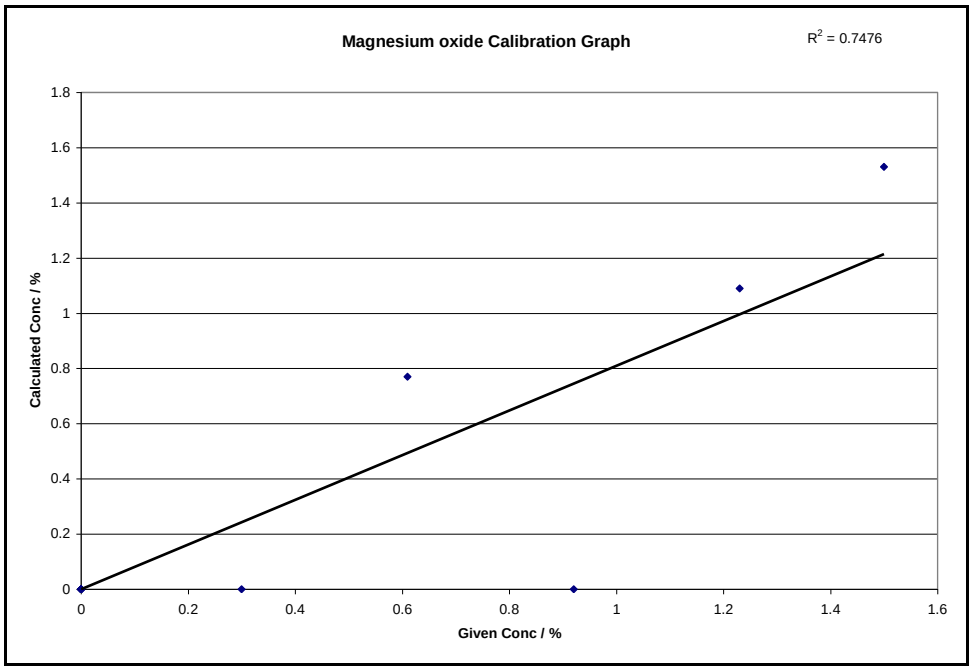


Figure C-0-9: Magnesium oxide with sodium iodide as non-wetting agent and FP corrections

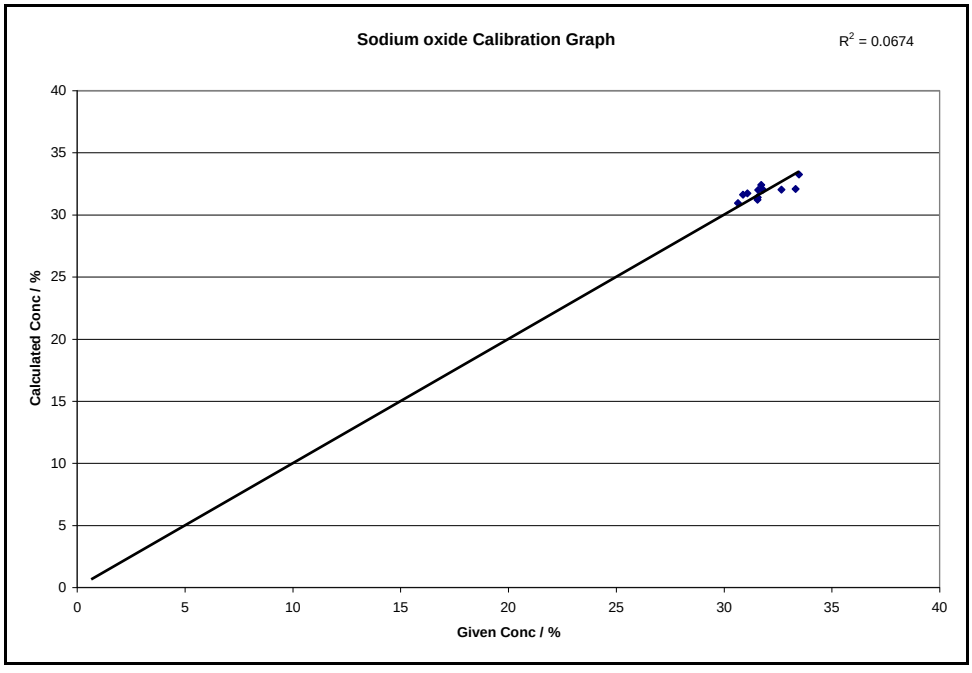


Figure C-0-10: Sodium oxide calibration graph with sodium iodide as non-wetting agent and FP corrections

Table C-4: Validation of calibration created with oxide calibration standards and sodium iodide as non-wetting agent

Glass bead number	Sample [g]	NaI [g]	Flux [g]	Crucible Before [g]	Crucible after [g]	Crucible Diff [g]	Mould before [g]	Mould after [g]	Mould Diff [g]	Glass bead mass [g]
Glass bead 1	0.25	0.10	9.68	26.65	26.79	0.14	34.13	43.78	9.65	9.79
Glass bead 2	0.25	0.10	9.85	30.86	30.92	0.06	34.13	44.04	9.90	9.96

Table C-5: Summary of experimental details with no non-wetting agent

Glass bead number	Sample [g]	Flux [g]	Crucible Before [g]	Crucible after [g]	Crucible Diff [g]	Mould before [g]	Mould after [g]	Mould Diff [g]	Glass bead mass [g]
FB 45	0.25	9.75	30.86	31.88	1.02	34.37	43.20	8.83	9.85
FB 46	-	10.00	31.89	32.08	0.19	34.37	44.94	10.57	10.76
FB 47	0.26	9.75	26.71	27.63	0.92	34.37	43.27	8.90	9.82
FB 48	-	10.01	27.63	27.58	-0.06	34.37	45.16	10.79	10.73
FB 49	0.25	9.75	30.88	32.23	1.34	34.37	42.87	8.51	9.85
FB 50	-	10.00	32.23	31.77	-0.45	34.37	45.51	11.14	10.68

Table C-6: Summary of experimental details with integrated flux

Glass bead number	Sample [g]	Integrated flux [g]	Mould Before [g]	Mould After [g]	Mould diff [g]
FB 40	-	10.00	34.37	44.12	9.75
FB 41	0.25	9.75	34.37	44.25	9.88
FB 42	0.25	9.75	34.37	44.12	9.75

Table C-7: Summary of experimental details with alternative non-wetting agents

Glass bead number	Sample [g]	NWA [g]	Flux [g]	Crucible Before [g]	Crucible After [g]	Mould before [g]	Mould After [g]	Glass bead mass [g]
FB 52	0.26	1.00	9.50	26.67	27.48	34.37	43.70	10.14
FB 53	0.26	1.00	9.51	30.86	31.85	34.37	43.96	10.58
FB 54	0.25	1.00	9.50	26.71	27.71	34.37	43.81	10.44
FB 55	0.25	1.14	9.51	30.88	31.98	34.37	43.75	10.48
FB 60	0.25	0.50	9.51	26.68	27.86	34.49	43.38	10.07
FB 61	0.27	0.50	8.75	30.86	32.04	34.49	42.94	9.64

Table C-8: Summary of experimental details with bromine gas as non-wetting agent

Glass bead number	CuO [g]	Flux [g]	Crucible before [g]	Crucible after [g]	Mould before [g]	Mould after [g]	Glass bead mass [g]
FB 76	-	10.01	30.88	32.03	34.48	43.17	9.85
FB 77	0.11	10.02	26.72	27.12	34.49	44.02	9.93
FB 86	0.05	9.95	26.68	28.11	34.13	42.50	9.80
FB 80	-	10.02	30.87	30.98	34.48	44.23	9.86
FB 81	-	10.01	26.69	27.04	34.48	43.97	9.83
FB 82	0.05	9.97	30.86	31.16	34.48	44.06	9.88
FB 83	0.07	9.95	26.67	27.53	34.48	43.47	9.85
FB 84	0.05	9.93	30.87	30.94	34.48	44.20	9.79
FB 85	0.05	9.97	30.87	31.10	34.48	44.07	9.82
FB 87	-	10.01	30.88	31.03	34.48	44.13	9.80

Table C-9: Mass of oxides and flux weighed to prepare calibration standards with bromine gas as non-wetting agent

	Blank 1	**Oxide Std 1**	**Oxide Std 2**	**Oxide Std 3**	**Oxide Std 4**	**Oxide Std 5**	**Oxide Std 6**	**Oxide Std 7**	**Oxide Std 8**	**Oxide Std 9**	**Oxide Std 10**
SiO_2	-	0.44	-	0.33	-	0.22	-	0.11	-	0.06	-
Fe_2O_3	-	-	0.06	0.11	-	-	0.17	-	0.22	0.29	-
MgO	-	-	0.16	-	0.13	-	-	0.10	-	0.07	0.03
Na_2SO_4	-	0.06	-	-	0.13	-	-	0.20	0.24	-	0.30
$CaCO_3$	-	-	0.01	-	0.08	0.06	0.04	-	-	-	0.02
Al_2O_3	-	-	-	0.06	-	0.04	0.04	0.02	0.01	-	-
CuO	-	0.01	-	-	0.02	0.03	0.04	-	-	-	0.06
NiO	-	-	0.05	-	-	0.05	-	0.04	0.02	0.01	-
$K_2Cr_2O_7$	-	-	0.12	-	0.09	-	0.06	0.02	-	-	0.04
Co_3O_4	-	0.01	0.02	-	0.03	-	0.04	-	-	-	0.06
MnO_2	-	-	0.01	0.02	0.05	-	-	0.03	0.05	-	-
$NaNO_3$	0.26	0.25	0.25	0.26	0.25	0.25	0.25	0.25	0.25	0.25	0.25
Na_2CO_3	0.25	0.25	0.26	0.25	0.25	0.25	0.25	0.25	0.25	0.26	0.26
Flux	10.77	10.23	10.36	10.24	10.66	10.34	10.51	10.40	10.23	10.34	10.25

Table C-10: Calibration results for preparation of oxide calibration standards with bromine gas as the non-wetting agent

	Blank 1	**Oxide Std 1**	**Oxide Std 2**	**Oxide Std 3**	**Oxide Std 4**	**Oxide Std 5**	**Oxide Std 6**	**Oxide Std 7**	**Oxide Std 8**	**Oxide Std 9**	**Oxide Std 10**
Crucible Before [g]	30.86	26.65	30.85	26.69	26.70	26.70	30.86	26.68	30.88	26.68	30.87
Crucible After [g]	31.04	26.77	31.02	26.76	26.78	26.73	31.06	26.76	31.00	26.83	30.85
Crucible Diff [g]	0.18	0.12	0.17	0.07	0.08	0.03	0.20	0.08	0.12	0.15	-0.02
Mould before [g]	34.48	34.13	34.48	34.13	34.48	34.13	34.48	34.48	34.48	34.13	34.48
Mould after [g]	45.18	44.82	45.17	44.86	45.59	44.90	45.30	45.41	45.24	44.81	45.40
Mould diff [g]	10.70	10.68	10.69	10.73	11.11	10.77	10.82	10.93	10.76	10.68	10.91
Bead Mass [g]	10.88	10.80	10.86	10.80	11.19	10.80	11.02	11.01	10.88	10.83	10.90
LOI [%]	1.25	1.75	1.62	1.89	1.90	1.53	0.98	1.34	1.23	1.61	0.87

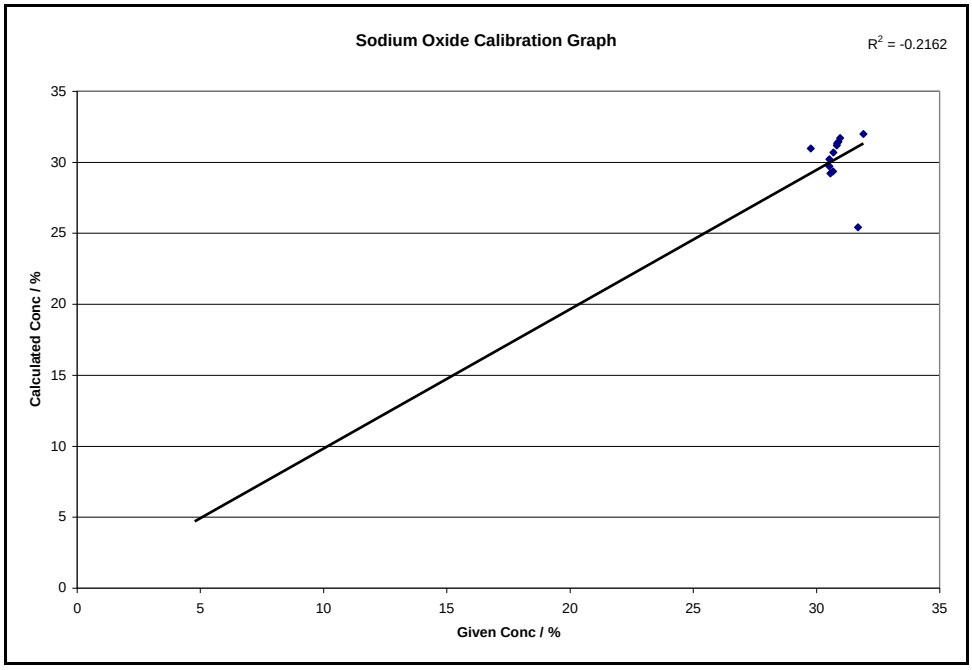


Figure C-0-11: Sodium oxide calibration graph with bromine gas as non-wetting agent

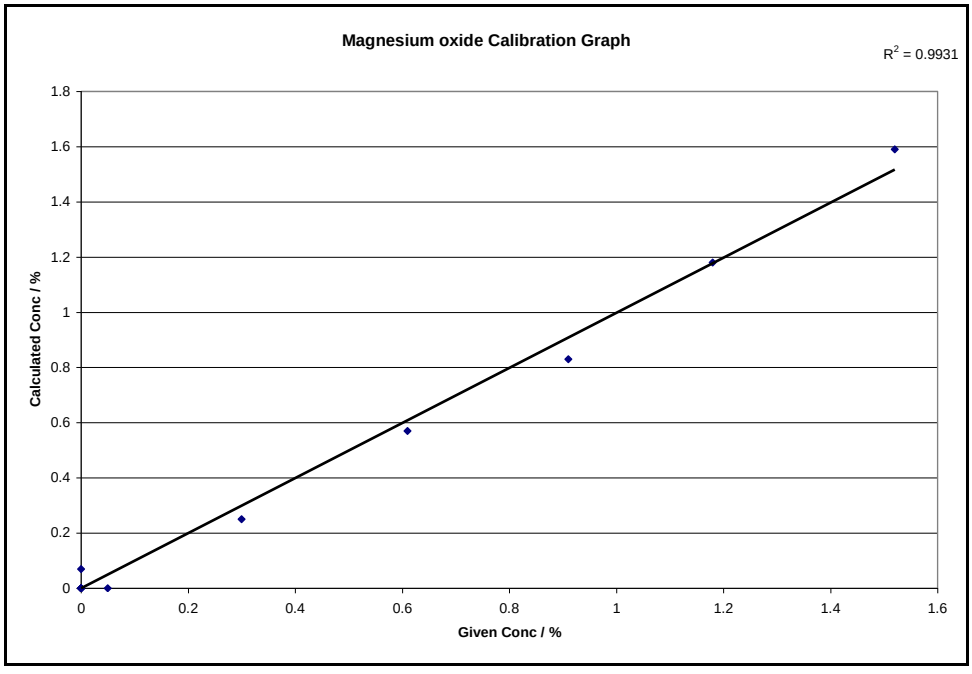


Figure C-0-12: Magnesium oxide calibration graph with bromine gas as non-wetting agent

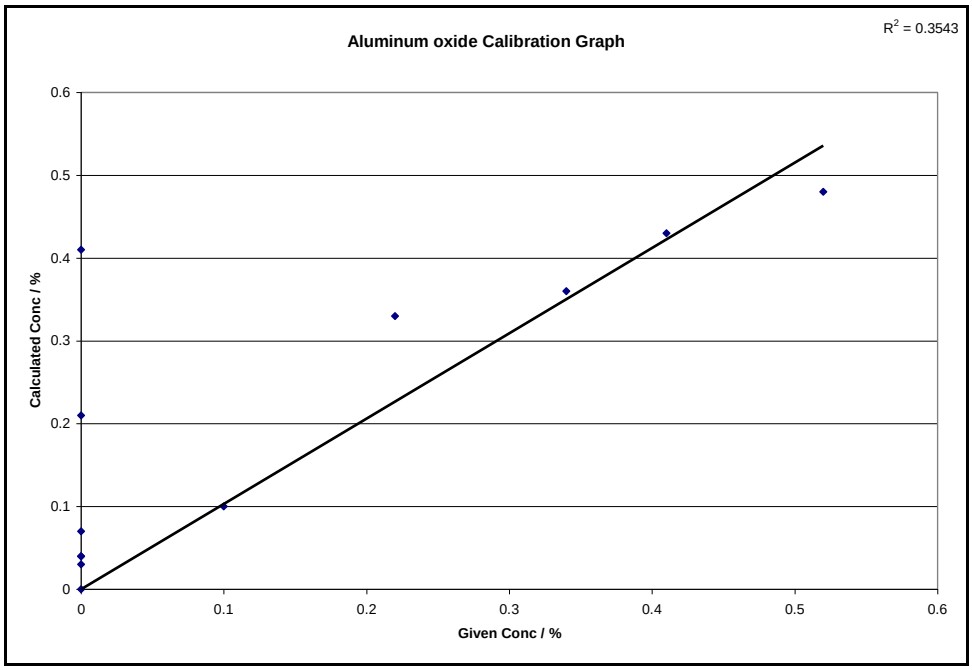


Figure C-0-13: Aluminum oxide calibration graph with bromine gas as non-wetting agent

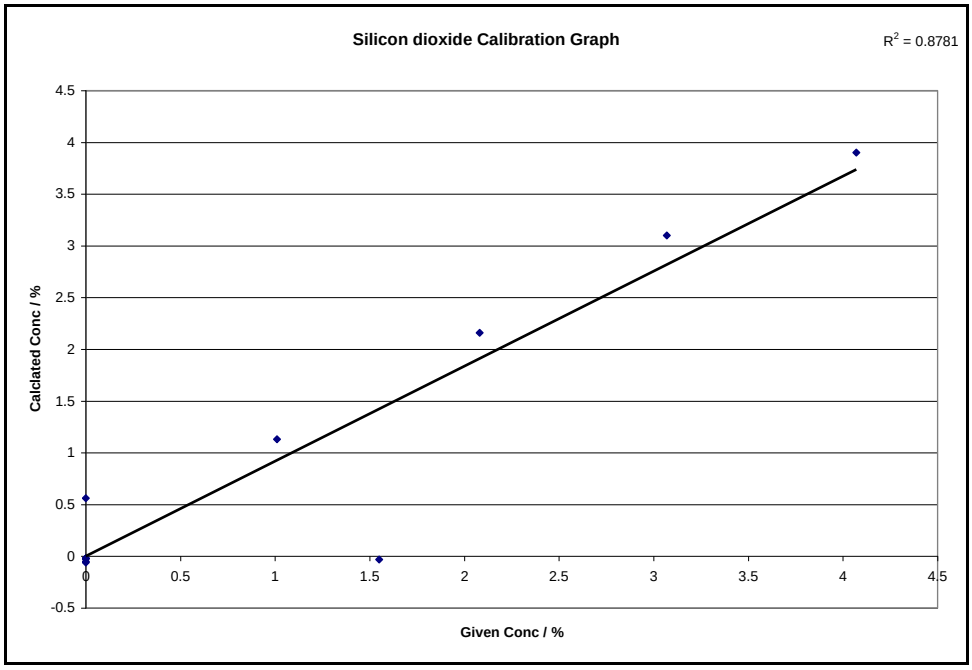


Figure C-0-14: Silicon dioxide calibration graph with bromine gas as non-wetting agent

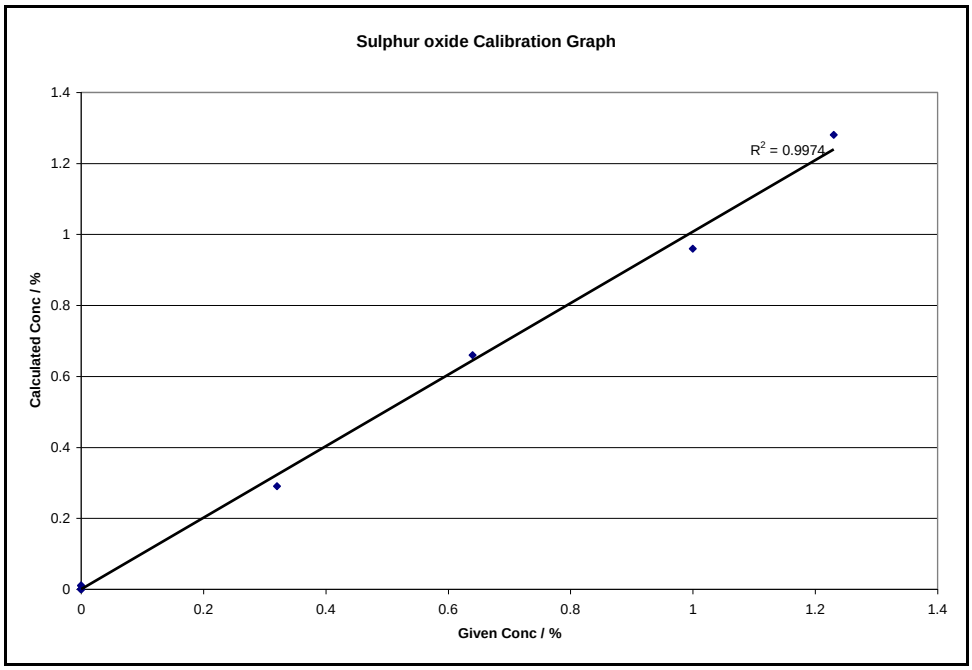


Figure C-0-15: Sulphur oxide calibration graph with bromine gas as non-wetting agent

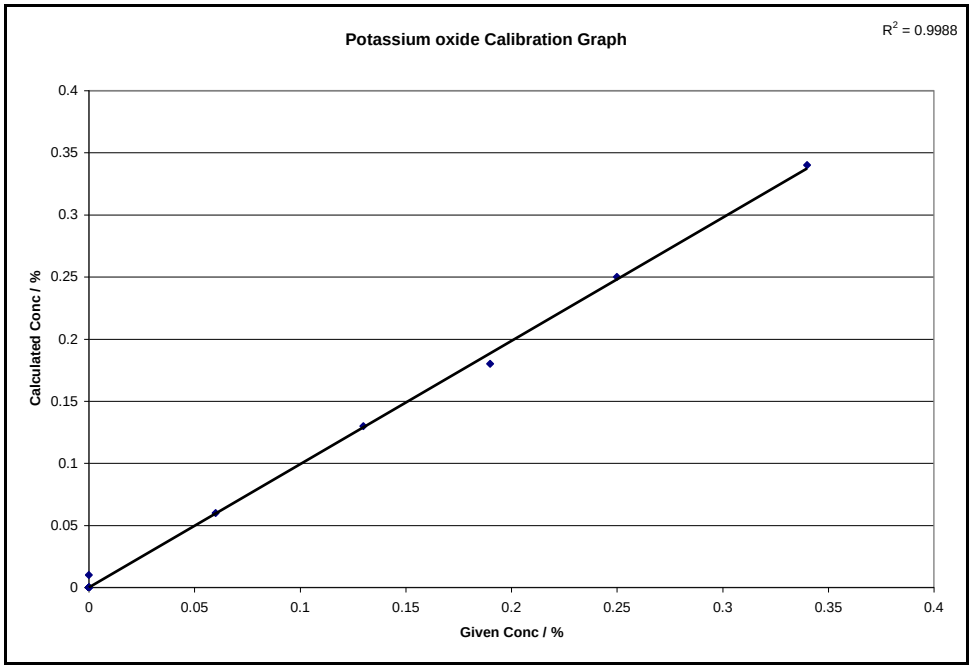


Figure C-0-16: Potassium oxide calibration graph with bromine gas as non-wetting agent

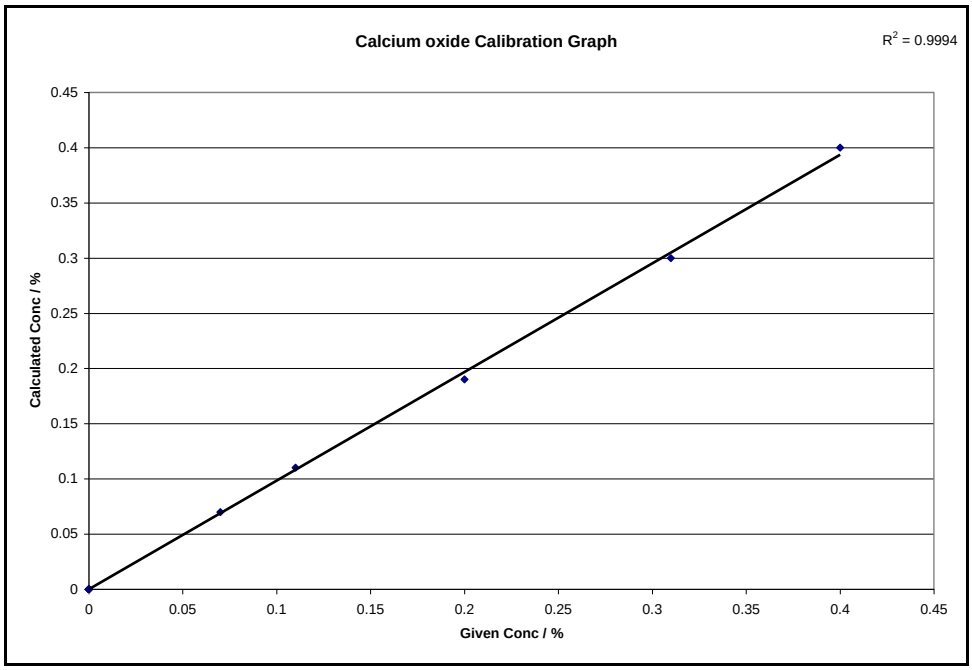


Figure C-0-17: Calcium oxide calibration graph with bromine gas as non-wetting agent

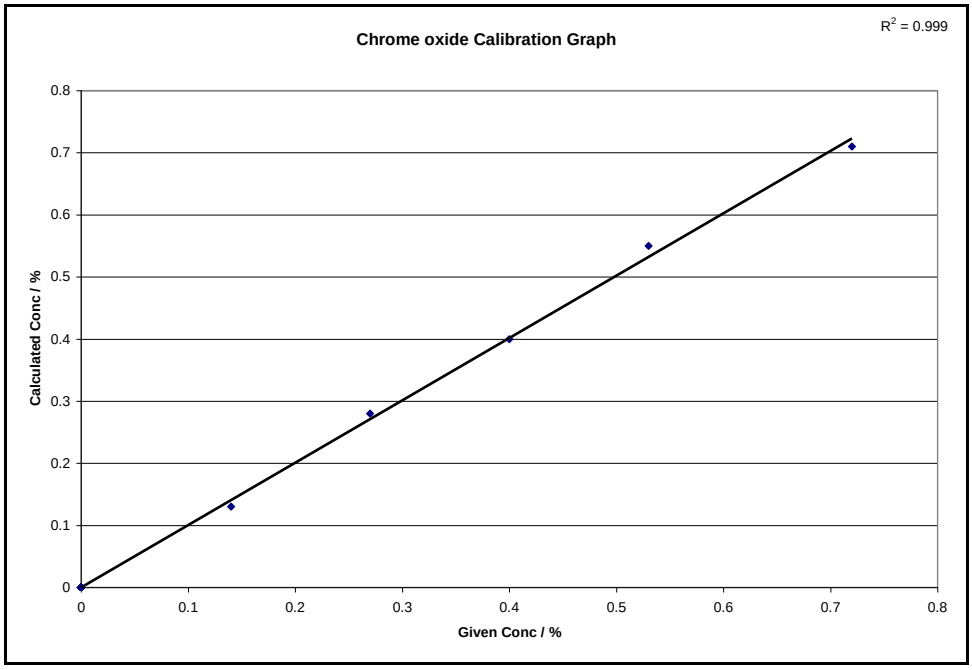


Figure C-0-18: Chromic oxide calibration graph with bromine gas as non-wetting agent

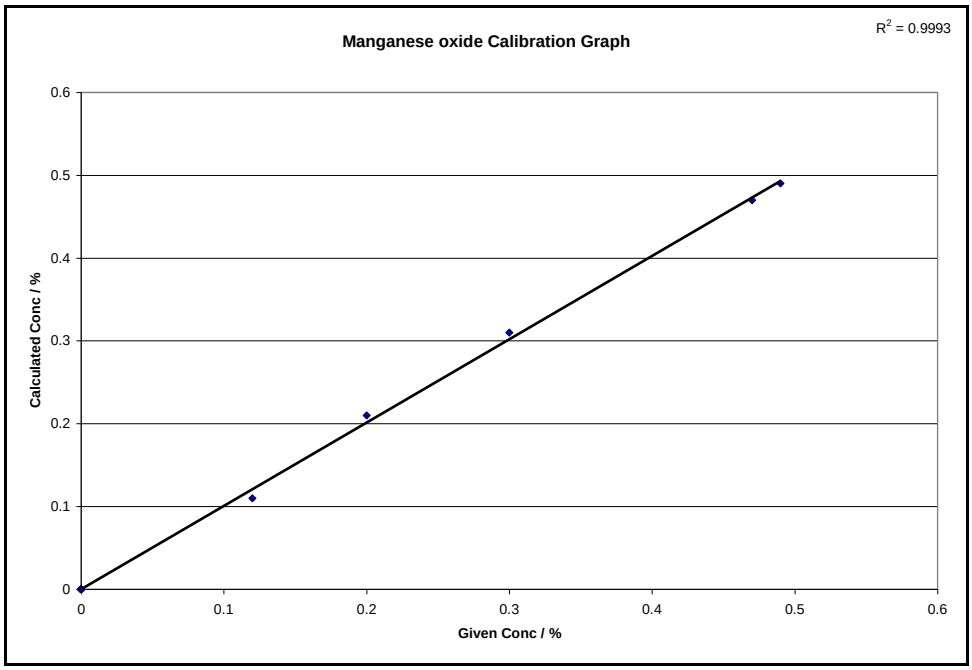


Figure C-0-19: Manganese oxide calibration graph with bromine gas as non-wetting agent

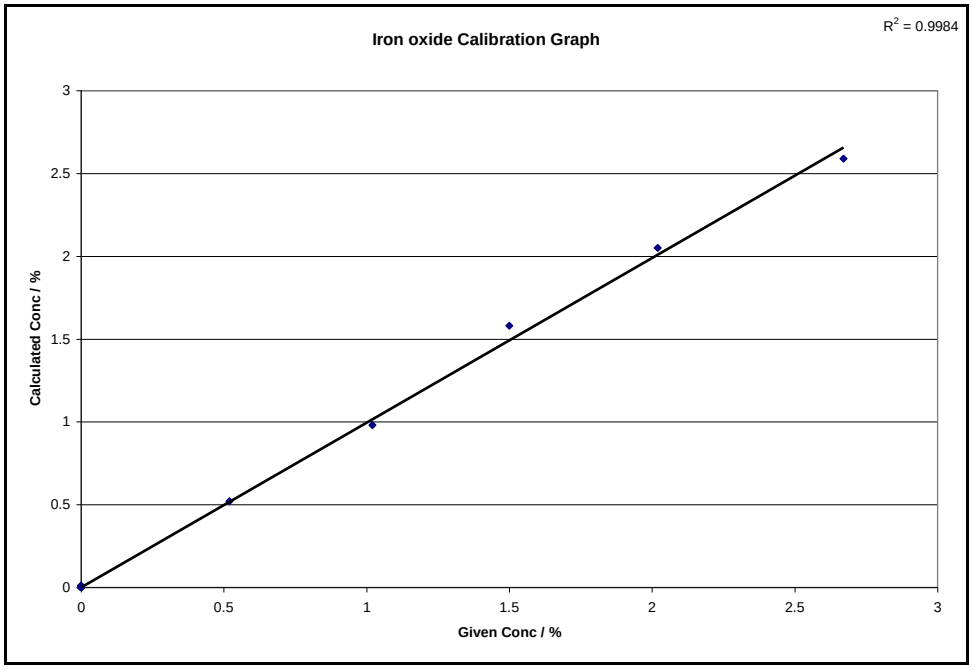


Figure C-0-20: Iron oxide calibration graph with bromine gas as non-wetting agent

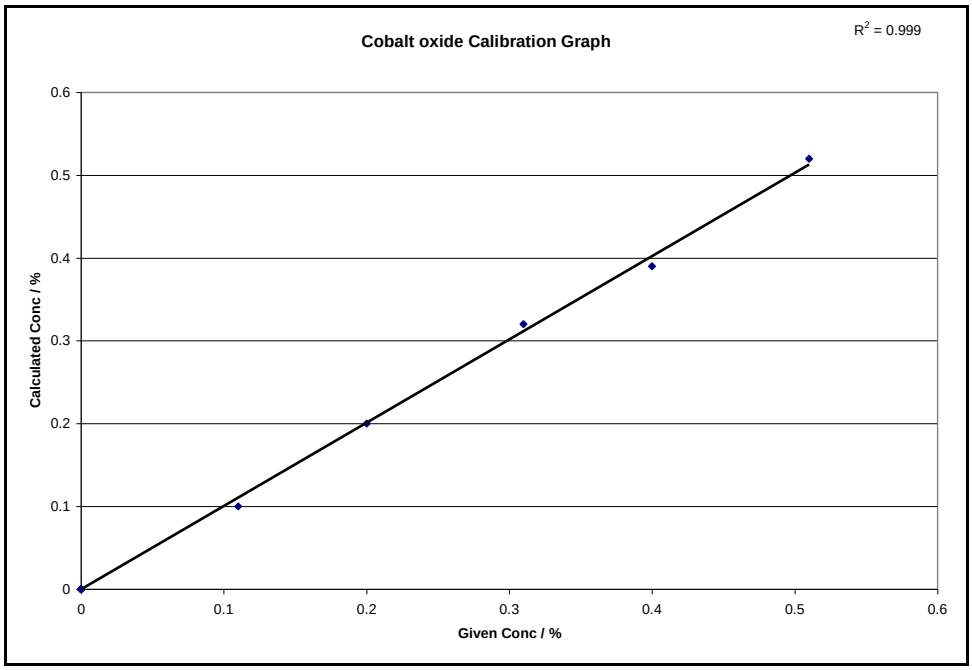


Figure C-0-21: Cobalt oxide calibration graph with bromine gas as non-wetting agent

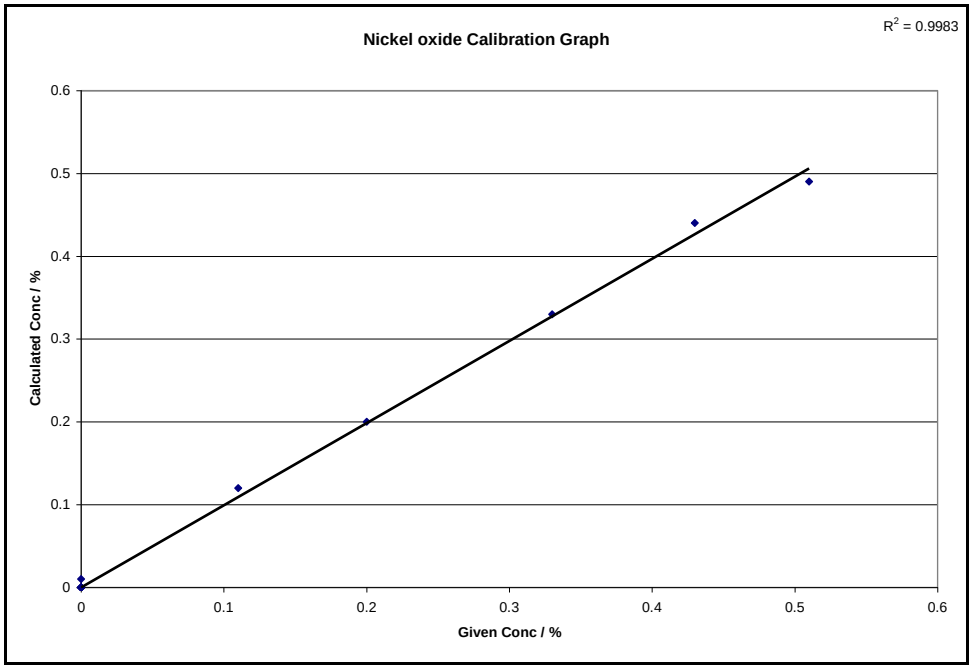


Figure C-0-22: Nickel oxide calibration graph with bromine gas as non-wetting agent

APPENDIX D

Table D-1: Experimental detail of samples prepared with different halides as non-wetting agents in the Katanax

Halide used	EDXRF Calibrated	CuO [g]	Halide [g]	Flux [g]	Crucible Before [g]	Crucible after [g]	Mould before [g]	Mould after [g]	Glass bead mass [g]
NaBr	Yes	-	0.22	10.86	30.32	30.81	34.43	44.71	11.07
-	Yes	0.05	-	10.96	30.35	32.28	34.35	43.13	11.01
-	Yes	0.11	-	10.93	30.21	32.14	34.11	42.94	11.04
NaCl	No	0.06	0.12	10.87	29.71	31.70	34.43	43.21	11.05
NaBr	No	0.06	0.12	10.88	29.74	29.93	33.87	44.40	11.06
NaBr	No	0.10	0.17	10.84	30.12	30.71	34.35	44.59	11.11
NaBr	No	0.04	0.04	7.00	30.35	31.42	36.51	42.28	7.07
NaBr	No	0.04	0.07	6.93	29.71	30.77	35.94	41.70	7.04
NaBr	No	0.04	0.15	6.90	30.32	30.42	36.41	43.12	7.08
KI	Yes	0.00	0.17	6.87	30.20	30.20	36.62	43.42	6.81
KI	Yes	0.04	0.04	7.01	29.71	29.77	36.51	43.31	6.80
KI	No	0.04	0.08	7.01	30.32	30.34	36.41	43.23	6.85
KI	No	0.04	0.14	6.91	30.35	30.35	35.95	42.77	6.82

Table D-2: Results obtained for samples prepared with different halides as non-wetting agents in the Katanax

Halide used	CuO Measured [%]
1 % Chloride	0.49
1 % Bromide	0.55
1.5 % Bromide	0.98
0.5 % Bromide	0.52
1 % Bromide	0.57
2 % Bromide	0.56
0.5 % Iodide	0.52
1 % Iodide	0.64
2 % Iodide	0.57

Table D-3: Mass of oxides, flux, additives ad non-wetting agent weighed to prepare oxide calibration standards with potassium iodide as the non-wetting agent in the Katanax

	OCS 1	**OCS 2**	**OCS 3**	**OCS 4**	**OCS 5**	**OCS 6**	**OCS 7**	**OCS 8**	**OCS 9**	**OCS 10**	**OCS 11**	**OCS 12**	**OCS 13**	**OCS 14**
SiO_2	0.424	-	0.351	-	0.281	0.124	0.218	0.056	0.140	-	0.100	-	0.038	-
Fe_2O_3	-	0.087	-	0.040	-	-	0.079	0.049	0.100	-	-	0.142	-	0.173
$MgSO_4$	-	0.603	-	0.472	-	0.452	0.354	-	-	0.230	-	0.120	0.315	-
Na_2SO_4	0.039	-	-	-	0.115	0.089	-	0.148	-	0.190	-	-	-	-
$CaCO_3$	-	0.063	-	0.051	-	-	-	-	-	0.014	-	0.038	0.037	-
$Al(NO_3)_3$	-	-	0.055	-	-	0.388	-	0.211	-	-	0.102	0.402	-	-
CuO	0.007	-	-	0.019	0.022	-	-	-	0.010	0.037	-	0.014	-	-
NiO	-	0.036	-	-	0.033	-	0.023	0.017	-	-	0.042	-	0.016	0.010
$K_2Cr_2O_7$	-	-	-	0.058	-	0.046	0.015	0.071	-	0.028	-	-	-	-
Co_3O_4	0.007	0.014	-	0.021	-	-	-	-	0.029	-	-	-	0.034	-
$KMnO_4$	-	-	0.076	-	0.018	-	0.019	-	0.024	-	0.030	-	-	0.038
KI	0.097	0.094	0.084	0.080	0.068	0.107	0.055	0.049	0.042	0.036	0.043	0.049	0.059	0.061
$NaNO_3$	0.250	0.260	0.257	0.263	0.253	0.255	0.249	0.250	0.250	0.264	0.272	0.249	0.255	0.250
Na_2CO_3	0.250	0.251	0.249	0.250	0.252	0.251	0.270	0.280	0.250	0.254	0.277	0.248	0.259	0.252
Flux	6.258	6.241	6.324	6.322	6.226	6.107	6.102	6.317	6.432	6.444	6.507	6.457	6.558	6.448

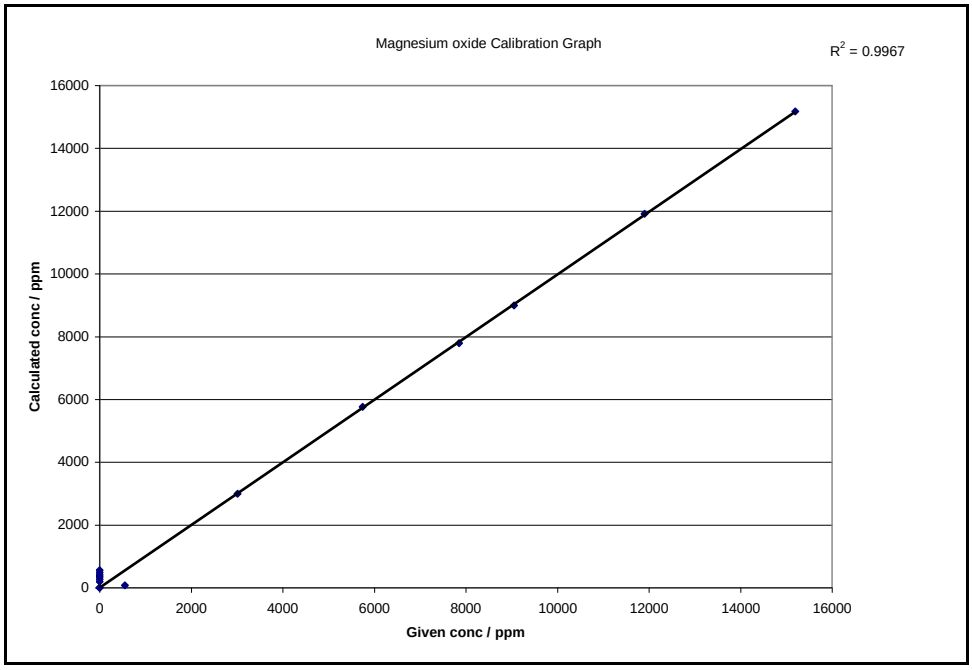


Figure D-0-1: Magnesium oxide calibration graph with potassium iodide as non-wetting agent and empirical corrections

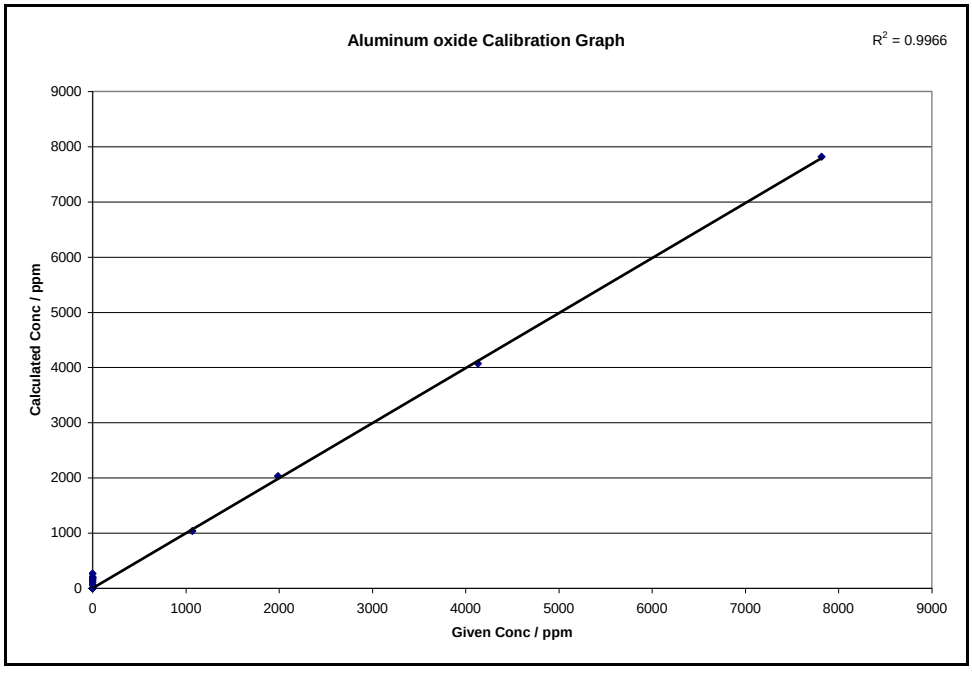


Figure D-0-2: Aluminum oxide calibration graph with potassium iodide as non-wetting agent and empirical corrections

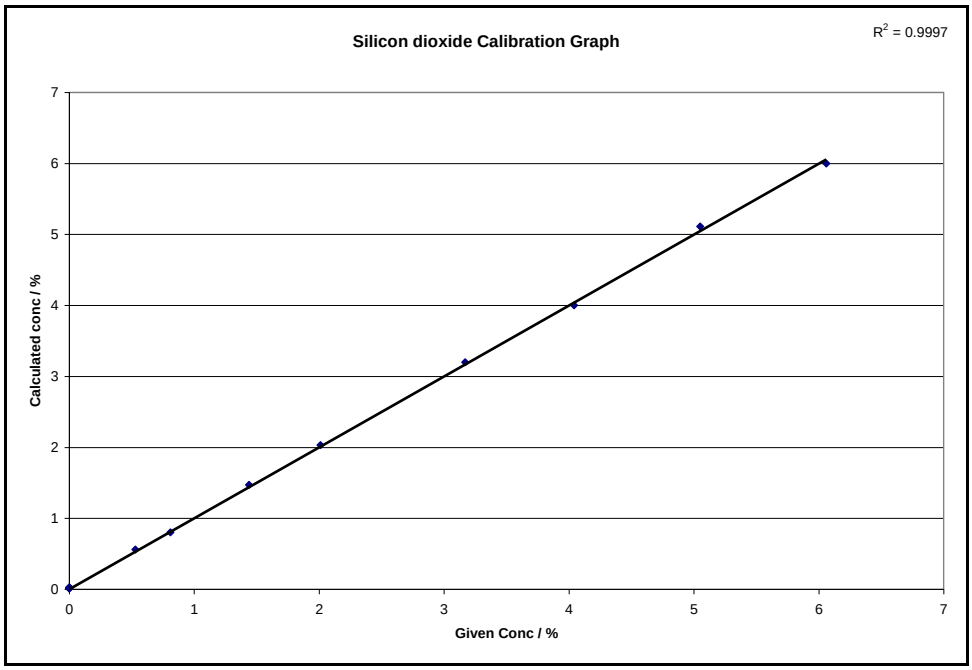


Figure D-0-3: Silicon dioxide calibration graph with potassium iodide as non-wetting agent and empirical corrections

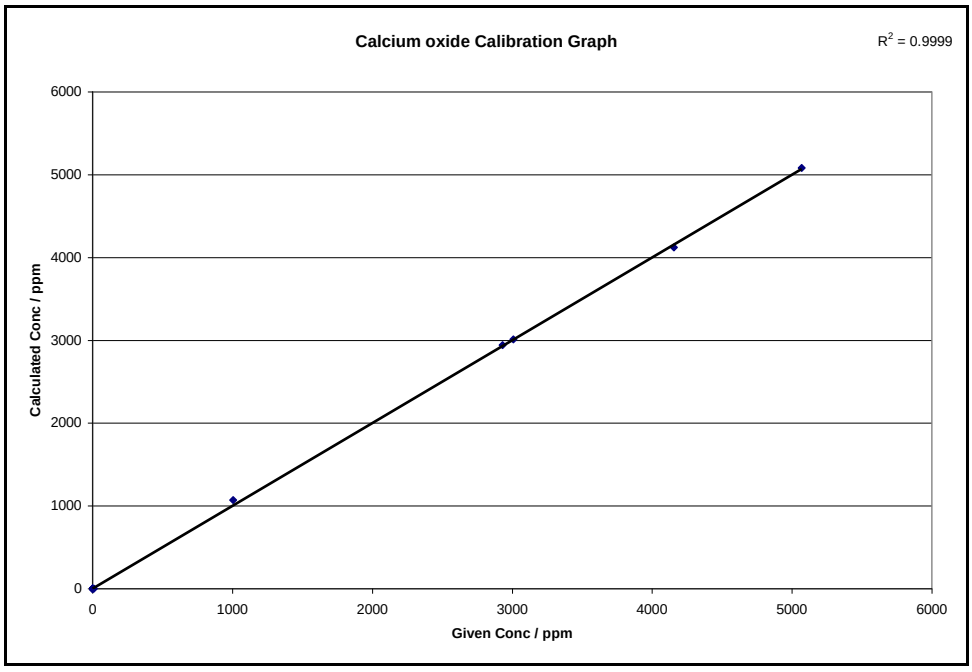


Figure D-0-4: Calcium oxide calibration graph with potassium iodide as non-wetting agent and empirical corrections

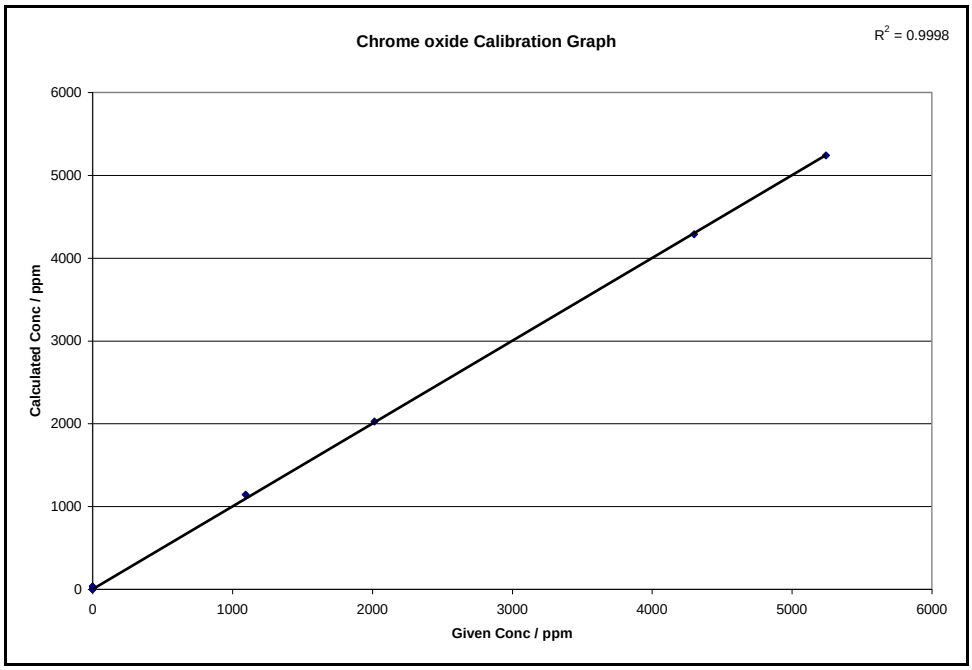


Figure D-0-5: Chromic oxide calibration graph with potassium iodide as non-wetting agent and empirical corrections

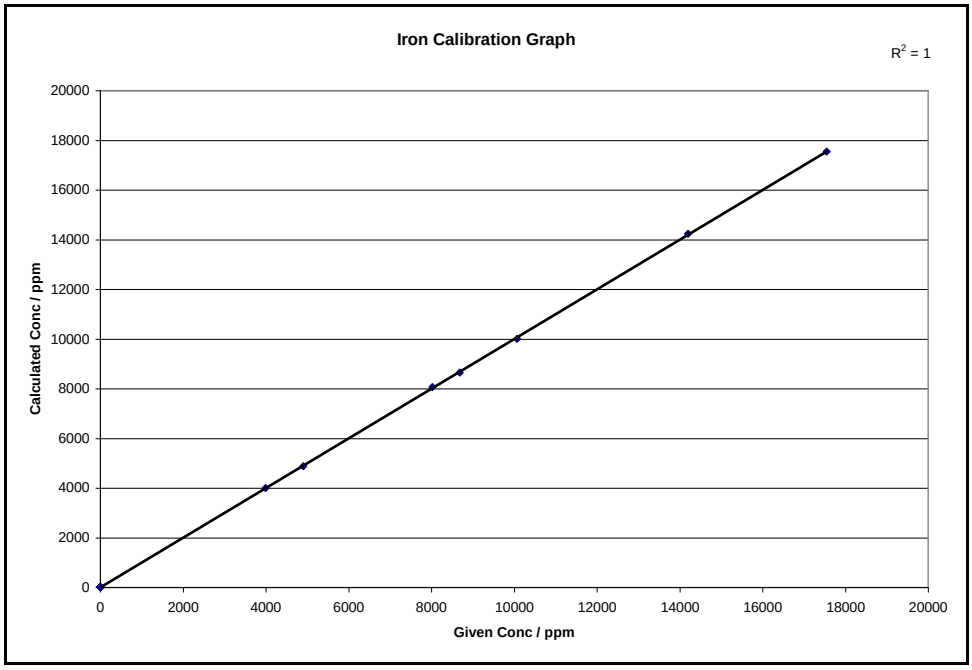


Figure D-0-6: Iron calibration graph with potassium iodide as non-wetting agent and empirical corrections

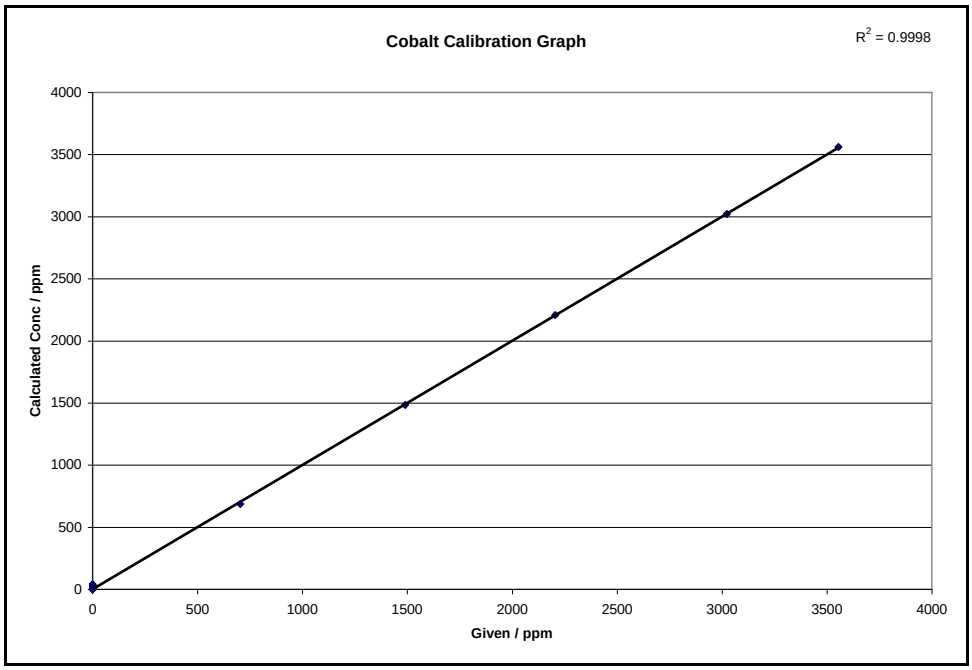


Figure D-0-7: Cobalt calibration graph with potassium iodide as non-wetting agent and empirical corrections

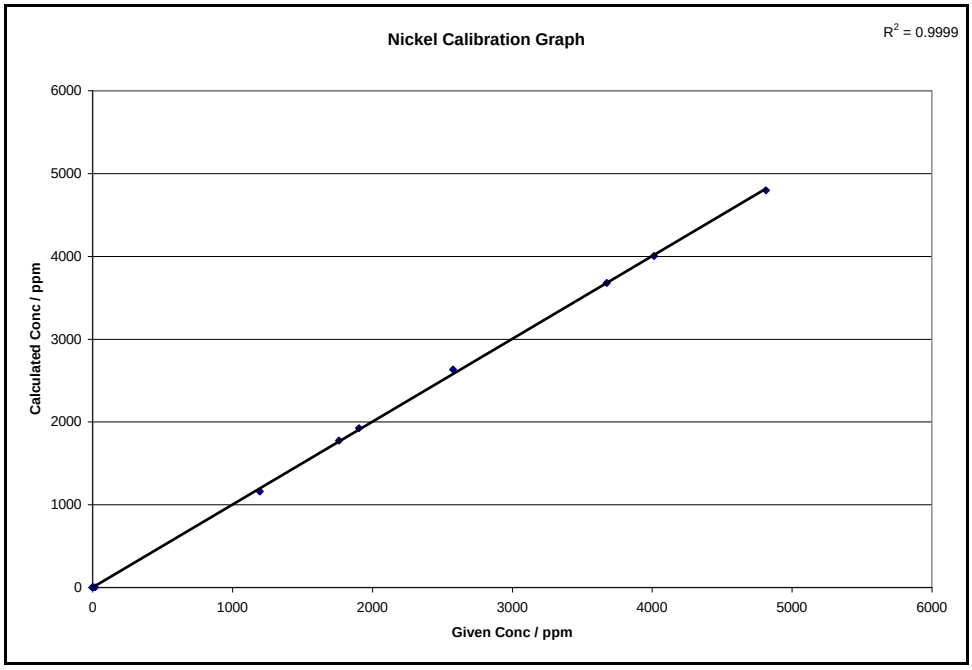


Figure D-0-8: Nickel calibration graph with potassium iodide as non-wetting agent and empirical corrections

APPENDIX E

Table E-1: Experimental details of samples prepared during oxidation with ammonium nitrate in the Electrofluxer

Glass bead number	Sample [g]	NH_4NO_3 [g]	NaI [g]	Flux [g]	KNO_3 [g]	Crucible Before [g]	Crucible after [g]	Mould before [g]	Mould after [g]	Glass bead mass [g]
Glass bead 1	0.25	1.00	0.10	8.75	-	26.69	27.87	34.13	41.87	8.92
Glass bead 2	0.25	1.03	0.10	9.67	-	30.86	31.12	34.13	43.73	9.85
Glass bead 3	0.25	1.00	0.10	9.51	1.00	30.86	32.00	34.48	43.46	11.46

Table E-2: Experimental details of samples prepared during oxidation with sodium nitrate in the Electrofluxer

Sample	Sample [g]	$NaNO_3$ [g]	$NaBO_3$ [g]	Flux [g]	Crucible before [g]	Crucible After [g]	Mould Before [g]	Mould After [g]	Glass bead mass [g]
PPL	0.26	0.51	1.50	9.02	30.87	30.94	44.44	9.96	10.02
AMB MER	0.25	0.55	1.51	9.01	26.68	27.00	44.10	9.62	9.93
AMB UG2	0.25	0.50	1.51	9.02	30.87	30.98	44.30	9.82	9.93
LMER	0.26	0.51	1.50	9.04	26.65	26.78	44.37	9.89	10.02

Table E-3: Experimental results of samples produced during oxidation with sodium nitrate in the Katanax

Glass bead	Crucible Before [g]	Crucible after [g]	Mould before [g]	Mould after [g]	Glass bead mass [g]	Cu Measured [ppm]	Ni Measured [ppm]	S Measured [ppm]
POF 1	30.34	30.54	36.50	43.73	7.43	1065.52	2515.48	7079.74
POF 2	30.13	30.55	35.94	42.97	7.45	1350.36	2973.04	6948.98
POF 3	29.74	31.26	36.40	42.43	7.54	1566.08	3161.97	7815.00
POF 4	30.21	30.89	35.94	42.85	7.59	1594.68	3139.41	7799.46
POF 5	30.32	30.64	36.61	43.86	7.57	1437.95	2995.31	7296.05
POF 6	29.71	30.73	36.41	42.96	7.58	1263.37	2872.70	7247.34
POF 7	29.74	30.24	36.50	43.73	7.73	1528.60	3116.15	7694.32
POF 8	30.21	30.45	35.94	43.47	7.77	1459.48	3064.77	7676.67
POF 9	30.32	30.99	36.50	43.29	7.46	1551.82	3430.13	8138.51
POF 10	29.71	30.12	36.61	43.58	7.37	1358.72	3121.20	7675.94
POF 11	30.14	30.65	36.40	43.48	7.58	1585.79	3132.70	7800.70
POF 12	30.35	31.54	35.94	42.41	7.65	1566.25	3215.06	7910.39
POF 13	30.21	31.30	36.41	42.92	7.60	1455.40	3076.73	7397.30
POF 14	29.74	30.09	36.61	43.87	7.60	1290.29	2922.66	7360.90
POF 15	30.13	30.61	36.50	42.75	6.72	1549.64	3063.09	7615.18
POF 16	29.72	30.64	35.94	43.86	8.84	1546.36	3098.31	7624.87
POF 17	30.21	30.59	36.50	43.63	7.51	1397.39	3073.33	7338.92
POF 18	30.33	30.96	36.61	43.44	7.45	1411.68	3014.57	7222.10
POF 19	29.75	30.26	35.94	42.96	7.53	1582.08	3255.11	7948.49
POF 20	30.35	30.76	36.41	42.92	6.92	1575.73	3153.77	7835.97
POF 21	30.13	31.05	36.50	43.25	7.67	1310.49	2879.88	7274.25
POF 22	29.72	30.35	36.61	43.64	7.67	1283.91	2891.12	7439.83
POF 23	29.75	30.74	36.50	43.31	7.80	1588.36	3076.63	7562.06
POF 24	30.22	31.65	36.40	42.71	7.74	1625.72	3116.20	7682.07
POF 25	29.74	30.28	36.50	43.41	7.44	1565.95	3267.01	7924.37
POF 26	30.33	31.62	36.40	42.51	7.40	1452.44	3223.84	7792.58
POF 27	30.14	31.24	36.61	43.07	7.56	1625.15	3222.04	7865.05
POF 28	29.72	30.28	35.94	42.96	7.57	1598.47	3234.17	7846.69
POF 29	30.35	30.84	36.50	43.61	7.60	1377.89	2996.93	7668.07
POF 30	30.21	31.02	36.61	43.51	7.70	1335.16	2998.41	7711.15
POF 31	30.14	31.14	36.41	43.14	7.74	1607.60	3100.95	7625.78
POF 32	29.75	30.94	36.61	43.17	7.75	1603.73	3134.09	7641.11
POF 33	29.72	30.21	36.50	43.59	7.58	1493.15	3123.08	7695.29
POF 34	29.75	29.93	36.61	44.05	7.62	1466.52	3060.74	7818.27
POF 35	30.33	31.49	35.94	42.37	7.58	1442.06	3163.09	7819.73
POF 36	30.13	30.99	36.41	43.26	7.70	1483.09	3048.75	7640.06

APPENDIX F

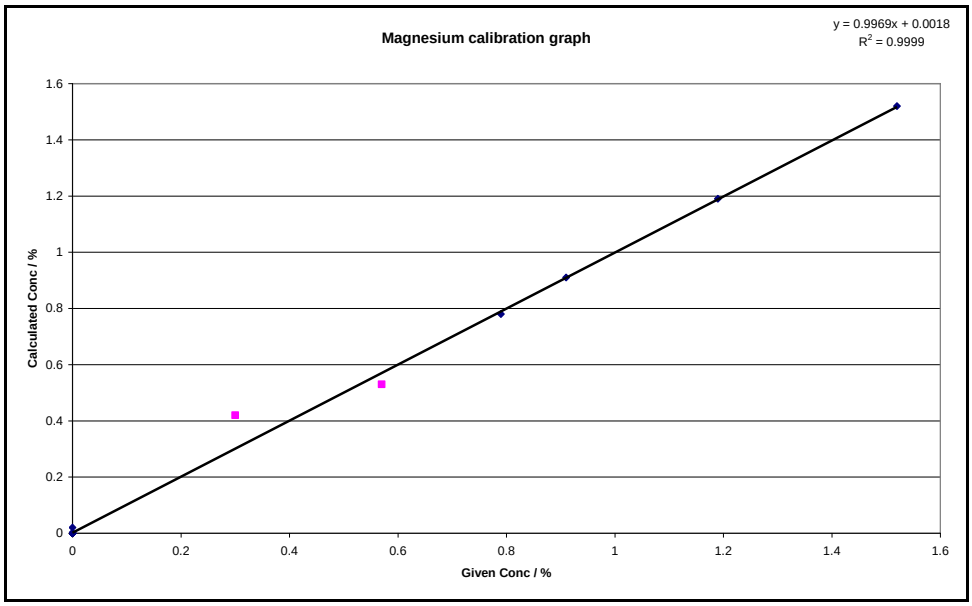


Figure F-0-1: Magnesium calibration graph on EDXRF with FP corrections

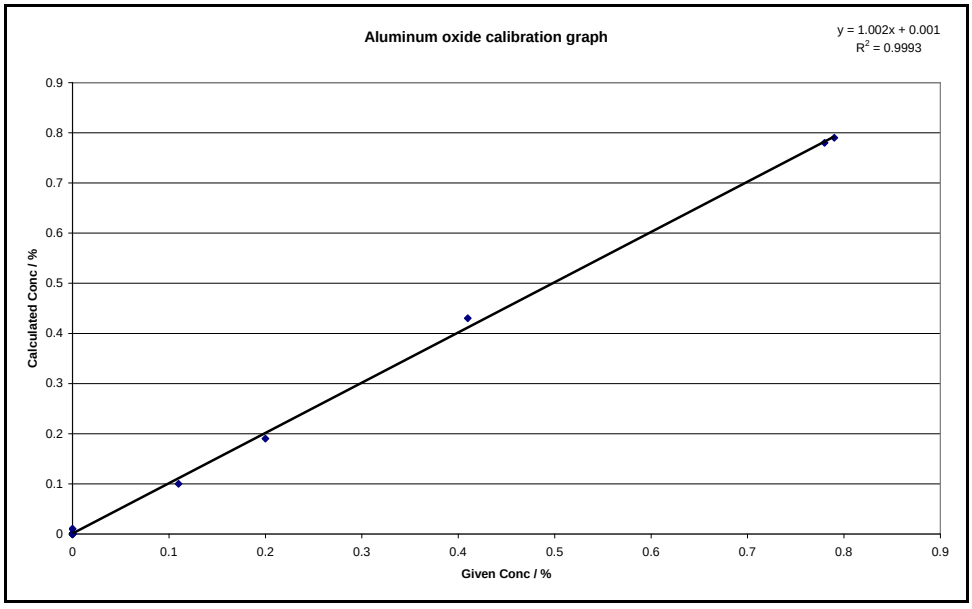


Figure F-0-2: Aluminum oxide calibration graph on EDXRF with FP corrections

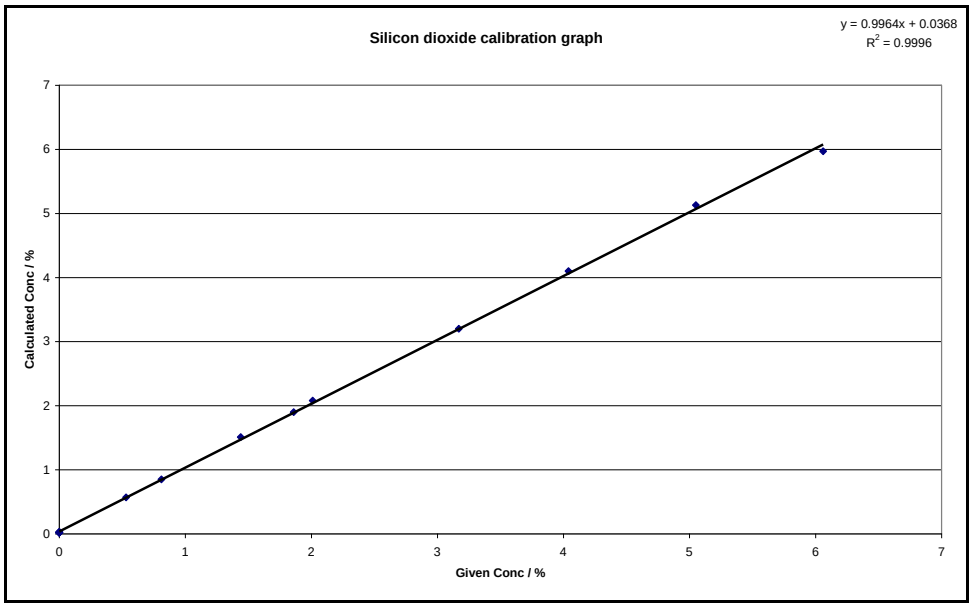


Figure F-0-3: Silicon dioxide calibration graph on EDXRF with FP corrections

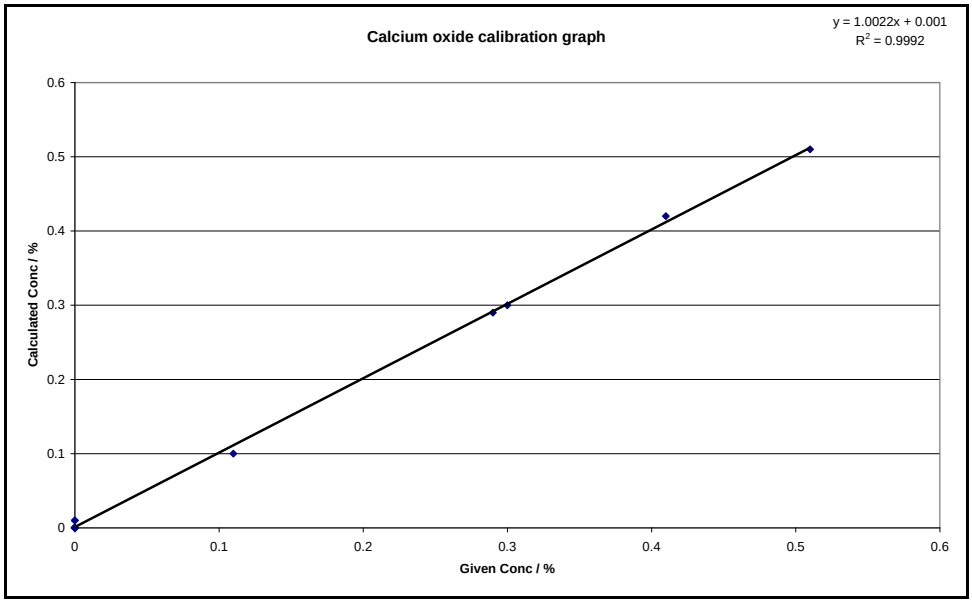


Figure F-0-4: Calcium oxide calibration graph on EDXRF with FP corrections

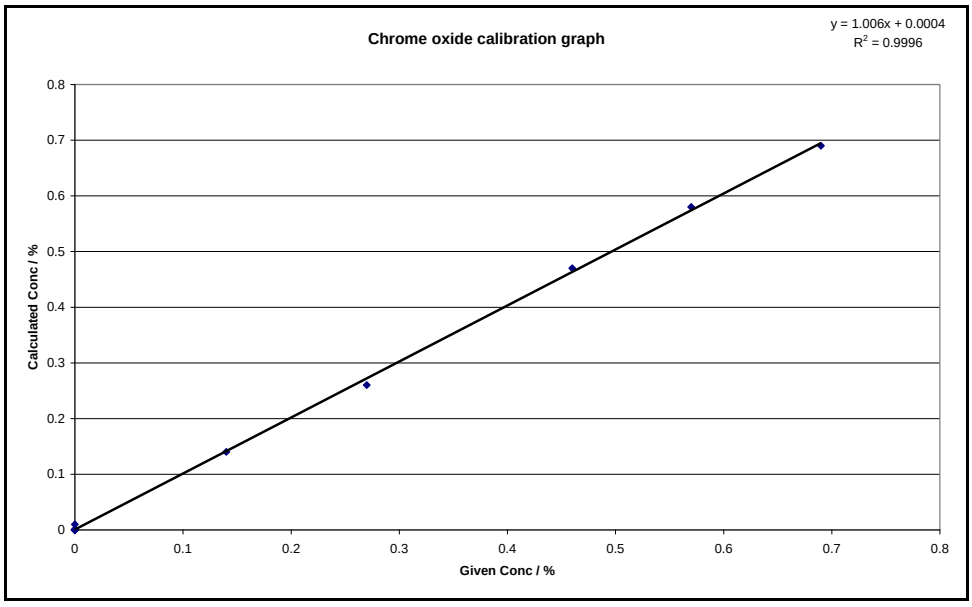


Figure F-0-5: Chromic oxide calibration graph on EDXRF with FP corrections

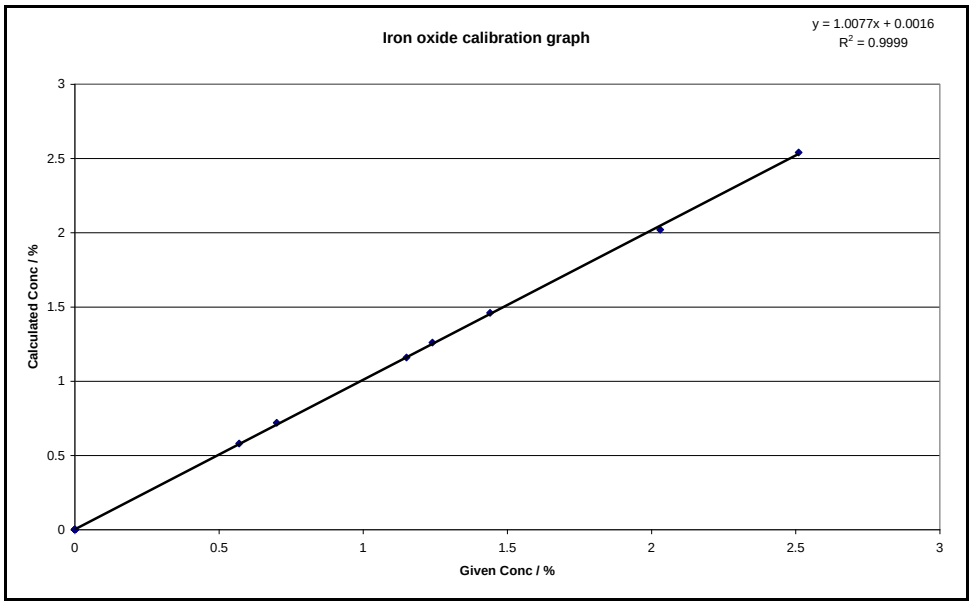


Figure F-0-6: Iron oxide calibration graph on EDXRF with FP corrections

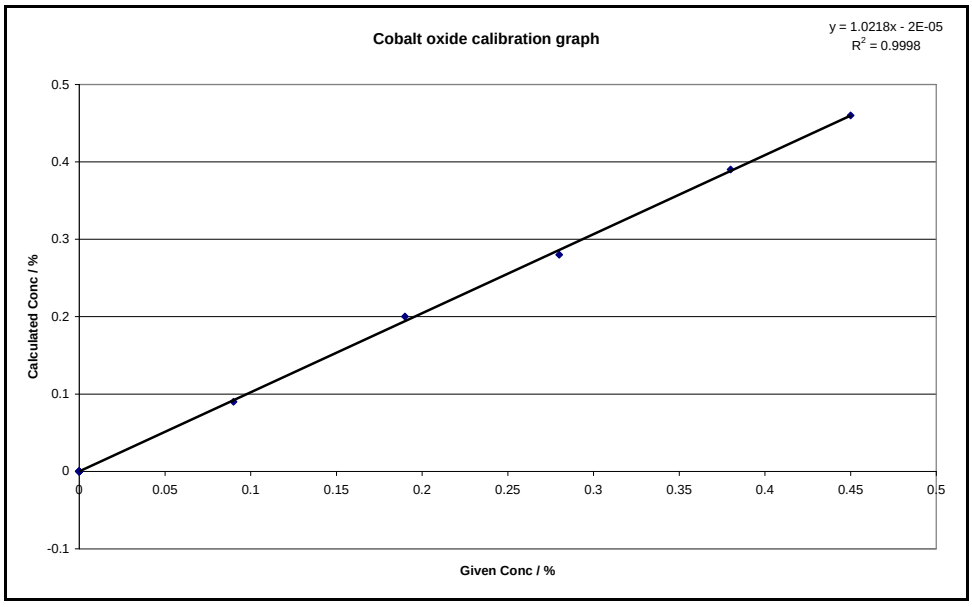


Figure F-0-7: Cobalt oxide calibration graph on EDXRF with FP corrections

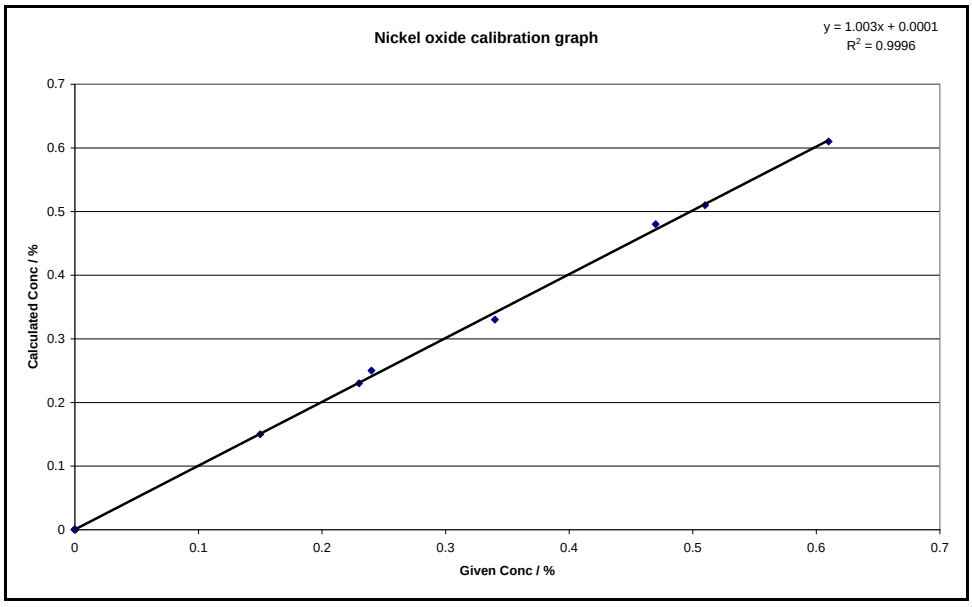


Figure F-0-8: Nickel oxide calibration graph on EDXRF with FP corrections

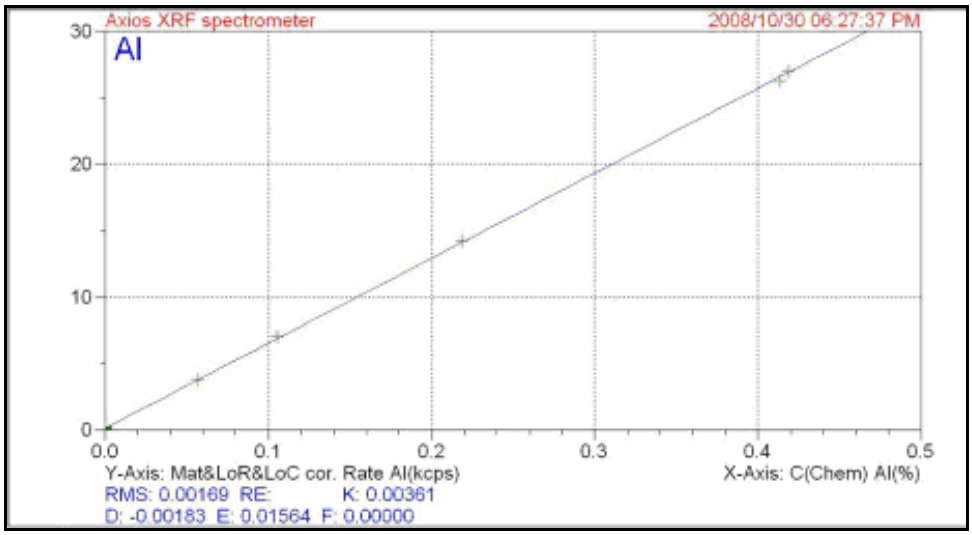


Figure F-0-9: Aluminum calibration graph on WDXRF with FP corrections

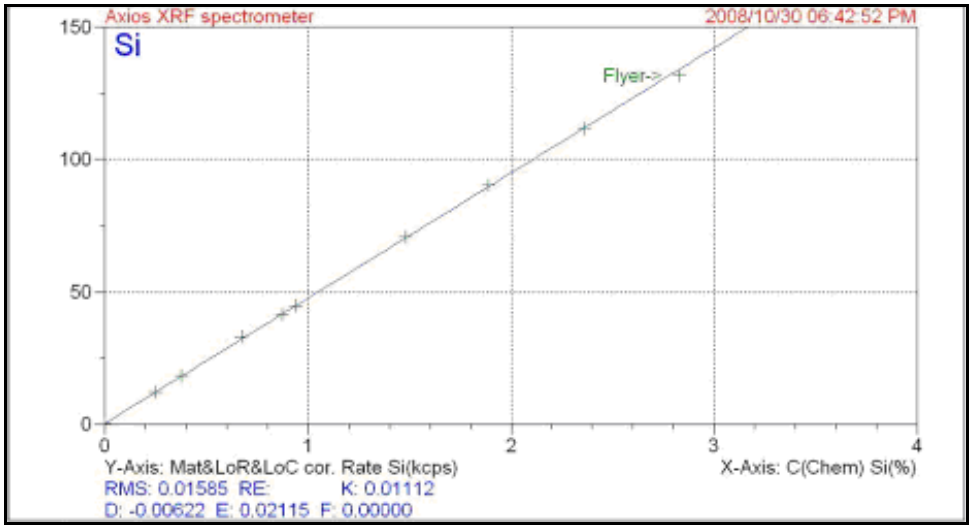


Figure F-0-10: Silica calibration graph on WDXRF with FP corrections

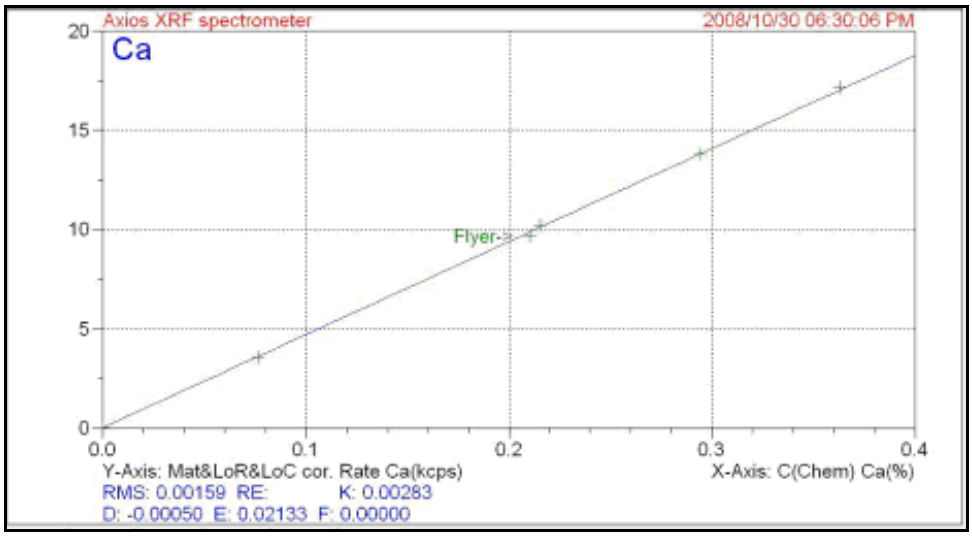


Figure F-0-11: Calcium calibration graph on WDXRF with FP corrections

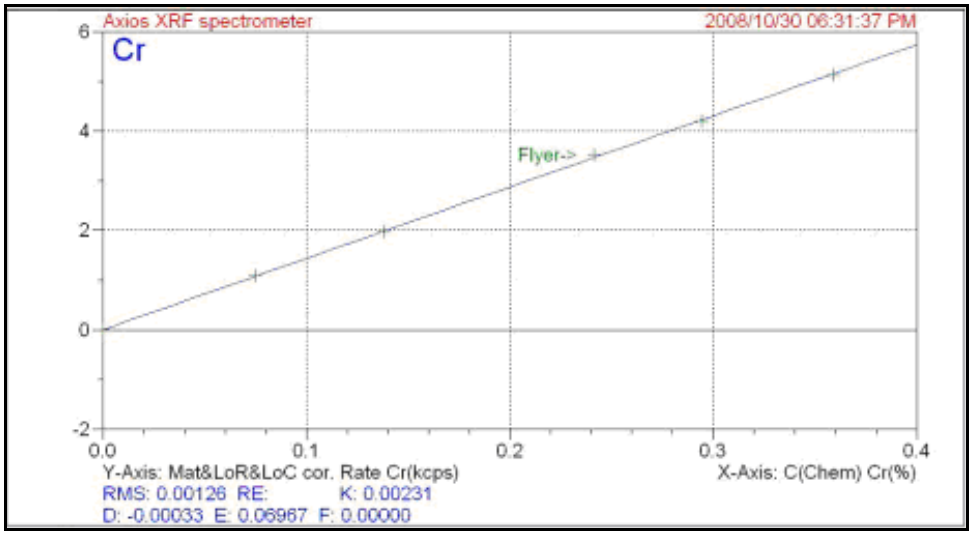


Figure F-0-12: Chrome calibration graph on WDXRF with FP corrections

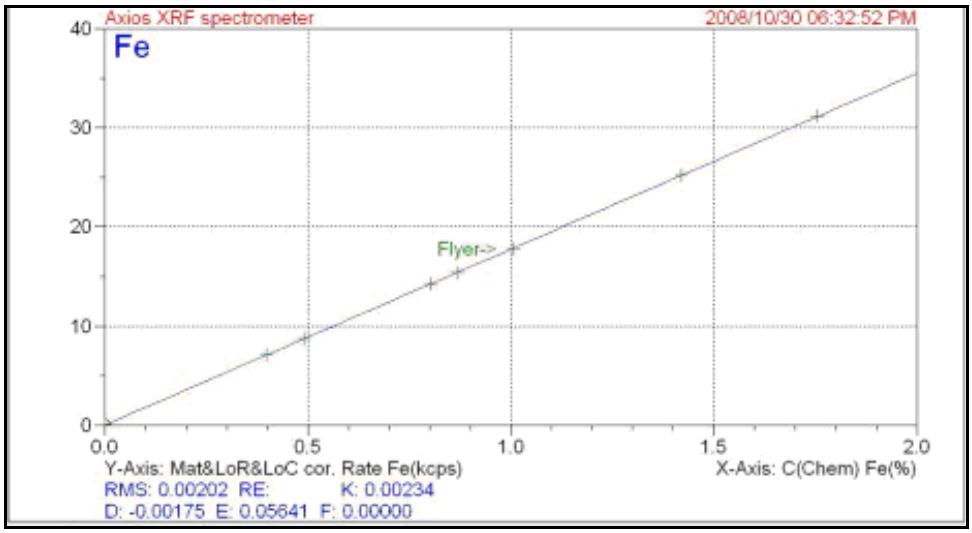


Figure F-0-13: Iron calibration graph on WDXRF with FP corrections

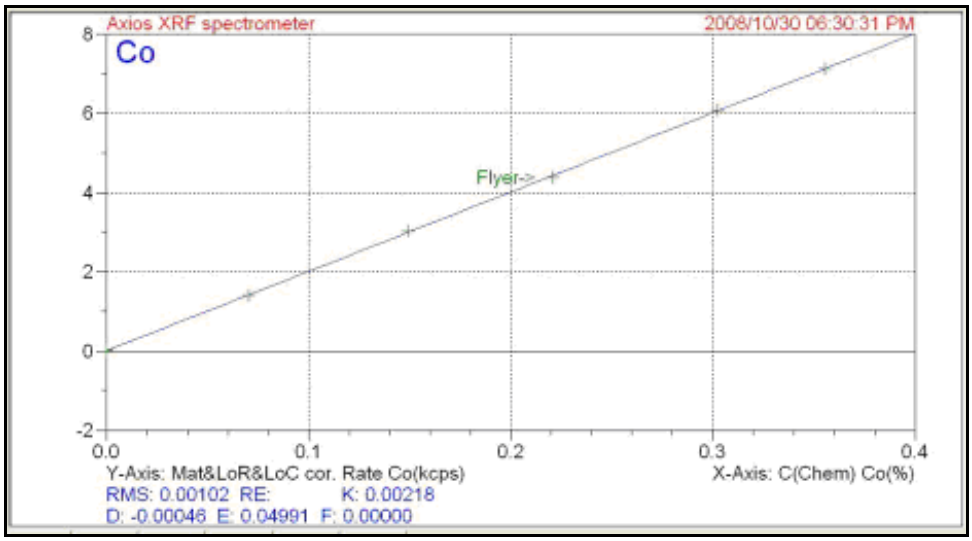


Figure F-0-14: Cobalt calibration graph on WDXRF with FP corrections

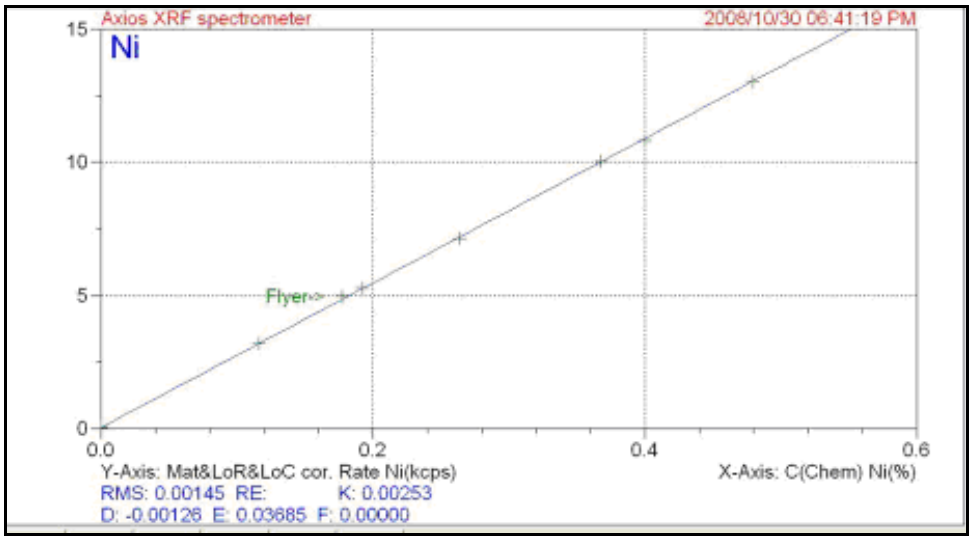


Figure F-0-15: Nickel calibration graph on WDXRF with FP corrections

APPENDIX G

Table G-1: Experimental detail of sample prepared for the validation of the final calibration on WDXRF

Glass bead number	Sample type	Sample [g]	$NaNO_3$ [g]	Na_2CO_3 [g]	$NaBO_3$ [g]	Flux [g]
POF 40	KM AMC	0.70	0.50	0.50	0.50	6.50
POF 41		0.70	0.50	0.50	0.50	6.50
POF 42	KM AUC	0.71	0.50	0.50	0.50	6.50
POF 43		0.71	0.50	0.50	0.50	6.50
POF 44	KM PPC	0.67	0.50	0.50	0.50	6.51
POF 45		0.67	0.50	0.50	0.50	6.52
POF 46	LMC QC 03	0.34	0.50	0.50	0.51	6.51
POF 47		0.35	0.50	0.50	0.50	6.50
POF 48	LUC QC 02	0.77	0.50	0.50	0.50	6.50
POF 49		0.76	0.51	0.50	0.50	6.50
POF 50	BMC QC 02	0.50	0.50	0.50	0.50	6.50
POF 51		0.50	0.50	0.50	0.50	6.51
POF 52	MUC QC 03	0.70	0.50	0.51	0.50	6.51
POF 53		0.70	0.50	0.50	0.50	6.50
POF 54	PPC QC 02	0.66	0.50	0.50	0.50	6.51
POF 55		0.66	0.51	0.50	0.50	6.50
VOC 1	AMCPS	1.01	0.51	0.50	0.52	6.52
VOC 2		1.00	0.50	0.50	0.50	6.52
VOC 3	AMMCW	1.00	0.50	0.50	0.51	6.53
VOC 4		1.00	0.51	0.50	0.50	6.54
VOC 5	ANUCPS	1.01	0.50	0.50	0.50	6.59
VOC 6		1.01	0.50	0.51	0.50	7.74
VOC 7	AUGPS	1.02	0.50	0.50	0.51	6.51
VOC 8		1.02	0.50	0.50	0.52	6.52
VOC 9	BRFDC 258	1.01	0.50	0.50	0.55	6.58
VOC 10		1.01	0.52	0.50	0.51	6.57
VOC 11	BRFDC 284	1.00	0.50	0.50	0.50	6.78
VOC 12		1.00	0.50	0.51	0.51	6.60
VOC 13	LMRPS	1.01	0.50	0.50	0.50	6.62
VOC 14		1.00	0.50	0.50	0.50	6.50
VOC 15	LUGPS	1.00	0.50	0.50	0.50	7.04
VOC 16		1.00	0.50	0.50	0.50	6.52
VOC 17	MDCPS	1.00	0.50	0.50	0.50	6.54
VOC 18		1.01	0.50	0.50	0.50	6.52
VOC 19	MTCPS	1.00	0.52	0.50	0.50	6.50
VOC 20		1.01	0.50	0.50	0.51	6.54
VOC 21	PPLPS	1.00	0.50	0.50	0.50	6.66
VOC 22		1.00	0.50	0.50	0.50	6.53
VOC 23	UWCPS	1.00	0.50	0.50	0.50	6.52
VOC 24		1.02	0.50	0.50	0.50	6.57
VOC 25	WNXPS	1.00	0.50	0.50	0.51	6.54
VOC 26		1.00	0.51	0.50	0.50	6.56
VOC 31	AMCPS	0.51	0.50	0.50	0.53	6.51
VOC 32		0.50	0.51	0.51	0.50	6.54
VOC 33	AMMCW	0.51	0.50	0.50	0.50	6.56
VOC 34		0.50	0.51	0.50	0.51	6.51
VOC 35	BRFDC 258	0.50	0.51	0.51	0.50	6.54
VOC 36		0.51	0.51	0.50	0.51	6.50
VOC 37	BRFDC 284	0.50	0.51	0.50	0.50	6.58

VOC 38		0.50	0.51	0.50	0.50	6.59
VOC 39	LMRPS	0.50	0.51	0.50	0.50	6.52
VOC 40		0.50	0.50	0.50	0.51	6.52
VOC 41	LUGPS	0.50	0.50	0.52	0.50	6.52
VOC 42		0.50	0.50	0.50	0.50	6.55

Table G-2: Raw results for copper oxide as analysed by WDXRF

Sample Type	WDXRF CuO results Glass bead A [ppm]	WDXRF CuO results Glass bead B [ppm]
KM AMC	2262	2282
KM AUC	939	985
KM PPC	1560	1618
LMC QC 03	Not used	2368
LUC QC 02	3134	2986
BMC QC 02	2691	2722
MUC QC 03	708	689
PPC QC 02	2037	2031
AMCPS	2470	2486
AMMCW	2794	2730
ANUCPS	479	532
AUGPS	695	804
BRFDC 258	3874	3867
BRFDC 284	3118	3322
LMRPS	1929	2066
LUGPS	1271	1365
MDCPS	1131	1296
MTCPS	539	545
PPLPS	2530	2614
UWCPS	930	871
WNXPS	2538	2560
AMCPS	1675	1549
AMMCW	1777	1764
BRFDC 258	2456	2478
BRFDC 284	1989	2081
LMRPS	1038	1068
LUGPS	748	701

Table G-3: Raw results for nickel oxide as analysed by WDXRF

Sample Type	WDXRF NiO results Glass bead A [ppm]	WDXRF NiO results Glass bead B [ppm]
KM AMC	3934	4006
KM AUC	1694	1740
KM PPC	2896	2974
LMC QC 03	Not used	4225
LUC QC 02	4780	4607
BMC QC 02	3983	4033
MUC QC 03	1067	1097
PPC QC 02	3547	3659
AMCPS	4873	4913
AMMCW	5672	5448
ANUCPS	927	876
AUGPS	1531	1613
BRFDC 258	6522	6482
BRFDC 284	5194	5616
LMRPS	2290	2373
LUGPS	1893	2008
MDCPS	1768	1863
MTCPS	1235	1283
PPLPS	4113	4095
UWCPS	1810	1741
WNXPS	4254	4319
AMCPS	2876	2743
AMMCW	3232	3235
BRFDC 258	3755	3746
BRFDC 284	3145	3148
LMRPS	1226	1250
LUGPS	1061	1067

Table G-4: Raw results of sulphur oxide as analysed by WDXRF

Sample Type	WDXRF SO_3 results Glass bead A [ppm]	WDXRF SO_3 results Glass bead B [ppm]
KM AMC	19182	19148
KM AUC	7281	7581
KM PPC	15063	15290
LMC QC 03	Not used	19886
LUC QC 02	20251	19607
BMC QC 02	19809	19625
MUC QC 03	4685	4371
PPC QC 02	18918	19096
AMCPS	26366	26768
AMMCW	29980	30286
ANUCPS	4341	3938
AUGPS	5903	5748
BRFDC 258	36118	36322
BRFDC 284	27472	29543
LMRPS	11208	11426
LUGPS	7898	8126
MDCPS	6797	6748
MTCPS	4748	4773
PPLPS	21821	22405
UWCPS	6845	6600
WNXPS	22159	22775
AMCPS	14776	14336
AMMCW	16470	16023
BRFDC 258	19969	19704
BRFDC 284	16219	15900
LMRPS	6319	6059
LUGPS	4581	4216

Table G-5: Raw results for iron oxide as analysed by WDXRF

Sample Type	WDXRF Fe_2O_3 results Glass bead A [ppm]	WDXRF Fe_2O_3 results Glass bead B [ppm]
KM AMC	20845	20909
KM AUC	13927	14003
KM PPC	17588	17981
LMC QC 03	Not used	13782
LUC QC 02	19274	18333
BMC QC 02	20852	20957
MUC QC 03	12284	12361
PPC QC 02	19879	20313
AMCPS	29499	29554
AMMCW	31255	31625
ANUCPS	17096	14807
AUGPS	15138	14878
BRFDC 258	32121	32432
BRFDC 284	26028	28856
LMRPS	18508	19098
LUGPS	19459	20357
MDCPS	16499	16635
MTCPS	16125	16221
PPLPS	24691	24931
UWCPS	15798	15551
WNXPS	25565	25662
AMCPS	16014	15971
AMMCW	16856	16812
BRFDC 258	17261	17523
BRFDC 284	15274	15004
LMRPS	10093	9964
LUGPS	10854	10953

Table G-6: Raw results for cobalt oxide as analysed by WDXRF

Sample Type	WDXRF CoO results Glass bead A [ppm]	WDXRF CoO results Glass bead B [ppm]
KM AMC	141	90
KM AUC	55	51
KM PPC	88	92
LMC QC 03	Not used	67
LUC QC 02	116	97
BMC QC 02	140	134
MUC QC 03	49	33
PPC QC 02	117	140
AMCPS	155	127
AMMCW	147	175
ANUCPS	44	51
AUGPS	48	66
BRFDC 258	155	163
BRFDC 284	151	164
LMRPS	59	49
LUGPS	39	36
MDCPS	67	70
MTCPS	34	56
PPLPS	113	107
UWCPS	54	77
WNXPS	79	103
AMCPS	58	81
AMMCW	92	78
BRFDC 258	94	88
BRFDC 284	69	64
LMRPS	34	40
LUGPS	32	25

Table G-7: Raw results for aluminium oxide as analysed by WDXRF

Sample Type	WDXRF Al_2O_3 results Glass bead A [ppm]	WDXRF Al_2O_3 results Glass bead B [ppm]
KM AMC	3283	3410
KM AUC	3965	4025
KM PPC	2834	2991
LMC QC 03	Not used	1191
LUC QC 02	6204	5959
BMC QC 02	1949	1870
MUC QC 03	2734	2834
PPC QC 02	2629	2638
AMCPS	2997	2806
AMMCW	3153	2999
ANUCPS	5492	4768
AUGPS	3300	3280
BRFDC 258	4738	4962
BRFDC 284	4373	5001
LMRPS	6809	6852
LUGPS	11823	12543
MDCPS	4361	4346
MTCPS	4417	4763
PPLPS	4893	4987
UWCPS	3408	3266
WNXPS	6030	6380
AMCPS	1793	1637
AMMCW	1887	1817
BRFDC 258	2665	2775
BRFDC 284	2682	2701
LMRPS	3844	4036
LUGPS	6848	6821

Table G-8: Raw results for calcium oxide as analysed by WDXRF

Sample Type	WDXRF CaO results Glass bead A [ppm]	WDXRF CaO results Glass bead B [ppm]
KM AMC	2375	2399
KM AUC	2594	2650
KM PPC	4453	4601
LMC QC 03	Not used	988
LUC QC 02	3230	3112
BMC QC 02	1356	1360
MUC QC 03	2245	2323
PPC QC 02	3295	3305
AMCPS	2535	2505
AMMCW	2678	2666
ANUCPS	3956	3452
AUGPS	2656	2631
BRFDC 258	3565	3626
BRFDC 284	3390	3681
LMRPS	4830	4944
LUGPS	4509	4726
MDCPS	3086	3166
MTCPS	3179	3108
PPLPS	6216	6343
UWCPS	2569	2449
WNXPS	4177	4223
AMCPS	1388	1359
AMMCW	1436	1438
BRFDC 258	1976	1967
BRFDC 284	1954	1970
LMRPS	2676	2627
LUGPS	2578	2605

Table G-9: Raw results for magnesium oxide as analysed by WDXRF

Sample Type	WDXRF MgO results Glass bead A [ppm]	WDXRF MgO results Glass bead B [ppm]
KM AMC	15790	15643
KM AUC	19742	20447
KM PPC	14902	15648
LMC QC 03	Not used	4708
LUC QC 02	16786	15781
BMC QC 02	7699	7567
MUC QC 03	21555	21827
PPC QC 02	13414	13537
AMCPS	23565	23554
AMMCW	22789	22053
ANUCPS	29853	25986
AUGPS	31559	31032
BRFDC 258	17801	18519
BRFDC 284	17408	20738
LMRPS	24052	24494
LUGPS	20877	22037
MDCPS	26457	29000
MTCPS	30077	30323
PPLPS	22501	22588
UWCPS	31255	29103
WNXPS	18631	19542
AMCPS	12075	12200
AMMCW	11483	11914
BRFDC 258	9102	9594
BRFDC 284	10576	10028
LMRPS	12914	13172
LUGPS	11177	11396

Table G-10: Raw results for chromic oxide as analysed by WDXRF

Sample Type	WDXRF CrO_3 results Glass bead A [ppm]	WDXRF CrO_3 results Glass bead B [ppm]
KM AMC	1316	1326
KM AUC	3167	3199
KM PPC	201	226
LMC QC 03	Not used	206
LUC QC 02	5806	5368
BMC QC 02	706	701
MUC QC 03	1493	1601
PPC QC 02	232	216
AMCPS	665	637
AMMCW	612	657
ANUCPS	2121	1869
AUGPS	2760	2573
BRFDC 258	520	554
BRFDC 284	511	592
LMRPS	2641	2681
LUGPS	15746	16247
MDCPS	3014	2987
MTCPS	3485	3487
PPLPS	372	402
UWCPS	2722	2688
WNXPS	1376	1366
AMCPS	380	357
AMMCW	348	378
BRFDC 258	290	331
BRFDC 284	332	329
LMRPS	1464	1391
LUGPS	8787	8678

Table G-11: Raw results for silicon dioxide as analysed by WDXRF

Sample Type	WDXRF SiO_2 results Glass bead A [ppm]	WDXRF SiO_2 results Glass bead B [ppm]
KM AMC	32485	33136
KM AUC	40585	41492
KM PPC	32628	33998
LMC QC 03	Not used	12140
LUC QC 02	35410	33819
BMC QC 02	19818	19868
MUC QC 03	45349	46330
PPC QC 02	31974	32229
AMCPS	47409	47395
AMMCW	44947	45189
ANUCPS	62581	54586
AUGPS	64270	62627
BRFDC 258	41969	42518
BRFDC 284	42046	46898
LMRPS	57201	58362
LUGPS	43298	44976
MDCPS	58341	60039
MTCPS	63256	62709
PPLPS	48205	49206
UWCPS	61727	59911
WNXPS	46446	47572
AMCPS	25914	25536
AMMCW	24265	24143
BRFDC 258	22909	22890
BRFDC 284	24486	24462
LMRPS	31027	30769
LUGPS	24587	24196